THE EFFECT OF INELASTIC BEHAVIOR OF BEAM-TO-COLUMN CONNECTION REGIONS ON THE SEISMIC PERFORMANCE OF RC FRAME STRUCTURES

A THESIS SUBMITTED TO
THE GRADUATE SCHOOL OF NATURAL AND APPLIED SCIENCES
OF
MIDDLE EAST TECHNICAL UNIVERSITY

BY

UMUT AKIN

IN PARTIAL FULFILLMENT OF THE REQUIREMENTS
FOR
THE DEGREE OF DOCTOR OF PHILOSOPHY
IN
CIVIL ENGINEERING

MARCH 2024

Approval of the thesis:

THE EFFECT OF INELASTIC BEHAVIOR OF BEAM-TO-COLUMN CONNECTION REGIONS ON THE SEISMIC PERFORMANCE OF RC FRAME STRUCTURES

submitted by **UMUT AKIN** in partial fulfillment of the requirements for the degree of **Doctor of Philosophy** i**n Civil Engineering, Middle East Technical University** by,

Prof. Dr. Naci Emre Altun
Dean, **Graduate School of Natural and Applied Sciences** _____

Prof. Dr. Erdem Canbay
Head of the Department, **Civil Engineering** _____

Assoc. Prof. Dr. Burcu Burak Bakır
Supervisor, **Civil Engineering, METU** _____

Examining Committee Members:

Prof. Dr. Murat Altuğ Erberik
Civil Engineering Dept., METU _____

Assoc. Prof. Dr. Burcu Burak
Civil Engineering Dept., METU _____

Prof. Dr. Afşin Sarıtaş
Civil Engineering Dept., METU _____

Dr. Halit Cenan Mertol
Civil Engineering Dept., Atılım University _____

Dr. Burcu Güldür Erkal
Civil Engineering Dept., Hacettepe University _____

Date: 06.03.2024

I hereby declare that all information in this document has been obtained and presented in accordance with academic rules and ethical conduct. I also declare that, as required by these rules and conduct, I have fully cited and referenced all material and results that are not original to this work.

Name Last name : Umut Akın

Signature :

ABSTRACT

THE EFFECT OF INELASTIC BEHAVIOR OF BEAM-TO-COLUMN CONNECTION REGIONS ON THE SEISMIC PERFORMANCE OF RC FRAME STRUCTURES

Akın, Umut
Doctor of Philosophy, Civil Engineering
Supervisor : Assoc. Prof. Dr. Burcu Burak Bakır

March 2024, 273 pages

The seismic behavior of reinforced concrete frame structures substantially depends on the response of beam-column connection regions as revealed by prior experimental research studies. Accurate evaluation of the nonlinear behavior of reinforced concrete frame structures under reversed cyclic loading requires an adequate definition of the beam-column joint response. In this research study, a joint shear strength prediction equation considering various material, geometrical properties and loading conditions is proposed, utilizing a comprehensive database composed of 251 experimentally investigated beam-column connection subassemblies. Moreover, a nonlinear inelastic joint shear behavior model is developed and verified by comparison with available experimental data. Finally, nonlinear analyses are performed utilizing the proposed joint model defined with the "panel zone" element of SAP 2000 software and the structural response is compared with experimental results of numerous subassemblies and a 3-story 3-bay reinforced concrete frame tested in the Middle East Technical University Structural Mechanics Laboratory. The utilization of the proposed joint model provides more accurate overall structural response and beam moment-rotation response estimations, which is crucial for evaluating the structural performance, when compared to rigid or semi

rigid joint assumptions. The comparison of the joint strength prediction equation with the contemporary code requirements indicates the improved accuracy of the proposed equation and the feasibility of integrating it into the structural design codes for obtaining the shear strength of both code conforming and nonconforming beam-column joints.

Keywords: Beam-Column Connection, Beam-Column Joint, Shear Strength, Shear Strain, Reinforced Concrete Frame Structure, Panel Zone, Nonlinear Analysis

ÖZ

BİRLEŞİM BÖLGELERİNDE GÖZLENEN İNELASTİK DAVRANIŞIN BETONARME ÇERÇEVE SİSTEMLERİN DEPREM YÜKÜ ALTINDAKİ DAVRANIŞLARINA ETKİSİ

Akın, Umut
Doktora, İnşaat Mühendisliği
Tez Yöneticisi: Doç. Dr. Burcu Burak Bakır

Mart 2024, 273 sayfa

Betonarme çerçeve yapıların deprem yüklemesi altındaki davranışları, deneysel araştırmalar sonucunda görüldüğü üzere kolon-kiriş birleşim bölgelerinin davranışına büyük ölçüde bağlıdır. Betonarme çerçeve yapıların tersinir tekrarlanır yükleme altındaki davranışlarını değerlendirebilmek için kolon-kiriş düğüm noktalarının davranışlarının doğru bir şekilde tanımlanması önem taşımaktadır. Bu araştırmada, 251 numuneden oluşan kapsamlı bir veri tabanı oluşturulmuş ve bu veri tabanındaki deneysel sonuçlar kullanılarak çeşitli malzeme ve geometri özellikleri olan farklı yükleme koşullarına sahip düğüm noktalarının kesme kapasitelerini tahmin etmekte kullanılabilecek bir denklem geliştirilmiştir. Ayrıca, deprem nedeniyle oluşan tersinir tekrarlanır yükleme altında düğüm noktalarının kesme davranışını tanımlayan doğrusal olmayan inelastik bir davranış modeli geliştirilmiş ve analitik bulgular deneysel sonuçlarla karşılaştırılarak modelin yapısal davranışı temsil etmedeki yeterliliği doğrulanmıştır. Son olarak, önerilen düğüm noktası davranış modeli "panel bölgesi" tanımı ile SAP 2000 yazılımında analitik olarak modellenmiş ve elde edilen yapısal davranış hem birleşim bölgesi numuneleri hem de Orta Doğu Teknik Üniversitesi Yapı Mekaniği Laboratuvarı'nda deneyi

gerçekleştirilen 3-katlı 3-açıklıklı betonarme çerçeveden elde edilen deneysel sonuçlar ile karşılaştırılmıştır. Önerilen düğüm noktası modelinin kullanımı, rijit veya yarı rijit düğüm noktası varsayımları ile karşılaştırıldığında, yapısal performansın değerlendirilmesinde çok önemli olan yapısal davranışın ve kiriş moment-dönme ilişkisinin deneysel verilere daha yakın elde edilmesini sağlar. Önerilen düğüm noktası kesme mukavemeti denkleminin dünyada ve Türkiye'de kullanılan farklı deprem yönetmelikleri ile karşılaştırılması sonucu önerilen denklemin daha doğru sonuçlar verdiği görülmüş ve bu da hem yönetmeliğe göre yeterli donatı kullanılarak tasarlanmış hem de yetersiz birleşim bölgeleri için bu denklemin tasarım yönetmeliklerine entegre edilmesinin fizibilitesini göstermiştir.

Anahtar Kelimeler: Kolon-Kiriş Birleşim Bölgesi, Kolon-Kiriş Düğüm Noktası, Kesme Mukavemeti, Kesme Birim Uzaması, Betonarme Çerçeve Yapı, Panel Bölgesi, Doğrusal Olmayan Analiz

Dedicated to the victims of Kahramanmaraş Earthquake.

ACKNOWLEDGMENTS

I wish to express my sincere gratitude to my thesis supervisor Assoc. Prof. Dr. Burcu Burak Bakır for her encouragement at the beginning of this journey and invaluable support, guidance and understanding throughout the long path we walked together.

I must extend my heartfelt gratitude towards my beloved sister, Fulya Akın, and my cherished parents, Fatma and Ahmet Akın, for their unwavering warmth and support during the challenging and intense periods of this journey. Their steadfast presence has been a cornerstone of my success, and without them, my achievements would have remained but a distant dream.

Furthermore, I cannot overlook the invaluable contribution of Arzu Şahin, whose relentless support and understanding have been a beacon of light for me. Equally, Beste and Yunus Kantekin deserve my deepest appreciation for not only their friendship and encouragement but also for the enriching technical discussions that have broadened my horizons and deepened my understanding, proving instrumental in my progress. I would also like to express my deep gratitude to Koray Kadaş for his enduring patience and thoughtful responses to my relentless stream of questions. Their collective support has been a pillar of strength, guiding me towards realizing my ambitions and for that, I am eternally grateful.

Lastly, I am profoundly proud for having the resilience not to surrender during the arduous and sometimes shadowy days of this endeavor. One should never forget that pursuing a Ph.D. is akin to running a marathon, not a sprint.

TABLE OF CONTENTS

ABSTRACT v

ÖZ vii

ACKNOWLEDGMENTS x

TABLE OF CONTENTS xi

LIST OF TABLES xvi

LIST OF FIGURES xix

LIST OF SYMBOLS xxv

CHAPTERS

1 INTRODUCTION 1

1.1 Reinforced Concrete Beam-Column Connections 1

1.2 Research Objective and Scope 3

2 LITERATURE REVIEW 7

2.1 Background Information 7

2.2 Joint Shear Strength (V_j) Equations of Contemporary Structural Codes 9

2.3 ACI 352-10 Recommendations for Design of Beam-Column Connections in Monolithic Reinforced Concrete Structures 9

2.4 ACI 318 Recommendations for Design of Beam-Column Connections in Monolithic Reinforced Concrete Structures 12

2.5 ASCE 41-17 Seismic Evaluation and Retrofit of Existing Buildings 16

2.6 CSA A23-19 Design of Concrete Structures 18

2.7 TEC 2007 – Turkish Earthquake Code 19

2.8 TEC 2018 – Turkish Earthquake Code 21

2.9 Conformity Requirements of Structural Codes 22
2.10 Parameters Affecting the Shear Strength of Beam-Column Joints 24
2.11 Joint Shear Reinforcement 24
2.12 Slab Participation 26
2.13 Presence of Transverse Beams 27
2.14 Presence of Axial Load on Column 29
2.15 Eccentricity 29
2.16 Analytical Modeling of Beam-Column Joints 31
3 CONSTRUCTION OF DATABASE 39
3.1 Overview 39
3.2 Selection of Specimens to be Included in the Database 40
3.3 Range of Specimen Properties 41
3.4 Selected Specimens 42
3.5 Constructed Database 47
4 ANALYTICAL MODEL 55
4.1 General Approach 55
4.2 Joint Shear Capacity Prediction Equation 56
4.2.1 Basic Prediction, $V_{j,pre.,basic}$ 57
4.2.2 Modification Factors 63
4.2.3 Joint Shear Capacity Prediction Equation 68
4.3 Determination of Joint Shear Performance Points 76
4.3.1 Definition of Joint Shear Performance Points 76
4.3.2 Prediction of Inelasticity Point P_{inel} 78
4.3.3 Construction of the Joint Shear Response Curve 79

4.4 Modification Factors for Strain Points 81
4.5 Construction of the Final Joint Shear Behavior Curve 83
5 VERIFICATION OF JOINT SHEAR STRENGTH PREDICTION..... 87
5.1 Overview 87
5.2 Evaluation of the Joint Shear Strength Predictions..... 88
5.3 Determination of the Accuracy of Each Modification Factor 114
5.4 Accuracy of the Joint Shear Strength Prediction 125
5.4.1 Comparison with ACI 352-10 126
5.4.2 Comparison with ACI 318-11 129
5.4.3 Comparison with ACI 318-14 131
5.4.4 Comparison with ACI 318-19 134
5.4.5 Comparison with ASCE 41-17 136
5.4.6 Comparison with CSA A23.03-19 139
5.4.7 Comparison with TEC2007 142
5.4.8 Comparison with TEC2018 145
6 VERIFICATION OF ANALYTICAL MODEL 151
6.1 Overview 151
6.2 Description of Modeling and Elements..... 151
6.2.1 Modeling of Beam-Column Connection Subassemblies 152
6.3 Loading Procedures..... 161
6.4 Loading Case Definition 163
6.5 Comparison of Analytical and Experimental Results 164
6.5.1 Specimens of Burak and Wight 165
6.5.2 Specimens of Raffaelle and Wight 179

6.5.3 Specimens of Shin and LaFave 186
6.5.4 Comparison of Joint Model with Rigid and Semi Rigid Joint Assumptions 192
7 APPLICATION OF JOINT MODEL TO FRAME ANALYSIS 199
7.1 Overview 199
7.2 Description of the Test Frame 201
7.2.1 Frame Properties 201
7.2.2 Material Properties 203
7.2.3 Frame Loading 204
7.3 Modeling of the Test Frame 208
7.3.1 Geometrical and Material Properties 208
7.3.2 Determination of Panel Zone Characteristics 214
7.3.3 Loads Applied to the Structure 226
7.3.4 Description of Nonlinear Time History Load Case 229
7.4 Verification of Analytical Results with Experimental Data 231
7.4.1 Comparison of the Cyclic Joint Response 232
7.4.2 Comparison of the Beam Moment – Rotation Response 237
7.4.3 Comparison of the Lateral Load – Story Drift Response 240
7.4.4 Evaluation of Analytical Model 248
7.4.5 Comparison of Rigid Joint Assumption with the Joint Model 249
8 SUMMARY AND CONCLUSIONS 255
8.1 Summary 255
8.2 Conclusions 257
8.3 Recommendations for Future Research 259

REFERENCES 261
CURRICULUM VITAE 271

LIST OF TABLES

TABLES

Table 2.1 Joint Shear Strength Factors, ACI 352-10 11
Table 2.2 Joint Shear Strength Factors, ACI 318-11 14
Table 2.3 Joint Shear Strength Factors, ACI 318-19 16
Table 2.4 Joint Shear Strength Factors, ASCE 41-17 17
Table 2.5 Code Conformity Requirements 22
Table 3.1 Specimen Types Included in the Database 40
Table 3.2 Range of Material and Geometrical Properties for the Specimens Included in the Database. 42
Table 3.3 Constructed Database 47
Table 4.1 ACI 352.10 Joint Shear Strength Factors 58
Table 4.2 Basic and Final Shear Strength Predictions 69
Table 4.3 Experimental and Analytical Ratios for Strain and Force Couples at the Performance Points 80
Table 5.1 Comparison of Experimental Joint Shear Strengths with Code Predictions 89
Table 5.2 Comparison of Experimental Joint Shear Strengths with Proposed Equation Predictions 102
Table 5.3 Correlation Coefficients for Different Volumetric Shear Reinforcement Ratio Definitions 114
Table 5.4 Correlation Coefficients for Shear Reinforcement Factors 115
Table 5.5 Comparison of Shear Strength Predictions of Contemporary Codes with Shear Reinforcement Factor (SR) 116
Table 5.6 Correlation Factors for Axial Stress Alternatives 118
Table 5.7 Correlation Coefficients for Axial Load Factor Alternatives 118
Table 5.8 Comparison of Shear Strength Predictions of Contemporary Codes with Axial Load Factor (AxF) 120

Table 5.9 Correlation Coefficients for Slab Index 122
Table 5.10 Correlation Coefficients for Slab Index Alternatives..... 122
Table 5.11 Comparison of Shear Strength Predictions of Contemporary Codes with Slab Factor (SF)..... 123
Table 5.12 Comparison of $V_{j,pre.}$ vs $V_{j,ACI\ 352\text{-}10}$ (Conforming Specimens)..... 126
Table 5.13 Comparison of $V_{j,pre.}$ vs $V_{j,ACI\ 352\text{-}10}$ (Nonconforming Specimens)..... 127
Table 5.14 Comparison of $V_{j,pre.}$ vs $V_{j,ACI\ 318\text{-}11}$ (Conforming Specimens)..... 129
Table 5.15 Comparison of $V_{j,pre.}$ vs $V_{j,ACI\ 318\text{-}11}$ (Nonconforming Specimens)..... 130
Table 5.16 Comparison of $V_{j,pre.}$ vs $V_{j,ACI\ 318\text{-}14}$ (Conforming Specimens)..... 131
Table 5.17 Comparison of $V_{j,pre.}$ vs $V_{j,ACI\ 318\text{-}14}$ (Nonconforming Specimens)..... 133
Table 5.18 Comparison of $V_{j,pre.}$ vs $V_{j,ACI\ 318\text{-}19}$ (Conforming Specimens)..... 134
Table 5.19 Comparison of $V_{j,pre.}$ vs $V_{j,ACI\ 318\text{-}19}$ (Nonconforming Specimens)..... 135
Table 5.20 Comparison of $V_{j,pre.}$ vs $V_{j,ACI\ 41\text{-}17}$ (Conforming Specimens)..... 137
Table 5.21 Comparison of $V_{j,pre.}$ vs $V_{j,ACI\ 41\text{-}17}$ (Nonconforming Specimens)..... 138
Table 5.22 Comparison of $V_{j,pre.}$ vs $V_{j,CSA.A23.03\text{-}19}$ (Conforming Specimens)..... 139
Table 5.23 Comparison of $V_{j,pre.}$ vs $V_{j,CSA.A23.03\text{-}19}$ (Nonconforming Specimens) . 141
Table 5.24 Comparison of $V_{j,pre.}$ vs $V_{j,TEC2007}$ (Conforming Specimens)..... 142
Table 5.25 Comparison of $V_{j,pre.}$ vs $V_{j,TEC2007}$ (Nonconforming Specimens)..... 144
Table 5.26 Comparison of $V_{j,pre.}$ vs $V_{j,TEC2018}$ (Conforming Specimens)..... 145
Table 5.27 Comparison of $V_{j,pre.}$ vs $V_{j,TEC2018}$ (Nonconforming Specimens)..... 147
Table 7.1 Test Frame Concrete Properties..... 203
Table 7.2 Test Frame Rebar Properties 203
Table 7.3 Confinement Score and Joint Shear Strength Factors for the Test Frame 217
Table 7.4 Axial Loads and Factors..... 218
Table 7.5 Shear Reinforcement Ratios for the Test Frame..... 218
Table 7.6 Joint Shear Strength Values of the Beam-Column Connections of Test Frame 220
Table 7.7 Basic Inelastic Strain Value Determination, Test Frame 221

Table 7.8 Strain Modification Factors, Test Frame.....222

LIST OF FIGURES

FIGURES

Figure 2.1. Forces Acting on Beam-Column Joints 10
Figure 2.2. Effective Joint Area Definition, ACI 318-11 14
Figure 2.3. Effective Joint Area Definition, TEC 2007 20
Figure 2.4. Eccentric Beam-Column Joints (Raffaelle & Wight, 1995) 30
Figure 2.5. Forces Acting on Eccentric Joints (Raffaelle & Wight, 1995) 31
Figure 2.6. Scissors Joint Model (Alath and Kunnath, 1995) 33
Figure 2.7. Plane Stress Element Model (Elmorsi et al., 2000) 34
Figure 2.8. Model of Shin and LaFave (2004) 35
Figure 2.9: Connection Model Proposed by Burak (2010) 37
Figure 2.10. Joint Model Proposed (Unal & Burak, 2013a) 38
Figure 4.1. $V_{j,pre.}$ Prediction Equation Development Flowchart 57
Figure 4.2. Proposed Shear Strength Factor 61
Figure 4.3. Effective Joint Width Definition 62
Figure 4.4. Shear Reinforcement Factor vs. $\rho_{singlelayer,core}$ 66
Figure 4.5. Joint Shear Force vs Joint Shear Strain Schematical Presentation 76
Figure 4.6. Digitization of Joint Shear Force vs Shear Strain Curves 77
Figure 4.7. Joint Performance Points Determination Flowchart 78
Figure 4.8. Proposed Joint Shear Force vs. Strain Response 80
Figure 4.9. Graphical Representation of Strain Modification Factor F_{BC} 82
Figure 4.10. Graphical Representation of Strain Modification Factor F_{SR} 83
Figure 4.11. Graphical Representation of Final Behavior Curve Definition for Joints 85
Figure 5.1. Effect of Shear Reinforcement Factor (SR) 117
Figure 5.2. Effect of Axial Load Factor (AxF) 121
Figure 5.3. Influence of Slab Factor (SF) 124
Figure 5.4. Comparison of $V_{j,pre.}$ vs $V_{j,ACI\ 352\text{-}10}$ (Conforming Specimens) 127
Figure 5.5. Comparison of $V_{j,pre.}$ vs $V_{j,ACI\ 352\text{-}10}$ (Nonconforming Specimens) 128

Figure 5.6. Comparison of $V_{j,pre.}$ vs $V_{j,ACI\ 318\text{-}11}$ (Conforming Specimens) 129
Figure 5.7. Comparison of $V_{j,pre.}$ vs $V_{j,ACI\ 318\text{-}11}$ (Nonconforming Specimens)..... 130
Figure 5.8. Comparison of $V_{j,pre.}$ vs $V_{j,ACI\ 318\text{-}14}$ (Conforming Specimens) 132
Figure 5.9. Comparison of $V_{j,pre.}$ vs $V_{j,ACI\ 318\text{-}14}$ (Nonconforming Specimens)..... 133
Figure 5.10. Comparison of $V_{j,pre.}$ vs $V_{j,ACI\ 318\text{-}19}$ (Conforming Specimens) 135
Figure 5.11. Comparison of $V_{j,pre.}$ vs $V_{j,ACI\ 318\text{-}19}$ (Conforming Specimens) 136
Figure 5.12. Comparison of $V_{j,pre.}$ vs $V_{j,ASCE\ 41\text{-}17}$ (Conforming Specimens) 137
Figure 5.13. Comparison of $V_{j,pre.}$ vs $V_{j,ASCE\ 41\text{-}17}$ (Nonconforming Specimens)... 138
Figure 5.14. Comparison of $V_{j,pre.}$ vs $V_{j,CSA\ A23.03\text{-}19}$ (Conforming Specimens)..... 140
Figure 5.15. Comparison of $V_{j,pre.}$ vs $V_{j,CSA\ A23.03\text{-}19}$ (Nonconforming Specimens) 141
Figure 5.16. Comparison of $V_{j,pre.}$ vs $V_{j,TEC2007}$ (Conforming Specimens)..... 143
Figure 5.17. Comparison of $V_{j,pre.}$ vs $V_{j,TEC2007}$ (Nonconforming Specimens)..... 144
Figure 5.18. Comparison of $V_{j,pre.}$ vs $V_{j,TEC2018}$ (Conforming Specimens)..... 145
Figure 5.19. Comparison of $V_{j,pre.}$ vs $V_{j,TEC2018}$ (Nonconforming Specimens)..... 147
Figure 5.20. Beam-Column Joint Failure Mechanism..... 148
Figure 6.1. Beam-Column Connection Subassembly (Burak & Wight, 2008)..... 152
Figure 6.2. Beam-Column Subassembly Model..... 153
Figure 6.3. Panel Zone Model 156
Figure 6.4. Takeda Hysteresis Model 157
Figure 6.5. Pivot Hysteresis Model 158
Figure 6.6. Comparison of Takeda and Pivot Hysteresis Models (Raffaelle & Wight, 1995)..... 160
Figure 6.7. Alternatives Evaluated for Moment Arm..... 161
Figure 6.8. Cyclic Deformation Time History Definition 162
Figure 6.9. Unit Displacement Defined at the Top of the Column 163
Figure 6.10. “Cyclic Loading” Load Case Definition 164
Figure 6.11. Specimen 1-S Joint Shear Force vs. Shear Strain Comparison 165
Figure 6.12. Specimen 1-S Lateral Load vs. Story Drift Comparison 166
Figure 6.13. Specimen 1-S Beam Moment - Rotation Comparison..... 166

Figure 6.14. Specimen 2-S Joint Shear Force vs. Joint Shear Strain Comparison 168
Figure 6.15. Specimen 2-S Lateral Load vs. Story Drift Comparison 168
Figure 6.16. Specimen 2-S Beam Moment – Rotation Response Comparison 169
Figure 6.17. Specimen 2-S Lateral Load vs. Story Drift Comparison for Various Moment Arm Assumptions 170
Figure 6.18. Specimen 3-S Joint Shear Force vs. Shear Strain Comparison 171
Figure 6.19. Specimen 3-S Lateral Load vs. Story Drift Comparison 172
Figure 6.20. Specimen 3-S Beam Moment – Rotation Response Comparison 172
Figure 6.21. Specimen 1-N Lateral Load vs. Story Drift Comparison..... 173
Figure 6.22. Specimen 1-N Beam Moment – Rotation Response Comparison.... 174
Figure 6.23. Specimen 2-N Joint Shear Force vs. Joint Shear Strain Comparison175
Figure 6.24. Specimen 2-N Lateral Load vs. Story Drift Comparison..... 176
Figure 6.25. Specimen 2-N Beam Moment – Rotation Response Comparison.... 176
Figure 6.26. Specimen 3-N Joint Shear Force vs. Shear Strain Comparison 177
Figure 6.27. Specimen 3-N Lateral Load vs. Story Drift Comparison..... 178
Figure 6.28. Specimen 3-N Beam Moment – Rotation Response Comparison.... 178
Figure 6.29. Specimen 1 Joint Shear Force vs. Shear Strain Comparison..... 180
Figure 6.30. Specimen 1 Lateral Load vs. Story Drift Comparison..... 180
Figure 6.31. Specimen 2 Joint Shear Force vs. Shear Strain Comparison..... 181
Figure 6.32. Specimen 2 Lateral Load vs. Story Drift Comparison..... 182
Figure 6.33. Specimen 3 Joint Shear Force vs. Shear Strain Comparison..... 183
Figure 6.34. Specimen 3 Lateral Load vs. Story Drift Comparison..... 183
Figure 6.35. Specimen 4 Joint Shear Force vs. Shear Strain Comparison..... 184
Figure 6.36. Specimen 4 Lateral Load vs. Story Drift Comparison..... 185
Figure 6.37. SL1 Joint Shear Force vs. Shear Strain Comparison 186
Figure 6.38. SL1 Lateral Load vs. Story Drift Comparison 187
Figure 6.39. SL2 Joint Shear Force vs. Shear Strain Comparison 188
Figure 6.40. SL2 Lateral Load vs. Story Drift Comparison 188
Figure 6.41. SL3 Joint Shear Force vs. Shear Strain Comparison 189
Figure 6.42. SL3 Lateral Load vs. Story Drift Comparison 190

Figure 6.43. SL4 Joint Shear Force vs. Shear Strain Comparison 191
Figure 6.44. SL4 Lateral Load vs. Story Drift Comparison..... 191
Figure 6.45. Analytical and Experimental Joint Reponse of Specimen 1-S 193
Figure 6.46. Comparison of Beam Moment-Rotation Response for Sp.1-S..... 194
Figure 6.47. Comparison of Lateral Load vs Story Drift for Sp.1-S..... 194
Figure 6.48. Analytical and Experimental Joint Reponse of Specimen 3-S 195
Figure 6.49. Comparison of Beam Moment Rotation Response for Sp. 3-S 196
Figure 6.50. Comparison of Lateral Load vs Story Drift for Sp. 3-S 196
Figure 7.1. Test Frame 201
Figure 7.2. Beam and Column Detailing 202
Figure 7.3. Interior and Exterior Beam-Column Joint Shear Reinforcement Detailing 202
Figure 7.4. Ground Acceleration Time Histories for Frame Test 204
Figure 7.5. Imposed Dead Load Magnitudes and Point of Application of Seismic Displacement Time Histories 205
Figure 7.6. D1 Displacement Time Histories Applied to the Frame 206
Figure 7.7. D2 Displacement Time Histories Applied to the Frame 206
Figure 7.8. D3 Displacement Time Histories Applied to the Frame 207
Figure 7.9. D4 Displacement Time Histories Applied to the Frame 207
Figure 7.10. 3D Model of the Test Frame..... 208
Figure 7.11. Sample Concrete Properties Definition (Floor 1) 209
Figure 7.12. Sample Cross Sectional Properties Definition (Floor 1) 210
Figure 7.13. Test Frame Beam Cracked Section Stiffness Determination 211
Figure 7.14. Moment-Rotation Relationship for Beams and Columns 212
Figure 7.15. Hinge Length Definition for Beams and Columns 213
Figure 7.16. Rigid End Zones 213
Figure 7.17. Panel Zone Assignment in the Model 215
Figure 7.18. Panel Zone Location in the Model 215
Figure 7.19. Sample Panel Zone Definition for Frame Model..... 216
Figure 7.20. Considered Moment Arm in Moment-Rotation Calculations 222

Figure 7.21. Joint Shear Force – Shear Strain Curves, Floor 1 Joints 223
Figure 7.22. Joint Shear Force – Shear Strain Curves, Floor 2 Joints 224
Figure 7.23. Joint Shear Force – Shear Strain Curves, Floor 3 Joints 225
Figure 7.24. Load Pattern Definitions for the Model 226
Figure 7.25. Superimposed Dead Loads on the Structure 227
Figure 7.26. Unit Displacement Assigned at Floor 3 228
Figure 7.27. Time History Function Application 229
Figure 7.28. Dead Load Case Definition 230
Figure 7.29. Sample Seismic Load Case Definition 231
Figure 7.30. Selected Interior and Exterior Joints for Verification 232
Figure 7.31. Interior Joint, D1 Response Comparison 233
Figure 7.32. Interior Joint, D2 Response Comparison 233
Figure 7.33. Interior Joint, D3 Response Comparison 234
Figure 7.34. Interior Joint, D4 Response Comparison 234
Figure 7.35. Exterior Joint, D1 Response Comparison 235
Figure 7.36. Exterior Joint, D2 Response Comparison 235
Figure 7.37. Exterior Joint, D3 Response Comparison 236
Figure 7.38. Exterior Joint, D4 Response Comparison 236
Figure 7.39. Beam Moment – Rotation Comparison, Exterior Beam Framing into Exterior Joint 238
Figure 7.40. Beam Moment – Rotation Comparison, Exterior Beam Framing into Interior Joint 238
Figure 7.41. Beam Moment – Rotation Comparison, Interior Beam Framing into Interior Joint 239
Figure 7.42. Story 1, D1 Lateral Load – Interstory Drift Response 240
Figure 7.43. Story 1, D2 Lateral Load – Interstory Drift Response 241
Figure 7.44. Story 1, D3 Lateral Load – Interstory Drift Response 241
Figure 7.45. Story 1, D4 Lateral Load – Interstory Drift Response 242
Figure 7.46. Story 2, D1 Lateral Load – Interstory Drift Response 242
Figure 7.47. Story 2, D2 Lateral Load – Interstory Drift Response 243

Figure 7.48. Story 2, D3 Lateral Load – Interstory Drift Response 243
Figure 7.49. Story 2, D4 Lateral Load – Interstory Drift Response 244
Figure 7.50. Story 3, D1 Lateral Load – Interstory Drift Response 244
Figure 7.51. Story 3, D2 Lateral Load – Interstory Drift Response 245
Figure 7.52. Story 3, D3 Lateral Load – Interstory Drift Response 245
Figure 7.53. Story 3, D4 Lateral Load – Interstory Drift Response 246
Figure 7.54. Roof Level, D1 Lateral Load – Interstory Drift Response 246
Figure 7.55. Roof Level, D2 Lateral Load – Roof Drift Response 247
Figure 7.56. Roof Level, D3 Lateral Load – Roof Drift Response 247
Figure 7.57. Roof Level, D4 Lateral Load – Roof Drift Response 248
Figure 7.58. Joint Model vs Rigid Joint Assumption, D1 249
Figure 7.59. Joint Model vs Rigid Joint Assumption, D2 250
Figure 7.60. Joint Model vs Rigid Joint Assumption, D3 250
Figure 7.61. Joint Model vs Rigid Joint Assumption, D4 251
Figure 7.62. Overall Beam Moment - Rot., Joint Model vs REZ Model, Beam Framing into Ext. Joint 252
Figure 7.63. Beam Moment - Rot., Joint Model vs REZ Model, Beam Ext Beam Framing into Int. Joint 252

LIST OF SYMBOLS

SYMBOLS

A_0 : shear reinforcement cross sectional area,

A_c, A_{ch} : area of column core measured from outside edge to outside edge of shear reinforcement;

A_g : gross area of the column section;

A_j : effective joint area

$A_{sh,req}$: minimum required joint shear reinforcement area;

A_{sh} : joint shear reinforcement area;

AxF : axial load factor;

AxI : axial load index;

b_1, b_2 : the distance between the centroidal axis of the beam to column edges;

b_b, b_w : width of the beam in the loading direction;

$b_{b,t}$, $b_{w,t}$: beam width in the transverse direction;

b_c'' : tied column core dimensions, calculated outside to outside edge of shear reinforcing bars, perpendicular to the shear reinforcement area A_{sh};

b_c : column width;

$b_{c,core}$: width of the column core

b_j : effective joint width;

C_b : compression force in the beam;

C_c : compression force in the column;

C_s : compression force in the slab;

d′′ : depth of the beam between top and bottom reinforcement;

d_b, $d_{b,core}$: beam depth and distance between top and bottom longitudinal beam reinforcement, respectively.

e : eccentricity between the centerlines of column and beam;

$f_c^{'}$: specified concrete compressive strength;

f_{cd} : design concrete compressive strength;

f_{ck} : characteristic concrete compressive strength;

f_{yh} : yield strength of transverse reinforcing bars;

h_b, $h_{b,l}$: beam depth in the direction of loading;

$h_{b,t}$: beam depth in the transverse direction;

h_c, h_{col} : column depth;

$h_{c,core}$: depth of the column core;

l_e : total length of the shear reinforcement in the loading direction,

N, P_f : column axial load;

n : number of specimens;

n_{gross} : number of shear reinforcement layers within the beam depth

k_f : strength factor for concrete;

k_n : effectiveness factor of confinement;

k_p : axial load ratio;

P_{cr} : joint shear force at the point of cracking;

P_{inel} : joint shear force at the point of inelasticity;

P_{max1} : joint shear force at the start of maximum force plateau;

P_{max2} : joint shear force at the end of maximum force plateau;

P_{final} : reduced joint shear strength, 90 % $P_{max1;}$

s, s_0, s_h : center-to-center spacing of shear reinforcement;

s_x : longitudinal spacing of shear reinforcement;

SF : slab factor;

SI : slab index;

SR : shear reinforcement factor;

SRI : shear reinforcement index;

T_b : tension in beam;

T_c : tension in column;

T_s : tension in slab;

t_f : slab thickness ;

V_b : shear in beam;

V_c : shear in column ;

v_j : joint shear stress;

$V_{j,exp}$: experimental joint shear strength;

$V_{j,pre}$: predicted joint shear strength;

V_n : nominal joint shear strength proposed by the evaluated code;

V_s : shear force in the slab;

x : smaller perpendicular distance from the face of the beam to the column side;

γ : joint shear strength factor;

γ_{cr} : joint shear strain at the point of cracking;

γ_{inel} : joint shear strain at the point of inelasticity;

γ_{max1} : joint shear strain at the start of maximum force plateau;

γ_{max2} : joint shear strain at the end of maximum force plateau;

γ_{final} : joint shear experienced at reduced joint shear force P_{final}

λ : modification factor used to account for the diminished mechanical qualities of lightweight concrete in comparison with normal weight concrete with equivalent compressive strength.

ρ_{core} : volumetric joint shear reinforcement ratio computed considering the core beam and column dimensions;

ρ_{gross} : volumetric joint shear reinforcement ratio computed considering the gross beam and column dimensions;

$\rho_{singlelayer,core}$: volumetric joint shear reinforcement ratio computed considering beam and column core dimensions, considering a single layer of shear reinforcement;

$\rho_{singlelayer,\,gross}$: volumetric joint shear reinforcement ratio computed considering the beam and column gross dimensions, considering a single layer of shear reinforcement.

CHAPTER 1

INTRODUCTION

1.1 Reinforced Concrete Beam-Column Connections

The structural integrity and performance of reinforced concrete moment-resisting frames (RCMRFs) under seismic excitation are critically dependent on the robustness of beam-column joints. These joints serve as crucial points within the frame, tasked with the essential function of maintaining structural coherence by effectively transferring shear forces both vertically and horizontally between beams and columns. This transfer is especially vital during seismic events, where the imposed loads can vary unpredictably in magnitude and direction.

To ensure that a structure can withstand such severe loading without significant degradation of stiffness or strength, the design of beam-column joints must be approached with meticulous attention to detail. They must be engineered to endure not only the anticipated service loads but also the extreme conditions posed by earthquakes. This entails a design that accommodates ductility, energy dissipation capacity, and means for load redistribution without compromising the structural integrity.

The connections are thus designed to act as the critical element for the moment-resisting frames, enabling them to exhibit desirable seismic behavior by dissipating energy, and by preventing the propagation of damage that could lead to catastrophic failure. The resilience of these joints under seismic deformations is essential, as it directly influences the ability of the structure to remain functional during and after earthquake loading, safeguarding both human life and property.

Contrary to the conventional rigid beam-column joint assumption, it has been confirmed that their inelastic behavior exerts a considerable influence on the structural response, particularly for buildings subjected to intense reversed cyclic loading. Despite a growing body of global research focusing on the behavior of beam-column connections, their design often does not receive adequate consideration. Neglecting the joint shear deformations leads to an inadequate prediction of the overall structural response, resulting in underestimation of story drifts and overestimation of beam rotations, consequently an unrealistic assessment of the structural performance. The significance of connection response in the lateral load resistance of reinforced concrete structures has been undeniably demonstrated through both experimental investigations and observations in the aftermath of earthquakes. The inadequate design of connections can lead to catastrophic outcomes, including loss of life and substantial property damage.

To date, the practical design of beam-column connections often adheres to simple guidelines. The central point governing the design is the 'strong column-weak beam' concept, which is applied without an in-depth comprehension of internal dynamics of the connections. The basis behind this concept is to localize damage within the plastic hinging zones of the beams while preventing column failure, even when subjected to substantial lateral forces. Essentially, this approach aims to prevent the premature yielding of column reinforcement relative to the beam reinforcement, thereby preventing the formation of plastic hinges at the base of the columns, which could lead to structural collapse. However, it is crucial to acknowledge that the successful implementation of the strong column-weak beam strategy requires that beam-column connections are capable of delivering reliable performance when faced with intense flexural and shear forces.

Despite their critical role in structural integrity, the dynamics and efficiency of beam-column connections remain one of the most overlooked aspects in the design of reinforced concrete moment-resisting frame structures. The primary factors contributing to this oversight include a scarcity of both experimental and analytical studies, along with the extensive diversity of connections in terms of their material

composition and geometric configurations. While research in this area is steadily increasing, a consensus has yet to emerge on the behavior of these connections during seismic events.

Although current structural codes provide some requirements for the design of beam-column connections, there is a notable variance in the methodologies prescribed by different codes. Additionally, there is a wide spectrum of connection configurations from wide beam-column joints to eccentric ones that require in depth investigation.

Analytical research studies investigate the various inelastic mechanisms related to the performance of beam-column joints when subjected to cyclic deformations. From a computational perspective, the aforementioned challenges in predicting connection response add layers of complexity to the analytical representation of their inelastic behavior. While numerous joint models have been proposed for the nonlinear analysis of reinforced concrete structures, the intricate interaction of factors influencing joint shear response, coupled with the extensive range of these parameters, has inhibited the development of a widely accepted analytical model that accurately captures the variations in beam-column connection behavior.

1.2 Research Objective and Scope

In the course of this study, the initial step involves conducting a detailed review of existing analytical and experimental research studies. Following this, a comprehensive database is compiled, including a broad spectrum of connection characteristics. Subsequently, a joint shear strength prediction equation and a nonlinear joint shear model are developed to represent the behavior of beam-column connections under reversed cyclic loading representing seismic loading. The final phase of the study involved validating the analytical model using the computational platform SAP2000. The proposed nonlinear analytical model is validated first in the light of the experimental results obtained from prior testing of beam-column connection subassemblies. In order to evaluate the effect of the nonlinear joint model

on the seismic behavior of frame structures, the results of a well detailed frame structure previously tested in the Middle East Technical University Structural Mechanics Laboratory is modeled and analyzed, then the analytical results are compared with the experimental ones.

Before compiling the database that would serve as the foundational tool for modeling, a thorough assessment of the prior studies is undertaken, reviewing both analytical and experimental studies related to the seismic behavior of beam-column connections. Evaluation of analytical studies contributed to a comprehensive understanding of the connection behavior and provided a fundamental point of reference for existing analytical models. In addition to indicating the influence of various geometric and material properties, experimental studies provided vital information for the database including reinforcement detailing, loading conditions, and observed overall structural and member responses. However, a significant challenge faced during the database assembly was the occasional incompleteness or lack of detailed data in the presented experimental data. The investigated methodologies and outcomes included the literature review, and the subsequent database construction are elaborated in Chapters 2 and 3, respectively.

An analytical model aimed at representing the nonlinear behavior of beam-column joints has been developed with two main considerations: the model should be applicable to a diverse array of specimens with varying attributes, and it should maintain a level of simplicity that makes it practical to use by professional engineers. The research study involved an extensive examination of a wide range of beam-column connections, differentiated by their geometric and material properties, in an effort to identify the most suitable analytical model that accurately characterizes the relationship between joint shear strength and strain. Among the numerous potential influencing factors, those with the most significant impact on connection performance were identified by correlation analyses and incorporated into the final model. Chapter 4 provides detailed information about the variables considered in determining the joint shear strength, as well as a comprehensive presentation of the development of a parametric joint shear strength prediction equation. Furthermore,

the development of the nonlinear joint model and the determination of indices, as well as Modification factors are presented in Chapter 4. First the determination of each Modification factor is presented considering the correlation of each parameter with the experimental joint shear strength. When the most influential parameters are determined, the effect of each parameter is evaluated statistically to reduce the mean absolute error (MAE) and the standard deviation (SD) for the performance points defined in the proposed model.

In Chapter 5, comparison of the proposed joint shear strength prediction equation with international structural seismic design codes used in practice is presented. The effect of each parameter is monitored individually to verify the efficiency of the defined factors on the prediction of the joint shear strength for the specimens included in the database. Furthermore, the evaluation and verification of the proposed equation, including the effect of all Modification factors ($V_{j,pre.}$) for conforming and nonconforming specimens based on the requirements of each structural code are presented.

The validation of the proposed joint model defining the nonlinear shear force vs shear strain behavior is presented in Chapter 6 of the dissertation. This involves the generation and analysis of computerized simulations of the experimental subassemblies, utilizing the SAP2000 structural analysis and design software. The developed joint model is integrated into the connection regions as panel zones defined in this software. The subassemblies are then subjected to loading based on the time history data from the related experimental investigations. The derived analytical outcomes are then compared with the experimental results to verify the accuracy of the model.

In Chapter 7, the verification is further advanced with the application of the proposed joint model to a well detailed reinforced concrete frame, which was tested in Middle East Technical University Structural Mechanics Laboratory in 2011. The proposed model is assigned to the interior and exterior connections of the frame model generated considering the geometrical and material properties of the frame, and

cyclic deformation time history data is applied to each floor compatible with the test setup, which was loaded by the implementation of story deformations imposed on the structure, representing 4 different earthquake levels. Further verification of the model by the aid of a frame analysis, presents the effect of the utilization of a nonlinear joint model to monitor the overall structural behavior and member responses, which improves the verification procedure completed by considering solely the subassemblies.

The thesis concludes with Chapter 8, which presents a comprehensive summary of the research, along with conclusions drawn from the analytical study and recommendations for further research.

CHAPTER 2

LITERATURE REVIEW

2.1 Background Information

Interest in the seismic performance of beam-column joints in reinforced concrete structures began to intensify in the 1960s. The pivotal experiments conducted by Hanson and Conner marked a pioneering step into the experimental evaluation of joint behavior under seismic loads, setting a benchmark for future research in this area. Their work is often referred to as the origin of systematic studies in this domain and is extensively cited by subsequent researchers.

In the wake of the significant research by Hanson and Connor, other prior works emerged as cornerstones in the field (Hanson & Conner, 1967). Park and Paulay made substantial contributions to the understanding of seismic design principles for reinforced concrete structures in New Zealand, emphasizing the importance of ductility and energy dissipation (Paulay et al., 1978). In Japan, the experimental studies by Ohmori et al. provided valuable insight into the influence of cyclic loading on the behavior of beam-column joints (Ohmori et al., 1989). Concurrently, in the United States, Bertero and Popov conducted influential research that improved understanding of seismic demands on joints, which played a pivotal role in shaping design codes.

The foundational research from these early studies catalyzed a series of experimental and analytical investigations, especially in regions with high seismic risks. The collective endeavors aimed to examine the complex failure mechanisms at beam-column connections during earthquakes, refine predictive models for joint

performance, improve material properties for better resilience, and lead to advanced computational methods for accurate seismic response simulation.

Experimental studies on beam-column joints predominantly examine their behavior under various loading conditions. The diversity in geometric configurations of the joints, coupled with a broad spectrum of material characteristics, introduces a considerable degree of variability in the behavior. This variability, influenced by the numerous combinations of joint features, presents a vast domain for experimental inquiry. Conversely, analytical research strives to encapsulate this behavior within mathematical frameworks. The primary challenge and goal of such studies lie in the development of a beam-column joint model that is both practically applicable and inclusive of the wide range of joint characteristics, while also delivering precise predictive outcomes.

Despite the increase in the number of experimental and analytical research studies on the behavior of beam-column joints, various aspects of their properties need further enhancement. The already mentioned variations in joint characteristics are signified when eccentric joints or wide beam-column connections are considered. These complexities extend the scope of the research and present challenges in achieving a universal agreement among scholars.

Subsequent sections of the literature review address various subtopics. Initially, the review outlines the definition, categorization, and shear capacity determination of beam-column joints, referencing the criteria for effective joint width and joint shear strength as stipulated by contemporary structural codes. Following this, key parameters influencing joint behavior are discussed, drawing on evidence from prior experimental and analytical studies.

The literature review concludes with a concise summary of prior work on the analytical modeling of beam-column joints.

2.2 Joint Shear Strength (V_j) Equations of Contemporary Structural Codes

While contemporary structural codes generally agree on the primary parameters influencing the shear capacity of beam-column joints, the methodologies for calculating shear strength differ among the codes. Furthermore, significant variations can be observed even within different editions of the same code. This section assesses the equations used for obtaining the shear strength of beam-column joints in four predominant North American Structural Codes. Additionally, the shear strength prediction procedure is investigated and presented in detail, considering the two versions of the Turkish Earthquake Code. Different versions of ACI 318 (2011, 2014, 2019) are also compared to trace the progression in shear capacity prediction methodology. The evaluated structural codes are ACI 352-10 (2010), ACI 318-11 (2011), ACI 318-14 (2014), ACI 318-19 (2019), ASCE 41-17 (2017), and CSA A23.03-19 (2019), TEC2007 (2007) and TEC2018 (2018). Despite a shared foundational approach, subtle discrepancies exist that influence the calculation of shear strength.

The forthcoming section provides detailed information on the common procedures and specific formulae used to estimate the shear strength of beam-column joints according to each code or guideline included in the thesis.

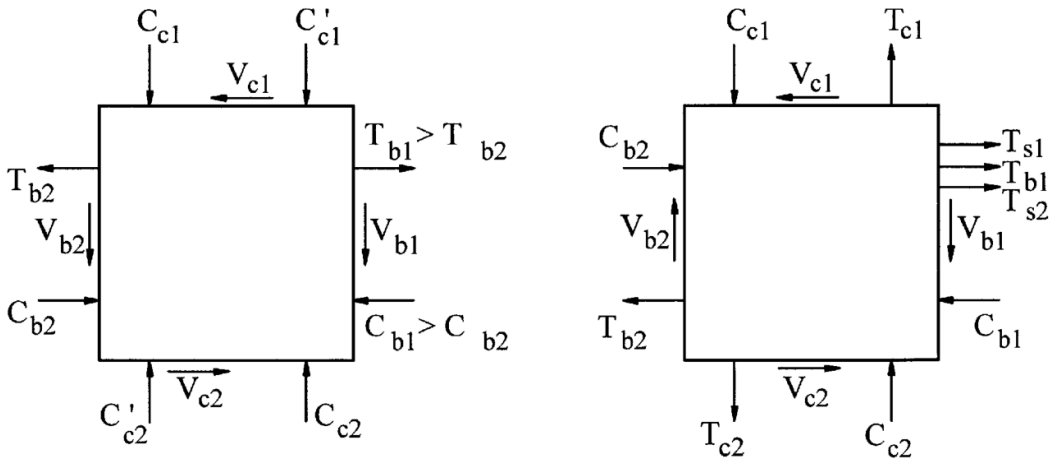
2.3 ACI 352-10 Recommendations for Design of Beam-Column Connections in Monolithic Reinforced Concrete Structures

The ACI 352-10 document, titled "Recommendations for Design of Beam-Column Connections in Monolithic Reinforced Concrete Structures," was published by the ACI-ASCE Committee 352 in 2002 and reapproved in 2010 (Joint ACI-ASCE Committee 352, 2010). This document, which supersedes the ACI 352R-91, is based on extensive laboratory tests and on-site studies, offering a comprehensive overview of the prevailing knowledge. The design specifications include dimensions,

reinforcement detailing, and construction of monolithic beam-column connections of cast-in-place reinforced concrete frame structures. The main requirements highlighted in the document encompass the sizing of structural members, the confinement of the column core within the joint, joint shear strength estimation, the comparative flexural strength of columns and beams framing into the joint, the anchorage of reinforcing bars, and the reinforcement detailing of adjoining columns and beams.

The ACI 352-10 guidelines categorize beam-column joints by expected loading conditions and the degree of confinement provided by adjacent structural elements. Joints are designated as Type 1 when they are not expected to undergo significant inelastic deformations, and as Type 2 when the adjoining frame members are engineered to maintain their strength under high intensity lateral loads.

The ACI 352-10 document also accounts for the forces exerted on the connection region stemming from a variety of loading cases, including externally applied loads, creep, shrinkage, temperature changes, settlement, and secondary effects. To explain these forces, the document presents them in two distinct free body diagrams that differentiate between gravity loading (for Type 1 joints) and lateral loading (for Type 2 joints), which are depicted in Figure 2.1.



(a) Due to gravity loads (b) Due to lateral loads

Figure 2.1. Forces Acting on Beam-Column Joints

where, T_b : Tension force in the beam.

C_b : Compression force in the beam.

V_b : Shear force in the beam.

T_c : Tension force in the column.

C_c : Compression force in the column.

V_c : Shear force in the column.

T_s : Tension force in the slab.

C_s : Compression force in the slab.

V_s : Shear force in the slab.

Regarding confinement, a beam is deemed to confine a joint if its width is at least three-quarters of the column width and its depth reaches at least three-quarters of the depth of the largest member framing into the joint. Joints with full confinement on all four sides are classified as Type A.1, those with confinement on at least two opposing sides are Type A.2, and all other configurations are Type A.3. The joint shear strength factors (γ) applicable to each type of joint are provided in Table 2.1.

Table 2.1 Joint Shear Strength Factors, ACI 352-10

Joint Type	A.1	A.2	A.3
1	24	20	15
2	20	15	12

Additionally, an effective joint area (A_j) is defined in relation to the dimensions of the beams and columns. The joint shear strength considered in design is derived by factoring in the effective joint area, the square root of the concrete compressive strength, representing the tensile strength, and the shear strength factor, determined

based on the level of confinement provided by the adjoining structural members, as presented above.

The definition of the effective joint area, which resists the applied shear force, accounts for the cross-sectional dimensions of the beams and columns, as well as the eccentricity of the beams that frame into the column in the direction of loading. The effective joint width (b_j) is determined by the lower value described by the criteria outlined in Eqn. 2.1. Subsequently, the joint shear strength, which utilizes the calculated effective joint area, is specified in Eqn. 2.2.

$$b_j = \min \begin{cases} (b_b + b_c)/2, \\ b_b + \sum \frac{m\, h_c}{2} \\ \qquad b_c \end{cases} \tag{2.1}$$

where, $m = 0.3$ for $e > b_c/8$

$m = 0.5$ for all other cases.

$$V_n = 0.083\, \gamma \sqrt{f'_c}\, b_j\, h_c \text{ (MPa)} \tag{2.2}$$

2.4 ACI 318 Recommendations for Design of Beam-Column Connections in Monolithic Reinforced Concrete Structures

The American Concrete Institute (ACI) 318 codes represent a pivotal body of knowledge and a cornerstone of civil engineering guidelines, essential for the design and construction of reinforced concrete structures(ACI Committee 318, 2011, 2014, 2019). The structural code has a set of comprehensive provisions that addresses numerous aspects of reinforced concrete buildings, which includes, but is not limited to, specifications for material properties, design requirements for various structural elements, detailing of reinforcement, and considerations for the effects of environmental factors on concrete durability.

The ACI codes are periodically updated to reflect the latest advancements in concrete technology, changes in practice, and updates based on new research findings. Each

revision is subjected to a rigorous review process by committees composed of experts in the field, ensuring that the codes remain at the forefront of industry standards.

Over time, the methodology employed by the ACI 318 for determining the strength of joints has undergone substantial modifications. With each new iteration of the code, the criteria for what is considered adequate confinement by neighboring members have been updated, reflecting a commitment to enhance the precision of these assessments. This section delves into the advancements made in predicting the shear strength of joints, highlighting the progressive revisions done in this subject.

ACI 318-11 (ACI Committee 318, 2011)

In divergence from the recommendations set forth in ACI 352-10, the ACI 318-11 defines only the shear strength coefficients pertinent to the seismic design of beam-column joints.

The classification of these joints accounts for the degree of confinement provided by adjoining structural members. A joint is considered to be adequately confined when at least three-fourths of the column face is covered by an adjoining beam. This criterion represents a significant deviation from ACI 352-10, where the impact of the beam depth on joint confinement is factored into the assessment, a consideration that ACI 318-11 does not incorporate.

Though the ACI 318-11 Code does not explicitly use the designation 'γ' to denote joint shear strength factors, the coefficients employed for shear strength evaluation across different joint configurations are systematically presented in Table 2.2.

Table 2.2 Joint Shear Strength Factors, ACI 318-11

Joint Type	γ
For joints confined by beams on all four faces	20
For joints confined by beams on three faces or on two opposite faces	15
For other cases	12

The definition of effective joint area according to ACI 318-11 is illustrated in Figure 2.2.

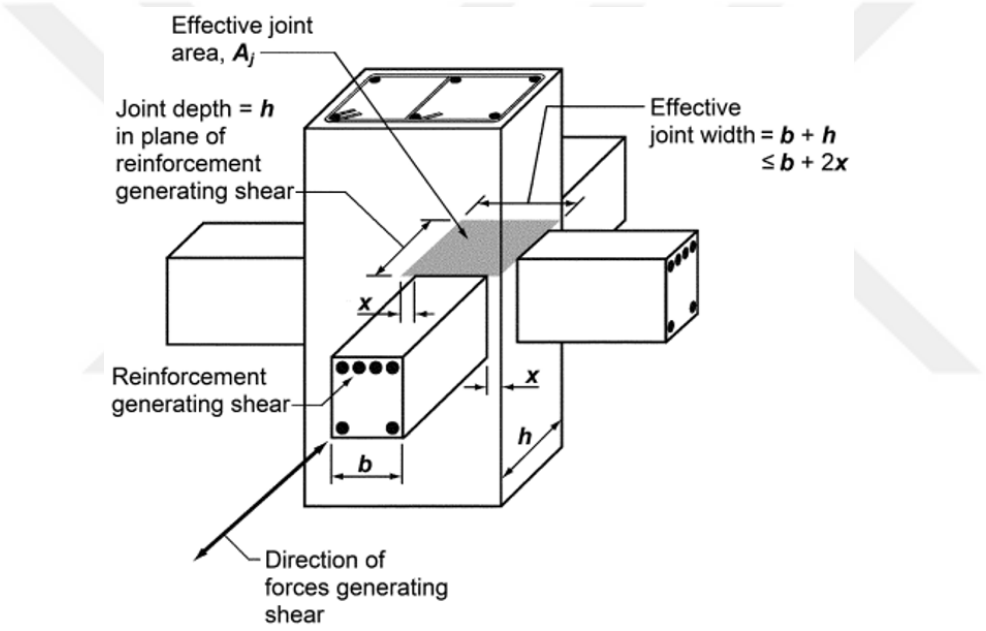


Figure 2.2. Effective Joint Area Definition, ACI 318-11

Effective joint width definition of ACI 318-11 is given in Eqn. 2.3.

$$b_j = \min \begin{cases} b_b + h_c, \\ b_b + 2x \\ b_c \end{cases} \tag{2.3}$$

where x is the smaller perpendicular distance from the face of the beam to the column side.

Consequently, the joint shear strength definition of ACI 318-11 is presented in Eqn. 2.4.

$$V_n = 0.0083\,\lambda\,\gamma\,\sqrt{f'_c}\;\; b_j\; h_c \text{ (MPa)} \qquad (2.4)$$

ACI 318-14 (ACI Committee 318, 2014)

ACI 318-14, titled "Building Code Requirements for Structural Concrete (ACI 318-14) and Commentary", was published in 2014. It replaced the earlier version, ACI 318-11, updating and refining the code with the intent to enhance clarity and incorporate the latest research findings on materials, and industry practices in concrete construction. ACI 318-14 was later superseded by ACI 318-19.

The solitary change introduced in the ACI 318-14 regarding shear strength calculations pertains to the updated criteria for confinement by beams connected to the joint. In this revision, effective confinement is achieved when a beam extends across a minimum of 3/4 of the joint effective width, a shift from the previous version, ACI 318-11, which considered the confinement in relation to the joint face.

ACI 318-19 (ACI Committee 318, 2019)

ACI 318-19 brings forth revised requirements concerning the confinement of joints by adjoining structural members. It emphasizes the significance of structural continuity of columns and beams along the direction of loading when determining the shear strength factor.

For a column to be recognized as continuous, it must project a minimum distance equal to one column depth, h_c, in the direction of joint shear. Furthermore, both longitudinal and transverse reinforcements from the bottom column must extend into the joint. Additionally, transverse beams adjoining a column are deemed to provide

confinement to the joint if they meet specific conditions outlined in subsequent clauses of the code.

a. The width of each transverse beam is at least three-quarters of the width of the column face which the beam frames into.

b. Transverse beams extend at least one beam depth, h_b, beyond the joint face.

c. Transverse beams contain at least two continuous top and bottom bars.

In compatibility with ACI 352-10 Recommendations, the ACI 318-19 Code also stipulates varying shear strength factors tailored to joints that are designed to withstand either gravity loads (γ_G) or earthquake loads (γ_{EQ}).

The prescribed factors for joints in continuous columns are listed in Table 2.3.

Table 2.3 Joint Shear Strength Factors, ACI 318-19

Beams in the loading direction	Beams in the transverse direction	γ_G	γ_{EQ}
Continuous or meets continuity requirements	Confining	24	20
Continuous or meets continuity requirements	Non-Confining	20	15
Other	Confining	20	15
Other	Non - Confining	15	12

2.5 ASCE 41-17 Seismic Evaluation and Retrofit of Existing Buildings

In ASCE 41-17 (ASCE/SEI 41, 2017), the classification of beam-column joints is determined exclusively by the number of structural members framing into the joint, without considering the proportional dimensions of beams and columns or the joint width itself. This code identifies five distinct types of joints, each categorized based on the presence of framing members, thereby omitting the width or depth ratios that are often factored into classifications in other codes.

The code categorizes beam-column joints based on the configuration and number of beams framing into the joint, resulting in five distinct classifications:

- Interior joint with transverse beams (IwT): This type of joint is characterized by the presence of four beams framing into the joint from all directions.
- Interior joint without transverse beams (I): This classification applies when two beams frame into the joint from opposite sides.
- Exterior joint with transverse beams (EwT): An exterior joint where three beams frame into the joint, two of which are oriented in the transverse direction.
- Exterior joint without transverse beams (E): This type of joint occurs when only one beam frames into the joint, and it is in the direction of loading.
- Knee joints (K): These joints are identified by a discontinuous column and are considered outside the scope of this particular study.

In ASCE 41-17, the classification of joint conformity is based solely on the spacing of the joint shear reinforcement, specifically the stirrups. If the spacing of the stirrups is less than or equal to half of the column depth ($h_c/2$), then the joint is considered Conforming (C). If the stirrup spacing exceeds this threshold, then the joint is classified as Non-Conforming (NC).

The joint shear strength factors based on the conformity clause and the type of the joint is presented in Table 2.4. As can be observed from this table, ASCE 41-17 is the only structural code that provides a joint shear strength equation applicable for deficient joints, the reinforcement detailing of which do not satisfy the minimum code requirements.

Table 2.4 Joint Shear Strength Factors, ASCE 41-17

Joint Shear. Reinf. Clause	IwT	I	EwT	E
C	20	15	15	12
NC	12	10	8	6

The definition of the effective joint width in ASCE 41-17 is specified in Eqn. 2.5 which also serves as the basis for calculating the shear strength of the joint.

$$b_j = min\begin{cases} b_b + h_c \\ b_b + 2x \\ b_c \end{cases} \quad (2.5)$$

The shear strength of a beam-column joint is computed by Eqn. 2.6.

$$V_n = 0.083\,\lambda\,\gamma\,\sqrt{f'_c}\;b_j\,h_c\ (\text{MPa}) \quad (2.6)$$

The parameter λ is a modifier that accounts for the type of concrete used in the joint construction. It is set to 0.75 when lightweight concrete is employed, reflecting the lower density of the material and strength characteristics compared to normal weight concrete. For joints made with normal weight concrete, which is more common and has typical density and strength properties, λ is assigned a value of 1.0.

2.6 CSA A23-19 Design of Concrete Structures

Within the Canadian Structural Code, CSA A23.3-19, titled "Design of Concrete Structures," the criterion for joint confinement by adjacent beams is quantified by the proportion of the beam width relative to the joint face width (Canadian Standards Association, 2019). Confinement is achieved when the width of the beam is at least three-fourths of the width of the joint face.

A joint is categorized as 'confined' when all four beams connecting to the joint meet this width requirement. In scenarios where only three or two opposite faces are framed by beams that fulfill the width condition, the joint is labeled as 'semi-confined'. Joints that do not meet these conditions are designated as 'unconfined'.

The effective joint area, denoted as A_j, is determined by taking the minimum of the gross cross-sectional area of the column, A_g, and the product of twice the beam width (b_w) and the column depth (h_{col}) as shown in Eqn. 2.7.

$$A_j = \min (A_g, 2b_w h_{col}) \quad (2.7)$$

The joint shear strength is calculated by Eqn. 2.8.

$$V_n = \gamma \lambda \varphi \sqrt{f'_c} A_j \text{ (MPa)} \quad (2.8)$$

The factor γ, which is used in the calculation of joint shear strength, varies depending on the confinement level of the joint. It is set to 1.3 for unconfined joints, 1.6 for semi-confined joints, and 2.2 for confined joints.

When these values are transformed into U.S. customary units, they correspond to 15.6, 19.2, and 26.4 respectively. It must be noted that, these coefficients are somewhat higher compared to those proposed by the structural codes in the United States for equivalent shear strength factors.

The coefficient λ represents the concrete density modifier. It is taken as 1.0 for normal density concrete, while a reduced value of 0.75 is utilized for low density concrete. In the context of facilities holding CSA certification, the concrete material factor, denoted as φ, is established at 0.70, for non-CSA certified entities, this factor is conservatively reduced to 0.65.

2.7 TEC2007 – Turkish Earthquake Code

The Turkish Earthquake Code, TEC2007, is a regulatory publication which outlines the essential design guidelines and requirements for buildings constructed in regions prone to seismic activity (Turkish Ministry of Public Works and Settlement, 2007).

The classification of beam-column joints accounts for the arrangement of beams framing into the joint and the ratio of beam width to column width, in a procedure that aligns with the guidelines set forth in ACI 318-19, ACI 352-10 and also CSA A23-19.

A connection is deemed 'confined' if beams are present on all sides and each beam width is at least three-quarters of the column width. Connections that do not meet these criteria are defined as 'unconfined'.

In relation with the definitions presented in Figure 2.3 for effective joint area, the effective joint width, b_j, is computed as,

$$\text{Effective joint width, } b_j = \min\{2\min(b_1, b_2), b_{w1}+h\} \quad (2.9)$$

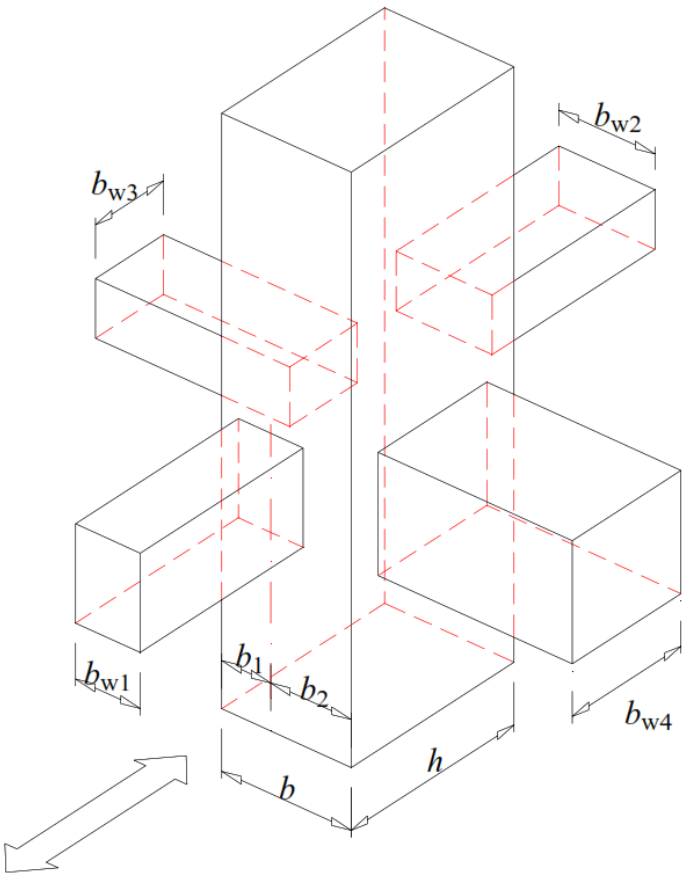


Figure 2.3. Effective Joint Area Definition, TEC2007

The joint shear strength is then calculated for confined and unconfined beam-column joints as presented in Eqn. 2.10.

$$\begin{aligned} &\text{For confined joints:} && V_n = 0.60\, b_j\, h\, f_{cd} \\ &\text{For unconfined joints:} && V_n = 0.45\, b_j\, h\, f_{cd} \end{aligned} \tag{2.10}$$

It must be underlined that, the only structural code defining the joint shear strength based on concrete compressive strength (f_{cd}), instead of $\sqrt{f_{cd}}$ is TEC2007. The equation is revised in the succeeding versions of the code, as explained in Section 2.8.

2.8 TEC2018 – Turkish Earthquake Code

The regulations set forth in TEC2007, the Turkish Earthquake Code, were superseded by an updated version, TEC2018 (Turkish Disaster and Emergency Management Presidency, 2018). This newer version included revisions to reflect the latest seismic research, changes in design philosophy, updates to material standards, and improvements in construction practices based on recent earthquake experiences and technological advancements.

From the perspective of the beam-column joints, the only revision is in terms of the joint shear strength prediction equations. The revised equations for confined and unconfined beam-column joints are presented in Eqn. 2.11.

$$\begin{aligned} &\text{For confined joints:} && V_n = 1.7\, b_j\, h\, \sqrt{f_{ck}} \\ &\text{For unconfined joints:} && V_n = 1.0\, b_j\, h \sqrt{f_{ck}} \end{aligned} \tag{2.11}$$

As mentioned in Section 2.7, the equation is revised basically in terms of the implication of concrete strength, namely the use of characteristic strength rather than design. The effect of this significant modification will be evaluated in Section 5.

2.9 Conformity Requirements of Structural Codes

The reliability of structural code provisions in determination of the shear strength of reinforced concrete members is critically influenced by the parameters governing the minimum area of shear reinforcement and the limits set for the spacing of shear reinforcement. During empirical investigations aimed at evaluating the accuracy of shear strength estimations provided by various structural codes, test specimens are systematically categorized. They are designated as "Conforming (C)" if they meet the code requirements for reinforcement detailing, or as "Non-Conforming (NC)" if they fall outside these limits.

It is noteworthy that among the considered structural codes, ASCE 41-17 distinguishes itself as the sole code with provisions that enable the prediction of shear capacities for specimens that do not conform to provided reinforcement detailing requirements. This capability is significant as it allows for a broader application of the code, encompassing a wider variety of scenarios that may not strictly adhere to conventional detailing practices.

To facilitate a comprehensive comparison and to provide a clear reference point for these critical parameters, a detailed summary is provided in Table 2.5. This table presents the maximum allowable shear reinforcement spacing and the minimum required shear reinforcement area as required by each evaluated structural code.

Table 2.5 Code Conformity Requirements

Structural Code	Maximum Shear Reinforcement Spacing ($s_{h,max}$)	Minimum Shear Reinforcement Area ($A_{sh,min}$)
ACI 352.10	$1/4\{\min(h_c, b_c)\}$ $6\,\Phi_{column\ bar}$ 150 mm	$0.3\,\frac{s_h\, b_c'' f_c'}{f_{yh}}\left(\frac{A_g}{A_c}-1\right)$ $0.09\,\frac{s_h\, b_c'' f_c'}{f_{yh}}$ $(f_{yh} \leq 420.0\ MPa)$

Table 2.5 Code Conformity Requirements (cont'd)

Structural Code	Maximum Shear Reinforcement Spacing ($s_{h,max}$)	Minimum Shear Reinforcement Area ($A_{sh,min}$)
ACI 318-11	$1/4\{\min(h_c, b_c)\}$ $6\,\Phi_{column\ bar}$ S_0	$0.3\,\frac{s_h\,b_c''\,f_c'}{f_{yh}}\left(\frac{A_g}{A_c}-1\right)$ $0.09\,\frac{s_h\,b_c''\,f_c'}{f_{yh}}$ $(f_{yh} \le 700.0\,MPa)$
ACI 318-14, ACI 318-19	$1/4\{\min(h_c, b_c)\}$ $6\,\Phi_{columnbar}$ S_0	$0.3\,\frac{s_h\,b_c''\,f_c'}{f_{yh}}\left(\frac{A_g}{A_c}-1\right)$ $0.09\,\frac{s_h\,b_c''\,f_c'}{f_{yh}}$ $0.2\ k_f\,k_n\frac{P_u}{f_{yh}\,A_{ch}}$ $(f_{yh} \le 700.0\,MPa)$
ASCE 41-17	$h_c/2$	-
CSA A23-19	$1/4\{\min(h_c, b_c)\}$ $6\,\Phi_{columnbar}$ S_x	$0.2\,k_n\,k_p\frac{A_g}{A_{ch}}\frac{f_c'}{f_{yh}}sh_c$ $0.09\,\frac{f_c'}{f_{yh}}sh_c$
TEC 2007, TEC 2018	100 mm (unconf. joints) 150 mm (conf. joints)	$0.3\,s\,b_k[\left(\frac{A_c}{A_{ck}}\right)-1]\frac{f_{ck}}{f_{ywk}}$ $0.075\,s\,b_k\,\frac{f_{ck}}{f_{ywk}}$ $0.6\,A_{sh,col,conf}$ (unconf. joints) $0.4\,A_{sh,col,conf}$ (conf. joints)

2.10 Parameters Affecting the Shear Strength of Beam-Column Joints

The behavior of beam-column joints when subjected to cyclic loading is influenced by several factors. As previously highlighted, the geometric and material characteristics of these joints, along with the specific conditions under which they are loaded, play a substantial role in determining their response. In the subsequent sections of this thesis, the impact of critical parameters will be discussed in detail, drawing upon findings from prior experimental and analytical research studies.

2.11 Joint Shear Reinforcement

The use of transverse shear reinforcement in the connection area has been demonstrated to significantly enhance the earthquake resilience of reinforced concrete structures. Research and field observations have also consistently shown that adequate shear reinforcement is vital for ensuring the seismic resilience of beam-column joints in reinforced concrete structures. Confining the joint core with transverse reinforcement aids in the effective transfer of both axial and shear forces between beams and columns, thereby improving the structural integrity and performance during seismic events.

Alameddine and Ehsani highlighted the role of transverse reinforcement in enhancing the resistance against excess shear forces applied to a joint after concrete cracking, reducing crack width before the yielding of transverse reinforcement, and delaying joint deterioration by confining the concrete (Alameddine & Ehsani, 1991). Through experimental research involving 12 specimens with joint shear reinforcement ratios ranging from 1.14% to 1.87%, it was concluded that transverse reinforcement not only increases the energy dissipation capacity but also postpones the pullout of main beam bars and the slippage of longitudinal column bars within the joint. This underscores the significant impact of transverse reinforcement on improving the structural integrity and durability of reinforced concrete beam-column joints, especially under conditions that simulate seismic activity.

Kim and Park studied the response of beam-column joints subjected to cyclic loading, testing 2 exterior and 3 interior beam-column joints with varying joint shear reinforcement ratios (C. G. Kim & Park, 2015). The joint shear reinforcement ratios varied between 0.58% and 0.93% whereas one exterior and one interior joint had no shear reinforcement in the joint. The test results revealed the enhancement in both the shear strength and deformation capacity of the joints, particularly noticeable in the exterior beam-column connections, as a result of increasing the joint shear reinforcement. This finding underscores the effectiveness of increased shear reinforcement in improving the structural resilience and performance of beam-column joints under reversed cyclic loading.

Moreover, in the parametric study conducted by Bonacci and Pantazoupoulou, aimed at exploring the impact of various design parameters on the behavior of beam-column connections, it was observed that shear reinforcement within the joint plays a crucial role in confining the concrete (Bonacci & Pantazoupoulou, 1993). This confinement leads to an increase in compressive resistance, which in turn helps to maintain the connection integrity. Furthermore, the research concluded that the contribution of joint hoops to the joint shear resistance mechanism is significant, especially in scenarios where the provided confinement by the adjoining members is minimal. This highlights the importance of incorporating adequate horizontal reinforcement in the design of beam-column connections to ensure their durability and effectiveness in resisting shear forces.

The experimental research by Ehsani and Wight emphasizes the effectiveness of shear reinforcement within the joint in improving the performance of specimens that lack transverse beams and slabs (Ehsani & Wight, 1985). It was observed that the use of transverse reinforcement also contributes to delaying the slippage of beam bars within the joint. This finding underscores the critical role that transverse reinforcement plays not only in enhancing structural integrity but also in prolonging the service life of connections by mitigating premature failures associated with bar slippage.

2.12 Slab Participation

Experimental investigations into beam-column joints that include reinforced concrete slabs have demonstrated that a properly designed slab can significantly enhance the shear capacity of a joint. However, it is particularly noteworthy that underestimating the effect of the slab, especially when evaluating the flexural strength ratio of a connection, might lead to an underestimation of the flexural capacity of the beam. This underestimation could result in beams being disproportionately stronger than columns, potentially causing a brittle failure of the structure, leading to column failure prior to beams. Therefore, accurately assessing the effect of slabs is of crucial importance for achieving a more realistic comprehension of both the connection and the overall structural behavior under lateral loads. This understanding is important for the design and analysis of structures to ensure their safety and integrity during seismic loading.

In their research study Burak and Wight highlighted the confinement effect provided by the slab for 3 eccentric and 3 concentric beam-column joints (Burak & Wight, 2008). It was revealed that the inclusion of floor slabs and spandrel beams in the test setup significantly diminished the influence of eccentricity, delaying the degradation of both shear strength and stiffness. Consequently, the specimens maintained their energy dissipation capacities and the extent of damage was notably reduced. This underscores the critical role that structural elements like slabs and spandrel beams play in enhancing the overall performance and durability of beam-column connections under lateral loading, particularly for eccentric joints.

Durrani and Zerbe tested 6 two span frames and 5 subassemblies where a total of 7 specimens had slabs (Durrani & Zerbe, 1987). After the evaluation of the test results, it was emphasized that the slab had significant impact on the strength, stiffness, and shear capacity of joints in their research. It was also noted that the participation of the slab can enhance the lateral load resistance of a joint by up to 40%. This highlights a critical insight since neglecting the contribution of slabs to the stiffness and strength of beams may lead to a substantial underestimation of the lateral load

resistance of the joint. This underestimation could affect the design and performance evaluation of structures, underscoring the importance of accounting for slab effects in structural analysis and design to ensure accurate assessments of structural behavior under lateral loads.

French and Boroojerdi observed that all tested subassemblies including slab demonstrated ductile behavior, with interstory drifts exceeding 8% (French & Boroojerdi, 1989). They noted an increase in flexural strengths of the beams ranging from 22% to 49% at 2% story drifts. Similarly, Cheung, Paulay, and Park also thesised enhancements in the negative moment flexural capacity and lateral loading capacity of the tested beam-column-slab subassemblies (Cheung et al., 1991). These findings underscore the significant role that proper design and integration of slabs play in improving the structural resilience and performance of beam-column connections under seismic loading.

2.13 Presence of Transverse Beams

The presence of transverse beams in beam-column connections plays a critical role in enhancing joint shear performance under cyclic loading. Research studies indicate that transverse beams contribute significantly to the overall stiffness and strength of the joint, leading to improved resistance against seismic forces. This enhancement in shear performance is attributed to the effective distribution of stresses and the additional confinement provided by transverse beams, which helps in mitigating the propagation of cracks and delaying the onset of significant damage. Consequently, structures equipped with such design features exhibit increased ductility, energy dissipation capacity, and resilience against cyclic loading, underscoring the importance of incorporating transverse beams in seismic-resistant design of reinforced concrete structures.

The effect of transverse beams on the performance of beam-column connections can be evaluated based on two key aspects: their role in resisting joint shear and their

contribution to providing confinement for the joint core. Transverse beams enhance the joint shear resistance by redistributing shear forces more effectively across the connection, thereby reducing the likelihood of shear failure. Additionally, they contribute to the confinement of the joint core, which is crucial for maintaining the integrity of the connection under seismic loads. This confinement helps to prevent premature crushing of the concrete in the joint core, improving the ductility and overall seismic performance of the connection. Together, these functions of transverse beams play a significant role in enhancing the structural resilience and safety of beam-column connections in reinforced concrete structures subjected to cyclic loading.

The investigation conducted by Durrani and Zerbe, encompassing an assessment of six specimens, underlines the significant contribution of transverse beams (Durrani & Zerbe, 1987). It was underlined that transverse beams served for two purposes, improving the shear resistance by furnishing additional area for shear force distribution and enhancing the confinement of the joint core, thereby enhancing the structural integrity and seismic resilience of the joint. Additionally, Ehsani and Wight highlighted that transverse beams significantly improve joint confinement and prevent beam bar pull-out, enhancing the structural integrity of beam-column connections (Ehsani & Wight, 1985).

In the research study conducted by Burak and Wight, a critical observation was made regarding the confining effects of transverse beams (Burak & Wight, 2008). The testing of the third specimen, oriented in the spandrel direction, indicated a degradation in both strength and stiffness. This deterioration was linked to the configuration of a wide and shallow normal beam in the transverse direction, which had a depth less than three-quarters that of the spandrel beam depth, failed to provide adequate confinement. As a result, an escalated level of the beam-column joint damage was recorded, highlighting the significance of ensuring sufficient transverse beam depth for optimal confinement.

2.14 Presence of Axial Load on Column

The axial load applied to columns has a significant impact on the shear strength of beam-column joints. An increase in axial load on the column typically enhances the joint shear strength, as the compressive forces contribute to the overall stiffness and resistance of the joint against shear deformations.

The impact of axial loading on columns within the evaluation of beam-column joint performance has been extensively debated among researchers, yielding varied conclusions. Kaku and Asakusa underlined that axial load on columns contributed to reduced pinching, enhanced stiffness, and improved anchorage for both hooked and straight beam bars within the joint (Kaku & Asakusa, 1991). Fujii and Morita have documented that an increase in axial load from $f_c'/12$ to $f_c'/4$ can increase the shear strength of exterior joints by approximately 11% (Fujii & Morita, 1991). On the other hand, Fu et al. stated that the impact of increasing axial load ratios on the energy dissipation capacity of beam-column joints varied significantly depending on the initial shear level of the joint (Fu et al., 2000). For joints subjected to low shear forces, an increase in axial load ratio is beneficial, enhancing their energy dissipation capacity. However, for joints experiencing moderate shear forces, the increase in axial load ratio did not exhibit a notable effect. In contrast, for joints under high shear forces, an increased axial load ratio was observed to be detrimental, leading to premature shear failure characterized by the crushing of joint core concrete.

2.15 Eccentricity

Eccentric connections are characterized by the alignment of the centroidal axis of the column with that of the beam, a configuration illustrated in Figure 2.4. Such alignments are frequently observed in the spandrel beams of buildings for architectural and aesthetic purposes, aiming to prevent any extension on the building facade by ensuring the centroidal axes of these beams do not coincide with those of the columns. While this approach enhances visual appeal of the structure, it

introduces specific structural considerations that necessitate careful planning and execution to preserve the structural integrity and functionality of the structure.

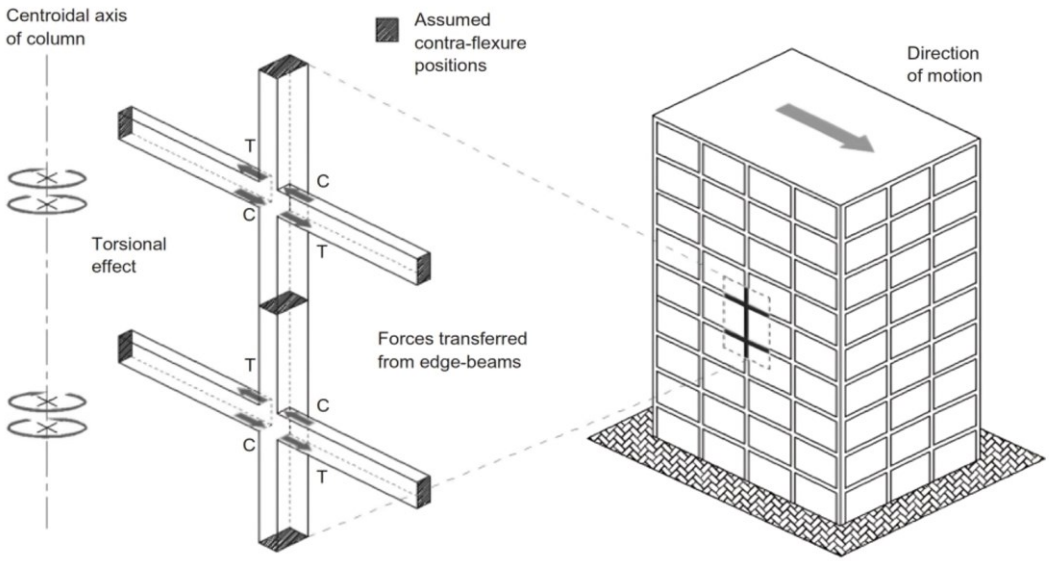


Figure 2.4. Eccentric Beam-Column Joints (Raffaelle & Wight, 1995)

Eccentric connections, often found in buildings, can complicate the structural behavior of beam-column joints under lateral loads. When the load path does not align with centerlines of the adjoining members, this may lead to extra forces and moments. Specifically, when lateral loads act along the spandrel beam axis, they can cause torsion in the beam-column connection region. Because of the twisting action effective on the joint, additional shear stresses that were not accounted for in simpler, concentric connection designs are produced. This situation can result in the reduction of the joint shear strength.

In Figure 2.5. the lateral load, the resulting eccentricity (the offset between the load path and the member centerlines), and the induced torsional moment is schematically presented.

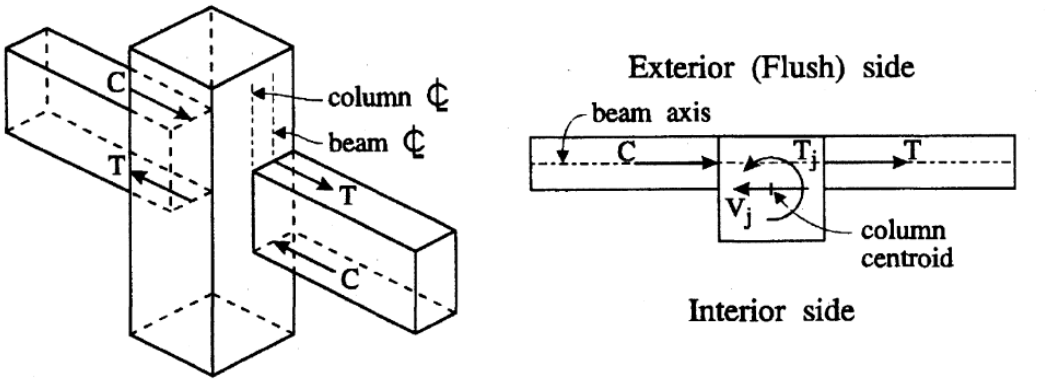


Figure 2.5. Forces Acting on Eccentric Joints (Raffaelle & Wight, 1995)

For the evaluation of the shear strengths of eccentric beam-column joints, contemporary structural codes basically address a penalty factor in the determination of the effective joint width.

2.16 Analytical Modeling of Beam-Column Joints

Analytical modeling of beam-column joints is a crucial aspect of structural engineering, aimed at understanding and predicting the behavior of connections under various loading conditions. This process involves the use of mathematical models and nonlinear analysis to simulate the structural response, focusing on factors such as load distribution, stress concentration, deformation, and failure modes. By accurately modeling these joints, engineers can optimize the design for both safety and efficiency, ensuring the integrity and durability of structures.

The performance of a connection involves various inelastic response mechanisms. The lack of understanding about certain parameters that may influence the behavior of joints, combined with limited experimental data on the individual effects of these parameters, make it challenging to develop a comprehensive model for beam-column joints. Despite the growing number of experimental and analytical studies, beam-column joints are often modeled as either rigid or semi rigid for simplicity, leading to inaccurate predictions of the structural response, such as underestimation of story

drifts and overestimation of structural rigidity and beam end rotations. The goal of research related to the analytical modeling of beam-column connections is to create a model that accurately represents the complex behavior of connections in a simple, comprehensive, and practical way.

The fundamental components utilized to characterize beam-column joint behavior in structural modeling include plastic hinges, rotational springs, and combined models. Each element has its own strengths and weaknesses in terms of simplicity and accuracy. Rigid end zones are frequently employed to accommodate the finite size of the connections. Subsequent paragraphs will explore various beam-column connection models developed to date.

As one of the earliest models, the research by Anderson and Townsend in 1977 highlighted the importance of considering the effect of degrading concrete and connection stiffness in analytical modeling of beam-column connections (Anderson & Townsend, 1977). This aspect was found to significantly influence the response of reinforced concrete structures, particularly in terms of seismic behavior. By incorporating these factors into the models, a more accurate representation of the structural response can be achieved, leading to improved assessment of seismic performance of structural members.

El Metwally and Chen conducted a study on the moment-rotation modeling of reinforced concrete beam-column connections (El-Metwally et al., 1990). A joint model that consisted of a concentrated rotational spring, the stiffness of which was determined by the linear elastic stiffness of the connection, ultimate moment capacity, and an internal variable 'a' representing the dissipated energy during cyclic loading, was proposed . This model aimed to capture the behavior of beam-column joints accurately, especially in terms of seismic response and inelastic performance by incorporating these key factors into the analysis.

Other beam-column joint models incorporated various elements like rotational springs, plastic hinges, rigid end zones, and plane stress elements. With the increasing amount of experimental and analytical research, a more comprehensive

understanding of the behavior of beam-column joint behavior has been achieved. This enhanced understanding is evident in the detailed modeling of connections, aiming to accurately capture the complex behavior during seismic events.

The model proposed by Alath and Kunnath known as the 'scissors model,' incorporates a rotational spring positioned between the beam and column centerlines (Alath & Kunnath, 1995).The connection finite size, including parts of beams and columns within the connection region, is represented by rigid zones located at the ends of the beams and columns. The moment-rotation behavior of the connection is depicted using hysteretic material assigned to the rotational spring. An illustration of the basic concept of the scissors model is provided in Figure 2.6.

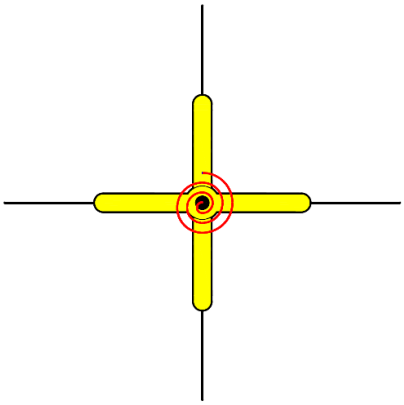


Figure 2.6. Scissors Joint Model (Alath and Kunnath, 1995)

Then, the model developed by Elmorsi et al. utilized plane stress elements, including a 12-node joint element and 10-node transition elements (Elmorsi et al., 2000). This complex model incorporated concrete and steel reinforcement models to capture material nonlinearity. By integrating these components with the kinematic model, the analytical model was completed to characterize shear deformations in the joint panel and flexural/shear deformations in the plastic hinging zones. A schematic representation of this model is presented in Figure 2.7.

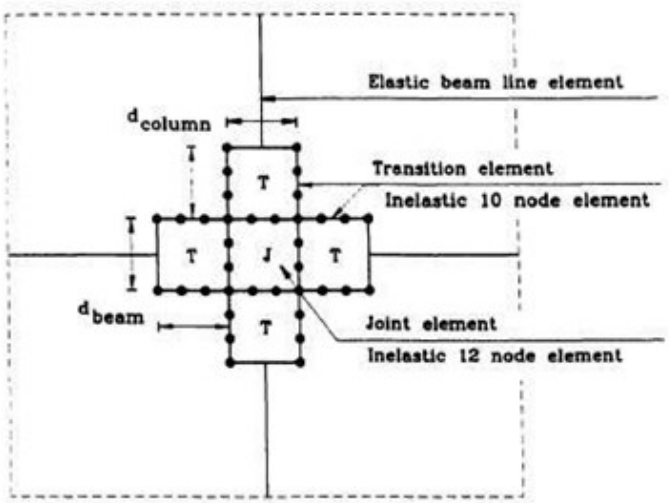


Figure 2.7. Plane Stress Element Model (Elmorsi et al., 2000)

The joint model proposed by Shin and LaFave consisted of seven rotational springs and a joint element (Shin & LaFave, 2004). The joint element is composed of rigid links, constrained by three rotational springs at the corners. Beams and columns were represented as elasto-plastic elements connected to the joint region through two springs, capturing bond slip and moment rotation characteristics. This joint model was implemented in Drain-2DX nonlinear structural analysis program, as presented in Figure 2.8.

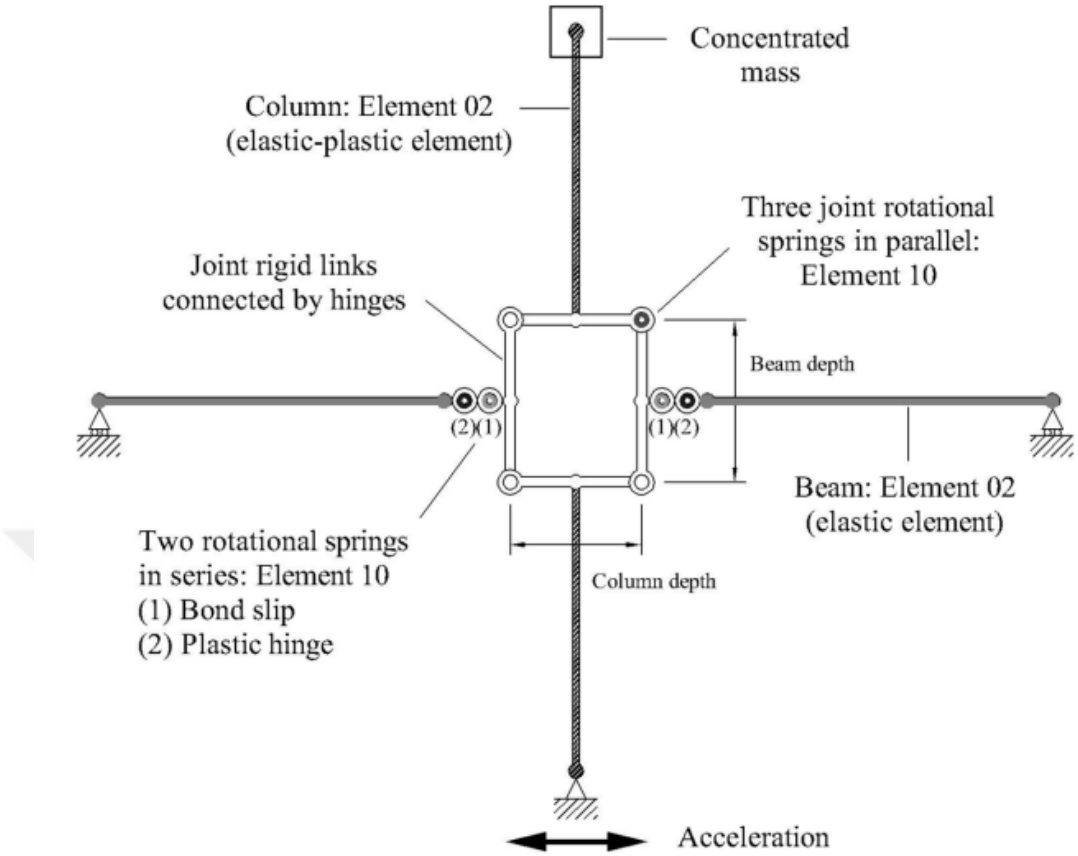


Figure 2.8. Model of Shin and LaFave (2004)

The study by Kim et al. focused on statistically analyzing the impact of various parameters on the shear strength of beam-column connections (J. Kim et al., 2007). Initially, the basic parametric model included eight variables, with less significant ones being excluded in subsequent stages. The fundamental joint shear strength prediction model proposed by the researchers is provided in Eqn. 2.12.

$$v_j = 1.04\left(\frac{s_{pro}}{s_{req}}\right)^{-0.00513}\left(\frac{b_b}{b_c}\right)^{0.0151}\left(\frac{A_{sh,pro}}{A_{sh,req}}\right)^{0.0241}\left(\frac{h_b}{h_c}\right)^{-0.301} \text{x } (JI)^{0.0886}(BI)^{0.236}(JP)^{1.28}(f'_c)^{0.765} \quad (2.12)$$

where, v_j = joint shear strength in MPa.

JP = 1.0 for interior connections, 0.75 for exterior connections, 0.50 for knee connections,

JI = joint transverse reinforcement index $[(\rho f_y)_{jointreinf}/f_c']$,

BI = beam reinforcement index $[(\rho f_y)_{beamreinf}/f_c']$,

S_{pro} = proposed spacing of joint transverse reinforcement,

S_{req} = required spacing of joint transverse reinforcement based on ACI 352-02 provisions.

The model developed by Burak focuses on capturing the inelastic response mechanisms of the beams and columns within the subassembly (Burak, 2010). This model represents beams and columns as elastic segments with rigid end zones intersecting at the connection point, the inelastic deformations of which were concentrated at member ends by the utilization of plastic hinges. To define the nonlinear response of plastic hinges, rotational springs were incorporated at the column and beam interfaces. Moreover, the joint model consisted of rigid links connected with hinges at the corners, with one corner featuring a nonlinear rotational spring. The moment-rotation relationship of beams, moment transfer through the connection versus shear strain of the joint, and axial load-moment relationship of columns were obtained by nonlinear analysis using Perform 3D. A visual representation of this joint model is illustrated in Figure 2.9

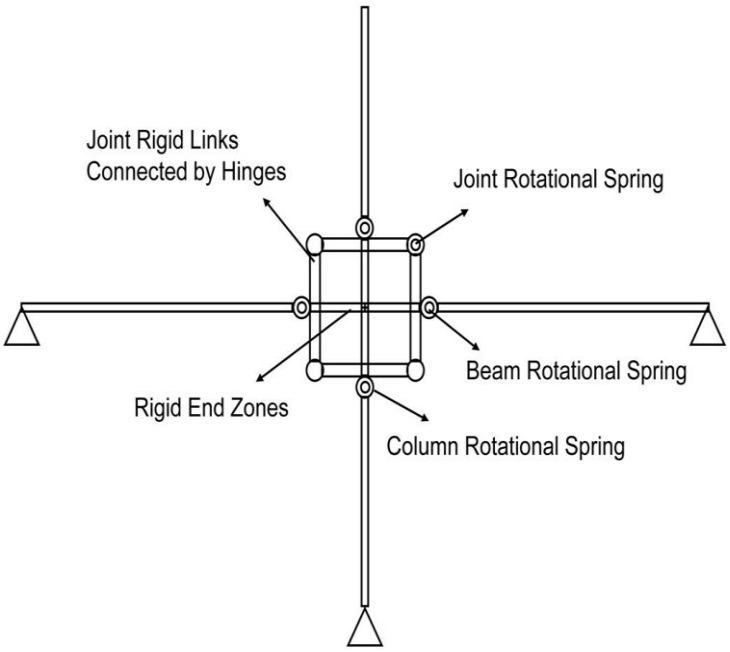


Figure 2.9: Connection Model Proposed by Burak (2010)

Unal and Burak developed a non-linear joint model, evaluating "JT" for confinement effect, "G" for elastic shear modulus, ρ_{joint} for joint transverse reinforcement ratio, "EE" for eccentricity effect, "CI" for column index, "NE" for axial load effect, "WB" for reduction in strength due to the presence of wide beams, and "SI" for slab index. The shear strength of the joint is predicted as presented in Eqn. 2.13. Then, a nonlinear beam-column joint model was constructed and verified using Perform 3D software, utilizing panel zones to define the joint characteristics. The proposed model is presented schematically in Figure 2.10

$$v_{j,u}\ (\text{MPa}) = \text{JT}\left(f_c\ f_y\right)^{1/6}\ \rho_{joint}\ \text{EE CI NE WB SI} \qquad (2.13)$$

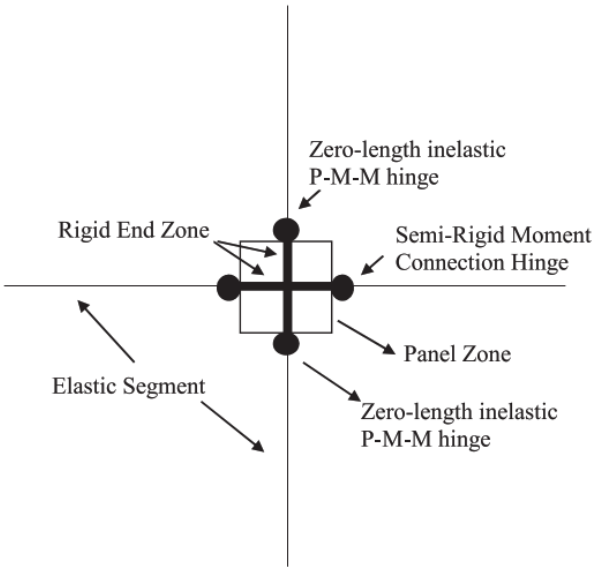


Figure 2.10. Joint Model Proposed (Unal & Burak, 2013a)

CHAPTER 3

CONSTRUCTION OF DATABASE

3.1 Overview

The initial phase of the analytical investigation involves establishing an extensive and intricate database. Numerous analytical and experimental studies have been examined, resulting in the creation of an initial database comprising 354 beam-column connection subassemblies from 58 distinct research studies. Following a reassessment of data adequacy, the final database is refined to include 251 specimens due to insufficient data or omission of specimens which did not experience joint shear failure.

Due to the more complex nature of data collection for beam-column connection tests compared to other structural members, the accuracy and reliability of experimental data are closely linked to the instrumentation employed during testing. Consequently, despite the research on connection subassemblies dates back to the 1960s, there is a scarcity of available detailed information. As a result, the primary challenge in compiling the database lies in the restricted availability of research projects offering adequate and reliable data, particularly concerning stress versus strain relationships within the connection region.

The database includes a wide array of beam-column connection subassemblies with diverse geometric, material, and loading attributes. However, specific limitations are defined, particularly for connections with unusual geometric and material properties, to ensure the accuracy and relevance of the analytical model to be developed. A general overview of the criteria considered during the selection of specimens for the database is outlined in the following sub-sections.

3.2 Selection of Specimens to be Included in the Database

An extensive database comprising specimens that have failed either by joint shear failure (JS) or joint shear failure preceded by beam plastic hinging (BJ) is compiled, encompassing a wide range of beam column connection region characteristics.

A variety of specimens with diverse geometric properties are examined. Apart from connection subassemblies featuring regular beams and columns, the database includes wide beam-column connections, eccentric connections, specimens with varying column aspect ratios, and subassemblies incorporating floor systems such as transverse beams and/or slabs.

The constructed database consists of 251 specimens with continuous columns obtained from 47 distinct experimental studies, encompassing both interior and exterior beam-column connections with or without transverse beams. Knee joints featuring discontinuous columns are omitted from the database due to insufficient experimental data, which hinders a meaningful comparison with code requirements. The types of specimens included in the database are outlined in Table 3.1.

Table 3.1 Specimen Types Included in the Database

Total number of specimens	251
Number of interior specimens with 2 transverse beams	19
Number of interior specimens with 1 transverse beam	8
Number of interior specimens without transverse beams	100
Number of exterior specimens with 2 transverse beams	21
Number of exterior specimens with 1 transverse beam	2
Number of exterior specimens without transverse beams	101

3.3 Range of Specimen Properties

The database contains a wide range of material properties in addition to different geometric features. The sub-sections provide summaries of the ranges of both geometric and material properties.

Compressive Strength (f_c')

Concrete compressive strength for selected specimens ranges from 19.30 MPa to 118.00 MPa, representing the specified compressive strength of the concrete.

Transverse Shear Reinforcement Ratio

The influence of confinement provided by the shear reinforcement is examined by utilizing specimens with a diverse range of shear reinforcement ratios. Some of the chosen specimens lack shear reinforcement, while others feature up to a 3.43 % volumetric ratio per one layer of shear reinforcement ($\rho_{singlelayer,core}$), as defined in 4.2.2.1.

Axial Load on Column

Within the considered specimens, the maximum axial load on the column transferred to the beam-column connection is 2890.0 kN (equivalent to 0.51 $f_c' A_g$), while no axial load was applied to some subassemblies.

Eccentricity

As one of the primary parameters under investigation, the study incorporates 18 beam-column connections with varying eccentricities between the beam and column centroidal axes. The selected specimens exhibit eccentricities ranging from 0.125 b_{column} to 0.306 b_{column}.

Beam Width to Column Width Ratio

The influence of the ratio of beam width to column width on the performance of beam-column joints is also assessed in relation to the confinement provided by the

beams. The minimum beam width to column width ratio in the database is 0.38, whereas the maximum value for this ratio is 3.10.

A general summary of the geometrical and material properties is presented in Table 3.2.

Table 3.2 Range of Material and Geometrical Properties for the Specimens Included in the Database.

		Min.	Max.
Concrete compressive strength, f_c'	(MPa)	19.3	118
Column depth, h_c	(mm)	150	600
Column width, b_c	(mm)	127	600
Depth of the beam in the loading direction, $h_{b,l}$	(mm)	203.2	610
Width of the beam in the loading direction, $b_{b,l}$	(mm)	110	939.8
Depth of the beam in the transverse direction, $h_{b,t}$	(mm)	300	609.6
Width of the beam in the transverse direction, $b_{b,t}$	(mm)	152.4	762

3.4 Selected Specimens

This section of the thesis provides a summary of the experiments included in the database. It outlines the key characteristics of the specimens and lists the primary parameters under investigation.

Burak and Wight carried out experiments on three 3/4 scale specimens (Burak & Wight, 2008). These specimens had slabs, transverse beams, and eccentric spandrel beams. Furthermore, one of the specimens featured a wide beam. Axial loads were applied to the columns in each subassembly. What sets this experimental study apart from other tests on eccentric connections is that the specimens were loaded in two principal directions, one plane at a time.

All four specimens of Raffaelle and Wight had spandrel beam eccentricities with varying beam dimensions and reinforcement detailing (Raffaelle & Wight, 1995).

All specimens were axially loaded, with a constant axial load of 20.0 kN. Specimens had neither slabs nor transverse beams.

Shin and LaFave conducted experiments on four exterior beam-column-slab connection specimens, two of which exhibited spandrel beam eccentricity (Shin & LaFave, 2004). The lateral loading was applied solely in the direction of the spandrel beam, without any axial load being placed on the column during the tests.

Gentry and Wight studied the performance of exterior wide beam-column connections by testing four specimens that had no slab or transverse beams (Gentry & Wight, 1994). While the column dimensions and reinforcement detailing remained the same across all specimens, longitudinal reinforcement of the wide beams was variable. A constant axial load of 20.0 kN was applied to the columns during the experiments.

LaFave and Wight conducted experiments on exterior wide beam-column connections (LaFave & Wight, 1999). The study involved cyclic loading in the wide beam direction for four specimens, with no axial loading. The subassemblies included slabs and transverse beams. For comparative analysis of behavior, one of the specimens featured a conventional beam in the loading direction.

Quintero-Febres and Wight carried out a study focusing on the seismic performance of reinforced concrete (RC) interior wide-beam connections (Quintero-Febres & Wight, 2001). The primary objective of this study was to assess how banded-floor systems respond to seismic loading. These systems, also known as wide-beam systems, involve slabs supported by broad, shallow beams that are framing into columns.

Durrani and Wight conducted an experimental and analytical study of internal beam-column connections subjected to reversed cyclic loading (Durrani & Wight, 1985). The study aimed to monitor the effect of the presence of transverse beams and slab on the beam-column connection performance. Of the six interior specimens that were tested, three had transverse beams and slab, while the other three had neither slab

nor transverse beams. Joint shear reinforcement was also one of the primary variables of this experimental investigation.

In their experimental study, Joh, Goto, and Shibata examined the impact of geometric properties of interior joints, with a particular focus on eccentricity (Joh et al., 1991a). The investigation included five specimens, four of which provided shear stress vs. shear strain data. Among these, two specimens were eccentric, and two were concentric. Notably, the test setup did not include slab and transverse beams, but axial load was applied to the columns.

Fujii and Morita examined the influence of the variations in the yield strength of beam bars, axial load of columns, and joint shear reinforcement area (Fujii & Morita, 1991). The conducted tests included an equal number of exterior and interior specimens, subjected to axial loading. The subassemblies did not have transverse beams or slabs.

Cheung, Paulay, and Park conducted tests on three beam-column-slab connections, with varying column depth to beam bar diameter ratios ranging from 21 to 25 (Cheung et al., 1991). Experimental results led to the conclusion that satisfactory performance of these connections was attributed to high joint shear reinforcement ratios and the utilization of small-diameter longitudinal beam bars, which prevents slippage. This indicates that the performance of a connections was influenced by specific design specifications related to reinforcement detailing and member depth to bar diameter ratios.

Teng and Zhou had two distinct series of specimens, each of which had three specimens (Teng & Zhou, 2003). All specimens were interior, four of which were eccentric. The distinguishing factors between the two series were the column depth and shear reinforcement ratio. It is important to highlight that all specimens had axial loading on the columns, in addition to being subjected to lateral cyclic loading.

Shiohara and Kusuhara tested six specimens, four of which were added to the database due to the lack of data on the maximum joint shear strength of the two

specimens (Shiohara & Kusuhara, 2006). The primary parameters investigated in this study included different loading protocols and the confinement effect of surrounding beams. The study investigated the seismic performance of interior reinforced concrete beam-column joint subassemblies, examining how a combination of design parameters influenced lateral capacity and post-yielding behavior. The research specifically focused on three key parameters: the amount of longitudinal reinforcement, the ratio of the joint flexural strength to that of the beam, and the ratio of the joint flexural strength to that of the column.

Wong and Kaung conducted experimental research on seventeen beam-column connections to investigate the impact of various parameters, including the horizontal and vertical reinforcement ratios within the joint, the effect of hooks of beam longitudinal bars, and anchorage (Wong & Kuang, 2008). However, four specimens from this test series were excluded from the database due to an anchorage problem caused by the absence of hooks in the beam longitudinal reinforcement extending inside the exterior joint, which was beyond the scope of the thesis. It is worth noting that all specimens were subjected to axial load, and no floor system was present.

Alameddine and Ehsani tested twelve specimens, varying in concrete compressive strengths, joint shear reinforcement ratios, and beam and column longitudinal reinforcement ratios (Alameddine & Ehsani, 1991). The connection subassemblies were two-dimensional and did not incorporate slabs, transverse beams or axial loading applied to the columns. The main purpose of this study was to assess the behavior of high strength reinforced concrete connections under inelastic cyclic loading.

Lee and Ko tested five specimens, three of which had an eccentric configuration (H.-J. Lee & Ko, 2008). Axial load was applied to the columns; however, no transverse beams or slab were included in the setup. The specimens were divided into two groups based on the orientation of the column. In the first group, the column was positioned to bear loads in the strong direction (parallel to the longer side), while the

second group was loaded in the weak direction. This study aimed to investigate and compare the behavior of the specimens with different column orientations.

Kusuhara et.al. tested three interior specimens, two of which had an eccentric configuration (Kusuhara et al., 2004). The subassemblies had no axial load, slab or transverse beams. The research aimed to explore the influence of beam eccentricity and joint shear reinforcement on the performance of the interior specimens.

Meinheit and Jirsa also focused on the shear strength of reinforced concrete beam-column connections (Meinheit & Jirsa, 1977). A total of 16 specimens were tested, all of which were loaded with high axial loads, ranging from 213.5 kN to 2655.6 kN.

Two interior (Units 1 and 2) and the two exterior (Units 3 and 4) reinforced concrete beam-column joints were tested by Park and Millburn, which were designed in accordance with the seismic provisions of NZS 3101 to demonstrate the effectiveness of the design requirements (Park & Milburn, 1983). This study aimed to illustrate and evaluate the effectiveness of various design approaches in meeting the seismic requirements outlined in the NZS 3101 code.

Based on the data obtained from the explored experimental studies, the constructed database is presented in Section 3.5.

3.5 Constructed Database

The constructed database consists of details about the research group conducted the experimental investigation and the specimen identifications. Moreover, dimensions of the members adjoining at the beam-column joint and material properties, as well as the axial load to the gross column sectional area are included in the database. The joint shear reinforcement ratio defined for the core section of the joint for a single layer of shear reinforcement $\rho_{singlelayer,core}$ is also included in the database.

Table 3.3 Constructed Database

Research.	Spec.	N / ($f_c'A_g$) (%)	$\rho_{sl.,core}$ (%)	f_c' (MPa)	b_c (mm)	h_c (mm)	$n_{b,l}$	$b_{b,l}$ (mm)	$h_{b,l}$ (mm)	$n_{b,tr}$	$b_{b,t}$ (mm)	$h_{b,t}$ (mm)
Burak & Wight, 2008	1-S	5.35	1.60	29.0	355.6	355.6	2	203.2	381.0	1	304.8	381.0
	2-S	3.98	0.92	39.0	533.4	355.6	2	254.0	457.2	1	304.8	457.2
	3-S	5.35	0.86	29.0	533.4	355.6	2	254.0	457.2	1	762.0	304.8
	1-N	5.35	1.60	29.0	355.6	355.6	1	304.8	381.0	2	203.2	381.0
	2-N	3.98	1.72	39.0	355.6	533.4	1	304.8	457.2	2	254.0	457.2
	3-N	5.35	1.60	29.0	355.6	533.4	1	762.0	304.8	2	254.0	457.2
Raffaelle & Wight, 1995	1	2.46	0.89	28.6	355.6	355.6	2	254.0	381.0	0	0.0	0.0
	2	2.62	0.89	26.8	355.6	355.6	2	177.8	381.0	0	0.0	0.0
	3	1.87	0.89	37.7	355.6	355.6	2	190.5	381.0	0	0.0	0.0
	4	3.64	0.89	19.3	355.6	355.6	2	190.5	558.8	0	0.0	0.0
Shin & LaFave, 2004	SL 1	0.00	0.63	29.9	457.2	330.2	2	279.4	406.4	1	330.2	406.4
	SL 2	0.00	0.63	36.1	457.2	330.2	2	177.8	406.4	1	330.2	406.4
	SL3	0.00	0.63	47.4	457.2	330.2	2	279.4	406.4	1	330.2	406.4
	SL4	0.00	1.13	31.2	279.4	368.3	2	279.4	406.4	1	279.4	406.4
Gentry & Wight, 1994	1	2.53	1.00	27.8	355.6	355.6	1	863.6	304.8	2	355.6	406.4
	2	2.53	1.00	27.8	355.6	355.6	1	762.0	304.8	2	355.6	406.4
	3	1.86	1.01	37.8	355.6	355.6	1	863.6	304.8	2	355.6	406.4
	4	1.86	1.00	37.8	355.6	355.6	1	863.6	304.8	2	355.6	406.4
LaFave & Wight, 1999	EWB-1	0.00	0.89	29.0	355.6	355.6	1	863.6	304.8	2	355.6	406.4
	EWB-2	0.00	0.89	30.3	355.6	355.6	1	863.6	304.8	2	254.0	609.6
	EWB-3	0.00	1.10	34.5	304.8	508.0	1	939.8	304.8	2	304.8	457.2
	ENB-1	0.00	1.10	24.8	304.8	508.0	1	304.8	558.8	2	304.8	457.2
Quintero-Febres & Wight, 2001	IWB-1	0.00	1.57	35.7	355.6	355.6	2	889.0	304.8	2	304.8	304.8
	IWB-2	0.00	1.57	27.5	355.6	355.6	2	660.4	304.8	2	304.8	304.8
	IWB-3	0.00	1.54	25.4	330.2	508.0	2	838.2	304.8	2	406.4	304.8

Table 3.3 Constructed Database (cont'd)

Research.	Spec.	$N / (f_c'A_g)$ (%)	$\rho_{sl.,core}$ (%)	f_c' (MPa)	b_c (mm)	h_c (mm)	$n_{b,l}$	$b_{b,l}$ (mm)	$h_{b,l}$ (mm)	$n_{b,tr}$	$b_{b,t}$ (mm)	$h_{b,t}$ (mm)
Durrani & Wight, 1985	X1	4.94	1.01	34.3	362.0	362.0	2	279.4	419.1	0	0.0	0.0
	X2	5.05	2.02	33.6	362.0	362.0	2	279.4	419.1	0	0.0	0.0
	X3	5.47	1.01	31.0	362.0	362.0	2	279.4	419.1	0	0.0	0.0
	S1	4.08	1.01	41.6	362.0	362.0	2	279.4	419.1	2	279.4	381.0
	S2	5.52	2.02	30.8	362.0	362.0	2	279.4	419.1	2	279.4	381.0
	S3	6.01	1.01	28.3	362.0	362.0	2	279.4	419.1	2	279.4	381.0
Joh et al., 1991b	B1	16.13	0.24	21.3	300.0	300.0	2	150.0	350.0	0	0.0	0.0
	B3	15.84	0.24	21.7	300.0	300.0	2	150.0	350.0	0	0.0	0.0
	B5	14.90	0.24	23.0	300.0	300.0	2	150.0	350.0	0	0.0	0.0
	B6	15.36	0.24	22.4	300.0	300.0	2	150.0	350.0	0	0.0	0.0
Fujii & Morita, 1991	A1	7.68	0.61	40.2	220.0	220.0	2	160.0	250.0	0	0.0	0.0
	A2	7.68	0.61	40.2	220.0	220.0	2	160.0	250.0	0	0.0	0.0
	A3	23.04	0.61	40.2	220.0	220.0	2	160.0	250.0	0	0.0	0.0
	A4	23.04	1.63	40.2	220.0	220.0	2	160.0	250.0	0	0.0	0.0
	B1	6.86	0.61	30.0	220.0	220.0	1	160.0	250.0	0	0.0	0.0
	B2	6.86	0.61	30.0	220.0	220.0	1	160.0	250.0	0	0.0	0.0
	B3	24.01	0.61	30.0	220.0	220.0	1	160.0	250.0	0	0.0	0.0
	B4	24.01	1.63	30.0	220.0	220.0	1	160.0	250.0	0	0.0	0.0
Kurose et al., 1991	J1(EW)	0.00	0.91	24.1	508.0	508.0	2	406.4	508.0	0	0.0	0.0
	J2(EW)	0.00	0.91	27.6	508.0	508.0	2	406.4	508.0	2	406.4	508.0
	J2(NS)	0.00	0.91	25.5	508.0	508.0	2	406.4	508.0	2	406.4	508.0
	J3(EW)	0.00	0.91	32.4	508.0	508.0	1	406.4	508.0	2	406.4	508.0
	J3 (NS)	0.00	0.91	32.4	508.0	508.0	2	406.4	508.0	1	406.4	508.0
Teng & Zhou, 2003	S1	11.14	0.90	33.0	400.0	300.0	2	200.0	400.0	0	0.0	0.0
	S2	10.81	0.90	34.0	400.0	300.0	2	200.0	400.0	0	0.0	0.0
	S3	10.50	0.90	35.0	400.0	300.0	2	200.0	400.0	0	0.0	0.0
	S4	11.59	1.35	37.0	400.0	200.0	2	200.0	400.0	0	0.0	0.0
	S5	10.99	1.35	39.0	400.0	200.0	2	200.0	400.0	0	0.0	0.0
	S6	11.28	1.35	38.0	400.0	200.0	2	200.0	400.0	0	0.0	0.0
Lawrence, 1991	1	0.00	1.21	23.2	500.0	500.0	2	250.0	500.0	0	0.0	0.0
Kusuhara et al., 2004	JE-0	0.00	0.33	27.0	320.0	280.0	2	180.0	300.0	0	0.0	0.0
	JE-55	0.00	0.33	27.0	320.0	280.0	2	180.0	300.0	0	0.0	0.0
	JE-55S	0.00	0.78	27.0	320.0	280.0	2	180.0	300.0	0	0.0	0.0
Shiohara & Kusuhara, 2006	A1	8.48	0.44	28.3	300.0	300.0	2	300.0	300.0	0	0.0	0.0
	B1	8.48	0.44	28.3	300.0	300.0	1	300.0	300.0	0	0.0	0.0
	B2	8.48	0.44	28.3	300.0	300.0	1	300.0	300.0	0	0.0	0.0

Table 3.3 Constructed Database (cont'd)

Research.	Spec.	N / ($f_c'A_g$) (%)	$\rho_{sl.,core}$ (%)	f_c' (MPa)	b_c (mm)	h_c (mm)	$n_{b,l}$	$b_{b,l}$ (mm)	$h_{b,l}$ (mm)	$n_{b,tr}$	$b_{b,t}$ (mm)	$h_{b,t}$ (mm)
(cont'd)	C1	8.48	0.44	28.3	300.0	300.0	2	300.0	300.0	2	300.0	300.0
Zaid et al., 1999	S3	3.97	0.54	28.0	300.0	300.0	2	200.0	300.0	0	0.0	0.0
Guimaraes et al., 1993	J4 (EW)	0.00	0.72	31.6	508.0	508.0	2	406.4	508.0	2	406.4	508.0
	J4 (NS)	0.00	0.72	31.6	508.0	508.0	2	406.4	508.0	2	406.4	508.0
	J5 (EW)	0.00	2.42	77.9	508.0	508.0	2	406.4	508.0	2	406.4	508.0
	J5 (NS)	0.00	2.42	77.9	508.0	508.0	2	406.4	508.0	2	406.4	508.0
	J6 (EW)	0.00	1.94	92.1	508.0	508.0	2	406.4	508.0	2	406.4	508.0
	J6 (NS)	0.00	1.94	92.1	508.0	508.0	2	406.4	508.0	2	406.4	508.0
H.-J. Lee & Ko, 2008	W0	10.09	0.73	28.9	600.0	400.0	1	300.0	450.0	0	0.0	0.0
	W75	9.59	0.73	30.4	600.0	400.0	1	300.0	450.0	0	0.0	0.0
	W150	10.02	0.73	29.1	600.0	400.0	1	300.0	450.0	0	0.0	0.0
Tsonos, 2007	E1	22.73	1.16	22.0	200.0	200.0	1	200.0	300.0	0	0.0	0.0
	G1	22.73	0.58	22.0	200.0	200.0	1	200.0	300.0	0	0.0	0.0
Alamed. & Ehsani, 1991	LL8	4.21	1.78	55.2	355.6	355.6	1	317.5	508.0	0	0.0	0.0
	LH8	4.21	2.50	55.2	355.6	355.6	1	317.5	508.0	0	0.0	0.0
	HL8	7.27	1.81	55.2	355.6	355.6	1	317.5	508.0	0	0.0	0.0
	HH8	7.27	2.54	55.2	355.6	355.6	1	317.5	508.0	0	0.0	0.0
	LL11	2.97	1.70	75.8	355.6	355.6	1	317.5	508.0	0	0.0	0.0
	LH11	2.88	2.46	75.8	355.6	355.6	1	317.5	508.0	0	0.0	0.0
	HL11	6.12	1.73	75.8	355.6	355.6	1	317.5	508.0	0	0.0	0.0
	HH11	6.31	2.46	75.8	355.6	355.6	1	317.5	508.0	0	0.0	0.0
	LL14	1.93	1.78	96.5	355.6	355.6	1	317.5	508.0	0	0.0	0.0
	LH14	1.82	2.50	96.5	355.6	355.6	1	317.5	508.0	0	0.0	0.0
Ehsani & Wight, 1985	1	5.90	0.90	33.6	299.7	299.7	1	259.1	480.1	0	0.0	0.0
	2	7.08	1.00	35.0	299.7	299.7	1	259.1	439.4	0	0.0	0.0
	3	6.06	1.34	40.9	299.7	299.7	1	259.1	480.1	0	0.0	0.0
	4	5.55	1.49	44.6	299.7	299.7	1	259.1	439.4	0	0.0	0.0
	5	5.81	0.90	42.6	299.7	299.7	1	259.1	480.1	2	259.1	480.1
	6	6.27	1.34	39.5	299.7	299.7	1	259.1	480.1	2	259.1	480.1
	7	8.55	1.00	29.0	299.7	299.7	1	259.1	439.4	2	259.1	439.4
	8	7.67	1.49	32.3	299.7	299.7	1	259.1	439.4	2	259.1	439.4
	9	12.62	0.75	24.3	340.4	340.4	1	299.7	480.1	0	0.0	0.0
	10	12.84	0.75	23.9	340.4	340.4	1	299.7	480.1	2	299.7	480.1
	11	6.56	0.77	39.8	340.4	340.4	1	299.7	480.1	0	0.0	0.0
	12	7.44	0.76	35.1	340.4	340.4	1	299.7	480.1	2	299.7	480.1

Table 3.3 Constructed Database (cont'd)

Research.	Spec.	N / ($f_c'A_g$) (%)	$\rho_{sl.,core}$ (%)	f_c' (MPa)	b_c (mm)	h_c (mm)	$n_{b,l}$	$b_{b,l}$ (mm)	$h_{b,l}$ (mm)	$n_{b,tr}$	$b_{b,t}$ (mm)	$h_{b,t}$ (mm)
Bolong & Yuzhou, 1991	J4	6.00	1.08	42.1	600.0	600.0	1	350.0	550.0	0	0.0	0.0
	J5	6.00	1.08	45.2	600.0	600.0	1	350.0	550.0	0	0.0	0.0
	J6	6.00	1.08	36.6	600.0	600.0	1	350.0	550.0	2	350.0	550.0
Kaku & Asakusa, 1991	3	0.00	0.51	41.7	220.0	220.0	1	160.0	220.0	0	0.0	0.0
	4	16.64	0.13	44.7	220.0	220.0	1	160.0	220.0	0	0.0	0.0
	5	9.01	0.13	36.7	220.0	220.0	1	160.0	220.0	0	0.0	0.0
	6	0.00	0.13	40.4	220.0	220.0	1	160.0	220.0	0	0.0	0.0
	9	0.00	0.52	40.6	220.0	220.0	1	160.0	220.0	0	0.0	0.0
	11	7.89	0.13	41.9	220.0	220.0	1	160.0	220.0	0	0.0	0.0
	12	0.00	0.13	35.1	220.0	220.0	1	160.0	220.0	0	0.0	0.0
	13	-4.45	0.52	46.4	220.0	220.0	1	160.0	220.0	0	0.0	0.0
	14	8.06	0.13	41.0	220.0	220.0	1	160.0	220.0	0	0.0	0.0
	15	8.33	0.13	39.7	220.0	220.0	1	160.0	220.0	0	0.0	0.0
Joh et al., 1991a	B8MH	13.96	0.47	28.1	300.0	300.0	2	200.0	350.0	0	0.0	0.0
	B8LH	14.58	0.24	26.9	300.0	300.0	2	200.0	350.0	0	0.0	0.0
	B9	15.32	0.69	25.6	300.0	300.0	2	200.0	350.0	0	0.0	0.0
	B10	15.75	0.69	24.9	300.0	300.0	2	200.0	350.0	0	0.0	0.0
	B11	15.14	0.69	25.9	300.0	300.0	2	200.0	350.0	0	0.0	0.0
Sugano et al., 1991	J4-0	33.34	1.47	30.4	440.0	440.0	2	300.0	400.0	0	0.0	0.0
	J6-0	16.75	1.47	60.5	440.0	440.0	2	300.0	400.0	0	0.0	0.0
	J8-0	13.06	1.47	77.6	440.0	440.0	2	300.0	400.0	0	0.0	0.0
	J8H-0	12.65	1.47	80.1	440.0	440.0	2	300.0	400.0	0	0.0	0.0
Murty et al., 2003	P1	0.00	0.62	27.3	200.0	250.0	2	200.0	400.0	0	0.0	0.0
	P2	0.00	0.62	26.3	200.0	250.0	2	200.0	400.0	0	0.0	0.0
	P3	0.00	0.62	27.0	200.0	250.0	2	200.0	400.0	0	0.0	0.0
	Q1	0.00	0.62	25.6	200.0	250.0	2	200.0	400.0	0	0.0	0.0
	Q2	0.00	0.62	27.2	200.0	250.0	2	200.0	400.0	0	0.0	0.0
	Q3	0.00	0.62	26.9	200.0	250.0	2	200.0	400.0	0	0.0	0.0
	R1	0.00	0.62	30.2	200.0	250.0	2	200.0	400.0	0	0.0	0.0
	R2	0.00	0.62	27.3	200.0	250.0	2	200.0	400.0	0	0.0	0.0
	R3	0.00	0.62	27.1	200.0	250.0	2	200.0	400.0	0	0.0	0.0
	S1	0.00	0.00	27.8	200.0	250.0	2	200.0	400.0	0	0.0	0.0
	S2	0.00	0.00	26.8	200.0	250.0	2	200.0	400.0	0	0.0	0.0
	S3	0.00	0.00	30.1	200.0	250.0	2	200.0	400.0	0	0.0	0.0
Park, 2002	O1	0.00	0.00	41.0	460.0	300.0	2	300.0	500.0	0	0.0	0.0

Table 3.3 Constructed Database (cont'd)

Research.	Spec.	N / ($f_c'A_g$) (%)	$\rho_{sl.,core}$ (%)	f_c' (MPa)	b_c (mm)	h_c (mm)	$n_{b,l}$	$b_{b,l}$ (mm)	$h_{b,l}$ (mm)	$n_{b,tr}$	$b_{b,t}$ (mm)	$h_{b,t}$ (mm)
Higazy et al., 1996	SB1	5.00	1.00	28.9	127.0	177.8	2	127.0	203.2	0	0.0	0.0
	SB2	-5.00	1.00	28.8	127.0	177.8	2	127.0	203.2	0	0.0	0.0
Meinheit & Jirsa, 1977	I	40.15	0.62	26.2	330.2	457.2	2	279.4	457.2	0	0.0	0.0
	II	25.39	0.62	41.8	330.2	457.2	2	279.4	457.2	0	0.0	0.0
	III	39.41	0.62	26.6	330.2	457.2	2	279.4	457.2	0	0.0	0.0
	IV	29.66	0.43	36.1	457.2	330.2	2	406.4	457.2	0	0.0	0.0
	V	3.94	0.62	35.9	330.2	457.2	2	279.4	457.2	0	0.0	0.0
	VI	48.35	0.62	36.7	330.2	457.2	2	279.4	457.2	0	0.0	0.0
	VII	47.25	0.43	37.2	457.2	330.2	2	406.4	457.2	0	0.0	0.0
	VIII	31.61	0.62	33.1	330.2	457.2	2	279.4	457.2	2	381.0	381.0
	IX	34.85	0.62	31.0	330.2	457.2	2	279.4	457.2	2	203.2	381.0
	X	35.76	0.62	29.6	330.2	457.2	2	279.4	457.2	2	203.2	381.0
	XI	41.93	0.43	25.6	457.2	330.2	2	406.4	457.2	2	152.4	381.0
	XII	30.42	2.77	35.2	330.2	457.2	2	279.4	457.2	0	0.0	0.0
	XIII	25.18	1.87	41.3	330.2	457.2	2	279.4	457.2	0	0.0	0.0
	XIV	32.25	1.28	33.2	457.2	330.2	2	406.4	457.2	0	0.0	0.0
Paulay et al., 1981	UNIT 2	15.00	1.50	22.5	457.0	457.0	1	356.0	610.0	0	0.0	0.0
	UNIT 3	5.30	0.77	26.9	457.0	457.0	1	356.0	610.0	0	0.0	0.0
Hwang et al., 2005	0T0	1.65	0.00	67.3	420.0	420.0	1	320.0	450.0	0	0.0	0.0
	3T3	1.61	0.73	69.0	420.0	420.0	1	320.0	450.0	0	0.0	0.0
	2T4	1.56	0.66	71.0	420.0	420.0	1	320.0	450.0	0	0.0	0.0
	1T44	1.53	0.88	72.8	420.0	420.0	1	320.0	450.0	0	0.0	0.0
Karayan. et al., 2008	A0	5.00	0.00	31.6	200.0	200.0	1	200.0	300.0	0	0.0	0.0
	A1	5.00	0.41	31.6	200.0	200.0	1	200.0	300.0	0	0.0	0.0
	A2	5.00	0.62	31.6	200.0	200.0	1	200.0	300.0	0	0.0	0.0
	B0	5.00	0.00	31.6	200.0	300.0	1	200.0	300.0	0	0.0	0.0
	B1	5.00	0.41	31.6	200.0	300.0	1	200.0	300.0	0	0.0	0.0
	C0	5.00	0.00	31.6	200.0	300.0	1	200.0	300.0	0	0.0	0.0
	C2	5.00	0.62	31.6	200.0	300.0	1	200.0	300.0	0	0.0	0.0
J.-Y. Lee et al., 2009	J1	0.00	1.07	40.0	350.0	350.0	2	300.0	400.0	0	0.0	0.0
	BJ1	0.00	1.07	40.0	350.0	350.0	2	300.0	400.0	0	0.0	0.0
	BJ2	0.00	0.80	40.0	350.0	350.0	2	300.0	400.0	0	0.0	0.0
	BJ3	0.00	0.80	40.0	350.0	350.0	2	300.0	400.0	0	0.0	0.0
	B1	0.00	0.80	40.0	350.0	350.0	2	300.0	400.0	0	0.0	0.0
Behnam et al., 2017	S3-BC2	12.82	1.61	34.7	300.0	360.0	1	600.0	300.0	2	360.0	300.0
	S4BC25	12.82	1.61	34.7	300.0	360.0	1	750.0	300.0	2	360.0	300.0

Table 3.3 Constructed Database (cont'd)

Research.	Spec.	N / ($f_c'A_g$) (%)	$\rho_{sl.,core}$ (%)	f_c' (MPa)	b_c (mm)	h_c (mm)	$n_{b,l}$	$b_{b,l}$ (mm)	$h_{b,l}$ (mm)	$n_{b,tr}$	$b_{b,t}$ (mm)	$h_{b,t}$ (mm)
Briss et al., 1978	B1	5.34	1.08	27.9	457.0	457.0	2	356.0	610.0	0	0.0	0.0
	B2	43.93	0.28	31.5	457.0	457.0	2	356.0	610.0	0	0.0	0.0
Park & Milburn, 1983	1	10.00	2.79	41.3	305.0	406.0	2	229.0	457.0	0	0.0	0.0
	2	10.00	1.48	46.9	305.0	406.0	2	229.0	457.0	0	0.0	0.0
	3	10.00	0.75	38.2	305.0	406.0	2	229.0	457.0	0	0.0	0.0
	4	10.00	0.90	38.9	305.0	406.0	1	229.0	457.0	0	0.0	0.0
Park & Ruitong, 1988	4	0.00	0.98	40.1	305.0	406.0	2	229.0	457.0	0	0.0	0.0
Leon, 1990	BCJ3	0.00	0.42	33.8	304.8	254.0	2	203.2	304.8	0	0.0	0.0
	BCJ4	0.00	0.35	24.8	355.6	254.0	2	203.2	304.8	0	0.0	0.0
Noguchi & Kashi., 1992	OKJ1	12.00	0.92	78.0	300.0	300.0	2	200.0	300.0	0	0.0	0.0
	OKJ2	12.00	0.92	78.0	300.0	300.0	2	200.0	300.0	0	0.0	0.0
	OKJ3	12.00	0.92	118.0	300.0	300.0	2	200.0	300.0	0	0.0	0.0
	OKJ4	12.00	0.92	78.0	300.0	300.0	2	200.0	300.0	0	0.0	0.0
	OKJ5	12.00	0.92	78.0	300.0	300.0	2	200.0	300.0	0	0.0	0.0
	OKJ6	12.00	0.92	59.0	300.0	300.0	2	200.0	300.0	0	0.0	0.0
Hegger et al., 2003	RK4	32.24	2.90	51.7	150.0	200.0	1	150.0	300.0	0	0.0	0.0
	RK5	30.36	2.96	54.9	150.0	200.0	1	150.0	300.0	0	0.0	0.0
	RK6	19.27	2.96	86.5	150.0	200.0	1	150.0	300.0	0	0.0	0.0
	RK7	30.47	2.05	54.7	150.0	200.0	1	150.0	400.0	0	0.0	0.0
	RK8	43.18	2.90	38.6	150.0	200.0	1	150.0	300.0	0	0.0	0.0
	RA1	26.00	0.00	53.1	150.0	240.0	2	150.0	300.0	0	0.0	0.0
	RA2	19.25	1.02	66.1	150.0	240.0	2	150.0	300.0	0	0.0	0.0
	RA3	31.98	2.17	43.6	150.0	240.0	2	150.0	300.0	0	0.0	0.0
	RA4	14.12	2.23	66.1	150.0	240.0	2	150.0	300.0	0	0.0	0.0
	RA5	24.66	1.21	56.2	150.0	240.0	2	150.0	300.0	0	0.0	0.0
	RA6	25.35	1.22	56.2	150.0	300.0	2	150.0	300.0	0	0.0	0.0
	RA7	15.93	3.43	79.7	150.0	240.0	2	150.0	300.0	0	0.0	0.0
Li & Leong, 2015	NS2	0.00	1.41	61.2	300.0	450.0	2	250.0	500.0	0	0.0	0.0
	NS3	0.00	1.99	60.5	300.0	450.0	2	250.0	500.0	0	0.0	0.0
	NS4	0.00	1.52	60.3	300.0	450.0	2	250.0	500.0	0	0.0	0.0
Attaalla, 1997	SOC3	5.02	1.11	47.2	127.0	177.8	2	127.0	203.2	0	0.0	0.0
	SHC1	4.48	0.74	56.6	127.0	177.8	2	127.0	203.2	0	0.0	0.0
	SHC2	4.40	1.11	59.6	127.0	177.8	2	127.0	203.2	0	0.0	0.0
Kun, 2003	H:0.0	0.00	2.11	50.6	300.0	300.0	2	250.0	300.0	0	0.0	0.0
	E:0.3	30.00	0.00	46.1	300.0	300.0	2	250.0	300.0	0	0.0	0.0

Table 3.3 Constructed Database (cont'd)

Research.	Spec.	N / ($f_c'A_g$) (%)	$\rho_{sl.,core}$ (%)	f_c' (MPa)	b_c (mm)	h_c (mm)	$n_{b,l}$	$b_{b,l}$ (mm)	$h_{b,l}$ (mm)	$n_{b,tr}$	$b_{b,t}$ (mm)	$h_{b,t}$ (mm)
(cont'd)	H:0.3	30.00	2.11	45.1	300.0	300.0	2	250.0	300.0	0	0.0	0.0
Wong & Kuang, 2008	BS-L	15.00	0.00	30.9	300.0	300.0	1	260.0	450.0	0	0.0	0.0
	BS-OL	15.00	0.00	30.9	300.0	300.0	1	260.0	450.0	0	0.0	0.0
	BS-LL	15.00	0.00	42.1	300.0	300.0	1	260.0	450.0	0	0.0	0.0
	BS-U	15.00	0.00	31.0	300.0	300.0	1	260.0	450.0	0	0.0	0.0
	L-LS	15.00	0.00	31.6	300.0	300.0	1	260.0	450.0	0	0.0	0.0
	V2T10	15.00	0.00	32.6	300.0	300.0	1	260.0	450.0	0	0.0	0.0
	V4T10	15.00	0.00	28.3	300.0	300.0	1	260.0	450.0	0	0.0	0.0
	H1T10	15.00	0.31	33.3	300.0	300.0	1	260.0	450.0	0	0.0	0.0
	H2T10	15.00	0.47	42.1	300.0	300.0	1	260.0	450.0	0	0.0	0.0
	L-600	15.00	0.00	36.4	300.0	300.0	1	260.0	600.0	0	0.0	0.0
	NN03	3.00	0.00	44.8	300.0	300.0	1	260.0	400.0	0	0.0	0.0
	NN15	15.00	0.00	46.0	300.0	300.0	1	260.0	400.0	0	0.0	0.0
	NN03	3.00	0.00	47.4	300.0	300.0	1	260.0	300.0	0	0.0	0.0
	NY03	3.00	0.53	34.9	300.0	300.0	1	260.0	400.0	0	0.0	0.0
	NY15	15.00	0.53	38.5	300.0	300.0	1	260.0	400.0	0	0.0	0.0
Lehman et al., 2004	PR14	10.00	0.00	31.8	406.4	457.2	2	406.4	457.2	0	0.0	0.0
	PR0850	10.00	0.00	35.0	406.4	457.2	2	406.4	457.2	0	0.0	0.0
	PR995	10.00	0.00	60.4	406.4	457.2	2	406.4	457.2	0	0.0	0.0
Uzumeri, 1977	1	51.82	0.00	30.8	381.0	381.0	1	304.8	508.0	1	304.8	508.0
	2	51.24	0.00	31.1	381.0	381.0	1	304.8	508.0	0	0.0	0.0
	5	49.92	0.00	31.9	381.0	381.0	1	381.0	508.0	1	304.8	508.0
Parker & Bullman, 1997	4a	0.00	0.00	39.2	300.0	300.0	1	250.0	500.0	0	0.0	0.0
	4b	8.50	0.00	39.2	300.0	300.0	1	250.0	500.0	0	0.0	0.0
	4c	17.21	0.00	36.8	300.0	300.0	1	250.0	500.0	0	0.0	0.0
	4d	0.00	0.00	39.2	300.0	300.0	1	250.0	500.0	0	0.0	0.0
	4e	8.33	0.00	40.0	300.0	300.0	1	250.0	500.0	0	0.0	0.0
	4f	17.73	0.00	37.6	300.0	300.0	1	250.0	500.0	0	0.0	0.0
	5a	0.00	0.64	42.4	300.0	300.0	1	250.0	500.0	0	0.0	0.0
	5b	7.72	0.64	43.2	300.0	300.0	1	250.0	500.0	0	0.0	0.0
	5c	15.43	0.64	43.2	300.0	300.0	1	250.0	500.0	0	0.0	0.0
	5d	0.00	0.86	43.2	300.0	300.0	1	250.0	500.0	0	0.0	0.0
	5e	7.44	0.86	44.8	300.0	300.0	1	250.0	500.0	0	0.0	0.0
	5f	15.43	0.86	43.2	300.0	300.0	1	250.0	500.0	0	0.0	0.0
Scott, 1992	C1	24.49	0.63	49.9	150.0	150.0	1	110.0	210.0	0	0.0	0.0
	C1A	20.37	0.63	60.0	150.0	150.0	1	110.0	210.0	0	0.0	0.0

Table 3.3 Constructed Database (cont'd)

Research.	Spec.	N / ($f_c'A_g$) (%)	$\rho_{sl.,core}$ (%)	f_c' (MPa)	b_c (mm)	h_c (mm)	$n_{b,l}$	$b_{b,l}$ (mm)	$h_{b,l}$ (mm)	$n_{b,tr}$	$b_{b,t}$ (mm)	$h_{b,t}$ (mm)
Scott, 1992 (cont'd)	C1AL	5.33	0.63	41.7	150.0	150.0	1	110.0	210.0	0	0.0	0.0
	C2	19.81	0.63	61.7	150.0	150.0	1	110.0	210.0	0	0.0	0.0
	C3	27.16	0.63	45.0	150.0	150.0	1	110.0	210.0	0	0.0	0.0
	C3L	5.01	0.63	44.4	150.0	150.0	1	110.0	210.0	0	0.0	0.0
	C4	23.60	0.65	51.8	150.0	150.0	1	110.0	210.0	0	0.0	0.0
	C4A	22.06	0.65	55.4	150.0	150.0	1	110.0	210.0	0	0.0	0.0
	C4AL	4.97	0.65	44.7	150.0	150.0	1	110.0	210.0	0	0.0	0.0
	C5	29.59	0.65	41.3	150.0	150.0	1	110.0	210.0	0	0.0	0.0
	C6	24.54	0.65	49.8	150.0	150.0	1	110.0	210.0	0	0.0	0.0
	C6L	3.88	0.65	57.3	150.0	150.0	1	110.0	210.0	0	0.0	0.0
	C7	27.78	0.41	44.0	150.0	150.0	1	110.0	300.0	0	0.0	0.0
	C8	21.98	0.41	55.6	150.0	150.0	1	110.0	300.0	0	0.0	0.0
	C9	27.22	0.41	44.9	150.0	150.0	1	110.0	300.0	0	0.0	0.0

.

CHAPTER 4

ANALYTICAL MODEL

In this section of the thesis, the development of beam-column joint shear strength prediction equation will be presented. Additionally, the performance points determined to represent the nonlinear behavior of the connection region will be addressed.

4.1 General Approach

The primary objective of this research is to provide an analytical framework that effectively reflects the critical performance points of the shear stress versus strain relationship and precisely computes the shear strength of beam-column connections. The model is intentionally designed to be user-friendly for practicing engineers, while providing comprehensive coverage of beam-column connection behavior.

Beam-column connections with a wide variety of geometrical, material and loading properties have been investigated. As the basic tendency of a parameter to affect the shear capacity is evaluated in the light of previous research, each parameter is then evaluated using several different approaches and the final effect of a parameter and the extend of the effect provided by the evaluated parameter is determined in relation with the singular and combined effect of all parameters. The effect of each parameter is interpreted with the main objective of reducing the mean absolute error of all Modification factors included, and variation of shear capacity predictions is tried to be kept at minimum. The utmost importance is given to keep the parameters as simple as possible such that the final equation can be used by practicing engineers.

In determination of both the joint shear capacity and performance points in the nonlinear response, a basic prediction is defined in relation to the concrete

compressive strength and the confinement provided by the adjoining members. In this way, the basic approach is kept in line with the methodology followed by contemporary structural standards.

Then, the basic prediction is enhanced by the use of additional coefficients in relation to the geometrical, material and loading conditions of each subassembly group. In each step, it is aimed to better the prediction by the utilization of introduced variables. The success of both the basic and enhanced predictions for the shear capacity is verified comparing the results with different editions of contemporary structural codes such as ACI 352 (2010), ACI 318 (2011, 2014 and 2019) and Turkish Earthquake Code (2007 and 2018). This comparison also provides information on the improvements observed as the code requirements are modified. Moreover, since the developed capacity prediction equation is applicable for both deficient and code conforming specimens, ASCE 41 (2017) is also used in the verification of the model, since the equation presented in the related standard is applicable for both deficient and conforming specimens.

After the maximum shear capacity prediction for the beam-column joint is completed, nonlinear behavior of the connection region is modeled using the performance points, based on $V_{j,pre.}$ The proposed performance points are then enhanced using geometrical and material properties of the connection, similar to the process followed in the capacity prediction equation.

A more detailed description of each step followed in the determination of the capacity and related performance points will be presented in the following sections.

4.2 Joint Shear Capacity Prediction Equation

Each beam-column joint has a characteristic shear response against cyclic loading, affected by many factors such as geometrical properties, material capacities and prior loading history, as discussed above. In this section, details of the proposed joint shear capacity prediction equation will be presented.

The shear capacity prediction equation construction methodology is schematically presented in the diagram below.

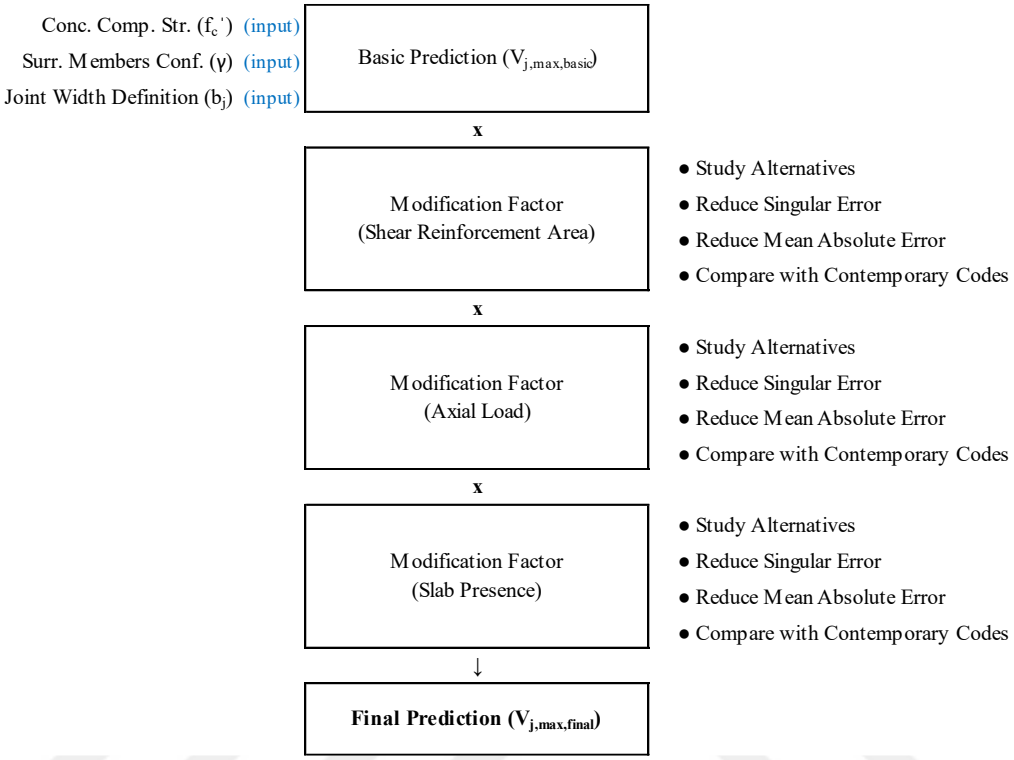


Figure 4.1. $V_{j,pre.}$ Prediction Equation Development Flowchart

4.2.1 Basic Prediction, $V_{j,pre.,basic}$

As discussed in Section 2.2, contemporary structural codes utilize a shear capacity prediction equation based on the concrete compressive strength (f_c'), confinement provided by the adjoining members and joint shear area based on effective joint shear width (b_j) definitions. In this study, the shear capacity prediction is also constructed on the square root of concrete compressive strength, which represents the tensile strength, joint shear area definition and shear strength factor based on the geometry of the beam-column connection region.

Joint Shear Strength Factor

It is important to underline that each structural code recommends a discrete shear strength factor based on the adjoining confinement provided by adjoining members. In the table below, shear strength factors (γ) recommended by ACI 352-10 for Type 2 connections, defined as connections designed to have sustained strength under deformation reversals into the inelastic range, are presented.

Table 4.1 ACI 352.10 Joint Shear Strength Factors

Classification	Connection type	
	1	2
A. Joints with a continuous column		
A.1 Joints effectively confined on all four vertical faces	24	20
A.2 Joints effectively confined on three vertical faces or on two opposite vertical faces	20	15
A.3 Other cases	15	12
B. Joints with a discontinuous column		
B.1 Joints effectively confined on all four vertical faces	20	15
B.2 Joints effectively confined on three vertical faces or on two opposite vertical faces	15	12
B.3 Other cases	12	8

In this research, instead of constant coefficients that result in stepwise predictions, a continuous approach is utilized based on the confinement provided by beams framing into the joint. Moreover, the efficiency of confinement provided by the beams in the loading direction is compared to the beams in the transverse direction, the effect of the beam width on confinement with respect to the member depth and the minimum and maximum coefficients that can be utilized in the determination of joint shear capacity are investigated. A “Confinement Score” based on the dimensions of adjoining beams is computed. In the following paragraphs, the proposed procedure is described.

Step 1: Determination of the Confinement Provided by a Single Beam

Similar to contemporary structural codes, the beam width to column width ratio is evaluated:

- If the beam covers equal or more than 3/4 width of the column face, the joint is considered to be fully confined.
- If the beam covers less than 3/4 width of the column, the confinement is obtained by interpolation.

$$\text{Beam Confinement (BC)} = b_b / (0.75 \times b_c) \leq 1.0 \quad (4.1)$$

Step 2: Determination of the Confinement Provided by All Adjoining Beams

When the contemporary structural codes are analyzed in terms of beam-column joint shear capacity determination, it is noticed that the confinement provided by a beam in the direction of loading is considered to be more effective than the confinement provided by a beam in the transverse direction. Similarly, in this research, the confinement effect of beams in the loading and transverse directions are investigated comparatively. In the final equation, the confinement provided by a beam in the loading direction is defined as twice the confinement provided by a member in the transverse direction.

The total confinement provided by the beams in the loading direction is computed as,

$$\sum BC_{beams,long} \quad (4.2)$$

where “BC” stands for “Beam Confinement”.

Since the efficiency of the confinement provided by the transverse beams is defined to be half of the confinement provided by the beams in the loading direction, the total confinement provided by the beams in the transverse direction is calculated as,

$$0.5 \sum BC_{beams,trans} \tag{4.3}$$

Consequently, the total confinement score (CS) provided by all beams framing into the joint is determined as presented in Eqn. 4.4.

$$\text{CS} = \sum BC_{beams,long} + 0.5 \sum BC_{beams,trans} \tag{4.4}$$

which sums up to a confinement score of 3.0 for a fully confined beam-column joint.

Step 3: Determination of Shear Strength Factor, γ

After the confinement provided by all beams adjoining the connection region is determined as confinement score (CS), the minimum and maximum confinement coefficients and the point where the confinement coefficient slope needs to be modified are determined.

Considering the coefficients recommended by ACI 352-10, a similar but continuous approach is utilized, after a comprehensive analysis is performed to reduce the mean absolute error and dispersion of data.

- For the specimens with a confinement score of 3 (4 sides fully confined), the maximum shear coefficient is determined as 20.
- For the specimens with a confinement score of 2 (2 beams in the longitudinal direction provides complete confinement or 1 beam in the longitudinal direction and 2 beams in the transverse direction provide full confinement), shear coefficient is defined as 14.
- The minimum confinement coefficient, for a joint with 0 confinement score, is determined as 6.

The comparison of continuous shear capacity coefficient definition with the definition of ACI 352-10 is presented in the figure below.

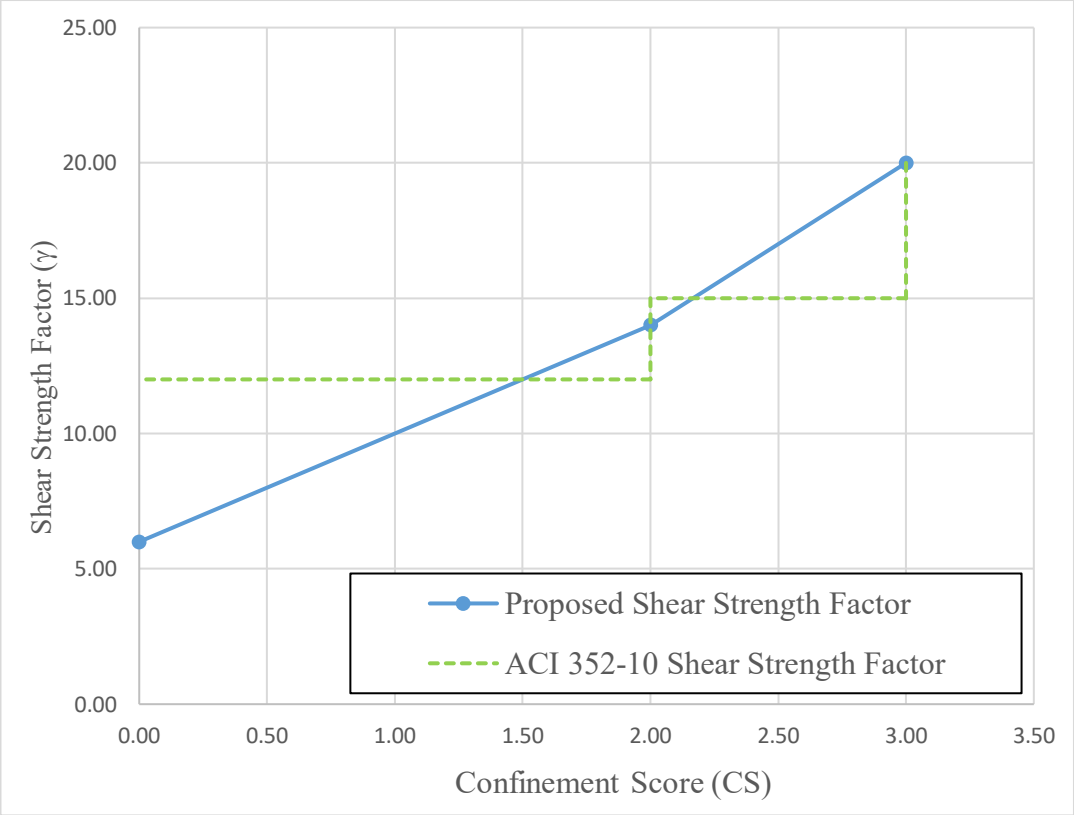


Figure 4.2. Proposed Shear Strength Factor

$$\gamma = \begin{cases} 6 + 4\,CS & \text{for specimens with } CS < 2.0 \\ 14 + 6\,(CS - 2.0) & \text{for specimens with } CS \geq 2.0 \end{cases} \quad (4.5)$$

Joint Shear Area

The effective joint area is defined as the multiplication of effective joint width (b_j) and column depth (h_c). In this research study, ACI 352-10 definition is taken as the benchmark for the determination of effective joint width, as presented in Section 2.3.

While defining the effective joint width, the eccentricity between the beam and column centerlines is considered in ACI 352-10 and a penalty factor, m, of 0.3 is imposed for eccentric beam-column connections. However, when the test results were examined, this assumption led to an underestimation of the joint shear strength. Therefore, the factor "m" is proposed as 0.5, same as the value for concentric

connections in ACI 352-10, without varying for different eccentricity ratios, also enabling a more practical application.

It must be underlined that, since the number of eccentric specimens tested for shear capacity under seismic loading is limited, the analytical investigation must be extended in the light of as new experimental results become available for a better understanding of the behavior.

Effective joint width definition utilized in the joint shear capacity prediction is presented in Eqn. 4.6.

$$\text{Effective joint width, } b_j = \min\left\{\frac{b_b+b_c}{2}\,,\, b_b + \sum m\frac{h_c}{2}\,,\, h_c\right\} \qquad (4.6)$$

where,

b_b = beam width in the loading direction,

b_c = column width,

h_c = column depth,

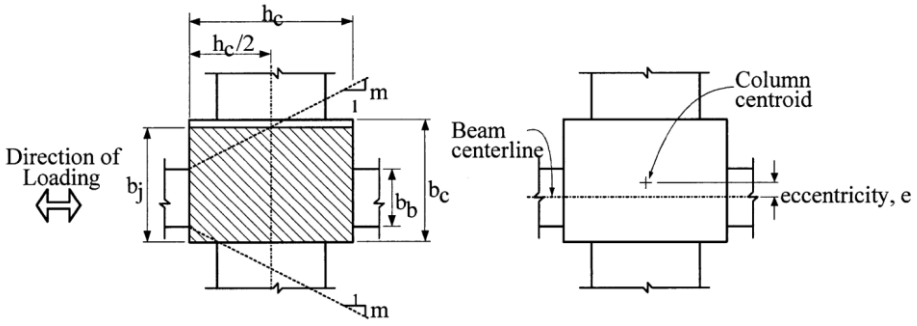


Figure 4.3. Effective Joint Width Definition

Consequently, basic shear capacity prediction equation is defined in Eqn. 4.7.

$$V_{j,pre.,basic} = 0.083\gamma\sqrt{f_c'}\,b_j \qquad (4.7)$$

4.2.2 Modification Factors

The cyclic response of beam-column connections is fundamentally determined by geometric properties and material qualities, in addition to the loading conditions, as previously stated. For the purpose of determining the maximum joint shear strength, a number of parameters that have high correlation factors are evaluated throughout this investigation.

Methodology Followed in the Determination of Modification Factors

In the determination process of the Modification factors, the initial step involves defining all key characteristics of a connection as standardized variables. Subsequently, basic indices are formulated to depict the influence of each identified attribute. These indices serve as a benchmark for evaluating various connection subassemblies that share common characteristics.

In the next step, the impact of each index on the connection behavior is examined, and an Modification factor is determined. This process involves analyzing the previously established indices and fine-tuning the Modification factor to accurately reflect the influence of the specific characteristic on the connection behavior.

For each Modification factor, a cross check analyses in between the coefficients is carried out where different versions of the Modification factor is applied and the resultant mean absolute error and data dispersion are minimized also relation with the other variables to reach to an optimized solution. In the determination of Modification factors, utmost importance is given to keep the factor simple for the purpose of practical use.

Finally, special conditions such as the effects of prior cyclic loading history and no joint shear reinforcement are investigated to improve the accuracy of the prediction equation.

In the following sections, the details of proposed Modification factors are presented.

4.2.2.1 Joint Shear Reinforcement Factor (SR)

Based on prior research and contemporary structural code requirements, one of the key parameters for the beam-column connection response is the joint shear reinforcement detailing.

To increase the accuracy of the shear reinforcement Modification factor, different joint shear volume definitions are investigated. In order to ascertain the option that exhibits the most significant correlation with the confinement effect, volumetric joint shear reinforcement ratios are computed for both gross and core joint volumes, in addition to the effective volume for a single layer of joint shear reinforcement as presented in Eqn.s. 4.8 to 4.11.

$$\rho_{gross} = \frac{n\, A_0\, l_e}{h_c\, b_c\, h_b} \tag{4.8}$$

$$\rho_{core} = \frac{n\, A_0\, l_e}{h_{c,core}\, b_{c,core}\, h_{b,core}} \tag{4.9}$$

$$\rho_{single\ layer,\ gross} = \frac{A_0\, l_e}{h_c\, b_c\, s} \tag{4.10}$$

$$\rho_{singlelayer,core} = \frac{A_0\, l_e}{h_{c,core}\, b_{c,core}\, s} \tag{4.11}$$

where,

A_0 : shear reinforcement cross sectional area,

l_e : total length of the shear reinforcement in the loading direction,

n_{gross} : number of shear reinforcement layers within the beam depth

s : shear reinforcement spacing,

h_c, b_c : column depth and width, respectively,

$h_{c,core}$, $b_{c,core}$: core column depth and width, respectively,

d_b, $d_{b,core}$: beam depth and distance between top and bottom longitudinal beam reinforcement, respectively.

The joint shear reinforcement index is determined after selecting the volumetric shear reinforcement ratio that exhibits the strongest correlation with the confinement effect. The index quantifies the degree of shear reinforcement enhancement or deterioration on the confinement of the beam-column joint, depending on whether it exceeds or falls below a specified threshold value, respectively.

Evaluation of the experimental data in the generated database is conducted to ascertain the most adequate value for this limit. The study assesses volumetric shear reinforcement ratios ranging from 0.0% to 3.5%. The single layer core volumetric shear reinforcement ratio of 1.00 % ($\rho_{singlelayer,core}$) is obtained to be the most reliable indicator of the confinement effect of shear reinforcement. Due to the higher correlation observed in the analytical study.

$$\text{Shear Reinforcement Index (SRI)} : \quad \rho_{singlelayer,core} - 0.01 \tag{4.12}$$

The proposed shear reinforcement factor is effective as an enhancement factor for joints with $\rho_{singlelayer,core} \geq 1.0$ % whereas the same factor penalizes the joints with shear reinforcement $\rho_{singlelayer,core} < 1.0$ %, which is utilized to obtain the shear strength of deficient joints.

After nonlinear correlation analysis, the best fit with the joint shear strength is observed to be the square root of shear reinforcement index. The resulting shear reinforcement factor is defined as given in Eqn. 4.13.

Shear Reinforcement Factor for Joints without Shear Reinforcement

The database presented in Section 3.5 covers a wide variety of specimens, including beam-column joints without any shear reinforcement. In the analysis of specimens, it is realized that even a negligible amount of shear reinforcement in the joint enhances the capacity considerably, compared to joints without any shear

reinforcement. From numerous alternatives that are examined, it is determined that a constant shear capacity reduction factor works best in the capacity prediction for joints with no shear reinforcement. The capacity reduction factor is determined to be 0.8.

The variation of shear reinforcement factor with respect to the single layer core volumetric shear reinforcement ratio is presented in Fig. 4.4. As can be observed from this figure, the shear reinforcement factor reduces the joint shear strength for deficient joints with reinforcement ratios less than 1.0%, while the increase in capacity gets reduced for higher reinforcement ratios.

Shear Reinforcement Factor (SR) :

$$\begin{aligned} &1 + \sqrt{SRI} \text{ for } \rho_{singlelayer,core} \geq 1.0\ \% \\ &1 - \sqrt{SRI} \text{ for } \rho_{singlelayer,core} < 1.0\ \%, \\ &0.8\ (1 - \sqrt{SRI}) \text{ for } \rho_{singlelayer,core} = 0.0\ \%, \end{aligned} \tag{4.13}$$

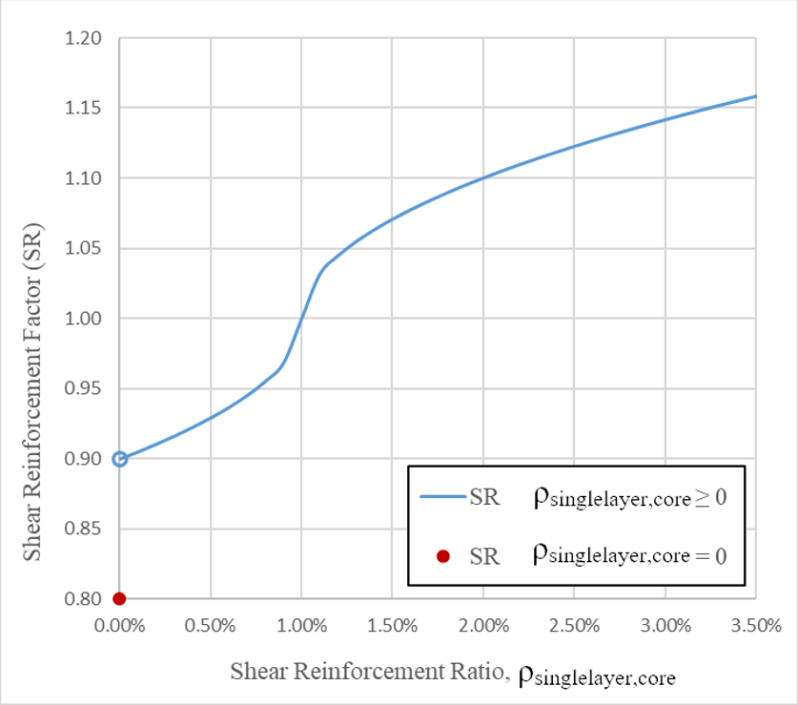


Figure 4.4. Shear Reinforcement Factor vs. $\rho_{singlelayer,core}$

4.2.2.2 Axial Load Factor (AxF)

Application of axial load on a column has been shown to enhance the shear strength of the beam-column joint by providing additional confinement to the connection region. The effect of axial load is quantified by establishing an axial load index, which is determined by normalizing the axial load with respect to the gross column area. The Axial load index is determined as presented below.

$$\text{Axial Load Index (AxI)} : \quad \frac{N}{(b_c\, h_c f_c')} \tag{4.14}$$

Analyzing different variations of the axial load effect based on the determined axial load index, the most accurate representation of the increasing impact of axial load on joint shear strength is obtained by taking half of the axial load index and the axial load factor is defined as shown in Eqn. 4.15.

$$\text{Axial Factor (AxF)} : \quad 1 + \frac{AxI}{2} \tag{4.15}$$

As reported in prior research studies (Fujii & Morita, 1991; Kaku & Asakusa, 1991) the effect of axial load on flexural strength of beams will be different in tension and compression failure zones based on the balanced axial load level. The possibility of a similar effect on joint shear strength is examined by considering limitations for the axial load level, however no such limit could be identified for the specimens included in the database. Consequently, the axial load factor kept constant for all axial load levels which aids in the simplicity of the Modification factor.

4.2.2.3 Factor for the Presence of Slab (SF)

Experimental results obtained for subassemblies included in the database indicated that specimens with slabs sustain higher joint shear forces. The additional confinement provided by the presence of slabs is examined considering the ratio of slab thickness to beam depth in the loading direction. The moment ratio of columns to beams is also evaluated including the slab reinforcement in the effective flange

width, however although this approach increases the computational time, it did not lead to an improved accuracy. Therefore, the slab index is simply defined as the ratio of slab thickness to beam depth in the direction of loading.

$$\text{Slab Index (SI)} : \quad \frac{t_f}{h_b} \tag{4.16}$$

The effect of slab on the enhancement of the joint shear capacity is then defined as presented in Eqn. 4.17.

$$\text{Slab Factor (SF)} : \quad 1 + SI^2 \tag{4.17}$$

4.2.3 Joint Shear Capacity Prediction Equation

As presented in the prior sections, to calculate the joint shear capacity effectively, firstly a basic shear capacity ($V_{j,pre.,basic}$) based on the concrete compressive strength (f_c'), confinement provided by the adjoining members and the effective joint width (b_j) is calculated.

Then, the basic prediction is enhanced by applying Modification factors accounting for the transverse shear reinforcement (SR), axial load (AxF) and slab (SF). The joint shear capacity prediction ($V_{j,pre.}$) equation developed based on these factors is presented in Eqn. 4.18.

$$V_{j,pre.} = V_{j,pre.,basic}\,(SR)\,(AxF)\,(SF) \tag{4.18}$$

Prior Loading Factor

Although only a limited number of subassemblies are loaded in two perpendicular directions for cyclic loading, it is observed that for the specimens loaded in two perpendicular directions or specimens with a biaxial loading where cyclic deformations are applied to the subassemblies in two perpendicular directions simultaneously, the joint shear strength reduces considerably. After evaluation of the

experimental data, it is determined that a reduction factor of 0.8 should be defined for such joints.

In the table presented below, the maximum shear capacity predictions for the specimens included in the database are presented.

Table 4.2 Basic and Final Shear Strength Predictions

Research.	Spec.	$V_{j,exp}$ kN	$V_{j,pre.,basic}$ kN	SR	AxF	SF	Load. Fact.	$V_{j,pre.}$ kN
Burak & Wight, 2008	1-S	778.4	628.1	1.08	1.03	1.07	1.00	744.0
	2-S	863.0	826.7	0.97	1.02	1.05	1.00	859.5
	3-S	827.4	712.8	0.96	1.03	1.05	1.00	739.1
	1-N	569.4	684.8	1.08	1.03	1.07	0.80	648.9
	2-N	809.6	1144.8	1.08	1.02	1.05	0.80	1063.2
	3-N	1156.5	1063.1	1.08	1.03	1.11	0.80	1045.6
Raffaelle & Wight, 1995	1	650.8	655.4	0.97	1.01	1.00	1.00	641.9
	2	420.6	462.0	0.97	1.01	1.00	1.00	452.9
	3	469.7	579.8	0.97	1.01	1.00	1.00	566.2
	4	412.4	414.8	0.97	1.02	1.00	1.00	408.6
Shin & LaFave, 2004	SL 1	631.6	801.9	0.94	1.00	1.06	1.00	800.5
	SL 2	631.6	521.0	0.94	1.00	1.06	1.00	520.1
	SL3	671.7	1027.4	0.94	1.00	1.06	1.00	1025.6
	SL4	791.8	810.6	1.04	1.00	1.06	1.00	892.1
Gentry & Wight, 1994	1	689.9	774.5	1.00	1.01	1.00	1.00	788.3
	2	733.5	774.5	1.00	1.01	1.00	1.00	788.3
	3	829.4	903.2	1.01	1.01	1.00	1.00	920.2
	4	934.3	903.2	1.00	1.01	1.00	1.00	916.1
LaFave & Wight, 1999	EWB-1	857.4	790.7	0.97	1.00	1.11	1.00	850.0
	EWB-2	929.0	798.3	0.97	1.00	1.11	1.00	858.2
	EWB-3	1244.4	996.0	1.03	1.00	1.11	1.00	1141.8
	ENB-1	688.4	845.2	1.03	1.00	1.03	1.00	900.8
Quintero-Febres & Wight, 2001	IWB-1	1386.1	1253.6	1.08	1.00	1.00	1.00	1348.4
	IWB-2	1352.9	1100.4	1.08	1.00	1.00	1.00	1183.7
	IWB-3	1510.2	1403.5	1.07	1.00	1.00	1.00	1506.6
Durrani & Wight, 1985	X1	1005.0	790.3	1.01	1.02	1.00	1.00	818.5
	X2	1054.8	782.3	1.10	1.03	1.00	1.00	883.2
	X3	803.5	751.3	1.01	1.03	1.00	1.00	780.0
	S1	1411.7	1242.3	1.01	1.02	1.06	1.00	1356.5
	S2	1384.6	1068.4	1.10	1.03	1.06	1.00	1280.0
	S3	1029.1	1024.4	1.01	1.03	1.06	1.00	1129.1
Joh et al., 1991b	JXO-B1	285.3	292.9	0.91	1.08	1.00	1.00	289.0
	JXO-B3	299.8	295.6	0.91	1.08	1.00	1.00	291.3

Table 4.2 Basic and Final Shear Strength Predictions (cont'd)

Research.	Spec.	$V_{j,exp}$ kN	$V_{j,pre.,basic}$ kN	SR	AxF	SF	Load. Fact.	$V_{j,pre.}$ kN
(cont'd)	JXO-B5	289.9	304.8	0.91	1.07	1.00	1.00	299.0
	JXO-B6	273.7	300.2	0.91	1.08	1.00	1.00	295.2
Fujii & Morita, 1991	A1	418.5	302.7	0.94	1.04	1.00	1.00	294.7
	A2	385.6	302.7	0.94	1.04	1.00	1.00	294.7
	A3	418.5	302.7	0.94	1.12	1.00	1.00	316.5
	A4	427.5	302.7	1.08	1.12	1.00	1.00	364.3
	B1	250.1	187.7	0.94	1.03	1.00	1.00	182.1
Fujii & Morita, 1991 (cont'd)	B2	217.2	187.7	0.94	1.03	1.00	1.00	182.1
	B3	277.0	187.7	0.94	1.12	1.00	1.00	197.2
	B4	291.9	187.7	1.08	1.12	1.00	1.00	227.0
Kurose et al., 1991	J1 (EW)	1825.3	1325.8	0.97	1.00	1.06	1.00	1365.8
	J2 (EW)	2617.8	2027.3	0.97	1.00	1.06	1.00	2088.5
	J2 (NS)	2393.1	1947.3	0.97	1.00	1.06	1.00	2006.2
	J3 (EW)	1834.4	1536.3	0.97	1.00	1.06	1.00	1582.7
	J3 (NS)	1896.7	1865.5	0.97	1.00	1.06	1.00	1921.9
Teng & Zhou, 2003	S1	717.3	486.3	0.97	1.06	1.00	1.00	497.2
	S2	717.3	493.6	0.97	1.05	1.00	1.00	503.8
	S3	716.4	459.1	0.97	1.05	1.00	1.00	467.9
	S4	391.2	343.3	1.06	1.06	1.00	1.00	384.7
	S5	391.2	352.5	1.06	1.05	1.00	1.00	393.8
	S6	391.2	289.9	1.06	1.06	1.00	1.00	324.4
Lawrence,1991	1	696.0	849.5	1.05	1.00	1.00	1.00	888.6
Kusuhara et al., 2004	JE-0	418.1	362.3	0.92	1.00	1.00	1.00	332.6
	JE-55	395.8	362.3	0.92	1.00	1.00	1.00	332.6
	JE-55S	400.1	362.3	0.95	1.00	1.00	1.00	345.4
Shiohara & Kusuhara, 2006	A1	586.8	556.3	0.93	1.04	1.00	1.00	536.7
	B1	456.1	397.4	0.93	1.04	1.00	1.00	383.3
	B2	427.4	397.4	0.93	1.04	1.00	1.00	383.3
	C1	696.7	794.8	0.93	1.04	1.00	1.00	766.7
Zaid et al.,1999	S3	635.5	431.9	0.93	1.02	1.00	1.00	410.6
Guimaraes et al., 1993	J4 (EW)	2560.2	2168.9	0.95	1.00	1.06	1.00	2181.7
	J4 (NS)	2101.7	2168.9	0.95	1.00	1.06	1.00	2181.7
	J5 (EW)	4812.4	3403.1	1.12	1.00	1.06	1.00	4046.7
	J5 (NS)	4109.4	3403.1	1.12	1.00	1.06	1.00	4046.7
	J6 (EW)	4438.3	3700.3	1.10	1.00	1.06	1.00	4312.0
	J6 (NS)	4163.5	3700.3	1.10	1.00	1.06	1.00	4312.0
H.-J. Lee & Ko, 2008)	W0	775.0	696.1	0.95	1.05	1.00	1.00	693.0
	W75	780.0	713.9	0.95	1.05	1.00	1.00	709.1
	W150	710.0	698.5	0.95	1.05	1.00	1.00	695.2

Table 4.2 Basic and Final Shear Strength Predictions (cont'd)

Research.	Spec.	$V_{j,exp}$ kN	$V_{j,pre.,basic}$ kN	SR	AxF	SF	Load. Fact.	$V_{j,pre.}$ kN
Tsonos, 2007	E1	219.8	155.7	1.04	1.11	1.00	1.00	180.4
	G1	195.0	155.7	0.94	1.11	1.00	1.00	162.2
Alameddine & Ehsani, 1991	LL8	860.3	737.7	1.09	1.02	1.00	1.00	819.9
	LH8	838.0	737.7	1.12	1.02	1.00	1.00	845.4
	HL8	986.6	737.7	1.09	1.04	1.00	1.00	833.5
	HH8	985.7	737.7	1.12	1.04	1.00	1.00	859.4
	LL11	769.1	865.1	1.08	1.01	1.00	1.00	951.4
	LH11	934.1	865.1	1.12	1.01	1.00	1.00	983.4
	HL11	967.5	865.1	1.09	1.03	1.00	1.00	967.6
	HH11	1020.9	865.1	1.12	1.03	1.00	1.00	1000.1
(cont'd)	LL14	877.6	975.9	1.09	1.01	1.00	1.00	1072.6
	LH14	890.5	975.9	1.12	1.01	1.00	1.00	1105.3
Ehsani & Wight, 1985	1	486.3	402.8	0.97	1.03	1.00	1.00	401.3
	2	502.6	410.9	0.99	1.04	1.00	1.00	422.8
	3	599.8	444.4	1.06	1.03	1.00	1.00	484.7
	4	623.3	464.2	1.07	1.03	1.00	1.00	510.6
	5	573.7	635.2	0.97	1.03	1.04	1.00	660.9
	6	601.4	611.6	1.06	1.03	1.04	1.00	697.7
	7	553.8	523.6	0.99	1.04	1.05	1.00	571.5
	8	601.5	552.8	1.07	1.04	1.05	1.00	647.1
	9	690.2	446.0	0.95	1.06	1.00	1.00	450.5
	10	641.5	619.1	0.95	1.06	1.04	1.00	654.1
	11	646.9	570.3	0.95	1.03	1.00	1.00	560.6
	12	755.3	749.8	0.95	1.04	1.04	1.00	772.7
Bolong & Yuzhou, 1991	J4	1928.0	1398.4	1.03	1.03	1.00	1.00	1481.0
	J5	1787.0	1449.0	1.03	1.03	1.00	1.00	1534.6
	J6	2412.0	1749.1	1.03	1.03	1.06	1.00	1955.9
Kaku & Asakusa, 1991	3	232.7	221.3	0.93	1.00	1.00	1.00	205.8
	4	256.3	229.1	0.91	1.08	1.00	1.00	225.1
	5	236.6	207.6	0.91	1.05	1.00	1.00	196.8
	6	224.3	217.8	0.91	1.00	1.00	1.00	197.5
	9	252.8	218.4	0.93	1.00	1.00	1.00	203.3
	11	247.4	221.9	0.91	1.04	1.00	1.00	209.2
	12	222.4	203.1	0.91	1.00	1.00	1.00	184.2
	13	224.3	233.5	0.93	1.00	1.00	1.00	217.3
	14	242.0	219.5	0.91	1.04	1.00	1.00	207.0
	15	246.9	216.0	0.91	1.04	1.00	1.00	204.0
Joh et al., 1991a)	B8-MH	306.6	432.6	0.93	1.07	1.00	1.00	429.3
	B8-LH	304.3	423.3	0.91	1.07	1.00	1.00	414.7
	B9	358.7	413.0	0.94	1.08	1.00	1.00	420.0

Table 4.2 Basic and Final Shear Strength Predictions (cont'd)

Research.	Spec.	$V_{j,exp}$ kN	$V_{j,pre.,basic}$ kN	SR	AxF	SF	Load. Fact.	$V_{j,pre.}$ kN
(cont'd)	B10	394.5	407.3	0.94	1.08	1.00	1.00	415.1
	B11	401.5	415.4	0.94	1.08	1.00	1.00	422.1
Sugano et al., 1991	J4-0	1409.3	988.9	1.07	1.17	1.00	1.00	1232.6
	J6-0	1676.2	1395.1	1.07	1.08	1.00	1.00	1615.3
	J8-0	1633.5	1579.6	1.07	1.07	1.00	1.00	1797.9
	J8H-0	2146.0	1605.3	1.07	1.06	1.00	1.00	1823.6
Murty et al., 2003	P1	232.2	303.6	0.94	1.00	1.00	1.00	284.9
	P2	274.2	298.0	0.94	1.00	1.00	1.00	279.6
	P3	244.3	301.9	0.94	1.00	1.00	1.00	283.3
	Q1	212.7	294.0	0.94	1.00	1.00	1.00	275.9
	Q2	297.4	303.0	0.94	1.00	1.00	1.00	284.4
	Q3	287.3	301.3	0.94	1.00	1.00	1.00	282.8
	R1	235.2	319.3	0.94	1.00	1.00	1.00	299.6
	R2	313.5	303.6	0.94	1.00	1.00	1.00	284.9
Murty et al., 2003 (cont'd)	R3	295.3	302.5	0.94	1.00	1.00	1.00	283.8
	S1	221.4	306.3	0.72	1.00	1.00	1.00	220.6
	S2	295.3	300.8	0.72	1.00	1.00	1.00	216.6
	S3	268.8	318.8	0.72	1.00	1.00	1.00	229.5
Park, 2002	O1	562.9	785.0	0.72	1.00	1.00	1.00	565.2
Higazy et al., 1996	SB1	151.9	141.0	0.99	1.03	1.00	1.00	143.5
	SB2	133.5	140.9	0.99	1.00	1.00	1.00	139.9
Meinheit & Jirsa, 1977	I	1089.8	828.9	0.94	1.20	1.00	1.00	934.1
	II	1596.8	1046.7	0.94	1.13	1.00	1.00	1107.1
	III	1227.6	835.4	0.94	1.20	1.00	1.00	938.5
	IV	1454.5	994.9	0.92	1.15	1.00	1.00	1056.0
	V	1530.1	969.6	0.94	1.02	1.00	1.00	927.9
	VI	1645.8	981.6	0.94	1.24	1.00	1.00	1144.0
	VII	1467.8	1010.9	0.92	1.24	1.00	1.00	1155.2
	VIII	1721.4	1330.8	0.94	1.16	1.00	1.00	1446.4
	IX	1596.8	1131.0	0.94	1.17	1.00	1.00	1246.5
	X	1476.7	1104.3	0.94	1.18	1.00	1.00	1221.8
	XI	1285.5	1060.4	0.92	1.21	1.00	1.00	1185.7
	XII	1948.2	960.2	1.13	1.15	1.00	1.00	1253.3
	XIII	1556.8	1040.6	1.09	1.13	1.00	1.00	1280.7
	XIV	1539.0	954.1	1.05	1.16	1.00	1.00	1167.0
Paulay et al., 1981	UNIT 2	990.0	731.4	1.07	1.08	1.00	1.00	841.9
	UNIT 3	752.5	799.7	0.95	1.03	1.00	1.00	781.7
Hwang et al., 2005	0T0	997.0	1058.1	0.72	1.01	1.00	1.00	768.1
	3T3	1132.0	1071.4	0.95	1.01	1.00	1.00	1023.5
	2T4	1080.0	1086.8	0.94	1.01	1.00	1.00	1031.4

Table 4.2 Basic and Final Shear Strength Predictions (cont'd)

Research.	Spec.	$V_{j,exp}$ kN	$V_{j,pre.,basic}$ kN	SR	AxF	SF	Load. Fact.	$V_{j,pre.}$ kN
(cont'd)	1T44	1039.0	1100.5	0.97	1.01	1.00	1.00	1070.5
Karayannis et al., 2008	A0	85.1	186.6	0.72	1.03	1.00	1.00	137.7
	A1	87.9	186.6	0.92	1.03	1.00	1.00	176.7
	A2	91.1	186.6	0.94	1.03	1.00	1.00	179.5
	B0	205.0	279.9	0.72	1.03	1.00	1.00	206.6
	B1	225.7	279.9	0.92	1.03	1.00	1.00	265.0
	C0	226.7	279.9	0.72	1.03	1.00	1.00	206.6
	C1	219.7	279.9	0.94	1.03	1.00	1.00	269.3
J.-Y. Lee et al., 2009	J1	1219.8	836.0	1.03	1.00	1.00	1.00	858.5
	BJ1	979.1	836.0	1.03	1.00	1.00	1.00	858.5
	BJ2	845.6	836.0	0.96	1.00	1.00	1.00	799.0
	BJ3	719.7	836.0	0.96	1.00	1.00	1.00	799.0
	B1	571.2	836.0	0.96	1.00	1.00	1.00	799.0
Behnam et al., 2017	S3-BC2	866.1	738.8	1.08	1.06	1.00	1.00	847.6
	S4BC2.5	1049.3	738.8	1.08	1.06	1.00	1.00	847.6
Briss et al., 1978	B1	1289.2	1140.2	1.03	1.03	1.00	1.00	1204.3
	B2	1306.3	1211.5	0.92	1.22	1.00	1.00	1352.6
Park & Milburn, 1983	1	991.4	809.5	1.13	1.05	1.00	1.00	963.8
	2	1038.9	862.6	1.07	1.05	1.00	1.00	968.7
	3	656.6	778.5	0.95	1.05	1.00	1.00	776.9
	4	657.2	561.2	0.97	1.05	1.00	1.00	571.1
Park & Ruitong, 1988	4	551.1	797.7	0.99	1.00	1.00	1.00	785.8
Leon, 1990	BCJ3	378.0	407.9	0.92	1.00	1.00	1.00	376.8
	BCJ4	414.0	354.8	0.92	1.00	1.00	1.00	326.2
Noguchi & Kashiwazaki, 1992	OKJ1	925.6	720.8	0.97	1.06	1.00	1.00	742.9
	OKJ2	920.4	720.8	0.97	1.06	1.00	1.00	742.9
	OKJ3	1157.0	886.6	0.97	1.06	1.00	1.00	913.7
	OKJ4	977.6	720.8	0.97	1.06	1.00	1.00	742.9
	OKJ5	962.0	720.8	0.97	1.06	1.00	1.00	742.9
	OKJ6	852.2	626.9	0.97	1.06	1.00	1.00	646.1
Hegger et al., 2003	RK4	357.0	179.0	1.14	1.16	1.00	1.00	236.6
	RK5	423.0	184.5	1.14	1.15	1.00	1.00	242.3
	RK6	556.0	231.6	1.14	1.10	1.00	1.00	289.5
	RK7	277.0	184.2	1.10	1.15	1.00	1.00	234.0
	RK8	273.0	154.7	1.14	1.22	1.00	1.00	214.0
	RA1	527.0	304.8	0.72	1.13	1.00	1.00	248.0
	RA2	597.0	340.1	1.01	1.10	1.00	1.00	378.0
	RA3	504.0	276.2	1.11	1.16	1.00	1.00	355.1
	RA4	771.0	340.1	1.11	1.07	1.00	1.00	404.5
	RA5	494.0	313.6	1.05	1.12	1.00	1.00	368.5

Table 4.2 Basic and Final Shear Strength Predictions (cont'd)

Research.	Spec.	$V_{j,exp}$ kN	$V_{j,pre.,basic}$ kN	SR	AxF	SF	Load. Fact.	$V_{j,pre.}$ kN
(cont'd)	RA6	663.0	392.0	1.05	1.13	1.00	1.00	462.5
	RA7	770.0	373.5	1.16	1.08	1.00	1.00	466.0
Li & Leong, 2015	NS2	916.7	1124.9	1.06	1.00	1.00	1.00	1196.8
	NS3	1080.4	1118.5	1.10	1.00	1.00	1.00	1229.8
	NS4	724.0	1116.6	1.07	1.00	1.00	1.00	1197.3
Attaalla, 1997	SOC3	133.0	180.2	1.03	1.03	1.00	1.00	191.0
	SHC1	127.0	197.3	0.95	1.02	1.00	1.00	191.5
	SHC2	145.0	202.5	1.03	1.02	1.00	1.00	214.0
Kun, 2003	H:0.0	869.3	681.9	1.11	1.00	1.00	1.00	753.7
	E:0.3	813.9	650.9	0.72	1.15	1.00	1.00	538.9
	H:0.3	743.9	643.8	1.11	1.15	1.00	1.00	818.3
Wong & Kuang, 2008	BS-L	315.5	387.6	0.72	1.08	1.00	1.00	300.0
	BS-OL	219.1	387.6	0.72	1.08	1.00	1.00	300.0
	BS-LL	398.8	452.4	0.72	1.08	1.00	1.00	350.1
	BS-U	341.2	388.2	0.72	1.08	1.00	1.00	300.5
	BS-L-LS	344.9	391.9	0.72	1.08	1.00	1.00	303.3
	L-V2T10	398.8	398.1	0.72	1.08	1.00	1.00	308.1
	L-V4T10	402.9	370.9	0.72	1.08	1.00	1.00	287.1
	L-H1T10	389.3	402.3	0.92	1.08	1.00	1.00	396.7
Wong & Kuang, 2008 (cont'd)	L-H2T10	479.3	452.4	0.93	1.08	1.00	1.00	451.0
	BS-L-600	283.9	420.6	0.72	1.08	1.00	1.00	325.6
	JA-NN03	304.2	466.7	0.72	1.02	1.00	1.00	341.0
	JA-NN15	325.1	472.9	0.72	1.08	1.00	1.00	366.0
	JB-NN03	317.0	480.0	0.72	1.02	1.00	1.00	350.8
	JA-NY03	302.6	411.9	0.93	1.02	1.00	1.00	389.5
	JA-NY15	323.7	432.6	0.93	1.08	1.00	1.00	433.2
Lehman et al., 2004	PEER14	960.8	1216.7	0.72	1.05	1.00	1.00	919.8
	PEER0850	768.7	1276.5	0.72	1.05	1.00	1.00	965.1
	PEER995	1313.1	1678.6	0.72	1.05	1.00	1.00	1269.0
Uzumeri, 1977	1	626.7	721.6	0.72	1.26	1.00	1.00	654.1
	2	608.9	604.7	0.72	1.26	1.00	1.00	546.9
	5	608.0	816.9	0.72	1.25	1.00	1.00	734.9
Parker & Bullman, 1997	4a	194.5	428.7	0.72	1.00	1.00	1.00	308.7
	4b	227.5	428.7	0.72	1.04	1.00	1.00	321.8
	4c	280.3	415.4	0.72	1.09	1.00	1.00	324.8
	4d	247.3	428.7	0.72	1.00	1.00	1.00	308.7
	4e	263.8	433.1	0.72	1.04	1.00	1.00	324.8
	4f	301.7	419.9	0.72	1.09	1.00	1.00	329.1
	5a	351.2	445.9	0.94	1.00	1.00	1.00	419.2
	5b	389.1	450.1	0.94	1.04	1.00	1.00	439.5

Table 4.2 Basic and Final Shear Strength Predictions (cont'd)

Research.	Spec.	$V_{j,exp}$ kN	$V_{j,pre.,basic}$ kN	SR	AxF	SF	Load. Fact.	$V_{j,pre.}$ kN
(cont'd)	5c	399.0	450.1	0.94	1.08	1.00	1.00	455.8
	5d	372.6	450.1	0.96	1.00	1.00	1.00	433.0
	5e	486.4	458.3	0.96	1.04	1.00	1.00	457.3
	5f	530.9	450.1	0.96	1.08	1.00	1.00	466.4
Scott, 1992	C1	112.8	113.3	0.94	1.12	1.00	1.00	119.5
	C1A	115.4	124.3	0.94	1.10	1.00	1.00	128.6
	C1AL	94.7	103.6	0.94	1.03	1.00	1.00	99.9
	C2	92.5	126.0	0.94	1.10	1.00	1.00	130.1
	C3	111.5	107.6	0.94	1.14	1.00	1.00	114.8
	C3L	93.0	106.9	0.94	1.03	1.00	1.00	102.9
	C4	129.5	115.5	0.94	1.12	1.00	1.00	121.4
	C4A	138.6	119.4	0.94	1.11	1.00	1.00	124.7
	C4AL	123.4	107.2	0.94	1.02	1.00	1.00	103.4
	C5	60.1	103.1	0.94	1.15	1.00	1.00	111.3
	C6	95.0	113.2	0.94	1.12	1.00	1.00	119.6
	C6L	113.3	121.4	0.94	1.02	1.00	1.00	116.4
	C7	87.2	106.4	0.92	1.14	1.00	1.00	111.9
	C8	74.4	119.6	0.92	1.11	1.00	1.00	122.6
	C9	76.0	107.5	0.92	1.14	1.00	1.00	112.7

4.3 Determination of Joint Shear Performance Points

4.3.1 Definition of Joint Shear Performance Points

Under cyclic loading with high drift ratios, joint shear-strain relationship well exceeds the elastic range. From the experimental data gathered from selected subassemblies, it is determined that the joint response can be idealized using 5 performance points. The idealization of the experimental joint shear force – joint shear strain relationship acquired by Shin (Shin & LaFave, 2004) is presented in Figure 4.5.

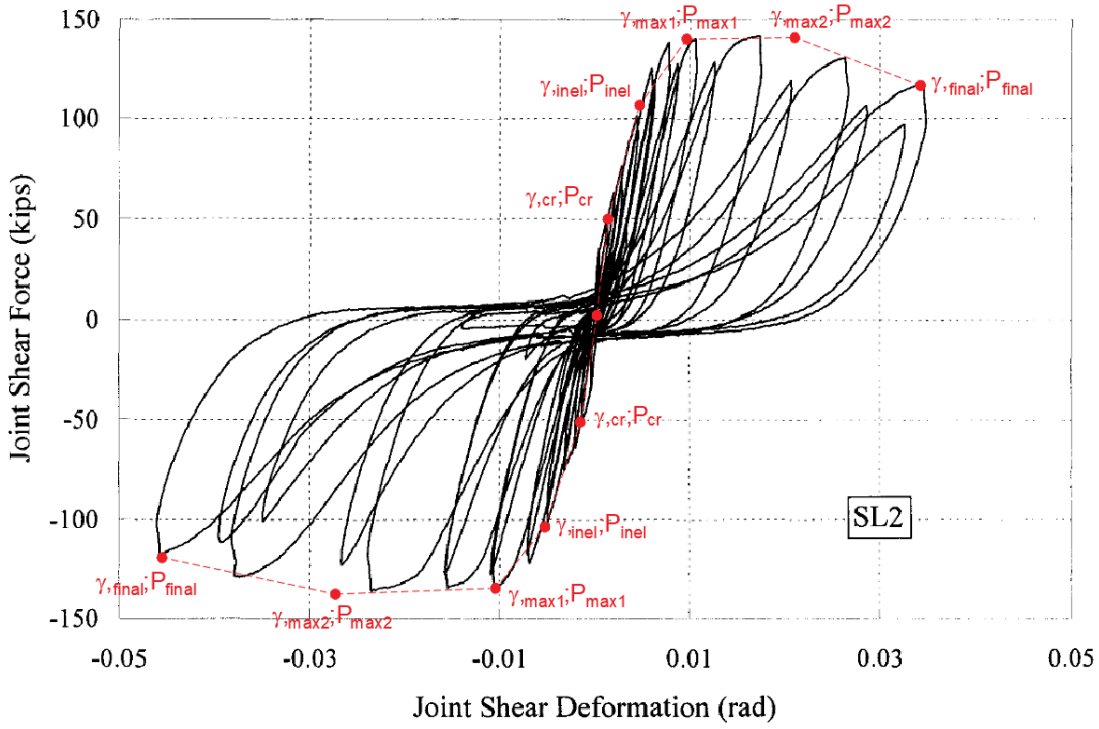


Figure 4.5. Joint Shear Force vs Joint Shear Strain Schematical Presentation

The behavior of reinforced concrete beam-column joints under excessive seismic deformations can be idealized by the selection of performance points. In the first phase, the joint undergoes a minor deformation with the formation of cracks identified as γ_{cr} in Figure 4.5. After the formation of cracks, joint rigidity slightly

reduces and the stress-strain response remains almost linear up to inelasticity point, γ_{inel}. As the inelastic strains accumulate, the curve reaches the maximum point, γ_{max1}, where the joint shear strength is reached. After this point, a plateau between γ_{max1} and γ_{max2} is observed, in which a minor strain hardening is observed which is taken as 2.0 % in the joint shear stress-strain model, ASCE 41-17 considers an allowable strain hardening limit of 6 for panel zones. Finally, strength degradation is observed where the beam-column joint capacity reduces considerably.

It must be noted that the number of experimental investigations that present the joint shear force – joint shear strain data is limited. Moreover, since not all the joints undergo excessive deformations under cyclic loading, the benchmark data for points γ_{max2} and γ_{final} are significantly limited. Consequently, the post-plateau behavior of joints is defined considering ASCE/SEI 41 nonlinear response recommendations as well as available experimental data.

To determine the nonlinear beam-column joint, available graphical data is digitized using an open-source software, *Engauge Digitizer* version 12.1. Sample digitization process is presented in Figure 4.6.

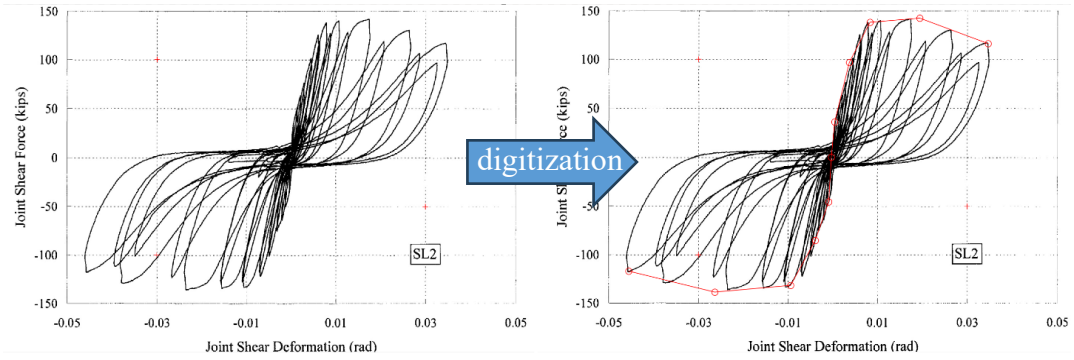


Figure 4.6. Digitization of Joint Shear Force vs Shear Strain Curves

Definition of joint shear stress components for the performance points is based on the proposed joint shear strength, $V_{j,pre.}$ Statistical data gathered from experimental force vs. strain curves are utilized to determine the performance points considering material and geometrical properties of the joints. Finally, strain Modification factors are derived for performance points. The algorithm for obtaining the joint force-strain

relationship is presented in Figure 4.7, which is explained in detail in the following sections.

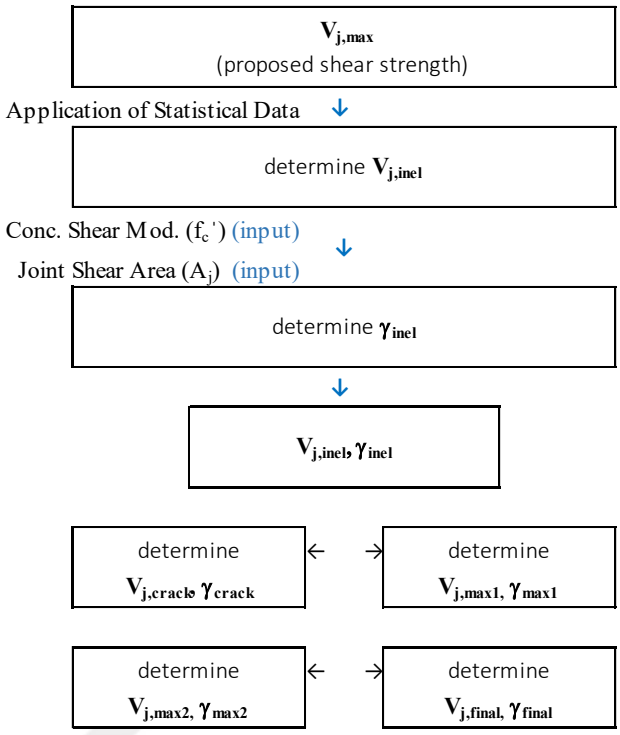


Figure 4.7. Joint Performance Points Determination Flowchart

4.3.2 Prediction of Inelasticity Point P_{inel}

The key point in developing the analytical model for the relationship between shear force and shear deformation of beam-column joints is identified as the inelastic point, P_{inel}, where the inelastic behavior becomes predominant represented by the significant reduction in the slope. This point is selected as the key point because the strain can be more accurately determined owing to the significant reduction in stiffness at this point.

Furthermore, since most of the experimental data of joint shear force versus shear strain response lack information on P_{max2} and P_{final} points due to constraints in either

the experimental setup or measuring instruments, P_{inel} emerges as the most dependable reference point for predicting the joint shear deformation.

Basic Joint Shear Strain Prediction for P_{inel}

In the initial estimation of the joint shear strain at the point of inelasticity (P_{inel}), a procedure similar to the joint shear strength prediction is employed. Initially, all data on shear force versus shear strain relationship are converted into digital format by *'Engauge Digitizer'*. Subsequently, the digitized shear force versus shear strain curves are transformed into linear form for five performance points, as depicted in Figure 4.6. The ratio of shear force at P_{inel} to the maximum joint shear capacity is computed as 0.682 statistically based on the experimental data.

$$V_{j,inel\ (exp)} = 0.682\ V_{j\ (exp)} \tag{4.19}$$

Based on the linear correlation between the shear modulus and modulus of elasticity, joint effective shear modulus utilized to predict the inelastic performance point, is considered to be 30% of the elastic shear modulus. Then, the shear strain at the inelasticity point is computed as presented in Eqn. 4.21.

$$G_{inel.} = G_{elastic} \times 0.30 \tag{4.20}$$

$$\gamma_{inel,basic} = \frac{v_{j0,inel}}{G_{inel.}} \tag{4.21}$$

4.3.3 Construction of the Joint Shear Response Curve

After the analysis of the experimental data for joint shear force vs joint shear strain, the basic ratios for analytical shear force and shear strain predictions are structured.

The average ratios obtained from experimental data and the proposed shear strain and force ratios are summarized in Table 4.3. Since experimental data for $\gamma_{j,max2}$ and $\gamma_{j,final}$ are limited, in the determination of proposed ratios for strain data is based on graphical verification of models carried out by Burak & Wight (2008); Raffaelle & Wight (1995); and Shin & LaFave (2004) which lead to a more accurate

representation of the nonlinear behavior as will be discussed in the following sections.

Table 4.3 Experimental and Analytical Ratios for Strain and Force Couples at the Performance Points

	Shear Force Ratios		Shear Strain Ratios	
	Experimental	Proposed	Experimental	Proposed
Cracking Pt.	0.341	**0.30**	0.097	**0.10**
Inel.Pt.	0.695	**0.70**	0.348	**0.30**
Max1 Pt.	1.000	**1.00**	1.000	**1.00**
Max2 Pt	1.000	**1.02**	2.368	**3.00**
Fail.Pt.	0.84	**0.90**	3.896	**7.00**

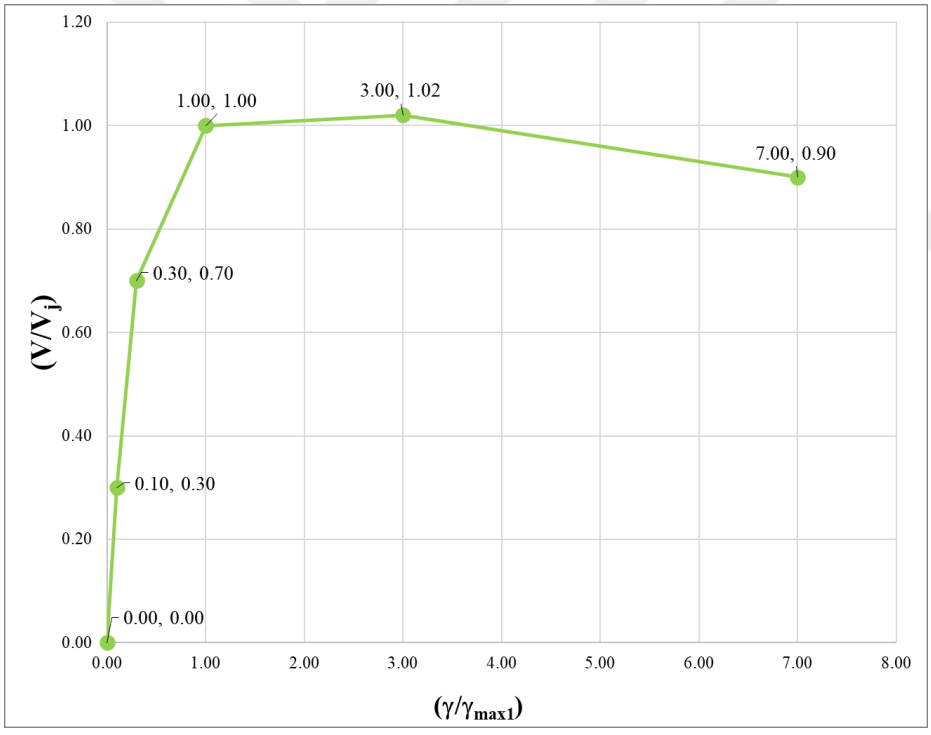


Figure 4.8. Proposed Joint Shear Force vs. Strain Response

The basic shear force shear strain curve is later modified by the application of additional Modification factors due to beam confinement and shear reinforcement

application within the joint volume. The details of modification factors and computation of strain values are presented in Section 4.2.2.

4.4 Modification Factors for Strain Points

In the analysis of both the joint shear strength and joint shear performance points of the experimental data presented in Section 3.5, it is identified that two of the most important characteristics are the confinement provided by the adjoining members to the joint and shear reinforcement applied in the joint volume.

As presented in Section 4.2.1, the edge point for member confinement is determined as 14, whereas the critical single layer volumetric joint shear reinforcement ratio ($\rho_{singlelayer,core}$) is defined as 1.0 %. Studying the experimental data, also considering the lack of dependable experimental data for γ_{max2} and γ_{final} points, Modification points to account for the lack of confinement provided by adjoining members and shear reinforcement within the joint volume is deemed necessary.

Strain Modification Factor due to Beam Confinement

In relation to the shear strength factor defined, for members with a factor less than 14, a strain enhancement factor is defined as presented in Eqn. 4.22. In order to determine the best fit, correlation of several modification factor alternatives are evaluated and the equation that minimizes the error is determined as $(14/\gamma)^2$.

$$F_{BC} = \begin{cases} 1.0 & \text{for beam-column joints with } \gamma \geq 14.0 \\ -0.25\,\gamma + 4.5 & \text{for beam-column joints with } \gamma < 14.0 \end{cases} \quad (4.22)$$

which leads to a strain enhancement factor of 2.5 for joints with shear strength factor of 8.0. The equation is graphically presented in Figure 4.9.

.

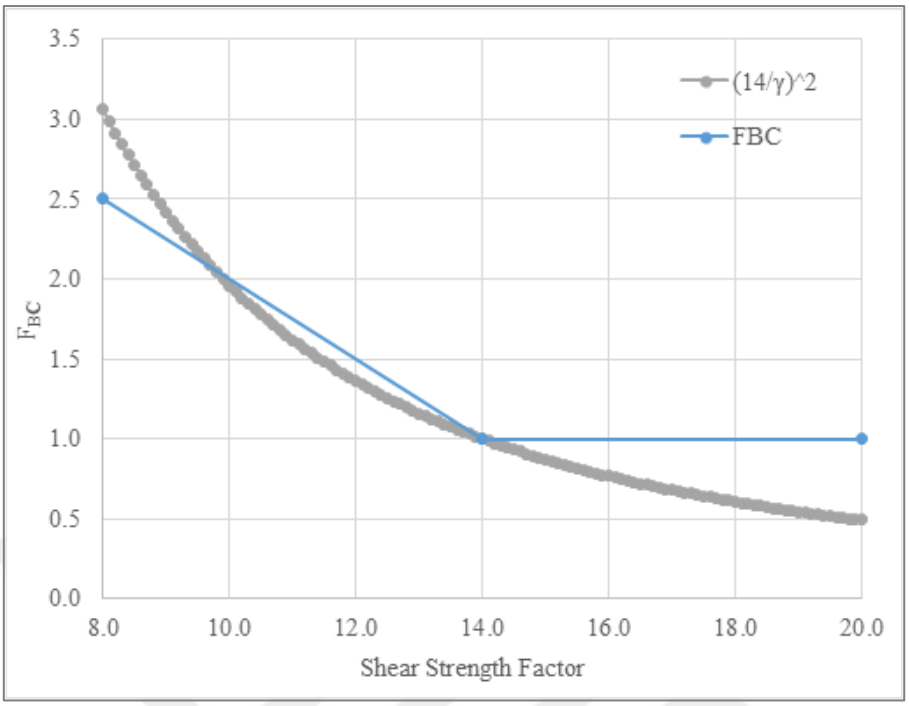


Figure 4.9. Graphical Representation of Strain Modification Factor F_{BC}

Strain Modification Factor due to Shear Reinforcement in the Joint Volume

Similar to the effect of inadequate confinement provided by adjoining members to the joint, the deficiency of shear reinforcement presence in the joint volume leads to increased strains than expected values.

After the evaluation of several alternatives for strain modification factor for shear reinforcement, the alternative which optimizes the shear strain behavior is determined as $(0.01 / \rho_{singlelayer,core})$. To simplify the definition of the factor, the following coefficients are identified as enhancement factors for joint shear strain points γ_{inel}, γ_{max1}, γ_{max2} and γ_{final}.

$$F_{SR} = \begin{cases} 1.0 & \text{for joints with } \rho_{singlelayer,core} \geq 1.0\ \% \\ 2.0 - 100\ \rho_{singlelayer,core} & \text{for joints with } \rho_{singlelayer,core} < 1.0\ \% \end{cases} \quad (4.23)$$

which leads to a strain enhancement factor of 2.0 for joints with no shear reinforcement and 1.0 for joints with joints with $\rho_{singlelayer,core} \geq 1.0$ % The equation is graphically presented in Figure 4.10.

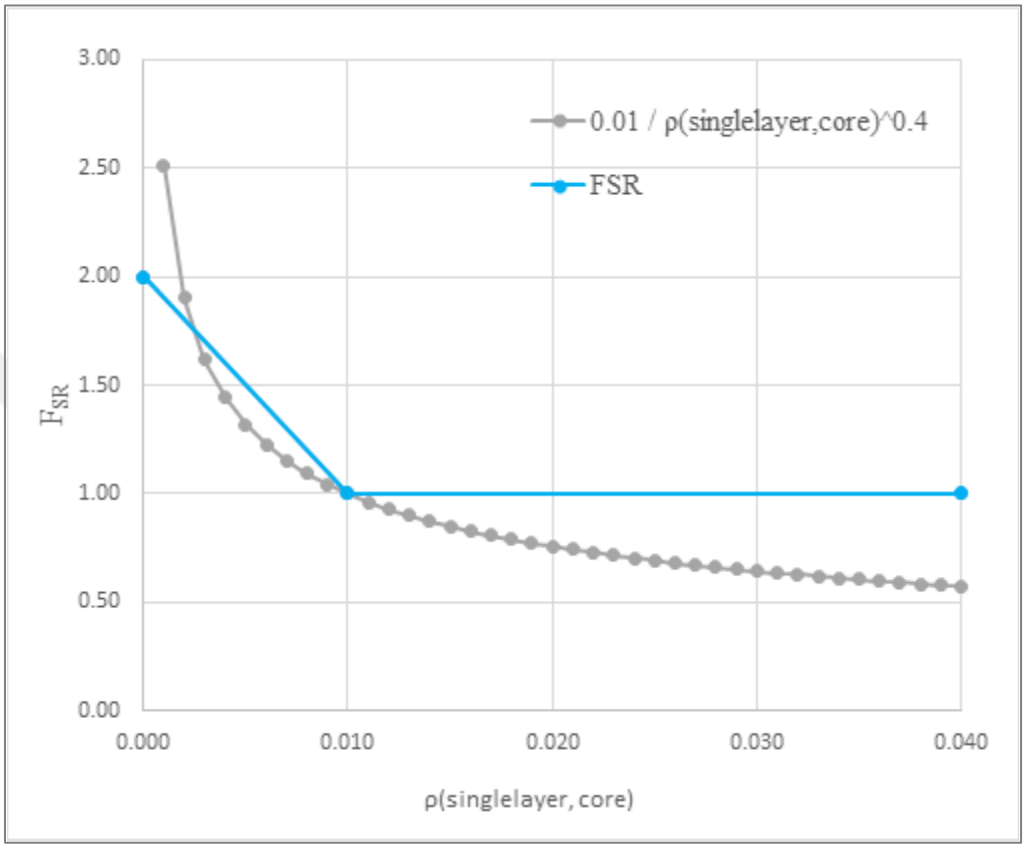


Figure 4.10. Graphical Representation of Strain Modification Factor F_{SR}

4.5 Construction of the Final Joint Shear Behavior Curve

The completion of the analytical study involves the creation of an analytical model that foresees the relationship between shear force and shear strain in beam-column connections when subjected to cyclic loading. The final model is developed considering a wide array of geometric and material characteristics, as previously mentioned. Below is a summary of the proposed equations, along with a graphical representation illustrating the shear force versus shear strain response, highlighting key performance points. The coefficients utilized are derived from the mean error

values and studying a number of alternatives to best fit the experimental data, within the compiled database of experimental studies.

Joint Shear Strength Prediction Equations

$$V_{j,pre.,basic} = 0.083\,\gamma\,\sqrt{f_c'}\,b_j$$

$$V_{j,pre.} = V_{j,pre.,basic}\,(SR)\,(AxF)\,(SF)$$

After the joint shear strength is determined, joint shear performance points are defined in relation to $V_{j,pre.}$.

$$\begin{aligned}
&\text{Point } 01, \quad V_{j,cr} = V_{j,pre.} \times 0.30\\
&\text{Point } 02, \quad V_{j,inel} = V_{j,pre.} \times 0.70\\
&\text{Point } 03, \quad V_{j,max1} = V_{j,pre.} \times 1.00\\
&\text{Point } 04, \quad V_{j,max2} = V_{j,pre.} \times 1.02\\
&\text{Point } 05, \quad V_{j,fail} = V_{j,pre.} \times 0.90
\end{aligned} \tag{4.24}$$

Joint Shear Strain Performance Points Prediction Equations

After the definition of joint force at inelasticity point, $V_{j,inel}$, shear strain expected at inelasticity point is determined accordingly, as previously presented in Eqn. 4.21.

$$\gamma_{inel,basic} = \frac{v_{j0,inel}}{G_{inel}}$$

As the strain prediction for inelasticity point is computed, the basic strain points are defined considering the mean values of experimental data presented in the database.

After the application of Modification factors for beam-column joints with shear strength factors less than 14 and with single layer core volumetric shear reinforcement rations ($\rho_{singlelayer,core}$) less than 1.0 %, the final curve for the shear behavior of beam-column connections is defined as in Figure 4.11.

Point 01, $\gamma_{j,cr} = \gamma_{j,max} \times 0.10$

Point 02, $\gamma_{j,inel} = \gamma_{j,max} \times 0.30$

Point 03, $\gamma_{j,max1} = \gamma_{j,max} \times 1.00$ (4.25)

Point 04, $\gamma_{j,max2} = \gamma_{j,max} \times 3.00$

Point 05, $\gamma_{j,fail} = \gamma_{j,max} \times 7.00$

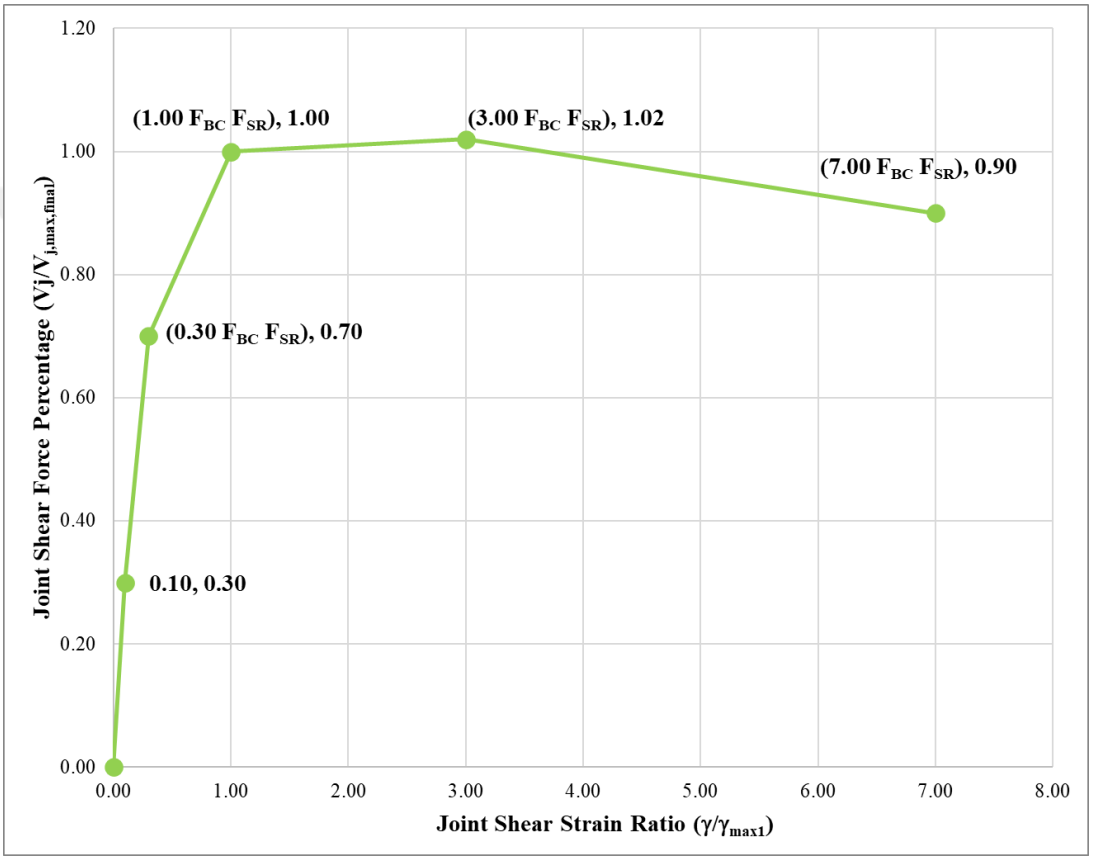


Figure 4.11. Graphical Representation of Final Behavior Curve Definition for Joints

CHAPTER 5

VERIFICATION OF JOINT SHEAR STRENGTH PREDICTION

5.1 Overview

In this section of the thesis, the accuracy of the joint shear strength equation will be evaluated in the light of joint shear strength equations provided in contemporary structural codes. The effect of each parameter in the joint shear strength prediction will be investigated and presented singularly and in combination with all considered parameters.

The basic joint shear strength predictions ($V_{j,pre.,basic}$), adjusted predictions considering each Modification factor and the final shear strength prediction ($V_{j,pre}$) will be compared to the joint shear capacity definitions of ACI 352-10, ACI 318 versions 2011, 2014 and 2019; and also, TEC versions 2007 and 2018 in order to evaluate the effectiveness of code revisions in terms of joint shear capacity predictions. Moreover, the comparison of the test results in the light of TEC2007 and TEC2018 enables to monitor the effect of compressive strength definition. TEC2007 is the only code utilizing the design compressive strength of concrete, f_{cd}, implying joint shear strength is based on the capacity of compression struts formed within the joint instead of the use of square root of characteristic compressive strength, $\sqrt{f_{ck}}$, representing tension failure in TEC2018 as discussed in Sections 2.7 and Section 2.8.

The precision of the shear capacity estimations in structural design codes greatly depends on the definition of minimum area and maximum spacing of shear reinforcement. When assessing the accuracy of shear strength predictions in structural codes, specimens are categorized as either "Conforming (C)" or "Nonconforming (NC)" considering the requirements provided in each structural code under evaluation. ASCE 41-17 stands out as the sole structural code that

provides predictions for the shear capacity of non-conforming specimens as well. The conformity requirements and detailed explanation of joint shear strength prediction procedures are presented in Section 2.2.

Table 5.1 provides the comparison of experimental joint shear strengths with design code equations based on absolute errors.

5.2 Evaluation of the Joint Shear Strength Predictions

The experimental shear strengths of the subassemblies in the database are compared with the shear capacity specifications of the structural codes and the proposed procedure for predicting joint shear strength, accounting for the specific criteria of each code individually.

The precision of the joint shear strength prediction for each structural code was initially evaluated by analyzing the absolute error for each specimen obtained by using Eqn 5.1 and the results are shown in Table 5.1. Additionally, the mean absolute error (MAE) values for various specimen types are calculated using Eqn. 5.2.

$$\text{Absolute Error (AE)} = \left| \frac{V_{j,pre} - V_{j,exp}}{V_{j,exp}} \right| \tag{5.1}$$

$$\text{Mean Absolute Error (MAE)} = \sum \frac{AE}{n} \tag{5.2}$$

where, “n” represents the number of subassemblies, where V_j denotes the joint shear strength, and the subscripts "pre" and "exp" indicate the predicted values by the structural codes and by the proposed equations and the experimental results, respectively.

Table 5.1 Comparison of Experimental Joint Shear Strengths with Code Predictions

Res.	Spec.	$V_{j,exp}$	ACI 352-10		ACI318-11		ACI 318-14		ACI 318-19		ASCE 41-17		CSA A23.03-19		TEC2007		TEC2018	
			V_j	AE	V_j	AE	V_j	AE	V_j,	AE	V_j	AE,	V_j	AE	V_j	AE	V_j	AE
		kN	kN	%	kN	%	kN	%	kN	%	kN	%	kN	%	kN	%	kN	%
Burak & Wight, 2008	1-S	778.4	489.3	37.1%	387.6	50.2%	484.5	37.8%	484.5	37.8%	484.5	37.8%	575.4	26.1%	558.8	28.2%	389.1	50.0%
	2-S	863.0	679.8	21.2%	561.8	34.9%	702.3	18.6%	702.3	18.6%	702.3	18.6%	953.3	10.5%	939.4	8.9%	564.1	34.6%
	3-S	827.4	586.2	29.2%	484.5	41.4%	605.6	26.8%	605.6	26.8%	605.6	26.8%	822.0	0.6%	698.5	15.6%	486.4	41.2%
	1-N	569.4	629.8	10.6%	678.2	19.1%	678.2	19.1%	678.2	19.1%	847.8	48.9%	575.4	1.1%	977.9	71.7%	681.0	19.6%
	2-N	809.6	1095.5	35.3%	1179.8	45.7%	1179.8	45.7%	1179.8	45.7%	1474.7	82.2%	1000.9	23.6%	1972	143.7%	1184.5	46.3%
	3-N	1156.5	1017.4	12.0%	1017.4	12.0%	1017.4	12.0%	1017.4	12.0%	1271.7	10.0%	863.1	25.4%	1466	26.8%	1021.4	11.7%
Raffaelle & Wight, 1995	1	650.8	577.5	11.3%	481.2	26.1%	601.5	7.6%	601.5	7.6%	601.5	7.6%	571.6	12.2%	689.2	5.9%	483.1	25.8%
	2	420.6	424.0	0.8%	326.1	22.5%	407.7	3.1%	407.7	3.1%	407.7	3.1%	553.4	31.6%	452.2	7.5%	327.4	22.1%
	3	469.7	530.4	12.9%	414.4	11.8%	517.9	10.3%	517.9	10.3%	517.9	10.3%	656.2	39.7%	681.3	45.0%	416.0	11.4%
	4	412.4	379.5	8.0%	296.5	28.1%	370.6	10.1%	370.6	10.1%	370.6	10.1%	469.5	13.9%	348.7	15.4%	297.6	27.8%
Shin & LaFave, 2004	SL 1	631.6	591.8	6.3%	502.7	20.4%	628.3	0.5%	628.3	0.5%	628.3	0.5%	697.8	10.5%	736.2	16.5%	504.7	20.1%
	SL 2	631.6	449.4	28.9%	351.5	44.4%	439.3	30.4%	439.3	30.4%	439.3	30.4%	596.4	5.6%	565.6	10.5%	352.9	44.1%
	SL3	671.7	834.2	24.2%	1035.6	54.2%	1035.6	54.2%	1294.5	92.7%	1294.5	92.7%	878.6	30.8%	1909.7	184.3%	1039.8	54.8%
	SL4	791.8	715.2	9.7%	715.2	9.7%	715.2	9.7%	715.2	9.7%	715.2	9.7%	597.4	24.5%	855.2	8.0%	574.5	27.4%
Gentry & Wight, 1994	1	689.9	829.9	20.3%	829.9	20.3%	829.9	20.3%	829.9	20.3%	829.9	20.3%	693.2	0.5%	936.9	35.8%	666.7	3.4%
	2	733.5	829.9	13.1%	829.9	13.1%	829.9	13.1%	829.9	13.1%	829.9	13.1%	693.2	5.5%	936.9	27.7%	666.7	9.1%
	3	829.4	967.7	16.7%	967.7	16.7%	967.7	16.7%	967.7	16.7%	967.7	16.7%	808.4	2.5%	1274.1	53.6%	777.3	6.3%
	4	934.3	967.7	3.6%	967.7	3.6%	967.7	3.6%	967.7	3.6%	967.7	3.6%	808.4	13.5%	1274.1	36.4%	777.3	16.8%
LaFave & Wight, 1999	EWB-1	857.4	847.2	1.2%	847.2	1.2%	847.2	1.2%	847.2	1.2%	847.2	1.2%	707.7	17.5%	976.5	13.9%	680.5	20.6%
	EWB-2	929.0	693.7	25.3%	693.7	25.3%	693.7	25.3%	693.7	25.3%	867.1	6.7%	588.5	36.6%	1023.0	10.1%	696.5	25.0%
	EWB-3	1244.4	905.5	27.2%	905.5	27.2%	905.5	27.2%	905.5	27.2%	1131.9	9.0%	768.2	38.3%	1423.4	14.4%	909.1	26.9%

Table 5.1 Comparison of Experimental Joint Shear Strengths with Code Predictions (cont'd)

Res.	Spec.	$V_{j,exp}$	ACI 352-10		ACI318-11		ACI 318-14		ACI 318-19		ASCE 41-17		CSA A23.03-19		TEC2007		TEC2018	
			V_j	AE	V_j	AE	V_j	AE	V_j,	AE	V_j	AE,	V_j	AE	V_j	AE	V_j	AE
		kN	kN	%	kN	%	kN	%	kN	%	kN	%	kN	%	kN	%	kN	%
(cont'd)	ENB-1	688.4	768.3	11.6%	768.3	11.6%	768.3	11.6%	768.3	11.6%	960.4	39.5%	651.8	5.3%	1024.9	48.9%	771.4	12.1%
Quintero-Febres & Wight, 2001	IWB-1	1386.1	1253.6	9.6%	1253.6	9.6%	1253.6	9.6%	1253.6	9.6%	1253.6	9.6%	1079.9	22.1%	1804.0	30.1%	1283.8	7.4%
	IWB-2	1352.9	1100.4	18.7%	1100.4	18.7%	1100.4	18.7%	1100.4	18.7%	1100.4	18.7%	948.0	29.9%	1390.1	2.7%	1126.9	16.7%
	IWB-3	1510.2	1403.5	7.1%	1403.5	7.1%	1403.5	7.1%	1403.5	7.1%	1403.5	7.1%	1209.1	19.9%	1704.7	12.9%	1437.4	4.8%
Durrani & Wight, 1985	X1	1005.0	846.8	15.7%	955.7	4.9%	955.7	4.9%	955.7	4.9%	955.7	4.9%	798.4	20.6%	1199.5	19.4%	767.7	23.6%
	X2	1054.8	838.2	20.5%	946.1	10.3%	946.1	10.3%	946.1	10.3%	946.1	10.3%	790.3	25.1%	1175.5	11.4%	759.9	28.0%
	X3	803.5	804.9	0.2%	908.5	13.1%	908.5	13.1%	908.5	13.1%	908.5	13.1%	758.9	5.6%	1083.9	34.9%	729.7	9.2%
	S1	1411.7	1242.3	12.0%	1402.2	0.7%	1402.2	0.7%	1402.2	0.7%	1402.2	0.7%	1208.0	14.4%	2178.7	54.3%	1436.0	1.7%
	S2	1384.6	1068.4	22.8%	1206.0	12.9%	1206.0	12.9%	1206.0	12.9%	1206.0	12.9%	1038.9	25.0%	1611.4	16.4%	1235.0	10.8%
	S3	1029.1	1024.4	0.5%	1156.3	12.4%	1156.3	12.4%	1156.3	12.4%	1156.3	12.4%	996.1	3.2%	1481.4	44.0%	1184.1	15.1%
Joh et al., 1991b	JXO-B1	285.3	310.1	8.7%	413.5	45.0%	413.5	45.0%	516.9	81.2%	516.9	81.2%	350.8	23.0%	510.7	79.0%	415.2	45.5%
	JXO-B3	299.8	313.0	4.4%	417.3	39.2%	417.3	39.2%	521.6	74.0%	521.6	74.0%	354.0	18.1%	520.1	73.5%	419.0	39.7%
	JXO-B5	289.9	279.7	3.5%	215.2	25.8%	269.0	7.2%	269.0	7.2%	269.0	7.2%	365.1	25.9%	276.5	4.6%	216.0	25.5%
	JXO-B6	273.7	275.5	0.6%	211.9	22.6%	264.9	3.2%	264.9	3.2%	264.9	3.2%	359.6	31.4%	268.3	2.0%	212.8	22.3%
Fujii & Morita, 1991	A1	418.5	264.0	36.9%	305.7	27.0%	305.7	27.0%	382.1	8.7%	382.1	8.7%	259.3	38.0%	518.9	24.0%	306.9	26.7%
	A2	385.6	264.0	31.5%	305.7	20.7%	305.7	20.7%	382.1	0.9%	382.1	0.9%	259.3	32.7%	518.9	34.6%	306.9	20.4%
	A3	418.5	264.0	36.9%	305.7	27.0%	305.7	27.0%	382.1	8.7%	382.1	8.7%	259.3	38.0%	518.9	24.0%	306.9	26.7%
	A4	427.5	264.0	38.2%	305.7	28.5%	305.7	28.5%	382.1	10.6%	382.1	10.6%	259.3	39.3%	518.9	21.4%	306.9	28.2%
	B1	250.1	228.1	8.8%	264.1	5.6%	264.1	5.6%	264.1	5.6%	264.1	5.6%	224.0	10.4%	387.3	54.9%	265.1	6.0%
	B2	217.2	228.1	5.0%	264.1	21.6%	264.1	21.6%	264.1	21.6%	264.1	21.6%	224.0	3.1%	387.3	78.3%	265.1	22.1%
	B3	277.0	228.1	17.7%	264.1	4.7%	264.1	4.7%	264.1	4.7%	264.1	4.7%	224.0	19.1%	387.3	39.8%	265.1	4.3%

Table 5.1 Comparison of Experimental Joint Shear Strengths with Code Predictions (cont'd)

Res.	Spec.	$V_{j,exp}$	ACI 352-10		ACI318-11		ACI 318-14		ACI 318-19		ASCE 41-17		CSA A23.03-19		TEC2007		TEC2018	
			V_j	AE	V_j	AE	V_j	AE	V_j,	AE	V_j	AE,	V_j	AE	V_j	AE	V_j	AE
		kN	kN	%	kN	%	kN	%	kN	%	kN	%	kN	%	kN	%	kN	%
(cont'd)	B4	291.9	228.1	21.9%	264.1	9.5%	264.1	9.5%	264.1	9.5%	264.1	9.5%	224.0	23.3%	387.3	32.7%	265.1	9.2%
Kurose et al., 1991	J1 (EW)	1825.3	1420.5	22.2%	1578.3	13.5%	1578.3	13.5%	1578.3	13.5%	1578.3	13.5%	1318.4	27.8%	1660.7	9.0%	1267.7	30.5%
	J2 (EW)	2617.8	2027.3	22.6%	2252.5	14.0%	2252.5	14.0%	2252.5	14.0%	2252.5	14.0%	1940.4	25.9%	2854.0	9.0%	2306.8	11.9%
	J2 (NS)	2393.1	1947.3	18.6%	2163.7	9.6%	2163.7	9.6%	2163.7	9.6%	2163.7	9.6%	1863.9	22.1%	2633.3	10.0%	2215.8	7.4%
	J3 (EW)	1834.4	1646.1	10.3%	1829.0	0.3%	1829.0	0.3%	1829.0	0.3%	1829.0	0.3%	1527.8	16.7%	2230.0	21.6%	1469.0	19.9%
	J3 (NS)	1896.7	1646.1	13.2%	1829.0	3.6%	1829.0	3.6%	1829.0	3.6%	1829.0	3.6%	1527.8	19.4%	2230.0	17.6%	1469.0	22.5%
Teng & Zhou, 2003	S1	717.3	514.9	28.2%	686.6	4.3%	686.6	4.3%	858.2	19.6%	858.2	19.6%	582.5	18.8%	1056.0	47.2%	689.3	3.9%
	S2	717.3	522.7	27.1%	522.7	27.1%	522.7	27.1%	653.4	8.9%	653.4	8.9%	591.3	17.6%	816.0	13.8%	524.8	26.8%
	S3	716.4	433.1	39.5%	353.5	50.6%	441.9	38.3%	441.9	38.3%	441.9	38.3%	599.9	16.3%	560.0	21.8%	355.0	50.5%
	S4	391.2	363.5	7.1%	484.7	23.9%	484.7	23.9%	605.8	54.9%	605.8	54.9%	411.2	5.1%	789.3	101.8%	486.6	24.4%
	S5	391.2	373.2	4.6%	373.2	4.6%	373.2	4.6%	466.5	19.2%	466.5	19.2%	422.2	7.9%	624.0	59.5%	374.7	4.2%
	S6	391.2	282.4	27.8%	245.6	37.2%	307.0	21.5%	307.0	21.5%	307.0	21.5%	416.7	6.5%	405.3	3.6%	246.6	37.0%
Lawrence	1	696.0	779.6	12.0%	599.7	13.8%	749.6	7.7%	749.6	7.7%	749.6	7.7%	1017.5	46.2%	773.3	11.1%	602.1	13.5%
Kusuhara et al., 2004	JE-0	418.1	362.3	13.3%	463.7	10.9%	463.7	10.9%	579.6	38.6%	579.6	38.6%	393.4	5.9%	645.1	54.3%	465.6	11.4%
	JE-55	395.8	343.4	13.2%	304.3	23.1%	380.4	3.9%	380.4	3.9%	380.4	3.9%	393.4	0.6%	423.4	7.0%	305.5	22.8%
	JE-55S	400.1	343.4	14.2%	304.3	23.9%	380.4	4.9%	380.4	4.9%	380.4	4.9%	393.4	1.7%	423.4	5.8%	305.5	23.6%
Shiohara & Kusuhara, 2006	A1	586.8	596.1	1.6%	596.1	1.6%	596.1	1.6%	596.1	1.6%	596.1	1.6%	497.9	15.1%	679.2	15.7%	478.8	18.4%
	B1	456.1	476.9	4.6%	476.9	4.6%	476.9	4.6%	476.9	4.6%	476.9	4.6%	404.6	11.3%	679.2	48.9%	478.8	5.0%
	B2	427.4	476.9	11.6%	476.9	11.6%	476.9	11.6%	476.9	11.6%	476.9	11.6%	404.6	5.3%	679.2	58.9%	478.8	12.0%
	C1	696.7	794.8	14.1%	794.8	14.1%	794.8	14.1%	794.8	14.1%	794.8	14.1%	684.7	1.7%	1018.8	46.2%	813.9	16.8%
Zaid et al.	S3	635.5	395.3	37.8%	474.3	25.4%	474.3	25.4%	592.9	6.7%	592.9	6.7%	402.4	36.7%	672.0	5.7%	476.2	25.1%

Table 5.1 Comparison of Experimental Joint Shear Strengths with Code Predictions (cont'd)

Res.	Spec.	$V_{j,exp}$	ACI 352-10		ACI318-11		ACI 318-14		ACI 318-19		ASCE 41-17		CSA A23.03-19		TEC2007		TEC2018	
			V_j	AE	V_j	AE	V_j	AE	V_j,	AE	V_j	AE,	V_j	AE	V_j	AE	V_j	AE
		kN	kN	%	kN	%	kN	%	kN	%	kN	%	kN	%	kN	%	kN	%
Guimaraes et al., 1993	J4 (EW)	2560.2	2168.9	15.3%	2409.9	5.9%	2409.9	5.9%	2409.9	5.9%	2409.9	5.9%	2076.0	18.9%	3266.8	27.6%	2468.0	3.6%
	J4 (NS)	2101.7	2168.9	3.2%	2409.9	14.7%	2409.9	14.7%	2409.9	14.7%	2409.9	14.7%	2076.0	1.2%	3266.8	55.4%	2468.0	17.4%
	J5 (EW)	4812.4	3403.1	29.3%	3781.2	21.4%	3781.2	21.4%	3781.2	21.4%	3781.2	21.4%	3257.3	32.3%	8042.4	67.1%	3872.4	19.5%
	J5 (NS)	4109.4	3403.1	17.2%	3781.2	8.0%	3781.2	8.0%	3781.2	8.0%	3781.2	8.0%	3257.3	20.7%	8042.4	95.7%	3872.4	5.8%
	J6 (EW)	4438.3	3700.3	16.6%	4111.5	7.4%	4111.5	7.4%	4111.5	7.4%	4111.5	7.4%	3541.8	20.2%	9508.5	114.2%	4210.6	5.1%
	J6 (NS)	4163.5	3700.3	11.1%	4111.5	1.3%	4111.5	1.3%	4111.5	1.3%	4111.5	1.3%	3541.8	14.9%	9508.5	128.4%	4210.6	1.1%
H.-J. Lee & Ko, 2008	W0	775.0	963.8	24.4%	1285.0	65.8%	1285.0	65.8%	1285.0	65.8%	1285.0	65.8%	1090.2	40.7%	1849.6	138.7%	1290.2	66.5%
	W75	780.0	988.5	26.7%	1318.0	69.0%	1318.0	69.0%	1318.0	69.0%	1318.0	69.0%	1118.2	43.4%	1945.6	149.4%	1323.3	69.6%
	W150	710.0	967.1	36.2%	1289.5	81.6%	1289.5	81.6%	1289.5	81.6%	1289.5	81.6%	1094.0	54.1%	1862.4	162.3%	1294.7	82.3%
Tsonos, 2007	E1	219.8	186.9	15.0%	186.9	15.0%	186.9	15.0%	186.9	15.0%	186.9	15.0%	158.5	27.9%	234.7	6.8%	187.6	14.6%
	G1	195.0	186.9	4.2%	186.9	4.2%	186.9	4.2%	186.9	4.2%	186.9	4.2%	158.5	18.7%	234.7	20.3%	187.6	3.8%
Alamed. & Ehsani, 1991	LL8	860.3	885.3	2.9%	935.4	8.7%	935.4	8.7%	935.4	8.7%	935.4	8.7%	793.6	7.8%	1860.0	116.2%	939.1	9.2%
	LH8	838.0	885.3	5.6%	935.4	11.6%	935.4	11.6%	935.4	11.6%	935.4	11.6%	793.6	5.3%	1860.0	121.9%	939.1	12.1%
	HL8	986.6	885.3	10.3%	935.4	5.2%	935.4	5.2%	935.4	5.2%	935.4	5.2%	793.6	19.6%	1860.0	88.5%	939.1	4.8%
	HH8	985.7	885.3	10.2%	935.4	5.1%	935.4	5.1%	935.4	5.1%	935.4	5.1%	793.6	19.5%	1860.0	88.7%	939.1	4.7%
	LL11	769.1	1038.1	35.0%	1096.8	42.6%	1096.8	42.6%	1096.8	42.6%	1096.8	42.6%	930.5	21.0%	2557.4	232.5%	1101.2	43.2%
	LH11	934.1	1038.1	11.1%	1096.8	17.4%	1096.8	17.4%	1096.8	17.4%	1096.8	17.4%	930.5	0.4%	2557.4	173.8%	1101.2	17.9%
	HL11	967.5	1038.1	7.3%	1096.8	13.4%	1096.8	13.4%	1096.8	13.4%	1096.8	13.4%	930.5	3.8%	2557.4	164.3%	1101.2	13.8%
	HH11	1020.9	1038.1	1.7%	1096.8	7.4%	1096.8	7.4%	1096.8	7.4%	1096.8	7.4%	930.5	8.8%	2557.4	150.5%	1101.2	7.9%
	LL14	877.6	1171.1	33.4%	1237.4	41.0%	1237.4	41.0%	1237.4	41.0%	1237.4	41.0%	1049.8	19.6%	3254.9	270.9%	1242.4	41.6%
	LH14	890.5	1171.1	31.5%	1237.4	38.9%	1237.4	38.9%	1237.4	38.9%	1237.4	38.9%	1049.8	17.9%	3254.9	265.5%	1242.4	39.5%

Table 5.1 Comparison of Experimental Joint Shear Strengths with Code Predictions (cont'd)

Res.	Spec.	$V_{j,exp}$	ACI 352-10		ACI318-11		ACI 318-14		ACI 318-19		ASCE 41-17		CSA A23.03-19		TEC2007		TEC2018	
			V_j	AE	V_j	AE	V_j	AE	V_j,	AE	V_j	AE,	V_j	AE	V_j	AE	V_j	AE
		kN	kN	%	kN	%	kN	%	kN	%	kN	%	kN	%	kN	%	kN	%
Ehsani & Wight, 1985	1	486.3	483.3	0.6%	518.5	6.6%	518.5	6.6%	518.5	6.6%	259.2	46.7%	439.9	9.5%	804.4	65.4%	520.5	7.0%
	2	502.6	493.1	1.9%	529.0	5.3%	529.0	5.3%	529.0	5.3%	264.5	47.4%	448.8	10.7%	837.4	66.6%	531.1	5.7%
	3	599.8	533.3	11.1%	572.1	4.6%	572.1	4.6%	572.1	4.6%	572.1	4.6%	485.4	19.1%	979.4	63.3%	574.4	4.2%
	4	623.3	557.1	10.6%	597.6	4.1%	597.6	4.1%	597.6	4.1%	597.6	4.1%	507.0	18.7%	1068.6	71.4%	600.0	3.7%
	5	573.7	680.6	18.6%	730.1	27.3%	730.1	27.3%	730.1	27.3%	389.4	32.1%	609.8	6.3%	1020.7	77.9%	586.4	2.2%
	6	601.4	655.3	9.0%	703.0	16.9%	703.0	16.9%	703.0	16.9%	703.0	16.9%	587.2	2.4%	946.4	57.4%	564.6	6.1%
	7	553.8	561.0	1.3%	601.8	8.7%	601.8	8.7%	601.8	8.7%	321.0	42.0%	502.7	9.2%	693.7	25.3%	483.4	12.7%
	8	601.5	592.2	1.5%	635.3	5.6%	635.3	5.6%	635.3	5.6%	635.3	5.6%	530.7	11.8%	773.0	28.5%	510.3	15.2%
	9	690.2	535.2	22.5%	569.2	17.5%	569.2	17.5%	569.2	17.5%	284.6	58.8%	482.9	30.0%	751.9	8.9%	571.5	17.2%
	10	641.5	663.3	3.4%	705.5	10.0%	705.5	10.0%	705.5	10.0%	376.2	41.3%	589.3	8.1%	739.1	15.2%	566.6	11.7%
	11	646.9	684.3	5.8%	727.8	12.5%	727.8	12.5%	727.8	12.5%	363.9	43.7%	617.4	4.6%	1229.0	90.0%	730.7	13.0%
	12	755.3	803.4	6.4%	854.4	13.1%	854.4	13.1%	854.4	13.1%	455.7	39.7%	713.7	5.5%	1084.1	43.5%	686.3	9.1%
Bolong & Yuzhou, 1991	J4	1928.0	1841.8	4.5%	2326.5	20.7%	2326.5	20.7%	2326.5	20.7%	2326.5	20.7%	1973.8	2.4%	4041.6	109.6%	2335.8	21.2%
	J5	1787.0	1908.4	6.8%	2410.6	34.9%	2410.6	34.9%	2410.6	34.9%	2410.6	34.9%	2045.2	14.4%	4339.2	142.8%	2420.3	35.4%
	J6	2412.0	1717.3	28.8%	2169.2	10.1%	2169.2	10.1%	2169.2	10.1%	2711.5	12.4%	1840.3	23.7%	3513.6	45.7%	2177.9	9.7%
Kaku & Asakusa, 1991	3	232.7	268.8	15.5%	311.3	33.8%	311.3	33.8%	311.3	33.8%	311.3	33.8%	264.1	13.5%	538.2	131.3%	312.5	34.3%
	4	256.3	278.3	8.6%	322.3	25.8%	322.3	25.8%	322.3	25.8%	322.3	25.8%	273.4	6.7%	576.9	125.1%	323.6	26.3%
	5	236.6	252.2	6.6%	292.0	23.4%	292.0	23.4%	292.0	23.4%	292.0	23.4%	247.8	4.7%	473.7	100.2%	293.2	23.9%
	6	224.3	264.6	18.0%	306.4	36.6%	306.4	36.6%	306.4	36.6%	306.4	36.6%	260.0	15.9%	521.4	132.4%	307.6	37.1%
	9	252.8	265.3	4.9%	307.2	21.5%	307.2	21.5%	307.2	21.5%	307.2	21.5%	260.6	3.1%	524.0	107.3%	308.4	22.0%
	11	247.4	269.5	8.9%	312.0	26.1%	312.0	26.1%	312.0	26.1%	312.0	26.1%	264.7	7.0%	540.8	118.6%	313.3	26.6%

Table 5.1 Comparison of Experimental Joint Shear Strengths with Code Predictions (cont'd)

Res.	Spec.	$V_{j,exp}$	ACI 352-10		ACI318-11		ACI 318-14		ACI 318-19		ASCE 41-17		CSA A23.03-19		TEC2007		TEC2018	
			V_j	AE	V_j	AE	V_j	AE	V_j,	AE	V_j	AE,	V_j	AE	V_j	AE	V_j	AE
		kN	kN	%	kN	%	kN	%	kN	%	kN	%	kN	%	kN	%	kN	%
Kaku & Asakusa (cont'd)	12	222.4	246.7	10.9%	285.6	28.4%	285.6	28.4%	285.6	28.4%	285.6	28.4%	242.3	9.0%	453.0	103.7%	286.7	28.9%
	13	224.3	283.6	26.4%	328.4	46.4%	328.4	46.4%	328.4	46.4%	328.4	46.4%	278.6	24.2%	598.9	166.9%	329.7	47.0%
	14	242.0	266.6	10.1%	308.7	27.5%	308.7	27.5%	308.7	27.5%	308.7	27.5%	261.9	8.2%	529.2	118.7%	309.9	28.1%
	15	246.9	262.3	6.2%	303.7	23.0%	303.7	23.0%	303.7	23.0%	303.7	23.0%	257.7	4.4%	512.4	107.5%	305.0	23.5%
Joh et al., 1991a	B8-MH	306.6	396.0	29.2%	475.2	55.0%	475.2	55.0%	594.0	93.7%	594.0	93.7%	403.1	31.5%	674.4	120.0%	477.1	55.6%
	B8-LH	304.3	387.4	27.3%	464.9	52.8%	464.9	52.8%	581.1	91.0%	581.1	91.0%	394.4	29.6%	645.6	112.2%	466.8	53.4%
	B9	358.7	378.0	5.4%	453.5	26.4%	453.5	26.4%	566.9	58.1%	566.9	58.1%	384.8	7.3%	614.4	71.3%	455.4	27.0%
	B10	394.5	372.8	5.5%	447.3	13.4%	447.3	13.4%	559.1	41.7%	559.1	41.7%	379.5	3.8%	597.6	51.5%	449.1	13.8%
	B11	401.5	380.2	5.3%	456.2	13.6%	456.2	13.6%	570.2	42.0%	570.2	42.0%	387.0	3.6%	621.6	54.8%	458.0	14.1%
Sugano et al., 1991	J4-0	1409.3	894.0	36.6%	1063.2	24.6%	1063.2	24.6%	1329.0	5.7%	1329.0	5.7%	902.0	36.0%	1569.5	11.4%	1067.4	24.3%
	J6-0	1676.2	1261.3	24.8%	1499.9	10.5%	1499.9	10.5%	1874.9	11.9%	1874.9	11.9%	1272.5	24.1%	3123.8	86.4%	1505.9	10.2%
	J8-0	1633.5	1428.1	12.6%	1698.3	4.0%	1698.3	4.0%	2122.9	30.0%	2122.9	30.0%	1440.8	11.8%	4004.7	145.2%	1705.1	4.4%
	J8H-0	2146.0	1451.4	32.4%	1726.0	19.6%	1726.0	19.6%	2157.5	0.5%	2157.5	0.5%	1464.3	31.8%	4136.3	92.7%	1732.9	19.2%
Murty et al., 2003	P1	232.2	325.3	40.1%	325.3	40.1%	325.3	40.1%	325.3	40.1%	325.3	40.1%	271.7	17.0%	364.0	56.8%	261.2	12.5%
	P2	274.2	319.2	16.4%	319.2	16.4%	319.2	16.4%	319.2	16.4%	319.2	16.4%	266.7	2.7%	350.7	27.9%	256.4	6.5%
	P3	244.3	323.5	32.4%	323.5	32.4%	323.5	32.4%	323.5	32.4%	323.5	32.4%	270.2	10.6%	360.0	47.4%	259.8	6.4%
	Q1	212.7	315.0	48.1%	315.0	48.1%	315.0	48.1%	315.0	48.1%	315.0	48.1%	263.1	23.7%	341.3	60.5%	253.0	18.9%
	Q2	297.4	324.7	9.2%	324.7	9.2%	324.7	9.2%	324.7	9.2%	324.7	9.2%	271.2	8.8%	362.7	22.0%	260.8	12.3%
	Q3	287.3	322.9	12.4%	322.9	12.4%	322.9	12.4%	322.9	12.4%	322.9	12.4%	269.7	6.1%	358.7	24.8%	259.3	9.7%
	R1	235.2	342.1	45.4%	342.1	45.4%	342.1	45.4%	342.1	45.4%	342.1	45.4%	285.8	21.5%	402.7	71.2%	274.8	16.8%
	R2	313.5	325.3	3.8%	325.3	3.8%	325.3	3.8%	325.3	3.8%	325.3	3.8%	271.7	13.3%	364.0	16.1%	261.2	16.7%

Table 5.1 Comparison of Experimental Joint Shear Strengths with Code Predictions (cont'd)

Res.	Spec.	$V_{j,exp}$	ACI 352-10		ACI318-11		ACI 318-14		ACI 318-19		ASCE 41-17		CSA A23.03-19		TEC2007		TEC2018	
			V_j	AE	V_j	AE	V_j	AE	V_j,	AE	V_j	AE,	V_j	AE	V_j	AE	V_j	AE
		kN	kN	%	kN	%	kN	%	kN	%	kN	%	kN	%	kN	%	kN	%
Murty et al., 2003 (cont'd)	R3	295.3	324.1	9.7%	324.1	9.7%	324.1	9.7%	324.1	9.7%	324.1	9.7%	270.7	8.3%	361.3	22.3%	260.3	11.9%
	S1	221.4	328.2	48.2%	328.2	48.2%	328.2	48.2%	328.2	48.2%	218.8	1.2%	274.2	23.8%	370.7	67.4%	263.6	19.1%
	S2	295.3	322.3	9.1%	322.3	9.1%	322.3	9.1%	322.3	9.1%	214.8	27.3%	269.2	8.9%	357.3	21.0%	258.8	12.4%
	S3	268.8	341.5	27.1%	341.5	27.1%	341.5	27.1%	341.5	27.1%	227.7	15.3%	285.3	6.1%	401.3	49.3%	274.3	2.1%
Park, 2002	O1	562.9	727.0	29.2%	880.1	56.4%	880.1	56.4%	1100.1	95.5%	733.4	30.3%	746.7	32.7%	1508.8	168.1%	883.6	57.0%
Higazy et al., 1996	SB1	151.9	151.1	0.5%	151.1	0.5%	151.1	0.5%	151.1	0.5%	151.1	0.5%	126.2	16.9%	174.0	14.5%	121.4	20.1%
	SB2	133.5	150.9	13.0%	150.9	13.0%	150.9	13.0%	150.9	13.0%	150.9	13.0%	126.1	5.6%	173.5	30.0%	121.2	9.2%
Meinheit & Jirsa, 1977	I	1089.8	888.1	18.5%	962.1	11.7%	962.1	11.7%	962.1	11.7%	962.1	11.7%	803.7	26.3%	1054.8	3.2%	772.7	29.1%
	II	1596.8	1121.5	29.8%	1214.9	23.9%	1214.9	23.9%	1214.9	23.9%	1214.9	23.9%	1014.9	36.4%	1682.1	5.3%	975.8	38.9%
	III	1227.6	895.0	27.1%	969.6	21.0%	969.6	21.0%	969.6	21.0%	969.6	21.0%	810.0	34.0%	1071.4	12.7%	778.8	36.6%
	IV	1454.5	1066.0	26.7%	1128.7	22.4%	1128.7	22.4%	1128.7	22.4%	1128.7	22.4%	942.8	35.2%	1451.7	0.2%	906.6	37.7%
	V	1530.1	1038.8	32.1%	1125.4	26.4%	1125.4	26.4%	1125.4	26.4%	1125.4	26.4%	940.1	38.6%	1443.4	5.7%	904.0	40.9%
	VI	1645.8	1051.8	36.1%	1139.4	30.8%	1139.4	30.8%	1139.4	30.8%	1139.4	30.8%	951.8	42.2%	1479.4	10.1%	915.2	44.4%
	VII	1467.8	1083.1	26.2%	1146.9	21.9%	1146.9	21.9%	1146.9	21.9%	1146.9	21.9%	958.0	34.7%	1498.9	2.1%	921.2	37.2%
	VIII	1721.4	1330.8	22.7%	1441.7	16.2%	1441.7	16.2%	1441.7	16.2%	1441.7	16.2%	1241.9	27.9%	1998.5	16.1%	1476.4	14.2%
	IX	1596.8	966.4	39.5%	1046.9	34.4%	1046.9	34.4%	1046.9	34.4%	1395.9	12.6%	874.5	45.2%	1249.1	21.8%	840.9	47.3%
	X	1476.7	943.6	36.1%	1022.2	30.8%	1022.2	30.8%	1022.2	30.8%	1362.9	7.7%	853.9	42.2%	1190.8	19.4%	821.1	44.4%
	XI	1285.5	899.0	30.1%	951.9	26.0%	951.9	26.0%	951.9	26.0%	1269.2	1.3%	795.1	38.1%	1032.6	19.7%	764.6	40.5%
	XII	1948.2	1028.8	47.2%	1114.5	42.8%	1114.5	42.8%	1114.5	42.8%	1114.5	42.8%	931.0	52.2%	1415.6	27.3%	895.2	54.0%
	XIII	1556.8	1115.0	28.4%	1207.9	22.4%	1207.9	22.4%	1207.9	22.4%	1207.9	22.4%	1009.0	35.2%	1662.6	6.8%	970.2	37.7%
	XIV	1539.0	1022.3	33.6%	1082.4	29.7%	1082.4	29.7%	1082.4	29.7%	1082.4	29.7%	904.2	41.3%	1335.1	13.2%	869.4	43.5%

Table 5.1 Comparison of Experimental Joint Shear Strengths with Code Predictions (cont'd)

Res.	Spec.	$V_{j,exp}$	ACI 352-10		ACI318-11		ACI 318-14		ACI 318-19		ASCE 41-17		CSA A23.03-19		TEC2007		TEC2018	
			V_j	AE	V_j	AE	V_j	AE	V_j,	AE	V_j	AE,	V_j	AE	V_j	AE	V_j	AE
		kN	kN	%	kN	%	kN	%	kN	%	kN	%	kN	%	kN	%	kN	%
Paulay et al., 1981	UNIT 2	990.0	877.7	11.3%	986.7	0.3%	986.7	0.3%	986.7	0.3%	986.7	0.3%	837.1	15.4%	1253.1	26.6%	990.7	0.1%
	UNIT 3	752.5	959.6	27.5%	1078.9	43.4%	1078.9	43.4%	1078.9	43.4%	1078.9	43.4%	915.3	21.6%	1498.1	99.1%	1083.2	43.9%
Hwang et al., 2005	0T0	997.0	1269.7	27.4%	1441.3	44.6%	1441.3	44.6%	1441.3	44.6%	720.7	27.7%	1222.8	22.7%	3165.8	217.5%	1447.1	45.1%
	3T3	1132.0	1285.7	13.6%	1459.4	28.9%	1459.4	28.9%	1459.4	28.9%	1459.4	28.9%	1238.2	9.4%	3245.8	186.7%	1465.3	29.4%
	2T4	1080.0	1304.2	20.8%	1480.4	37.1%	1480.4	37.1%	1480.4	37.1%	1480.4	37.1%	1256.0	16.3%	3339.8	209.2%	1486.4	37.6%
	1T44	1039.0	1320.6	27.1%	1499.1	44.3%	1499.1	44.3%	1499.1	44.3%	1499.1	44.3%	1271.8	22.4%	3424.5	229.6%	1505.1	44.9%
Karayannis et al., 2008	A0	85.1	224.0	163.1%	224.0	163.1%	224.0	163.1%	224.0	163%	112.0	31.6%	190.0	123.2%	337.1	296.0%	224.9	164.2%
	A1	87.9	224.0	154.7%	224.0	154.7%	224.0	154.7%	224.0	154%	112.0	27.3%	190.0	116.1%	337.1	283.3%	224.9	155.7%
	A2	91.1	224.0	145.8%	224.0	145.8%	224.0	145.8%	224.0	145%	224.0	145.8%	190.0	108.5%	337.1	269.9%	224.9	146.8%
	B0	205.0	335.9	63.9%	335.9	63.9%	335.9	63.9%	335.9	63.9%	168.0	18.1%	285.0	39.0%	505.6	146.6%	337.3	64.5%
	B1	225.7	335.9	48.9%	335.9	48.9%	335.9	48.9%	335.9	48.9%	335.9	48.9%	285.0	26.3%	505.6	124.1%	337.3	49.5%
	C0	226.7	335.9	48.2%	335.9	48.2%	335.9	48.2%	335.9	48.2%	168.0	25.9%	285.0	25.7%	505.6	123.0%	337.3	48.8%
	C2	219.7	335.9	52.9%	335.9	52.9%	335.9	52.9%	335.9	52.9%	335.9	52.9%	285.0	29.8%	505.6	130.2%	337.3	53.6%
J.-Y. Lee et al., 2009	J1	1219.8	895.7	26.6%	964.6	20.9%	964.6	20.9%	964.6	20.9%	964.6	20.9%	805.7	33.9%	1306.7	7.1%	774.8	36.5%
	BJ1	979.1	895.7	8.5%	964.6	1.5%	964.6	1.5%	964.6	1.5%	964.6	1.5%	805.7	17.7%	1306.7	33.5%	774.8	20.9%
	BJ2	845.6	895.7	5.9%	964.6	14.1%	964.6	14.1%	964.6	14.1%	964.6	14.1%	805.7	4.7%	1306.7	54.5%	774.8	8.4%
	BJ3	719.7	895.7	24.4%	964.6	34.0%	964.6	34.0%	964.6	34.0%	964.6	34.0%	805.7	12.0%	1306.7	81.5%	774.8	7.6%
	B1	571.2	895.7	56.8%	964.6	68.9%	964.6	68.9%	964.6	68.9%	964.6	68.9%	805.7	41.1%	1306.7	128.8%	774.8	35.6%
Benham et al.	S3-BC2	866.1	791.6	8.6%	791.6	8.6%	791.6	8.6%	791.6	8.6%	791.6	8.6%	661.2	23.7%	998.1	15.2%	635.8	26.6%
	S4BC2.5	1049.3	791.6	24.6%	791.6	24.6%	791.6	24.6%	791.6	24.6%	791.6	24.6%	661.2	37.0%	998.1	4.9%	635.8	39.4%
Briss et al.	B1	1289.2	1221.7	5.2%	1373.4	6.5%	1373.4	6.5%	1373.4	6.5%	1373.4	6.5%	1147.3	11.0%	1553.8	20.5%	1103.1	14.4%

Table 5.1 Comparison of Experimental Joint Shear Strengths with Code Predictions (cont'd)

Res.	Spec.	$V_{j,exp}$	ACI 352-10		ACI318-11		ACI 318-14		ACI 318-19		ASCE 41-17		CSA A23.03-19		TEC2007		TEC2018	
			V_j	AE	V_j	AE	V_j	AE	V_j,	AE	V_j	AE,	V_j	AE	V_j	AE	V_j	AE
		kN	kN	%	kN	%	kN	%	kN	%	kN	%	kN	%	kN	%	kN	%
	B2	1306.3	1298.1	0.6%	1459.3	11.7%	1459.3	11.7%	1459.3	11.7%	1459.3	11.7%	1219.0	6.7%	1754.3	34.3%	1172.2	10.3%
Park & Milburn, 1983	1	991.4	867.3	12.5%	990.8	0.1%	990.8	0.1%	990.8	0.1%	990.8	0.1%	827.6	16.5%	1363.8	37.6%	795.8	19.7%
	2	1038.9	924.3	11.0%	1055.8	1.6%	1055.8	1.6%	1055.8	1.6%	1055.8	1.6%	882.0	15.1%	1548.7	49.1%	848.0	18.4%
	3	656.6	834.1	27.0%	952.9	45.1%	952.9	45.1%	952.9	45.1%	952.9	45.1%	796.0	21.2%	1261.4	92.1%	765.3	16.6%
	4	657.2	673.4	2.5%	769.2	17.0%	769.2	17.0%	769.2	17.0%	769.2	17.0%	652.6	0.7%	1284.5	95.4%	772.3	17.5%
Park & Ruitong	4	551.1	854.6	55.1%	976.3	77.2%	976.3	77.2%	976.3	77.2%	976.3	77.2%	815.5	48.0%	1324.2	140.3%	784.1	42.3%
Leon, 1990	BCJ3	378.0	373.3	1.2%	448.0	18.5%	448.0	18.5%	560.0	48.2%	560.0	48.2%	380.1	0.6%	696.9	84.4%	449.8	19.0%
	BCJ4	414.0	352.0	15.0%	448.0	8.2%	448.0	8.2%	560.0	35.3%	560.0	35.3%	380.1	8.2%	597.3	44.3%	449.8	8.6%
Noguchi & Kashi., 1992	OKJ1	925.6	659.7	28.7%	791.7	14.5%	791.7	14.5%	989.6	6.9%	989.6	6.9%	671.7	27.4%	1872.0	102.2%	794.9	14.1%
	OKJ2	920.4	659.7	28.3%	791.7	14.0%	791.7	14.0%	989.6	7.5%	989.6	7.5%	671.7	27.0%	1872.0	103.4%	794.9	13.6%
	OKJ3	1157.0	811.4	29.9%	973.7	15.8%	973.7	15.8%	1217.2	5.2%	1217.2	5.2%	826.1	28.6%	2832.0	144.8%	977.7	15.5%
	OKJ4	977.6	659.7	32.5%	791.7	19.0%	791.7	19.0%	989.6	1.2%	989.6	1.2%	671.7	31.3%	1872.0	91.5%	794.9	18.7%
	OKJ5	962.0	659.7	31.4%	791.7	17.7%	791.7	17.7%	989.6	2.9%	989.6	2.9%	671.7	30.2%	1872.0	94.6%	794.9	17.4%
	OKJ6	852.2	573.8	32.7%	688.5	19.2%	688.5	19.2%	860.7	1.0%	860.7	1.0%	584.2	31.4%	1416.0	66.2%	691.3	18.9%
Hegger et al., 2003	RK4	357.0	214.8	39.8%	214.8	39.8%	214.8	39.8%	214.8	39.8%	214.8	39.8%	182.3	48.9%	413.6	15.9%	215.7	39.6%
	RK5	423.0	221.4	47.7%	221.4	47.7%	221.4	47.7%	221.4	47.7%	221.4	47.7%	187.8	55.6%	439.2	3.8%	222.3	47.5%
	RK6	556.0	277.9	50.0%	277.9	50.0%	277.9	50.0%	277.9	50.0%	277.9	50.0%	235.8	57.6%	692.0	24.5%	279.0	49.8%
	RK7	277.0	221.0	20.2%	221.0	20.2%	221.0	20.2%	221.0	20.2%	221.0	20.2%	187.5	32.3%	437.6	58.0%	221.9	19.9%
	RK8	273.0	185.6	32.0%	185.6	32.0%	185.6	32.0%	185.6	32.0%	185.6	32.0%	157.5	42.3%	308.8	13.1%	186.4	31.7%
	RA1	527.0	326.6	38.0%	326.6	38.0%	326.6	38.0%	326.6	38.0%	217.7	58.7%	272.8	48.2%	509.8	3.3%	262.3	50.2%
	RA2	597.0	364.4	39.0%	364.4	39.0%	364.4	39.0%	364.4	39.0%	364.4	39.0%	304.4	49.0%	634.6	6.3%	292.7	51.0%

Table 5.1 Comparison of Experimental Joint Shear Strengths with Code Predictions (cont'd)

Res.	Spec.	$V_{j,exp}$	ACI 352-10		ACI318-11		ACI 318-14		ACI 318-19		ASCE 41-17		CSA A23.03-19		TEC2007		TEC2018	
			V_j	AE	V_j	AE	V_j	AE	V_j,	AE	V_j	AE,	V_j	AE	V_j	AE	V_j	AE
		kN	kN	%	kN	%	kN	%	kN	%	kN	%	kN	%	kN	%	kN	%
Hegger et al (cont'd)	RA3	504.0	295.9	41.3%	295.9	41.3%	295.9	41.3%	295.9	41.3%	295.9	41.3%	247.2	50.9%	418.6	17.0%	237.7	52.8%
	RA4	771.0	364.4	52.7%	364.4	52.7%	364.4	52.7%	364.4	52.7%	364.4	52.7%	304.4	60.5%	634.6	17.7%	292.7	62.0%
	RA5	494.0	336.0	32.0%	336.0	32.0%	336.0	32.0%	336.0	32.0%	336.0	32.0%	280.7	43.2%	539.5	9.2%	269.9	45.4%
	RA6	663.0	420.0	36.7%	420.0	36.7%	420.0	36.7%	420.0	36.7%	420.0	36.7%	350.8	47.1%	674.4	1.7%	337.3	49.1%
	RA7	770.0	400.1	48.0%	400.1	48.0%	400.1	48.0%	400.1	48.0%	400.1	48.0%	334.2	56.6%	765.1	0.6%	321.4	58.3%
Li & Leong, 2015	NS2	916.7	1205.3	31.5%	1314.9	43.4%	1314.9	43.4%	1314.9	43.4%	1314.9	43.4%	1098.4	19.8%	2203.2	140.3%	1056.1	15.2%
	NS3	1080.4	1198.4	10.9%	1307.3	21.0%	1307.3	21.0%	1307.3	21.0%	1307.3	21.0%	1092.1	1.1%	2178.0	101.6%	1050.1	2.8%
	NS4	724.0	1196.4	65.2%	1305.2	80.3%	1305.2	80.3%	1305.2	80.3%	1305.2	80.3%	1090.2	50.6%	2170.8	199.8%	1048.3	44.8%
Attaalla, 1997	SOC3	133.0	193.1	45.2%	193.1	45.2%	193.1	45.2%	193.1	45.2%	193.1	45.2%	161.3	21.3%	284.1	113.6%	155.1	16.6%
	SHC1	127.0	211.4	66.5%	211.4	66.5%	211.4	66.5%	211.4	66.5%	211.4	66.5%	176.6	39.1%	340.6	168.2%	169.8	33.7%
	SHC2	145.0	217.0	49.7%	217.0	49.7%	217.0	49.7%	217.0	49.7%	217.0	49.7%	181.3	25.0%	358.7	147.4%	174.3	20.2%
Kun, 2003	H:0.0	869.3	730.6	16.0%	797.1	8.3%	797.1	8.3%	797.1	8.3%	797.1	8.3%	665.8	23.4%	1214.4	39.7%	640.2	26.4%
	E:0.3	813.9	697.4	14.3%	760.8	6.5%	760.8	6.5%	760.8	6.5%	507.2	37.7%	635.5	21.9%	1106.4	35.9%	611.1	24.9%
	H:0.3	743.9	689.8	7.3%	752.5	1.2%	752.5	1.2%	752.5	1.2%	752.5	1.2%	628.6	15.5%	1082.4	45.5%	604.4	18.8%
Wong & Kuang, 2008	L	315.5	465.1	47.4%	498.3	57.9%	498.3	57.9%	498.3	57.9%	249.1	21.0%	422.7	34.0%	741.6	135.1%	500.3	58.6%
	OL	219.1	465.1	112.3%	498.3	127.4%	498.3	127.4%	498.3	127%	249.1	13.7%	422.7	92.9%	741.6	238.5%	500.3	128.3%
	LL	398.8	542.8	36.1%	581.6	45.8%	581.6	45.8%	581.6	45.8%	290.8	27.1%	493.4	23.7%	1010.4	153.4%	584.0	46.4%
	U	341.2	465.8	36.5%	499.1	46.3%	499.1	46.3%	499.1	46.3%	249.5	26.9%	423.4	24.1%	744.0	118.1%	501.1	46.9%
	L-LS	344.9	470.3	36.4%	503.9	46.1%	503.9	46.1%	503.9	46.1%	252.0	26.9%	427.5	24.0%	758.4	119.9%	505.9	46.7%
	L-V2T10	398.8	477.7	19.8%	511.8	28.3%	511.8	28.3%	511.8	28.3%	255.9	35.8%	434.2	8.9%	782.4	96.2%	513.9	28.9%
	L-V4T10	402.9	445.1	10.5%	476.9	18.4%	476.9	18.4%	476.9	18.4%	238.4	40.8%	404.6	0.4%	679.2	68.6%	478.8	18.8%

Table 5.1 Comparison of Experimental Joint Shear Strengths with Code Predictions (cont'd)

Res.	Spec.	$V_{j,exp}$	ACI 352-10		ACI318-11		ACI 318-14		ACI 318-19		ASCE 41-17		CSA A23.03-19		TEC2007		TEC2018	
			V_j	AE	V_j	AE	V_j	AE	V_j,	AE	V_j	AE,	V_j	AE	V_j	AE	V_j	AE
		kN	kN	%	kN	%	kN	%	kN	%	kN	%	kN	%	kN	%	kN	%
Wong & Kuang, 2008 (cont'd)	L-H1T10	389.3	482.8	24.0%	517.3	32.9%	517.3	32.9%	517.3	32.9%	258.6	33.6%	438.9	12.7%	799.2	105.3%	519.4	33.4%
	L-H2T10	479.3	542.8	13.3%	581.6	21.3%	581.6	21.3%	581.6	21.3%	581.6	21.3%	493.4	3.0%	1010.4	110.8%	584.0	21.8%
	L-600	283.9	504.8	77.8%	540.8	90.5%	540.8	90.5%	540.8	90.5%	270.4	4.8%	458.8	61.6%	873.6	207.7%	543.0	91.3%
	JA-NN03	304.2	560.0	84.1%	600.0	97.2%	600.0	97.2%	600.0	97.2%	300.0	1.4%	509.0	67.3%	1075.2	253.5%	602.4	98.0%
	JA-NN15	325.1	567.4	74.5%	608.0	87.0%	608.0	87.0%	608.0	87.0%	304.0	6.5%	515.8	58.7%	1104.0	239.6%	610.4	87.8%
	JB-NN03	317.0	576.0	81.7%	617.2	94.7%	617.2	94.7%	617.2	94.7%	308.6	2.7%	523.6	65.2%	1137.6	258.9%	619.6	95.5%
	JA-NY03	302.6	494.3	63.3%	529.6	75.0%	529.6	75.0%	529.6	75.0%	529.6	75.0%	449.3	48.5%	837.6	176.8%	531.7	75.7%
	JA-NY15	323.7	519.1	60.4%	556.2	71.8%	556.2	71.8%	556.2	71.8%	556.2	71.8%	471.9	45.8%	924.0	185.4%	558.4	72.5%
Lehman et al., 2004	PEER14	960.8	1303.6	35.7%	1303.6	35.7%	1303.6	35.7%	1303.6	35.7%	869.1	9.5%	1089.0	13.3%	1573.5	63.8%	1047.1	9.0%
	PEER085	768.7	1367.7	77.9%	1367.7	77.9%	1367.7	77.9%	1367.7	77.9%	911.8	18.6%	1142.5	48.6%	1732.0	125.3%	1098.6	42.9%
	PEER995	1313.1	1798.5	37.0%	1798.5	37.0%	1798.5	37.0%	1798.5	37.0%	1199.0	8.7%	1502.4	14.4%	2995.0	128.1%	1444.6	10.0%
Uzumeri, 1977	1	626.7	902.0	43.9%	1002.2	59.9%	1002.2	59.9%	801.7	27.9%	400.9	36.0%	837.2	33.6%	1190.3	89.9%	805.0	28.4%
	2	608.9	725.6	19.2%	806.2	32.4%	806.2	32.4%	806.2	32.4%	403.1	33.8%	684.0	12.3%	1203.7	97.7%	809.5	32.9%
	5	608.0	1021.1	67.9%	1021.1	67.9%	1021.1	67.9%	816.9	34.3%	408.4	32.8%	853.0	40.3%	1235.7	103.2%	820.2	34.9%
Parker & Bullman, 1997	4a	194.5	514.5	164.4%	561.2	188.5%	561.2	188.5%	561.2	188%	280.6	44.2%	476.1	144.7%	940.8	383.6%	563.5	189.6%
	4b	227.5	514.5	126.1%	561.2	146.7%	561.2	146.7%	561.2	146%	280.6	23.3%	476.1	109.3%	940.8	313.5%	563.5	147.7%
	4c	280.3	498.5	77.8%	543.8	94.0%	543.8	94.0%	543.8	94.0%	271.9	3.0%	461.3	64.6%	883.2	215.1%	546.0	94.8%
	4d	247.3	514.5	108.0%	561.2	126.9%	561.2	126.9%	561.2	126%	280.6	13.5%	476.1	92.5%	940.8	280.4%	563.5	127.9%
	4e	263.8	519.7	97.0%	566.9	114.9%	566.9	114.9%	566.9	114%	283.5	7.5%	481.0	82.3%	960.0	263.9%	569.2	115.8%
	4f	301.7	503.9	67.0%	549.7	82.2%	549.7	82.2%	549.7	82.2%	274.8	8.9%	466.3	54.6%	902.4	199.1%	551.9	82.9%
	5a	351.2	535.1	52.4%	583.7	66.2%	583.7	66.2%	583.7	66.2%	583.7	66.2%	495.2	41.0%	1017.6	189.8%	586.0	66.9%

Table 5.1 Comparison of Experimental Joint Shear Strengths with Code Predictions (cont'd)

Res.	Spec.	$V_{j,exp}$	ACI 352-10		ACI318-11		ACI 318-14		ACI 318-19		ASCE 41-17		CSA A23.03-19		TEC2007		TEC2018	
			V_j	AE	V_j	AE	V_j	AE	V_j,	AE	V_j	AE,	V_j	AE	V_j	AE	V_j	AE
		kN	kN	%	kN	%	kN	%	kN	%	kN	%	kN	%	kN	%	kN	%
Parker & Bullman (cont'd)	5b	389.1	540.1	38.8%	589.2	51.4%	589.2	51.4%	589.2	51.4%	589.2	51.4%	499.9	28.5%	1036.8	166.5%	591.5	52.0%
	5c	399.0	540.1	35.4%	589.2	47.7%	589.2	47.7%	589.2	47.7%	589.2	47.7%	499.9	25.3%	1036.8	159.9%	591.5	48.3%
	5d	372.6	540.1	44.9%	589.2	58.1%	589.2	58.1%	589.2	58.1%	589.2	58.1%	499.9	34.1%	1036.8	178.3%	591.5	58.8%
	5e	486.4	550.0	13.1%	600.0	23.4%	600.0	23.4%	600.0	23.4%	600.0	23.4%	509.0	4.7%	1075.2	121.1%	602.4	23.9%
	5f	530.9	540.1	1.7%	589.2	11.0%	589.2	11.0%	589.2	11.0%	589.2	11.0%	499.9	5.8%	1036.8	95.3%	591.5	11.4%
Scott, 1992	C1	112.8	137.2	21.7%	158.3	40.4%	158.3	40.4%	158.3	40.4%	79.2	29.8%	134.3	19.1%	299.4	165.5%	158.9	40.9%
	C1A	115.4	150.4	30.4%	173.6	50.5%	173.6	50.5%	173.6	50.5%	86.8	24.8%	147.3	27.7%	360.0	212.1%	174.3	51.1%
	C1AL	94.7	125.4	32.4%	144.7	52.8%	144.7	52.8%	144.7	52.8%	72.4	23.6%	122.8	29.6%	250.2	164.2%	145.3	53.4%
	C2	92.5	152.6	64.8%	176.0	90.2%	176.0	90.2%	176.0	90.2%	88.0	4.9%	149.3	61.4%	370.2	300.0%	176.7	91.0%
	C3	111.5	130.3	16.9%	150.3	34.8%	150.3	34.8%	150.3	34.8%	75.2	32.6%	127.5	14.4%	270.0	142.2%	150.9	35.4%
	C3L	93.0	129.4	39.2%	149.3	60.6%	149.3	60.6%	149.3	60.6%	74.7	19.7%	126.7	36.3%	266.4	186.5%	149.9	61.2%
	C4	129.5	139.8	8.0%	161.3	24.6%	161.3	24.6%	161.3	24.6%	80.6	37.7%	136.8	5.7%	310.8	140.1%	161.9	25.1%
	C4A	138.6	144.6	4.3%	166.8	20.3%	166.8	20.3%	166.8	20.3%	83.4	39.8%	141.5	2.1%	332.4	139.8%	167.5	20.8%
	C4AL	123.4	129.9	5.3%	149.8	21.5%	149.8	21.5%	149.8	21.5%	74.9	39.3%	127.1	3.1%	268.2	117.4%	150.4	22.0%
	C5	60.1	124.8	107.5%	144.0	139.4%	144.0	139.4%	144.0	139%	72.0	19.7%	122.2	103.1%	247.8	312.0%	144.6	140.4%
	C6	95.0	137.1	44.2%	158.1	66.4%	158.1	66.4%	158.1	66.4%	79.1	16.8%	134.2	41.2%	298.8	214.5%	158.8	67.1%
	C6L	113.3	147.0	29.7%	169.6	49.7%	169.6	49.7%	169.6	49.7%	84.8	25.2%	143.9	27.0%	343.8	203.4%	170.3	50.3%
	C7	87.2	128.8	47.7%	148.7	70.4%	148.7	70.4%	148.7	70.4%	74.3	14.8%	126.1	44.6%	264.0	202.7%	149.2	71.1%
	C8	74.4	144.8	94.6%	167.1	124.6%	167.1	124.6%	167.1	124%	83.6	12.3%	141.8	90.5%	333.6	348.3%	167.8	125.5%
	C9	76.0	130.1	71.1%	150.2	97.5%	150.2	97.5%	150.2	97.5%	75.1	1.3%	127.4	67.5%	269.4	254.3%	150.8	98.3%

For the comparison of basic shear strength prediction ($V_{j,pre.,basic}$), enhanced shear strength prediction with each singular Modification factor ($V_{j,pre.,basic}$) $(AF)_n$ and the final shear strength prediction ($V_{j,pre}$), the corresponding shear capacity predictions and related absolute error (AE) values are presented in the Table 5.2. The proposed equation is evaluated based on the effect of each factor separately and additionally, as a group where all the Modification factors are applied simultaneously.

In the following sections, the efficiency of each Modification factor is evaluated separately, and corresponding mean absolute error (MAE) and standard deviation (SD) values are presented.

Table 5.2 Comparison of Exp. Joint Shear Strengths with Proposed Equation Pre.

Research.	Spec.	$V_{j,exp}$	$V_{j,pre.,basic}$		$(V_{j,pre.,basic})$ (SR)			$(V_{j,pre.,basic})$ (AxF)			$(V_{j,pre.,basic})$ (SF)			Load. Fact.	$V_{j,pre.}$	
			V_j	AE	SR	V_j	AE	AxF	V_j	AE	SF	V_j	AE		V_j	AE
		kN	kN	%		kN	%		kN	%		kN	%		kN	%
Burak & Wight, 2008	1-S	778.4	628.1	19.3%	1.08	676.51	13.1%	1.03	644.86	17.2%	1.07	672.72	13.6%	1.00	744.0	4.4%
	2-S	863.0	826.7	4.2%	0.97	803.10	6.9%	1.02	843.10	2.3%	1.05	867.48	0.5%	1.00	859.5	0.4%
	3-S	827.4	712.8	13.8%	0.96	685.93	17.1%	1.03	731.91	11.5%	1.05	748.04	9.6%	1.00	739.1	10.7%
	1-N	569.4	684.8	20.3%	1.08	737.60	29.5%	1.03	703.09	23.5%	1.07	733.47	28.8%	0.80	648.9	14.0%
	2-N	809.6	1144.8	41.4%	1.08	1241.73	53.4%	1.02	1167.56	44.2%	1.05	1201.33	48.4%	0.80	1063.2	31.3%
	3-N	1156.5	1063.1	8.1%	1.08	1145.64	0.9%	1.03	1091.55	5.6%	1.11	1181.23	2.1%	0.80	1045.6	9.6%
Raffaelle & Wight, 1995	1	650.8	655.4	0.7%	0.97	634.09	2.6%	1.01	663.42	1.9%	1.00	655.37	0.7%	1.00	641.9	1.4%
	2	420.6	462.0	9.9%	0.97	447.01	6.3%	1.01	468.07	11.3%	1.00	462.01	9.9%	1.00	452.9	7.7%
	3	469.7	579.8	23.4%	0.97	560.94	19.4%	1.01	585.17	24.6%	1.00	579.76	23.4%	1.00	566.2	20.5%
	4	412.4	414.8	0.6%	0.97	401.33	2.7%	1.02	422.36	2.4%	1.00	414.80	0.6%	1.00	408.6	0.9%
Shin & LaFave, 2004	SL 1	631.6	801.9	27.0%	0.94	753.44	19.3%	1.00	801.89	27.0%	1.06	852.01	34.9%	1.00	800.5	26.7%
	SL 2	631.6	521.0	17.5%	0.94	489.53	22.5%	1.00	521.01	17.5%	1.06	553.58	12.4%	1.00	520.1	17.7%
	SL3	671.7	1027.4	53.0%	0.94	965.28	43.7%	1.00	1027.35	53.0%	1.06	1091.56	62.5%	1.00	1025.6	52.7%
	SL4	791.8	810.6	2.4%	1.04	839.64	6.0%	1.00	810.56	2.4%	1.06	861.22	8.8%	1.00	892.1	12.7%
Gentry & Wight, 1994	1	689.9	774.5	12.3%	1.00	778.40	12.8%	1.01	784.34	13.7%	1.00	774.54	12.3%	1.00	788.3	14.3%
	2	733.5	774.5	5.6%	1.00	778.40	6.1%	1.01	784.34	6.9%	1.00	774.54	5.6%	1.00	788.3	7.5%
	3	829.4	903.2	8.9%	1.01	911.68	9.9%	1.01	911.60	9.9%	1.00	903.19	8.9%	1.00	920.2	10.9%
	4	934.3	903.2	3.3%	1.00	907.69	2.9%	1.01	911.60	2.4%	1.00	903.19	3.3%	1.00	916.1	1.9%
LaFave & Wight, 1999	EWB-1	857.4	790.7	7.8%	0.97	765.03	10.8%	1.00	790.70	7.8%	1.11	878.56	2.5%	1.00	850.0	0.9%
	EWB-2	929.0	798.3	14.1%	0.97	772.38	16.9%	1.00	798.30	14.1%	1.11	887.00	4.5%	1.00	858.2	7.6%
	EWB-3	1244.4	996.0	20.0%	1.03	1027.61	17.4%	1.00	996.04	20.0%	1.11	1106.71	11.1%	1.00	1141.8	8.2%

Table 5.2 Comparison of Exp. Joint Shear Strengths with Proposed Equation Pre. (cont'd)

Research.	Spec.	$V_{j,exp}$	$V_{j,pre.,basic}$		$(V_{j,pre.,basic})$ (SR)			$(V_{j,pre.,basic})$ (AxF)			$(V_{j,pre.,basic})$ (SF)			Load. Fact.	$V_{j,pre.}$	
			V_j	AE	SR	V_j	AE	AxF	V_j	AE	SF	V_j	AE		V_j	AE
		kN	kN	%		kN	%		kN	%		kN	%		kN	%
(cont'd)	ENB-1	688.4	845.2	22.8%	1.03	871.96	26.7%	1.00	845.16	22.8%	1.03	873.10	26.8%	1.00	900.8	30.9%
Quintero-Febres & Wight, 2001	IWB-1	1386.1	1253.6	9.6%	1.08	1348.43	2.7%	1.00	1253.61	9.6%	1.00	1253.61	9.6%	1.00	1348.4	2.7%
	IWB-2	1352.9	1100.4	18.7%	1.08	1183.66	12.5%	1.00	1100.42	18.7%	1.00	1100.42	18.7%	1.00	1183.7	12.5%
	IWB-3	1510.2	1403.5	7.1%	1.07	1506.61	0.2%	1.00	1403.55	7.1%	1.00	1403.55	7.1%	1.00	1506.6	0.2%
Durrani & Wight, 1985	X1	1005.0	790.3	21.4%	1.01	798.73	20.5%	1.02	809.84	19.4%	1.00	790.30	21.4%	1.00	818.5	18.6%
	X2	1054.8	782.3	25.8%	1.10	861.45	18.3%	1.03	802.07	24.0%	1.00	782.33	25.8%	1.00	883.2	16.3%
	X3	803.5	751.3	6.5%	1.01	759.26	5.5%	1.03	771.81	3.9%	1.00	751.25	6.5%	1.00	780.0	2.9%
	S1	1411.7	1242.3	12.0%	1.01	1255.58	11.1%	1.02	1267.70	10.2%	1.06	1315.35	6.8%	1.00	1356.5	3.9%
	S2	1384.6	1068.4	22.8%	1.10	1176.49	15.0%	1.03	1097.93	20.7%	1.06	1131.23	18.3%	1.00	1280.0	7.6%
	S3	1029.1	1024.4	0.5%	1.01	1035.33	0.6%	1.03	1055.17	2.5%	1.06	1084.61	5.4%	1.00	1129.1	9.7%
Joh et al., 1991b	JXO-B1	285.3	292.9	2.7%	0.91	267.44	6.2%	1.08	316.54	11.0%	1.00	292.91	2.7%	1.00	289.0	1.3%
	JXO-B3	299.8	295.6	1.4%	0.91	269.89	10.0%	1.08	319.01	6.4%	1.00	295.59	1.4%	1.00	291.3	2.9%
	JXO-B5	289.9	304.8	5.2%	0.91	278.31	4.0%	1.07	327.52	13.0%	1.00	304.81	5.2%	1.00	299.0	3.2%
	JXO-B6	273.7	300.2	9.7%	0.91	274.13	0.1%	1.08	323.29	18.1%	1.00	300.24	9.7%	1.00	295.2	7.8%
Fujii & Morita, 1991	A1	418.5	302.7	27.7%	0.94	283.79	32.2%	1.04	314.28	24.9%	1.00	302.66	27.7%	1.00	294.7	29.6%
	A2	385.6	302.7	21.5%	0.94	283.79	26.4%	1.04	314.28	18.5%	1.00	302.66	21.5%	1.00	294.7	23.6%
	A3	418.5	302.7	27.7%	0.94	283.79	32.2%	1.12	337.52	19.3%	1.00	302.66	27.7%	1.00	316.5	24.4%
	A4	427.5	302.7	29.2%	1.08	326.68	23.6%	1.12	337.52	21.0%	1.00	302.66	29.2%	1.00	364.3	14.8%
	B1	250.1	187.7	24.9%	0.94	176.04	29.6%	1.03	194.19	22.4%	1.00	187.75	24.9%	1.00	182.1	27.2%
	B2	217.2	187.7	13.6%	0.94	176.04	19.0%	1.03	194.19	10.6%	1.00	187.75	13.6%	1.00	182.1	16.2%
	B3	277.0	187.7	32.2%	0.94	176.04	36.4%	1.12	210.29	24.1%	1.00	187.75	32.2%	1.00	197.2	28.8%

Table 5.2 Comparison of Exp. Joint Shear Strengths with Proposed Equation Pre. (cont'd)

Research.	Spec.	$V_{j,exp}$	$V_{j,pre.,basic}$		$(V_{j,pre.,basic})$ (SR)			$(V_{j,pre.,basic})$ (AxF)			$(V_{j,pre.,basic})$ (SF)			Load. Fact.	$V_{j,pre.}$	
			V_j	AE	SR	V_j	AE	AxF	V_j	AE	SF	V_j	AE		V_j	AE
		kN	kN	%		kN	%		kN	%		kN	%		kN	%
(cont'd)	B4	291.9	187.7	35.7%	1.08	202.65	30.6%	1.12	210.29	28.0%	1.00	187.75	35.7%	1.00	227.0	22.3%
Kurose et al., 1991	J1 EW)	1825.3	1325.8	27.4%	0.97	1285.49	29.6%	1.00	1325.77	27.4%	1.06	1408.64	22.8%	1.00	1365.8	25.2%
	J2(EW)	2617.8	2027.3	22.6%	0.97	1965.66	24.9%	1.00	2027.26	22.6%	1.06	2153.96	17.7%	1.00	2088.5	20.2%
	J2(NS)	2393.1	1947.3	18.6%	0.97	1888.15	21.1%	1.00	1947.32	18.6%	1.06	2069.03	13.5%	1.00	2006.2	16.2%
	J3(EW)	1834.4	1536.3	16.2%	0.97	1489.64	18.8%	1.00	1536.33	16.2%	1.06	1632.35	11.0%	1.00	1582.7	13.7%
	J3(NS)	1896.7	1865.5	1.6%	0.97	1808.85	4.6%	1.00	1865.54	1.6%	1.06	1982.14	4.5%	1.00	1921.9	1.3%
Teng & Zhou, 2003	S1	717.3	486.3	32.2%	0.97	470.93	34.3%	1.06	513.41	28.4%	1.00	486.33	32.2%	1.00	497.2	30.7%
	S2	717.3	493.6	31.2%	0.97	478.01	33.4%	1.05	520.33	27.5%	1.00	493.65	31.2%	1.00	503.8	29.8%
	S3	716.4	459.1	35.9%	0.97	444.57	37.9%	1.05	483.22	32.5%	1.00	459.12	35.9%	1.00	467.9	34.7%
	S4	391.2	343.3	12.2%	1.06	363.61	7.1%	1.06	363.20	7.2%	1.00	343.31	12.2%	1.00	384.7	1.7%
	S5	391.2	352.5	9.9%	1.06	373.30	4.6%	1.05	371.84	4.9%	1.00	352.47	9.9%	1.00	393.8	0.7%
	S6	391.2	289.9	25.9%	1.06	307.07	21.5%	1.06	306.29	21.7%	1.00	289.93	25.9%	1.00	324.4	17.1%
Lawrence	1	696.0	849.5	22.1%	1.05	888.63	27.7%	1.00	849.53	22.1%	1.00	849.53	22.1%	1.00	888.6	27.7%
Kusuhara et al., 2004	JE-0	418.1	362.3	13.3%	0.92	332.61	20.4%	1.00	362.28	13.3%	1.00	362.28	13.3%	1.00	332.6	20.4%
	JE-55	395.8	362.3	8.5%	0.92	332.61	16.0%	1.00	362.28	8.5%	1.00	362.28	8.5%	1.00	332.6	16.0%
	JE-55S	400.1	362.3	9.4%	0.95	345.41	13.7%	1.00	362.28	9.4%	1.00	362.28	9.4%	1.00	345.4	13.7%
Shiohara & Kusuhara, 2006	A1	586.8	556.3	5.2%	0.93	514.84	12.3%	1.04	579.93	1.2%	1.00	556.34	5.2%	1.00	536.7	8.5%
	B1	456.1	397.4	12.9%	0.93	367.74	19.4%	1.04	414.24	9.2%	1.00	397.39	12.9%	1.00	383.3	16.0%
	B2	427.4	397.4	7.0%	0.93	367.74	14.0%	1.04	414.24	3.1%	1.00	397.39	7.0%	1.00	383.3	10.3%
	C1	696.7	794.8	14.1%	0.93	735.49	5.6%	1.04	828.47	18.9%	1.00	794.77	14.1%	1.00	766.7	10.0%
Zaid	S3	635.5	431.9	32.0%	0.93	402.64	36.6%	1.02	440.44	30.7%	1.00	431.87	32.0%	1.00	410.6	35.4%

Table 5.2 Comparison of Exp. Joint Shear Strengths with Proposed Equation Pre. (cont'd)

Research.	Spec.	$V_{j,exp}$	$V_{j,pre.,basic}$		$(V_{j,pre.,basic})$ (SR)			$(V_{j,pre.,basic})$ (AxF)			$(V_{j,pre.,basic})$ (SF)			Load. Fact.	$V_{j,pre.}$	
			V_j	AE	SR	V_j	AE	AxF	V_j	AE	SF	V_j	AE		V_j	AE
		kN	kN	%		kN	%		kN	%		kN	%		kN	%
Guimaraes et al., 1993	J4 (EW)	2560.2	2168.9	15.3%	0.95	2053.36	19.8%	1.00	2168.92	15.3%	1.06	2304.48	10.0%	1.00	2181.7	14.8%
	J4 (NS)	2101.7	2168.9	3.2%	0.95	2053.36	2.3%	1.00	2168.92	3.2%	1.06	2304.48	9.6%	1.00	2181.7	3.8%
	J5 (EW)	4812.4	3403.1	29.3%	1.12	3808.70	20.9%	1.00	3403.12	29.3%	1.06	3615.81	24.9%	1.00	4046.7	15.9%
	J5 (NS)	4109.4	3403.1	17.2%	1.12	3808.70	7.3%	1.00	3403.12	17.2%	1.06	3615.81	12.0%	1.00	4046.7	1.5%
	J6 (EW)	4438.3	3700.3	16.6%	1.10	4058.39	8.6%	1.00	3700.33	16.6%	1.06	3931.60	11.4%	1.00	4312.0	2.8%
	J6 (NS)	4163.5	3700.3	11.1%	1.10	4058.39	2.5%	1.00	3700.33	11.1%	1.06	3931.60	5.6%	1.00	4312.0	3.6%
H.-J. Lee & Ko, 2008	W0	775.0	696.1	10.2%	0.95	659.71	14.9%	1.05	731.19	5.7%	1.00	696.07	10.2%	1.00	693.0	10.6%
	W75	780.0	713.9	8.5%	0.95	676.62	13.3%	1.05	748.15	4.1%	1.00	713.90	8.5%	1.00	709.1	9.1%
	W150	710.0	698.5	1.6%	0.95	661.99	6.8%	1.05	733.48	3.3%	1.00	698.47	1.6%	1.00	695.2	2.1%
Tsonos, 2007	E1	219.8	155.7	29.1%	1.04	162.01	26.3%	1.11	173.42	21.1%	1.00	155.72	29.1%	1.00	180.4	17.9%
	G1	195.0	155.7	20.1%	0.94	145.65	25.3%	1.11	173.42	11.1%	1.00	155.72	20.1%	1.00	162.2	16.8%
Alamed & Ehsani, 1991	LL8	860.3	737.7	14.2%	1.09	803.04	6.7%	1.02	753.25	12.4%	1.00	737.72	14.2%	1.00	819.9	4.7%
	LH8	838.0	737.7	12.0%	1.12	828.00	1.2%	1.02	753.25	10.1%	1.00	737.72	12.0%	1.00	845.4	0.9%
	HL8	986.6	737.7	25.2%	1.09	804.27	18.5%	1.04	764.54	22.5%	1.00	737.72	25.2%	1.00	833.5	15.5%
	HH8	985.7	737.7	25.2%	1.12	829.24	15.9%	1.04	764.54	22.4%	1.00	737.72	25.2%	1.00	859.4	12.8%
	LL11	769.1	865.1	12.5%	1.08	937.45	21.9%	1.01	877.90	14.1%	1.00	865.06	12.5%	1.00	951.4	23.7%
	LH11	934.1	865.1	7.4%	1.12	969.48	3.8%	1.01	877.50	6.1%	1.00	865.06	7.4%	1.00	983.4	5.3%
	HL11	967.5	865.1	10.6%	1.09	938.83	3.0%	1.03	891.54	7.9%	1.00	865.06	10.6%	1.00	967.6	0.0%
	HH11	1020.9	865.1	15.3%	1.12	969.48	5.0%	1.03	892.34	12.6%	1.00	865.06	15.3%	1.00	1000.1	2.0%
	LL14	877.6	975.9	11.2%	1.09	1062.32	21.0%	1.01	985.34	12.3%	1.00	975.92	11.2%	1.00	1072.6	22.2%
	LH14	890.5	975.9	9.6%	1.12	1095.34	23.0%	1.01	984.81	10.6%	1.00	975.92	9.6%	1.00	1105.3	24.1%

Table 5.2 Comparison of Exp. Joint Shear Strengths with Proposed Equation Pre. (cont'd)

Research.	Spec.	$V_{j,exp}$	$V_{j,pre.,basic}$		$(V_{j,pre.,basic})$ (SR)			$(V_{j,pre.,basic})$ (AxF)			$(V_{j,pre.,basic})$ (SF)			Load. Fact.	$V_{j,pre.}$	
			V_j	AE	SR	V_j	AE	AxF	V_j	AE	SF	V_j	AE		V_j	AE
		kN	kN	%		kN	%		kN	%		kN	%		kN	%
Ehsani & Wight, 1985	1	486.3	402.8	17.2%	0.97	389.76	19.8%	1.03	414.64	14.7%	1.00	402.76	17.2%	1.00	401.3	17.5%
	2	502.6	410.9	18.2%	0.99	408.30	18.8%	1.04	425.50	15.3%	1.00	410.94	18.2%	1.00	422.8	15.9%
	3	599.8	444.4	25.9%	1.06	470.49	21.6%	1.03	457.89	23.7%	1.00	444.43	25.9%	1.00	484.7	19.2%
	4	623.3	464.2	25.5%	1.07	496.85	20.3%	1.03	477.11	23.5%	1.00	464.23	25.5%	1.00	510.6	18.1%
	5	573.7	635.2	10.7%	0.97	614.68	7.1%	1.03	653.64	13.9%	1.04	663.64	15.7%	1.00	660.9	15.2%
	6	601.4	611.6	1.7%	1.06	647.48	7.7%	1.03	630.79	4.9%	1.04	639.02	6.3%	1.00	697.7	16.0%
	7	553.8	523.6	5.4%	0.99	520.27	6.1%	1.04	546.02	1.4%	1.05	551.63	0.4%	1.00	571.5	3.2%
	8	601.5	552.8	8.1%	1.07	591.60	1.6%	1.04	573.96	4.6%	1.05	582.30	3.2%	1.00	647.1	7.6%
	9	690.2	446.0	35.4%	0.95	423.80	38.6%	1.06	474.18	31.3%	1.00	446.03	35.4%	1.00	450.5	34.7%
	10	641.5	619.1	3.5%	0.95	588.26	8.3%	1.06	658.86	2.7%	1.04	646.85	0.8%	1.00	654.1	2.0%
	11	646.9	570.3	11.8%	0.95	542.76	16.1%	1.03	588.97	9.0%	1.00	570.25	11.8%	1.00	560.6	13.3%
	12	755.3	749.8	0.7%	0.95	713.06	5.6%	1.04	777.73	3.0%	1.04	783.42	3.7%	1.00	772.7	2.3%
Bolong & Yuzhou, 1991	J4	1928.0	1398.4	27.5%	1.03	1437.86	25.4%	1.03	1440.37	25.3%	1.00	1398.41	27.5%	1.00	1481.0	23.2%
	J5	1787.0	1449.0	18.9%	1.03	1489.86	16.6%	1.03	1492.45	16.5%	1.00	1448.98	18.9%	1.00	1534.6	14.1%
	J6	2412.0	1749.1	27.5%	1.03	1798.44	25.4%	1.03	1801.57	25.3%	1.06	1846.81	23.4%	1.00	1955.9	18.9%
Kaku & Asakusa, 1991	3	232.7	221.3	4.9%	0.93	205.80	11.6%	1.00	221.32	4.9%	1.00	221.32	4.9%	1.00	205.8	11.6%
	4	256.3	229.1	10.6%	0.91	207.78	18.9%	1.08	248.21	3.1%	1.00	229.15	10.6%	1.00	225.1	12.2%
	5	236.6	207.6	12.3%	0.91	188.27	20.4%	1.05	216.98	8.3%	1.00	207.63	12.3%	1.00	196.8	16.8%
	6	224.3	217.8	2.9%	0.91	197.53	12.0%	1.00	217.85	2.9%	1.00	217.85	2.9%	1.00	197.5	12.0%
	9	252.8	218.4	13.6%	0.93	203.30	19.6%	1.00	218.38	13.6%	1.00	218.38	13.6%	1.00	203.3	19.6%
	11	247.4	221.9	10.3%	0.91	201.21	18.7%	1.04	230.60	6.8%	1.00	221.85	10.3%	1.00	209.2	15.5%

Table 5.2 Comparison of Exp. Joint Shear Strengths with Proposed Equation Pre. (cont'd)

Research.	Spec.	$V_{j,exp}$	$V_{j,pre.,basic}$		$(V_{j,pre.,basic})$ (SR)			$(V_{j,pre.,basic})$ (AxF)			$(V_{j,pre.,basic})$ (SF)			Load. Fact.	$V_{j,pre.}$	
			V_j	AE	SR	V_j	AE	AxF	V_j	AE	SF	V_j	AE		V_j	AE
		kN	kN	%		kN	%		kN	%		kN	%		kN	%
Kaku,& Asakusa (cont'd)	12	222.4	203.1	8.7%	0.91	184.16	17.2%	1.00	203.05	8.7%	1.00	203.05	8.7%	1.00	184.2	17.2%
	13	224.3	233.5	4.1%	0.93	217.34	3.1%	1.00	233.46	4.1%	1.00	233.46	4.1%	1.00	217.3	3.1%
	14	242.0	219.5	9.3%	0.91	199.02	17.8%	1.04	228.30	5.7%	1.00	219.46	9.3%	1.00	207.0	14.5%
	15	246.9	216.0	12.5%	0.91	195.84	20.7%	1.04	224.94	8.9%	1.00	215.95	12.5%	1.00	204.0	17.4%
Joh et al., 1991a	B8-MH	306.6	432.6	41.1%	0.93	401.27	30.9%	1.07	462.84	51.0%	1.00	432.65	41.1%	1.00	429.3	40.0%
	B8-LH	304.3	423.3	39.1%	0.91	386.50	27.0%	1.07	454.17	49.3%	1.00	423.31	39.1%	1.00	414.7	36.3%
	B9	358.7	413.0	15.1%	0.94	390.13	8.8%	1.08	444.59	23.9%	1.00	412.95	15.1%	1.00	420.0	17.1%
	B10	394.5	407.3	3.2%	0.94	384.76	2.5%	1.08	439.34	11.4%	1.00	407.27	3.2%	1.00	415.1	5.2%
	B11	401.5	415.4	3.5%	0.94	392.41	2.3%	1.08	446.81	11.3%	1.00	415.36	3.5%	1.00	422.1	5.1%
Sugano et al., 1991	J4-0	1409.3	988.9	29.8%	1.07	1056.51	25.0%	1.17	1153.68	18.1%	1.00	988.86	29.8%	1.00	1232.6	12.5%
	J6-0	1676.2	1395.1	16.8%	1.07	1490.52	11.1%	1.08	1511.90	9.8%	1.00	1395.07	16.8%	1.00	1615.3	3.6%
	J8-0	1633.5	1579.6	3.3%	1.07	1687.65	3.3%	1.07	1682.76	3.0%	1.00	1579.58	3.3%	1.00	1797.9	10.1%
	J8H-0	2146.0	1605.3	25.2%	1.07	1715.16	20.1%	1.06	1706.86	20.5%	1.00	1605.33	25.2%	1.00	1823.6	15.0%
Murty et al., 2003	P1	232.2	303.6	30.7%	0.94	284.88	22.7%	1.00	303.57	30.7%	1.00	303.57	30.7%	1.00	284.9	22.7%
	P2	274.2	298.0	8.7%	0.94	279.61	2.0%	1.00	297.96	8.7%	1.00	297.96	8.7%	1.00	279.6	2.0%
	P3	244.3	301.9	23.6%	0.94	283.31	16.0%	1.00	301.90	23.6%	1.00	301.90	23.6%	1.00	283.3	16.0%
	Q1	212.7	294.0	38.2%	0.94	275.87	29.7%	1.00	293.97	38.2%	1.00	293.97	38.2%	1.00	275.9	29.7%
	Q2	297.4	303.0	1.9%	0.94	284.36	4.4%	1.00	303.01	1.9%	1.00	303.01	1.9%	1.00	284.4	4.4%
	Q3	287.3	301.3	4.9%	0.94	282.78	1.6%	1.00	301.34	4.9%	1.00	301.34	4.9%	1.00	282.8	1.6%
	R1	235.2	319.3	35.8%	0.94	299.63	27.4%	1.00	319.29	35.8%	1.00	319.29	35.8%	1.00	299.6	27.4%
	R2	313.5	303.6	3.2%	0.94	284.88	9.1%	1.00	303.57	3.2%	1.00	303.57	3.2%	1.00	284.9	9.1%

Table 5.2 Comparison of Exp. Joint Shear Strengths with Proposed Equation Pre. (cont'd)

Research.	Spec.	$V_{j,exp}$	$V_{j,pre.,basic}$		$(V_{j,pre.,basic})$ (SR)			$(V_{j,pre.,basic})$ (AxF)			$(V_{j,pre.,basic})$ (SF)			Load. Fact.	$V_{j,pre.}$	
			V_j	AE	SR	V_j	AE	AxF	V_j	AE	SF	V_j	AE		V_j	AE
		kN	kN	%		kN	%		kN	%		kN	%		kN	%
(cont'd)	R3	295.3	302.5	2.4%	0.94	283.83	3.9%	1.00	302.46	2.4%	1.00	302.46	2.4%	1.00	283.8	3.9%
	S1	221.4	306.3	38.3%	0.72	220.56	0.4%	1.00	306.34	38.3%	1.00	306.34	38.3%	1.00	220.6	0.4%
	S2	295.3	300.8	1.8%	0.72	216.56	26.7%	1.00	300.78	1.8%	1.00	300.78	1.8%	1.00	216.6	26.7%
	S3	268.8	318.8	18.6%	0.72	229.50	14.6%	1.00	318.76	18.6%	1.00	318.76	18.6%	1.00	229.5	14.6%
Park,2002	O1	562.9	785.0	39.5%	0.72	565.19	0.4%	1.00	784.99	39.5%	1.00	784.99	39.5%	1.00	565.2	0.4%
Higazy et al., 1996	SB1	151.9	141.0	7.2%	0.99	140.04	7.8%	1.03	144.55	4.8%	1.00	141.03	7.2%	1.00	143.5	5.5%
	SB2	133.5	140.9	5.5%	0.99	139.87	4.8%	1.00	140.86	5.5%	1.00	140.86	5.5%	1.00	139.9	4.8%
Meinheit & Jirsa, 1977	I	1089.8	828.9	23.9%	0.94	777.90	28.6%	1.20	995.24	8.7%	1.00	828.86	23.9%	1.00	934.1	14.3%
	II	1596.8	1046.7	34.5%	0.94	982.36	38.5%	1.13	1179.57	26.1%	1.00	1046.70	34.5%	1.00	1107.1	30.7%
	III	1227.6	835.4	32.0%	0.94	784.02	36.1%	1.20	1000.00	18.5%	1.00	835.37	32.0%	1.00	938.5	23.6%
	IV	1454.5	994.9	31.6%	0.92	919.65	36.8%	1.15	1142.44	21.5%	1.00	994.89	31.6%	1.00	1056.0	27.4%
	V	1530.1	969.6	36.6%	0.94	909.99	40.5%	1.02	988.71	35.4%	1.00	969.59	36.6%	1.00	927.9	39.4%
	VI	1645.8	981.6	40.4%	0.94	921.29	44.0%	1.24	1218.93	25.9%	1.00	981.64	40.4%	1.00	1144.0	30.5%
	VII	1467.8	1010.9	31.1%	0.92	934.47	36.3%	1.24	1249.75	14.9%	1.00	1010.93	31.1%	1.00	1155.2	21.3%
	VIII	1721.4	1330.8	22.7%	0.94	1248.98	27.4%	1.16	1541.10	10.5%	1.00	1330.79	22.7%	1.00	1446.4	16.0%
	IX	1596.8	1131.0	29.2%	0.94	1061.52	33.5%	1.17	1328.14	16.8%	1.00	1131.04	29.2%	1.00	1246.5	21.9%
	X	1476.7	1104.3	25.2%	0.94	1036.45	29.8%	1.18	1301.80	11.8%	1.00	1104.34	25.2%	1.00	1221.8	17.3%
	XI	1285.5	1060.4	17.5%	0.92	980.16	23.8%	1.21	1282.67	0.2%	1.00	1060.36	17.5%	1.00	1185.7	7.8%
	XII	1948.2	960.2	50.7%	1.13	1087.89	44.2%	1.15	1106.26	43.2%	1.00	960.22	50.7%	1.00	1253.3	35.7%
	XIII	1556.8	1040.6	33.2%	1.09	1137.50	26.9%	1.13	1171.68	24.7%	1.00	1040.64	33.2%	1.00	1280.7	17.7%
	XIV	1539.0	954.1	38.0%	1.05	1004.95	34.7%	1.16	1107.96	28.0%	1.00	954.11	38.0%	1.00	1167.0	24.2%

Table 5.2 Comparison of Exp. Joint Shear Strengths with Proposed Equation Pre. (cont'd)

Research.	Spec.	$V_{j,exp}$	$V_{j,pre.,basic}$		$(V_{j,pre.,basic})$ (SR)			$(V_{j,pre.,basic})$ (AxF)			$(V_{j,pre.,basic})$ (SF)			Load. Fact.	$V_{j,pre.}$	
			V_j	AE	SR	V_j	AE	AxF	V_j	AE	SF	V_j	AE		V_j	AE
		kN	kN	%		kN	%		kN	%		kN	%		kN	%
Paulay & Scarpas	UNIT 2	990.0	731.4	26.1%	1.07	783.15	20.9%	1.08	786.24	20.6%	1.00	731.39	26.1%	1.00	841.9	15.0%
	UNIT 3	752.5	799.7	6.3%	0.95	761.51	1.2%	1.03	820.90	9.1%	1.00	799.71	6.3%	1.00	781.7	3.9%
Hwang et al., 2005	0T0	997.0	1058.1	6.1%	0.72	761.85	23.6%	1.01	1066.86	7.0%	1.00	1058.12	6.1%	1.00	768.1	23.0%
	3T3	1132.0	1071.4	5.4%	0.95	1015.36	10.3%	1.01	1080.03	4.6%	1.00	1071.40	5.4%	1.00	1023.5	9.6%
	2T4	1080.0	1086.8	0.6%	0.94	1023.44	5.2%	1.01	1095.33	1.4%	1.00	1086.82	0.6%	1.00	1031.4	4.5%
	1T44	1039.0	1100.5	5.9%	0.97	1062.36	2.2%	1.01	1108.91	6.7%	1.00	1100.51	5.9%	1.00	1070.5	3.0%
Karayannis et al., 2008	A0	85.1	186.6	119.3%	0.72	134.37	57.9%	1.03	191.30	124.7%	1.00	186.63	119.3%	1.00	137.7	61.8%
	A1	87.9	186.6	112.2%	0.92	172.34	96.0%	1.03	191.30	117.5%	1.00	186.63	112.2%	1.00	176.7	100.9%
	A2	91.1	186.6	104.8%	0.94	175.14	92.2%	1.03	191.30	109.9%	1.00	186.63	104.8%	1.00	179.5	97.0%
	B0	205.0	279.9	36.5%	0.72	201.56	1.7%	1.03	286.94	40.0%	1.00	279.95	36.5%	1.00	206.6	0.8%
	B1	225.7	279.9	24.1%	0.92	258.51	14.6%	1.03	286.94	27.2%	1.00	279.95	24.1%	1.00	265.0	17.4%
	C0	226.7	279.9	23.5%	0.72	201.56	11.1%	1.03	286.94	26.6%	1.00	279.95	23.5%	1.00	206.6	8.9%
	C1	219.7	279.9	27.4%	0.94	262.71	19.6%	1.03	286.94	30.6%	1.00	279.95	27.4%	1.00	269.3	22.6%
J.-Y. Lee et al., 2009	J1	1219.8	836.0	31.5%	1.03	858.51	29.6%	1.00	835.96	31.5%	1.00	835.96	31.5%	1.00	858.5	29.6%
	BJ1	979.1	836.0	14.6%	1.03	858.51	12.3%	1.00	835.96	14.6%	1.00	835.96	14.6%	1.00	858.5	12.3%
	BJ2	845.6	836.0	1.1%	0.96	799.01	5.5%	1.00	835.96	1.1%	1.00	835.96	1.1%	1.00	799.0	5.5%
	BJ3	719.7	836.0	16.1%	0.96	799.01	11.0%	1.00	835.96	16.1%	1.00	835.96	16.1%	1.00	799.0	11.0%
	B1	571.2	836.0	46.4%	0.96	799.01	39.9%	1.00	835.96	46.4%	1.00	835.96	46.4%	1.00	799.0	39.9%
Behnam et al., 2017	S3-BC2	866.1	738.8	14.7%	1.08	796.54	8.0%	1.06	786.16	9.2%	1.00	738.79	14.7%	1.00	847.6	2.1%
	S4BC2.5	1049.3	738.8	29.6%	1.08	796.54	24.1%	1.06	786.16	25.1%	1.00	738.79	29.6%	1.00	847.6	19.2%
Briss et al.	B1	1289.2	1140.2	11.6%	1.03	1173.00	9.0%	1.03	1170.64	9.2%	1.00	1140.21	11.6%	1.00	1204.3	6.6%

Table 5.2 Comparison of Exp. Joint Shear Strengths with Proposed Equation Pre. (cont'd)

Research.	Spec.	$V_{j,exp}$	$V_{j,pre.,basic}$		$(V_{j,pre.,basic})$ (SR)			$(V_{j,pre.,basic})$ (AxF)			$(V_{j,pre.,basic})$ (SF)			Load. Fact.	$V_{j,pre.}$	
			V_j	AE	SR	V_j	AE	AxF	V_j	AE	SF	V_j	AE		V_j	AE
		kN	kN	%		kN	%		kN	%		kN	%		kN	%
(cont'd)	B2	1306.3	1211.5	7.3%	0.92	1109.00	15.1%	1.22	1477.65	13.1%	1.00	1211.54	7.3%	1.00	1352.6	3.5%
Park & Milburn, 1983	1	991.4	809.5	18.3%	1.13	917.86	7.4%	1.05	849.98	14.3%	1.00	809.50	18.3%	1.00	963.8	2.8%
	2	1038.9	862.6	17.0%	1.07	922.57	11.2%	1.05	905.77	12.8%	1.00	862.64	17.0%	1.00	968.7	6.8%
	3	656.6	778.5	18.6%	0.95	739.93	12.7%	1.05	817.46	24.5%	1.00	778.53	18.6%	1.00	776.9	18.3%
	4	657.2	561.2	14.6%	0.97	543.87	17.2%	1.05	589.22	10.3%	1.00	561.16	14.6%	1.00	571.1	13.1%
Park & Rui.1988	4	551.1	797.7	44.7%	0.99	785.79	42.6%	1.00	797.66	44.7%	1.00	797.66	44.7%	1.00	785.8	42.6%
Leon, 1990	BCJ3	378.0	407.9	7.9%	0.92	376.77	0.3%	1.00	407.91	7.9%	1.00	407.91	7.9%	1.00	376.8	0.3%
	BCJ4	414.0	354.8	14.3%	0.92	326.21	21.2%	1.00	354.80	14.3%	1.00	354.80	14.3%	1.00	326.2	21.2%
Noguchi & Kashi, 1992	OKJ1	925.6	720.8	22.1%	0.97	700.85	24.3%	1.06	764.07	17.5%	1.00	720.82	22.1%	1.00	742.9	19.7%
	OKJ2	920.4	720.8	21.7%	0.97	700.85	23.9%	1.06	764.07	17.0%	1.00	720.82	21.7%	1.00	742.9	19.3%
	OKJ3	1157.0	886.6	23.4%	0.97	862.02	25.5%	1.06	939.78	18.8%	1.00	886.58	23.4%	1.00	913.7	21.0%
	OKJ4	977.6	720.8	26.3%	0.97	700.85	28.3%	1.06	764.07	21.8%	1.00	720.82	26.3%	1.00	742.9	24.0%
	OKJ5	962.0	720.8	25.1%	0.97	700.85	27.1%	1.06	764.07	20.6%	1.00	720.82	25.1%	1.00	742.9	22.8%
	OKJ6	852.2	626.9	26.4%	0.97	609.54	28.5%	1.06	664.52	22.0%	1.00	626.91	26.4%	1.00	646.1	24.2%
Hegger et al., 2003	RK4	357.0	179.0	49.8%	1.14	203.73	42.9%	1.16	207.90	41.8%	1.00	179.04	49.8%	1.00	236.6	33.7%
	RK5	423.0	184.5	56.4%	1.14	210.34	50.3%	1.15	212.50	49.8%	1.00	184.50	56.4%	1.00	242.3	42.7%
	RK6	556.0	231.6	58.3%	1.14	264.03	52.5%	1.10	253.89	54.3%	1.00	231.58	58.3%	1.00	289.5	47.9%
	RK7	277.0	184.2	33.5%	1.10	203.06	26.7%	1.15	212.21	23.4%	1.00	184.16	33.5%	1.00	234.0	15.5%
	RK8	273.0	154.7	43.3%	1.14	176.03	35.5%	1.22	188.10	31.1%	1.00	154.70	43.3%	1.00	214.0	21.6%
	RA1	527.0	304.8	42.2%	0.72	219.48	58.4%	1.13	344.46	34.6%	1.00	304.83	42.2%	1.00	248.0	52.9%
	RA2	597.0	340.1	43.0%	1.01	344.82	42.2%	1.10	372.83	37.5%	1.00	340.10	43.0%	1.00	378.0	36.7%

Table 5.2 Comparison of Exp. Joint Shear Strengths with Proposed Equation Pre. (cont'd)

Research.	Spec.	$V_{j,exp}$	$V_{j,pre.,basic}$		$(V_{j,pre.,basic})$ (SR)			$(V_{j,pre.,basic})$ (AxF)			$(V_{j,pre.,basic})$ (SF)			Load. Fact.	$V_{j,pre.}$	
			V_j	AE	SR	V_j	AE	AxF	V_j	AE	SF	V_j	AE		V_j	AE
		kN	kN	%		kN	%		kN	%		kN	%		kN	%
Hegger et al., 2003 (cont'd)	RA3	504.0	276.2	45.2%	1.11	306.15	39.3%	1.16	320.39	36.4%	1.00	276.22	45.2%	1.00	355.1	29.5%
	RA4	771.0	340.1	55.9%	1.11	377.80	51.0%	1.07	364.11	52.8%	1.00	340.10	55.9%	1.00	404.5	47.5%
	RA5	494.0	313.6	36.5%	1.05	328.08	33.6%	1.12	352.27	28.7%	1.00	313.60	36.5%	1.00	368.5	25.4%
	RA6	663.0	392.0	40.9%	1.05	410.52	38.1%	1.13	441.68	33.4%	1.00	392.00	40.9%	1.00	462.5	30.2%
	RA7	770.0	373.5	51.5%	1.16	431.61	43.9%	1.08	403.20	47.6%	1.00	373.45	51.5%	1.00	466.0	39.5%
Li & Leong, 2015	NS2	916.7	1124.9	22.7%	1.06	1196.78	30.6%	1.00	1124.93	22.7%	1.00	1124.93	22.7%	1.00	1196.8	30.6%
	NS3	1080.4	1118.5	3.5%	1.10	1229.83	13.8%	1.00	1118.48	3.5%	1.00	1118.48	3.5%	1.00	1229.8	13.8%
	NS4	724.0	1116.6	54.2%	1.07	1197.35	65.4%	1.00	1116.63	54.2%	1.00	1116.63	54.2%	1.00	1197.3	65.4%
Attaalla, 1997	SOC3	133.0	180.2	35.5%	1.03	186.33	40.1%	1.03	184.75	38.9%	1.00	180.23	35.5%	1.00	191.0	43.6%
	SHC1	127.0	197.3	55.4%	0.95	187.32	47.5%	1.02	201.74	58.9%	1.00	197.33	55.4%	1.00	191.5	50.8%
	SHC2	145.0	202.5	39.7%	1.03	209.38	44.4%	1.02	206.98	42.7%	1.00	202.53	39.7%	1.00	214.0	47.6%
Kun, 2003	H:0.0	869.3	681.9	21.6%	1.11	753.68	13.3%	1.00	681.92	21.6%	1.00	681.92	21.6%	1.00	753.7	13.3%
	E:0.3	813.9	650.9	20.0%	0.72	468.64	42.4%	1.15	748.53	8.0%	1.00	650.89	20.0%	1.00	538.9	33.8%
	H:0.3	743.9	643.8	13.5%	1.11	711.54	4.3%	1.15	740.37	0.5%	1.00	643.80	13.5%	1.00	818.3	10.0%
Wong & Kuang, 2008	BS-L	315.5	387.6	22.8%	0.72	279.04	11.6%	1.08	416.62	32.1%	1.00	387.56	22.8%	1.00	300.0	4.9%
	BS-OL	219.1	387.6	76.9%	0.72	279.04	27.4%	1.08	416.62	90.2%	1.00	387.56	76.9%	1.00	300.0	36.9%
	BS-LL	398.8	452.4	13.4%	0.72	325.71	18.3%	1.08	486.30	21.9%	1.00	452.37	13.4%	1.00	350.1	12.2%
	BS-U	341.2	388.2	13.8%	0.72	279.49	18.1%	1.08	417.30	22.3%	1.00	388.18	13.8%	1.00	300.5	11.9%
	BS-L-LS	344.9	391.9	13.6%	0.72	282.18	18.2%	1.08	421.32	22.2%	1.00	391.92	13.6%	1.00	303.3	12.0%
	L-V2T10	398.8	398.1	0.2%	0.72	286.61	28.1%	1.08	427.93	7.3%	1.00	398.08	0.2%	1.00	308.1	22.7%
	L-V4T10	402.9	370.9	7.9%	0.72	267.04	33.7%	1.08	398.71	1.0%	1.00	370.89	7.9%	1.00	287.1	28.7%

Table 5.2 Comparison of Exp. Joint Shear Strengths with Proposed Equation Pre. (cont'd)

Research.	Spec.	$V_{j,exp}$	$V_{j,pre.,basic}$		$(V_{j,pre.,basic})$ (SR)			$(V_{j,pre.,basic})$ (AxF)			$(V_{j,pre.,basic})$ (SF)			Load. Fact.	$V_{j,pre.}$	
			V_j	AE	SR	V_j	AE	AxF	V_j	AE	SF	V_j	AE		V_j	AE
		kN	kN	%		kN	%		kN	%		kN	%		kN	%
Wong & Kuang, 2008 (cont'd)	L-H1T10	389.3	402.3	3.3%	0.92	369.02	5.2%	1.08	432.50	11.1%	1.00	402.33	3.3%	1.00	396.7	1.9%
	L-H2T10	479.3	452.4	5.6%	0.93	419.49	12.5%	1.08	486.30	1.5%	1.00	452.37	5.6%	1.00	451.0	5.9%
	L-600	283.9	420.6	48.2%	0.72	302.86	6.7%	1.08	452.19	59.3%	1.00	420.64	48.2%	1.00	325.6	14.7%
	NN03	304.2	466.7	53.4%	0.72	335.99	10.5%	1.02	473.66	55.7%	1.00	466.66	53.4%	1.00	341.0	12.1%
	NN15	325.1	472.9	45.5%	0.72	340.46	4.7%	1.08	508.33	56.4%	1.00	472.86	45.5%	1.00	366.0	12.6%
	NN03	317.0	480.0	51.4%	0.72	345.60	9.0%	1.02	487.21	53.7%	1.00	480.01	51.4%	1.00	350.8	10.7%
	NY03	302.6	411.9	36.1%	0.93	383.71	26.8%	1.02	418.06	38.2%	1.00	411.88	36.1%	1.00	389.5	28.7%
	NY15	323.7	432.6	33.6%	0.93	403.01	24.5%	1.08	465.05	43.7%	1.00	432.60	33.6%	1.00	433.2	33.8%
Lehman et al., 2004	PEER14	960.8	1216.7	26.6%	0.72	876.03	8.8%	1.05	1277.55	33.0%	1.00	1216.71	26.6%	1.00	919.8	4.3%
	PEER0850	768.7	1276.5	66.1%	0.72	919.10	19.6%	1.05	1340.35	74.4%	1.00	1276.53	66.1%	1.00	965.1	25.6%
	PEER995	1313.1	1678.6	27.8%	0.72	1208.60	8.0%	1.05	1762.55	34.2%	1.00	1678.61	27.8%	1.00	1269.0	3.4%
Uzumeri, 1977	1	626.7	721.6	15.1%	0.72	519.53	17.1%	1.26	908.52	45.0%	1.00	721.57	15.1%	1.00	654.1	4.4%
	2	608.9	604.7	0.7%	0.72	435.36	28.5%	1.26	759.60	24.7%	1.00	604.67	0.7%	1.00	546.9	10.2%
	5	608.0	816.9	34.3%	0.72	588.15	3.3%	1.25	1020.76	67.9%	1.00	816.88	34.3%	1.00	734.9	20.9%
Parker & Bullman, 1997	4a	194.5	428.7	120.4%	0.72	308.68	58.7%	1.00	428.72	120.4%	1.00	428.72	120.4%	1.00	308.7	58.7%
	4b	227.5	428.7	88.4%	0.72	308.68	35.7%	1.04	446.95	96.4%	1.00	428.72	88.4%	1.00	321.8	41.4%
	4c	280.3	415.4	48.2%	0.72	299.08	6.7%	1.09	451.13	61.0%	1.00	415.39	48.2%	1.00	324.8	15.9%
	4d	247.3	428.7	73.4%	0.72	308.68	24.8%	1.00	428.72	73.4%	1.00	428.72	73.4%	1.00	308.7	24.8%
	4e	263.8	433.1	64.2%	0.72	311.81	18.2%	1.04	451.12	71.0%	1.00	433.07	64.2%	1.00	324.8	23.1%
	4f	301.7	419.9	39.2%	0.72	302.31	0.2%	1.09	457.10	51.5%	1.00	419.88	39.2%	1.00	329.1	9.1%
	5a	351.2	445.9	27.0%	0.94	419.20	19.4%	1.00	445.88	27.0%	1.00	445.88	27.0%	1.00	419.2	19.4%

Table 5.2 Comparison of Exp. Joint Shear Strengths with Proposed Equation Pre. (cont'd)

Research.	Spec.	$V_{j,exp}$	$V_{j,pre.,basic}$		$(V_{j,pre.,basic})$ (SR)			$(V_{j,pre.,basic})$ (AxF)			$(V_{j,pre.,basic})$ (SF)			Load. Fact.	$V_{j,pre.}$	
			V_j	AE	SR	V_j	AE	AxF	V_j	AE	SF	V_j	AE		V_j	AE
		kN	kN	%		kN	%		kN	%		kN	%		kN	%
Parker & Bullman, 1997 (cont'd)	5b	389.1	450.1	15.7%	0.94	423.13	8.7%	1.04	467.43	20.1%	1.00	450.06	15.7%	1.00	439.5	12.9%
	5c	399.0	450.1	12.8%	0.94	423.13	6.1%	1.08	484.79	21.5%	1.00	450.06	12.8%	1.00	455.8	14.2%
	5d	372.6	450.1	20.8%	0.96	432.98	16.2%	1.00	450.06	20.8%	1.00	450.06	20.8%	1.00	433.0	16.2%
	5e	486.4	458.3	5.8%	0.96	440.92	9.3%	1.04	475.37	2.3%	1.00	458.32	5.8%	1.00	457.3	6.0%
	5f	530.9	450.1	15.2%	0.96	432.98	18.4%	1.08	484.79	8.7%	1.00	450.06	15.2%	1.00	466.4	12.1%
(Scott, 1992)	C1	112.8	113.3	0.5%	0.94	106.44	5.6%	1.12	127.19	12.8%	1.00	113.31	0.5%	1.00	119.5	5.9%
	C1A	115.4	124.3	7.7%	0.94	116.72	1.2%	1.10	136.91	18.7%	1.00	124.25	7.7%	1.00	128.6	11.5%
	C1AL	94.7	103.6	9.4%	0.94	97.30	2.7%	1.03	106.35	12.3%	1.00	103.59	9.4%	1.00	99.9	5.5%
	C2	92.5	126.0	36.1%	0.94	118.36	27.9%	1.10	138.48	49.6%	1.00	126.00	36.1%	1.00	130.1	40.6%
	C3	111.5	107.6	3.5%	0.94	101.08	9.3%	1.14	122.22	9.6%	1.00	107.61	3.5%	1.00	114.8	3.0%
	C3L	93.0	106.9	15.0%	0.94	100.40	8.0%	1.03	109.56	17.8%	1.00	106.89	15.0%	1.00	102.9	10.7%
	C4	129.5	115.5	10.8%	0.94	108.60	16.1%	1.12	129.07	0.3%	1.00	115.45	10.8%	1.00	121.4	6.2%
	C4A	138.6	119.4	13.9%	0.94	112.32	19.0%	1.11	132.57	4.4%	1.00	119.40	13.9%	1.00	124.7	10.0%
	C4AL	123.4	107.2	13.1%	0.94	100.89	18.2%	1.02	109.91	10.9%	1.00	107.25	13.1%	1.00	103.4	16.2%
	C5	60.1	103.1	71.4%	0.94	96.97	61.2%	1.15	118.34	96.7%	1.00	103.09	71.4%	1.00	111.3	85.1%
	C6	95.0	113.2	19.1%	0.94	106.49	12.1%	1.12	127.09	33.8%	1.00	113.20	19.1%	1.00	119.6	25.8%
	C6L	113.3	121.4	7.1%	0.94	114.23	0.8%	1.02	123.78	9.2%	1.00	121.43	7.1%	1.00	116.4	2.7%
	C7	87.2	106.4	22.0%	0.92	98.24	12.6%	1.14	121.18	38.9%	1.00	106.40	22.0%	1.00	111.9	28.3%
	C8	74.4	119.6	60.7%	0.92	110.43	48.4%	1.11	132.76	78.4%	1.00	119.61	60.7%	1.00	122.6	64.7%
	C9	76.0	107.5	41.3%	0.92	99.24	30.5%	1.14	122.12	60.6%	1.00	107.49	41.3%	1.00	112.7	48.3%

5.3 Determination of the Accuracy of Each Modification Factor

In the selection of each Modification factor, first a basic comparative study is carried out considering the alternatives that can be utilized for the modification of the equation. Correlation factors between the alternatives are evaluated and then, the alternatives are modified in order to reduce the error for the case where Modification factor is applied singularly and as a group.

Determination of Joint Shear Reinforcement Factor (SR)

As described in Section 4.2.2.1, different alternatives for volumetric joint shear reinforcement ratios are evaluated in the determination of a better accuracy for the influence of joint shear reinforcement. Namely, ρ_{gross}, ρ_{core}, $\rho_{single\ layer,\ gross}$ and $\rho_{singlelayer,core}$ definitions are investigated. The computed correlation coefficients are presented in Table 5.3.

Table 5.3 Correlation Coefficients for Different Volumetric Shear Reinforcement Ratio Definitions

SR Ratio Alternative	Correlation Coefficient
ρ_{gross}	0.341
ρ_{core}	0.356
$\rho_{single\ layer,\ gross}$	0.383
$\rho_{single\ layer,core}$	0.419

After evaluation of the correlation coefficients, $\rho_{singlelayer,core}$, which has the highest correlation coefficient, is utilized in the shear reinforcement factor definition, based on the recommendations provided in a prior research study (Unal & Burak, 2012).

Table 5.4 Correlation Coefficients for Shear Reinforcement Factors

SR Factor	Correlation Coefficient
$1 \pm \mathrm{SI}$	0.383
$1 \pm \mathrm{SI}^2$	0.281
$1 \pm \mathrm{SI}^3$	0.063
$1 \pm \sqrt{\mathrm{SI}}$	0.400
$1 \pm \sqrt[3]{\mathrm{SI}}$	0.393
$1 \pm 10\ \mathrm{SI}$	0.383

Consequently, the shear reinforcement factor is determined as $(1 \pm \sqrt{\mathrm{SI}})$, after a comparative process to reduce the MAE in the shear capacity predictions, increasing the number of under predicted specimens shear capacities to be conservative and reducing the standard deviations when compared to the evaluated structural codes. In Section 5.4. contemporary structural codes are compared with the proposed joint shear strength prediction equation. To evaluate the effect of Shear Reinforcement Factor (SR), both the basic joint shear strength prediction, the prediction modified using SR, are presented.

Table 5.5 Comparison of Shear Strength Predictions of Contemporary Codes with Shear Reinforcement Factor (SR)

	$V_{j,ACI}$ 352-10	$V_{j,ACI}$ 318-11	$V_{j,ACI}$ 318-14	$V_{j,ACI}$ 318-19	$V_{j,ASCE}$ 41-17	$V_{j,CSA}$ 23-03	$V_{j,}$ TEC2007	$V_{j,}$ TEC2018	$V_{j.pre,basic}$	SR $V_{j.pre,,basic}$
Total Number of Specimens	251	251	251	251	251	251	251	251	251	251
No. of Over Predicted Specimens	138	151	153	163	121	117	228	130	100	77
MAE_{over}	34.4%	42.9%	42.5%	42.7%	32.0%	31.4%	96.3%	43.7%	28.2%	21.1%
No. of Under Pred. Specimens	113	100	98	88	130	134	23	121	151	174
MAE_{under}	21.3%	20.1%	17.8%	16.8%	19.4%	21.9%	12.3%	23.0%	19.3%	18.9%
Standard Deviation	38.5%	42.6%	41.6%	41.7%	33.2%	34.8%	82.4%	44.2%	30.4%	23.8%
Overall Mean Absolute Error	28.5%	33.8%	32.9%	33.6%	25.5%	26.3%	88.6%	33.7%	22.9%	19.6%

It should be noted that the specimens included in Table 5.5 include both the conforming and non-conforming specimens for each code. Although a more detailed comparison of the proposed equation including all Modification factors with each code is provided separately in Section 5.4 presenting the predictions for conforming and non-conforming specimens individually, Table aids in evaluating the effect of the proposed Modification factor on all the specimens. From the evaluated design codes, only ASCE 41-17 provides the shear capacity predictions for both conforming and non-conforming specimens.

From the presented results, it can be noticed that the proposed Modification factor improves the accuracy of the shear strength prediction by reducing the mean absolute error from 22.9 % to 19.6 %. Also, it is important to note that the number of under predicted specimens increased from 141 to 174, while reducing the MAE of the mentioned group from 19.3 % to 18.9 %. Additionally, the standard deviation is reduced from 30.4% to 23.8%, representing reduced data scatter.

The comparison of predictions with and without the utilization of shear reinforcement factor (SR) is presented in Figure 5.1.

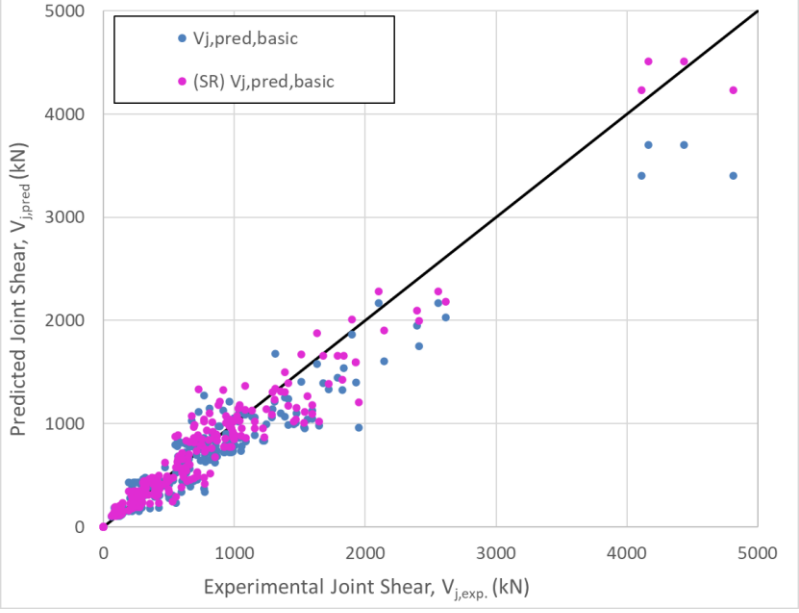


Figure 5.1. Effect of Shear Reinforcement Factor (SR)

Determination of Axial Load Factor (AxF)

For the determination of the influence of axial load on the enhancement of joint shear strength, two alternatives for the axial load index are investigated. The correlation of the axial stress effective on the joint gross volume, $N / (f_c' \, b_c \, h_c)$, and joint core volume are evaluated, the correlation coefficients of which are presented in Table 5.6.

Table 5.6 Correlation Factors for Axial Stress Alternatives

Axial Stress Alternative	Correlation Coefficient
Stress on Gross Vol. $N / (f_c' \, b_c \, h_c)$	0.115
Stress on Core Vol. $N / (f_c' \, b_{c,core} \, h_{c,core})$	0.036

After the evaluation of correlation coefficients, the axial load index is defined based on the axial stress ratio on the joint gross volume, $AI = \frac{N}{(b_c \, h_c f_c')}$.

For the determination of the axial load factor, a number of alternatives are evaluated, both monitoring the effect of the Modification factor on the mean absolute error of the group, and the correlation coefficients of the respective factors.

Some of the alternatives evaluated and corresponding correlation coefficients are presented in Table 5.7.

Table 5.7 Correlation Coefficients for Axial Load Factor Alternatives

Axial Load Factor	Correlation Coefficient
$1 + \sqrt[3]{AI}$	0.053
$1 + AI^2$	0.070
$1 + AI/2$	0.115
$1 + AI/3$	0.115

Consequently, based on the correlation analyses, the axial load factor is determined as presented below, and as prescribed in Section 4.2.2.2, which reduces the MAE and improves the accuracy of the equation.

Axial Factor (AxF) : $1 + \frac{\text{AxI}}{2}$

Table 5.8 presents the comparison between modern structural codes and the proposed equation for predicting joint shear strength, considering the Modification factor for axial load. Both the basic joint shear strength prediction and the modified prediction incorporating the axial load factor (AxF) are provided to assess the impact of AxF. In the evaluation of the results, only the specimens on which axial load is applied are presented.

Table 5.8 Comparison of Shear Strength Predictions of Contemporary Codes with Axial Load Factor (AxF)

	$V_{j,ACI}$ 352-10	$V_{j,ACI}$ 318-11	$V_{j,ACI}$ 318-14	$V_{j,ACI}$ 318-19	$V_{j,ASCE}$ 41-17	$V_{j,CSA}$ 23-03-19	$V_{j,}$ TEC2007	$V_{j,}$ TEC2018	$V_{j,pre.,basic}$	AxF $V_{j,pre.,basic}$
Total Number of Specimens	190	190	190	190	190	190	190	190	190	190
No. of Over Predicted Specimens	104	115	116	126	87	91	169	102	69	83
MAE_{over}	35.1%	43.9%	43.6%	42.6%	30.4%	31.9%	104.0%	45.8%	29.0%	29.2%
No. of Under Pred. Specimens	86	75	74	64	103	99	21	88	121	107
MAE_{under}	23.1%	22.3%	20.2%	19.1%	21.9%	23.9%	12.6%	25.3%	20.7%	17.6%
Standard Deviation	39.9%	43.7%	42.8%	42.4%	33.8%	35.9%	84.2%	45.9%	30.9%	32.1%
Overall Mean Absolute Error	29.7%	35.4%	34.5%	34.7%	25.8%	27.7%	93.9%	36.3%	23.7%	22.7%

In the evaluation of axial load factor (AxF), it is noticed that the factor is especially effective for the group of specimens where the shear strength of the joint is under predicted, with the basic procedure. The mean absolute error of the specimens is reduced by nearly 3.0 %, whereas this effect is also noticeable in the mean absolute error of the total group, with an increase of 1.0% in the accuracy.

Figure 5.2 presents the effect of axial load factor on the prediction accuracy.

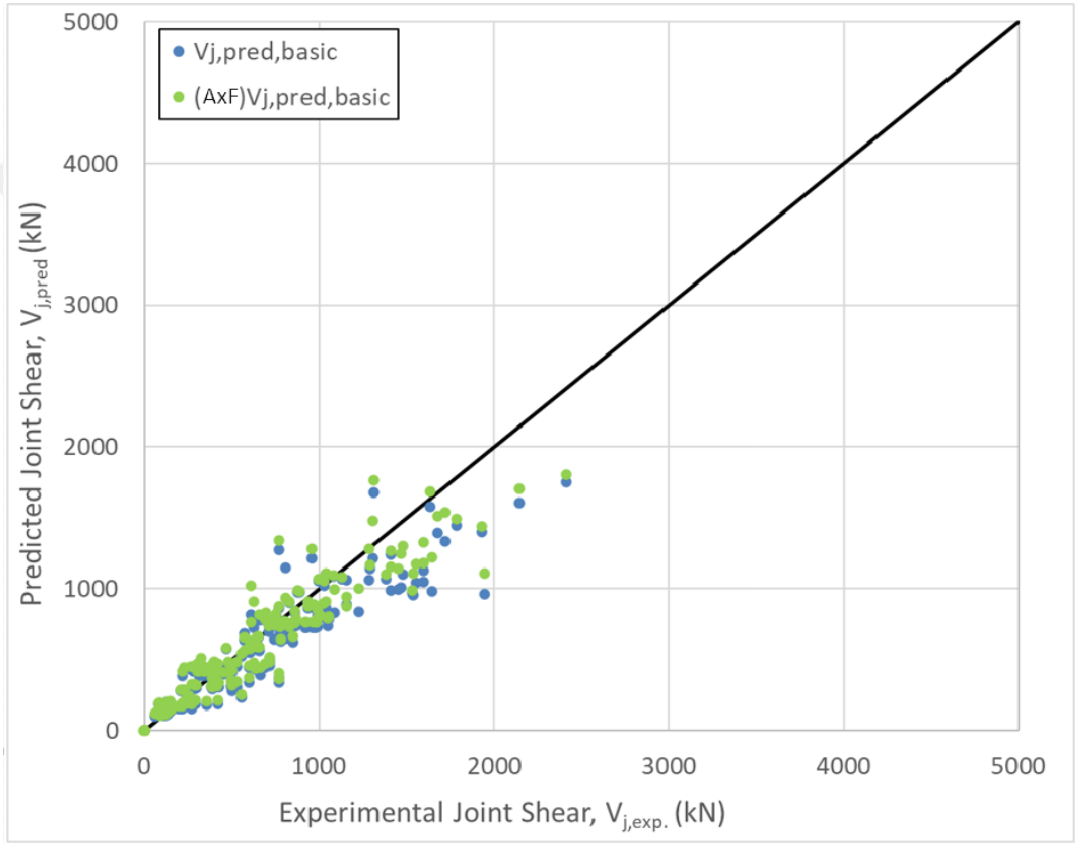


Figure 5.2. Effect of Axial Load Factor (AxF)

Determination of Slab Factor (SF)

Similar to the determination of axial load factor (AxF) and shear reinforcement factor (SR), the slab factor is determined taking into consideration the correlation of the slab index and slab factor, also focusing on the reduction of the mean absolute error for specimens with slabs. In the determination of the slab index (SI), slab thickness slab (t_f), and beam depth (h_b) are taken as the main variables.

Table 5.9 Correlation Coefficients for Slab Index

Slab Index	Correlation Coefficient
$\sqrt[3]{t_f/\ h_b}$	0.435
$\sqrt[2]{t_f/\ h_b}$	0.437
t_f/h_b	0.469
$(t_f/h_b)^2$	0.451
$(t_f/h_b)^3$	0.413

Considering the alternative slab indices that are evaluated, the slab factor is defined based on correlation analyses. The correlation of the enhancing effect due to the confinement provided by the presence of slab is evaluated as presented in Table 5.10.

Table 5.10 Correlation Coefficients for Slab Index Alternatives

Slab Factor Alternative	**Correlation Coefficient**
$1 + (t_f/h_b)$	0.447
$1+(t_f/h_b)^2$	0.451
$1+(t_f/h_b)^3$	0.414
$1+(t_f/h_b)^4$	0.363

Accordingly, the slab factor (SF) is determined as, $1+ (t_f\ /\ h_b)^2$ as previously described in 4.2.2.3, which leads to a reduction in the mean absolute error.

Table 5.11 presents the effect of considering the slab in the prediction equation.

Table 5.11 Comparison of Shear Strength Predictions of Contemporary Codes with Slab Factor (SF)

	$V_{j,ACI\ 352-10}$	$V_{j,ACI\ 318-11}$	$V_{j,ACI\ 318-14}$	$V_{j,ACI\ 318-19}$	$V_{j,ASCE\ 41-17}$	$V_{j,CSA\ 23-03}$	$V_{j,TEC2007}$	$V_{j,TEC2018}$	$V_{j,pre.,basic}$	SF $V_{j,pre.,basic}$
Total Number of Specimens	35	35	35	35	35	35	35	35	35	35
No. of Over Predicted Specimens	10	12	12	12	10	6	31	9	8	15
MAE_{over}	12.4%	19.9%	19.9%	23.1%	33.5%	13.8%	48.5%	18.9%	16.7%	13.6%
No. of Under Pred. Specimens	25	23	23	23	25	29	4	26	27	20
MAE_{under}	17.6%	16.3%	13.0%	13.0%	15.8%	17.4%	15.8%	19.4%	14.1%	12.3%
Standard Deviation	16.7%	22.4%	19.7%	23.5%	29.8%	15.7%	46.0%	21.9%	16.8%	17.3%
Overall Mean Absolute Error	16.1%	17.6%	15.4%	16.5%	20.8%	16.7%	44.7%	19.3%	14.7%	12.9%

It can be inferred from the comparison presented in Table 5.11, although the basic prediction ($V_{j,pre,basic}$) successfully predicts the joint shear strength within the group, the addition of the Modification factor, SF, improves the accuracy of the prediction for both the specimens that are under or over predicted as shown in Figure 5.3. The shear strength prediction is improved by 3.1 % for the over predicted specimens, whereas the improvement is 1.8 % for the under predicted specimens.

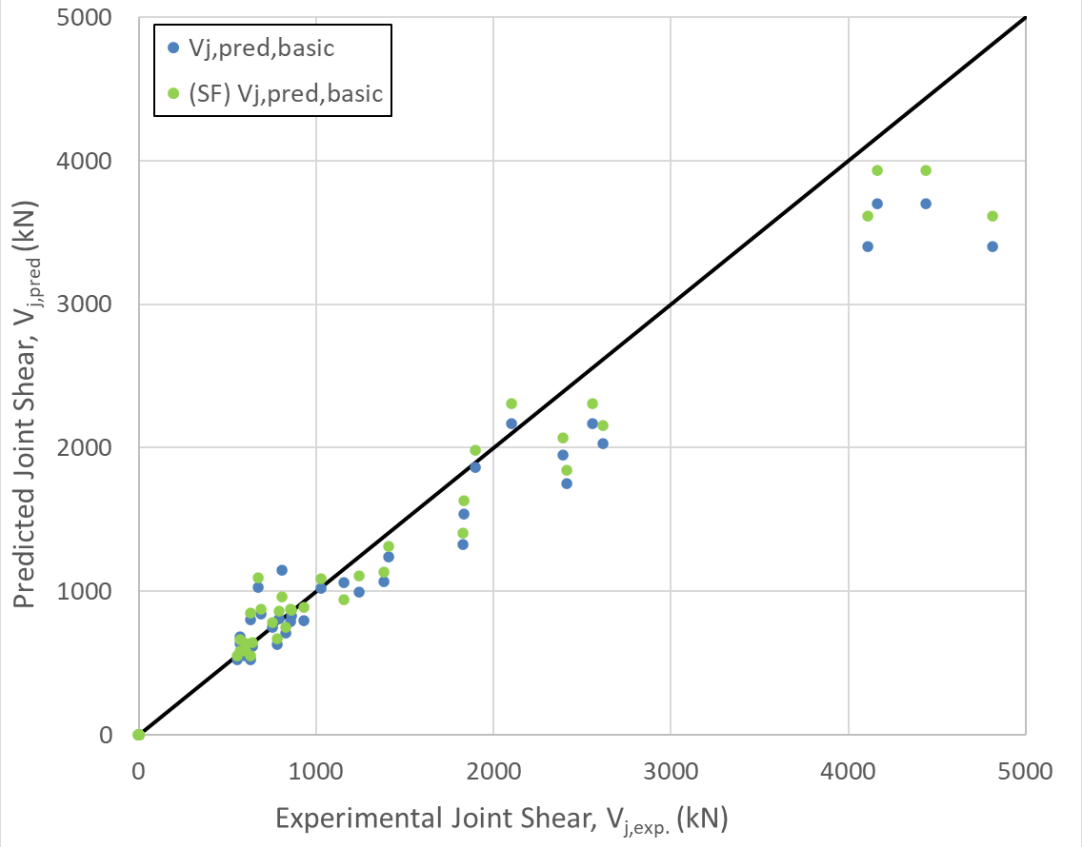


Figure 5.3. Influence of Slab Factor (SF)

5.4 Accuracy of the Joint Shear Strength Prediction

As presented in Section 4.2.1, a basic prediction equation is constructed using the fundamental characteristics of the beam-column joint, including the concrete compressive strength (f_c'), effective joint area (b_j h_c) and shear strength factor (γ). The details of determination of the Modification factors are described in Section 5.3, investigating the effect of each factor individually.

In this section, the accuracy of the proposed shear strength prediction equation is compared with the shear strength equations of contemporary structural codes, emphasizing the conformity requirements for each structural code, previously defined in Section 2.2.

In contemporary structural codes, although the key parameters considered for the determination of beam-column joint shear strength are mostly consistent, the computation methods vary across different codes. Even within the same code, different versions may adopt different approaches in succeeding revisions. This article evaluates and compares the beam-column joint shear strength prediction equations presented in four prominent North American Structural Codes and Turkish Earthquake Code. Various versions of ACI 318 (2011, 2014, and 2019) are assessed to highlight improvements in shear capacity predictions over time. The selected codes include ACI 352-10, ACI 318-11, ACI 318-14, ACI 318-19, ASCE 41-17, and CSA A23.3-19, TEC2007 and TEC2018.

Although these codes share a similar fundamental approach, there are notable differences that influence shear strength calculations.

The accuracy of the equations is examined in terms of the mean absolute error, the number of under and over predicted specimens and standard deviation. Moreover, the graphical representations of the comparison for the conforming and nonconforming specimens are presented.

Although the above mentioned structural codes cannot be used to predict the shear strength of the nonconforming specimens, except ASCE 41-17, which predicts the joint shear capacity of both conforming and nonconforming specimens, the predictions for the nonconforming specimens are also compared to obtain a viable option for deficient subassemblies and evaluate the performance of prediction equations for deficient joints.

The section is finalized with the observations gathered from the comparative analyses of the predictions.

5.4.1 Comparison with ACI 352-10

In this section of the thesis, the shear strength predictions obtained from the proposed equation are compared to ACI 352-10 requirements. In Table 5.12, a statistical comparison carried out for the "conforming" specimens is presented.

Table 5.12 Comparison of $V_{j,pre.}$ vs $V_{j,ACI\ 352\text{-}10}$ (Conforming Specimens)

	$V_{j,pre.}$	$V_{j,ACI\ 352\text{-}10}$
Total Number of Specimens	70	70
No. of Over Predicted Specimens	20	16
MAE_{over}	11.3%	14.9%
No. of Under Pred. Specimens	50	54
MAE_{under}	12.6%	19.0%
Standard Deviation	14.7%	18.1%
Overall Mean Absolute Error	12.2%	18.1%

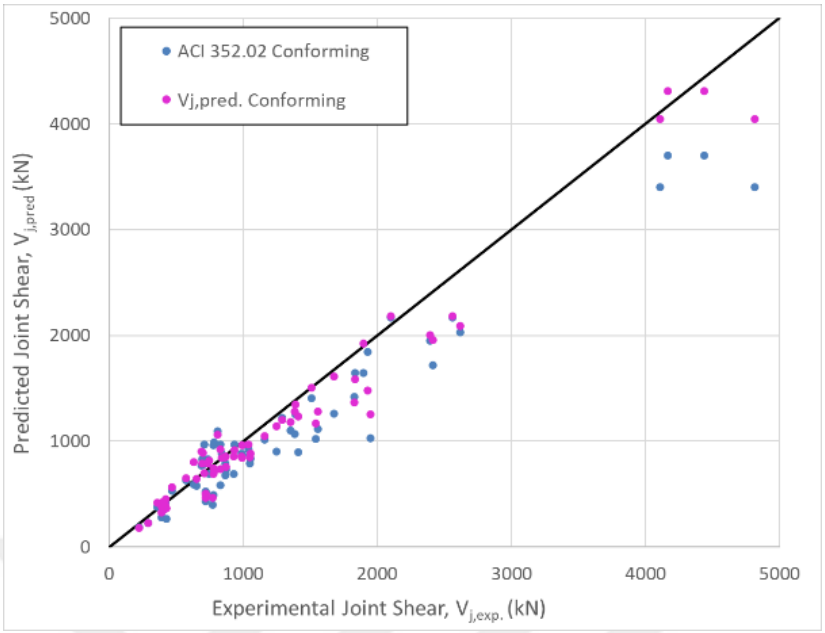


Figure 5.4. Comparison of $V_{j,pre.}$ vs $V_{j,ACI\ 352\text{-}10}$ (Conforming Specimens)

From Table 5.11 and Figure 5.4, it can be observed that the proposed shear strength equation predicts the joint strength with a higher accuracy for the code conforming specimens according to ACI 352-10. The mean absolute error value is lower for both the over predicted and under predicted specimens. When the results for the overall group are monitored, the accuracy of the proposed equation is 5.9 % higher than ACI 352-10 prediction. The standard deviation is also lower for both the over and under predicted specimens as verified by the lower data dispersion in Figure 5.4.

Table 5.13 Comparison of $V_{j,pre.}$ vs $V_{j,ACI\ 352\text{-}10}$ (Nonconforming Specimens)

	$V_{j,pre.}$	$V_{j,ACI\ 352\text{-}10}$
Total Number of Specimens	181	181
No. of Over Predicted Specimens	80	122
MAE_{over}	23.2%	36.9%
No. of Under Pred. Specimens	101	59
MAE_{under}	17.7%	23.4%
Standard Deviation	26.3%	41.3%
Overall Mean Absolute Error	20.1%	32.5%

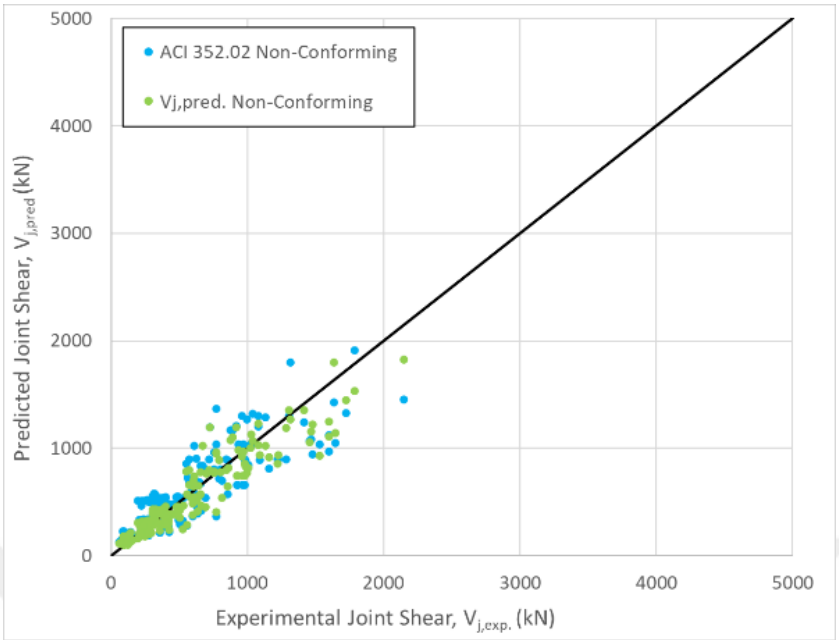


Figure 5.5. Comparison of $V_{j,pre.}$ vs $V_{j,ACI\ 352\text{-}10}$ (Nonconforming Specimens)

As previously stated, since this design code cannot be used to predict the shear strength of nonconforming joints, the evaluation presented below is for observing the general tendency of the accuracy of proposed equation. Thus, generalized results will be drawn from Figure 5.5.

From the results it can be concluded that the proposed equation predicts the joint shear capacity of the nonconforming group of ACI 352-10, with a moderately low data scatter. The number of under predicted specimens is 101 and for such a large group, the accuracy can be considered high with a MAE of % 17.7. As expected, the code prediction equation is not applicable for nonconforming joints, also observed in the comparison.

5.4.2 Comparison with ACI 318-11

In this subsection, the comparison of shear strength predictions of ACI 318-11 and proposed shear strength equation is presented. The comparison will first focus on the conforming specimens based on ACI 318-11 requirements. Then, the comparison for nonconforming specimens is also discussed.

Table 5.14 Comparison of $V_{j,pre.}$ vs $V_{j,ACI\ 318\text{-}11}$ (Conforming Specimens)

	$V_{j,pre.}$	$V_{j,ACI\ 318\text{-}11}$
Total Number of Specimens	63	63
No. of Over Predicted Specimens	16	15
MAE_{over}	13.9%	27.3%
No. of Under Pred. Specimens	47	48
MAE_{under}	14.7%	19.6%
Standard Deviation	16.7%	26.5%
Overall Mean Absolute Error	14.5%	21.4%

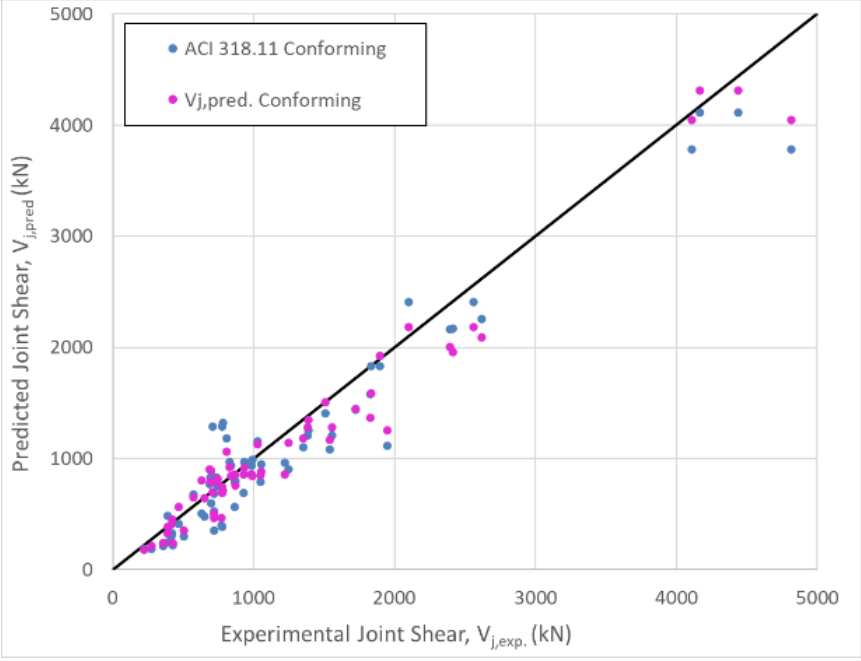


Figure 5.6. Comparison of $V_{j,pre.}$ vs $V_{j,ACI\ 318\text{-}11}$ (Conforming Specimens)

The first observation from the statistical results is that the proposed model predicts the joint shear capacities of the conforming group with a significant margin, as the overall MAE of $V_{j,pre}$ is 6.9% lower than that of $V_{j,ACI318-11}$. When the over-predicted and under predicted specimens are analyzed, the same result can be inferred since the MAE values of both groups are lower for $V_{j,pre}$ equation. Also focusing on the comparison of the standard deviation values, $V_{j,pre}$ equation predicts the shear joint strength with a significantly lower data dispersion, also revealed in Figure 5.6.

Table 5.15 Comparison of $V_{j,pre.}$ vs $V_{j,ACI\ 318-11}$ (Nonconforming Specimens)

	$V_{j,pre.}$	$V_{j,ACI\ 318-11}$
Total Number of Specimens	188	188
No. of Over Predicted Specimens	84	136
MAE_{over}	22.1%	44.6%
No. of Under Pred. Specimens	104	52
MAE_{under}	16.6%	20.6%
Standard Deviation	25.4%	43.3%
Overall Mean Absolute Error	19.0%	38.0%

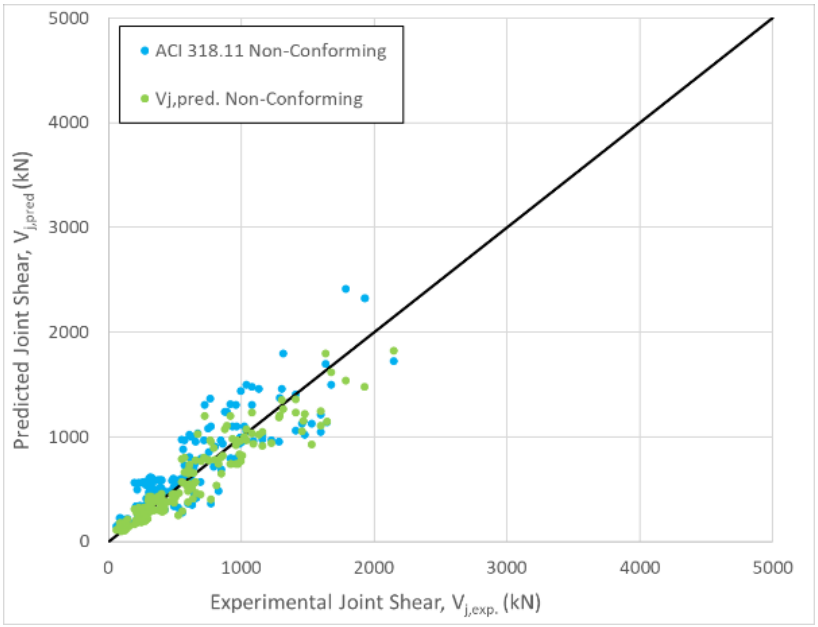


Figure 5.7. Comparison of $V_{j,pre.}$ vs $V_{j,ACI\ 318-11}$ (Nonconforming Specimens)

The proposed equation predicts the joint shear capacity of the nonconforming specimens with a MAE of 19.0 %, with a relatively low standard deviation of % 25.4. Expectedly, the equation proposed in ACI 318-14 is not adequate in determination of nonconforming specimens which can be monitored by the evaluation of results presenting considerably high MAE and standard deviation.

5.4.3 Comparison with ACI 318-14

In this section, an analysis comparing the predictions of shear strength as per ACI 318-14 standards and the proposed shear strength model is presented. Initially, the comparison will focus on specimens that adhere to the ACI 318-14 guidelines. Subsequently, the predictions on the nonconforming specimens are also evaluated.

Table 5.16 Comparison of $V_{j,pre.}$ vs $V_{j,ACI\ 318\text{-}14}$ (Conforming Specimens)

	$V_{j,pre.}$	$V_{j,ACI\ 318\text{-}14}$
Total Number of Specimens	59	59
No. of Over Predicted Specimens	16	17
MAE_{over}	13.9%	25.2%
No. of Under Pred. Specimens	43	42
MAE_{under}	13.1%	14.8%
Standard Deviation	15.8%	24.4%
Overall Mean Absolute Error	13.4%	17.8%

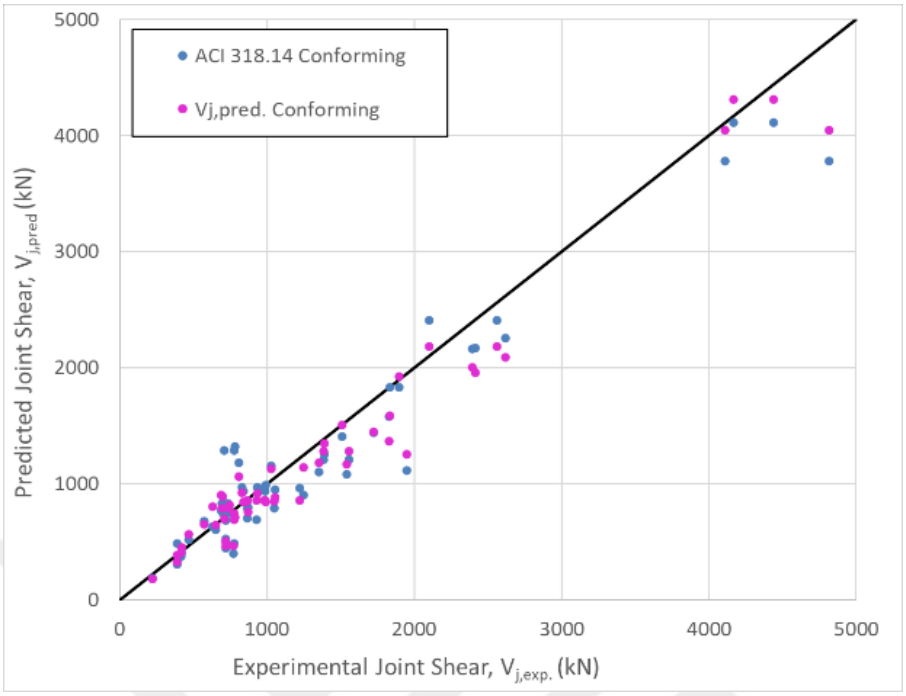


Figure 5.8. Comparison of $V_{j,pre.}$ vs $V_{j,ACI\ 318\text{-}14}$ (Conforming Specimens)

Considering conforming specimens, the proposed shear strength prediction equation yields more accurate results with a MAE of 13.4%, when compared to ACI 318-14 results with a MAE of 17.8%. It is important to underline that the difference in MAE of over-predicted specimens is more significant with a difference of 11.3%, which indicated the predicted equation is more conservative. Additionally, the standard deviations are lower for both the over predicted and under predicted specimens, indicating a lower dispersion.

Table 5.17 Comparison of $V_{j,pre.}$ vs $V_{j,ACI\ 318\text{-}14}$ (Nonconforming Specimens)

	$V_{j,pre.}$	$V_{j,ACI\ 318\text{-}14}$
Total Number of Specimens	192	192
No. of Over Predicted Specimens	84	136
MAE_{over}	22.1%	44.6%
No. of Under Pred. Specimens	108	56
MAE_{under}	17.1%	20.1%
Standard Deviation	25.6%	43.4%
Overall Mean Absolute Error	19.3%	37.5%

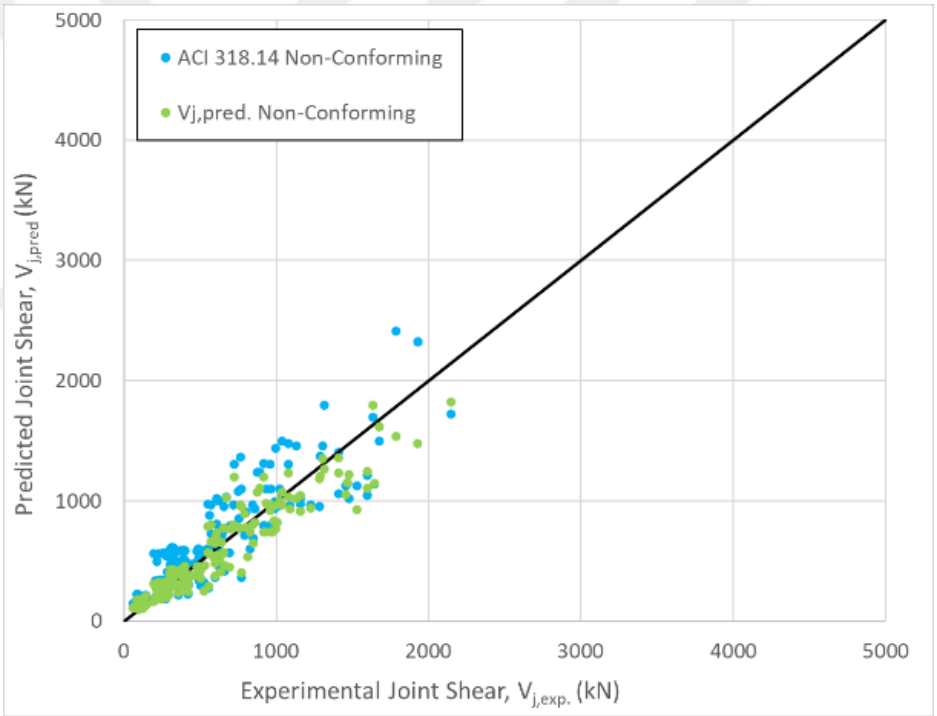


Figure 5.9. Comparison of $V_{j,pre.}$ vs $V_{j,ACI\ 318\text{-}14}$ (Nonconforming Specimens)

The proposed joint shear equation predicts the shear strength of the nonconforming sample set based on ACI 318-14 requirements with a mean absolute error (MAE) of 19.3% and a standard deviation of 25.4%.

As expected, the equation introduced in ACI 318-14 is not suitable for assessing nonconforming specimens, as evidenced by the evaluation of results with significantly high MAE and standard deviation.

5.4.4 Comparison with ACI 318-19

The shear strength prediction procedure of ACI 318-19 is significantly revised when compared to the previous versions of the code, as discussed in Section 2.4. Since this version is the latest guidelines that is currently in use, it is important to compare and understand its implications thoroughly. This comparison will aid in determining the effectiveness of the code requirements and the improvements when compared to the prior versions.

Table 5.18 Comparison of $V_{j,pre.}$ vs $V_{j,ACI\ 318\text{-}19}$ (Conforming Specimens)

	$V_{j,pre.}$	$V_{j,ACI318\text{-}19}$
Total Number of Specimens	59	59
No. of Over Predicted Specimens	16	18
MAE_{over}	13.9%	26.6%
No. of Under Pred. Specimens	43	41
MAE_{under}	13.1%	14.6%
Standard Deviation	15.8%	25.2%
Overall Mean Absolute Error	13.4%	18.2%

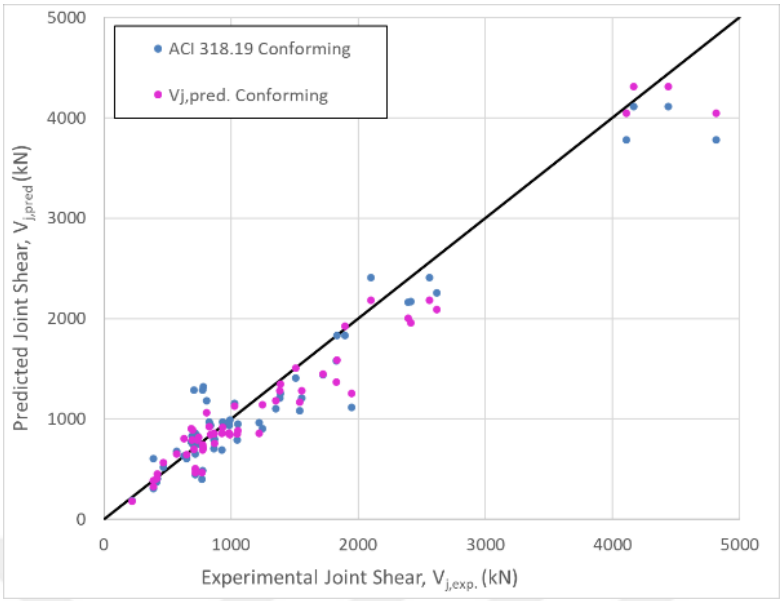


Figure 5.10. Comparison of $V_{j,pre.}$ vs $V_{j,ACI\ 318\text{-}19}$ (Conforming Specimens)

From the comparison, it can be inferred that the proposed equation has a better performance than $V_{j,ACI318\text{-}19}$, with lower mean absolute errors both for over and under predicted joints, a lower standard deviation indicating more consistent predictions, and a lower overall mean absolute error.

Table 5.19 Comparison of $V_{j,pre.}$ vs $V_{j,ACI\ 318\text{-}19}$ (Nonconforming Specimens)

	$V_{j,pre.}$	$V_{j,ACI318\text{-}19}$
Total Number of Specimens	192	192
No. of Over Predicted Specimens	84	145
MAE_{over}	22.1%	44.7%
No. of Under Pred. Specimens	108	47
MAE_{under}	17.1%	18.7%
Standard Deviation	25.6%	43.0%
Overall Mean Absolute Error	19.3%	38.4%

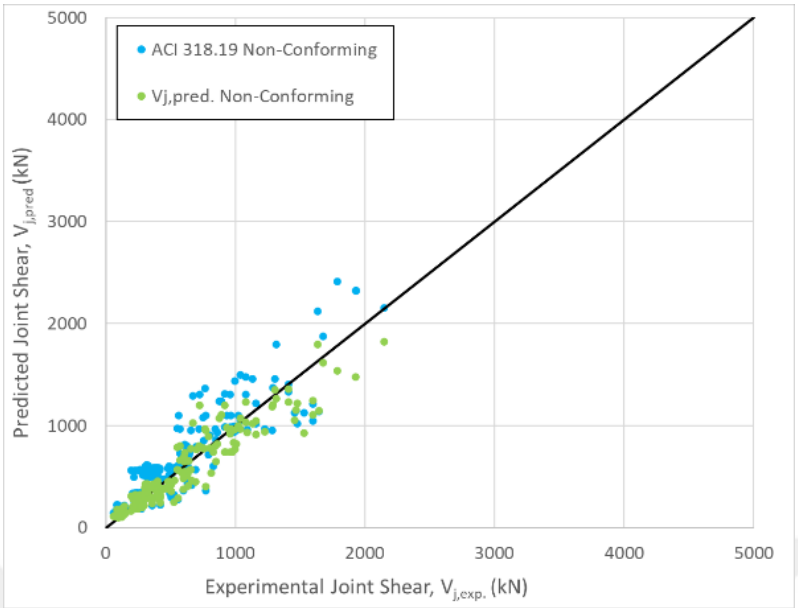


Figure 5.11. Comparison of $V_{j,pre.}$ vs $V_{j,ACI\ 318\text{-}19}$ (Conforming Specimens)

When the nonconforming group of specimens per ACI 318-19 are investigated, the same pattern is observed. The proposed equation predicts the joint shear capacity of the group with a successful MAE of 19.3 %. Additionally, the standard deviation is 25.6 %, underlining a low scatter of data around the mean value.

As for the previously evaluated standards, ACI 318-19 joint shear strength equation is not applicable for nonconforming specimens and leads to overprediction of joint shear strength, which is unconservative.

5.4.5 Comparison with ASCE 41-17

In this section, the comparison of the joint shear strength equation of ASCE 41-17 with proposed equation is presented. This comparison is crucial as ASCE 41-17 provides prediction methods for both conforming and nonconforming specimens, setting it apart from other design codes. First, the performance of the proposed model for conforming specimens is presented. Later, the evaluation is carried out for the nonconforming specimens.

Table 5.20 Comparison of $V_{j,pre.}$ vs $V_{j,ACI\ 41\text{-}17}$ (Conforming Specimens)

	$V_{j,pre.}$	$V_{j,ASCE\ 41.17}$
Total Number of Specimens	193	193
No. of Over Predicted Specimens	65	110
MAE_{over}	19.2%	33.0%
No. of Under Pred. Specimens	128	83
MAE_{under}	15.9%	15.5%
Standard Deviation	21.4%	32.6%
Overall Mean Absolute Error	17.0%	25.5%

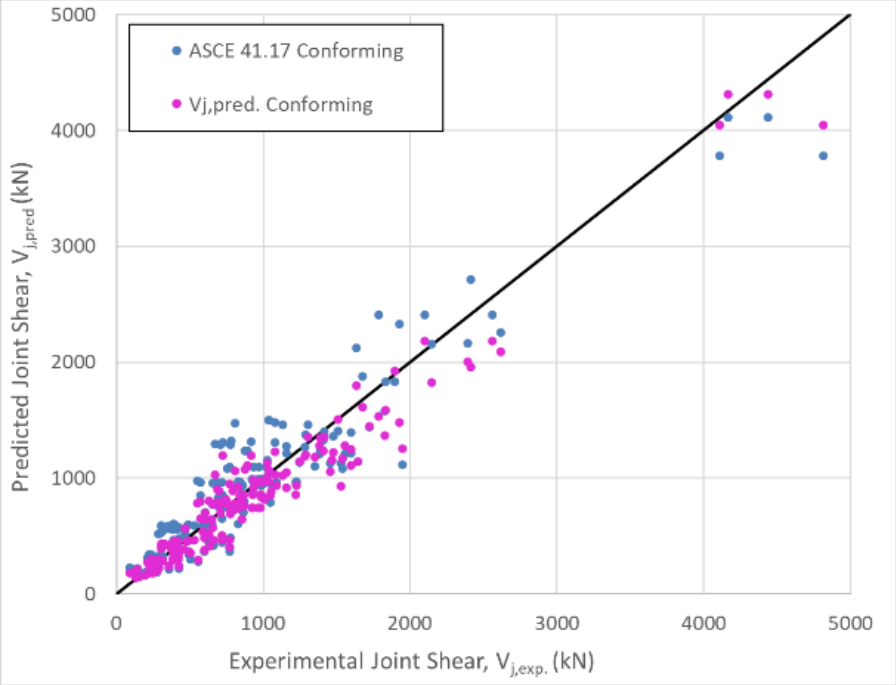


Figure 5.12. Comparison of $V_{j,pre.}$ vs $V_{j,ASCE\ 41\text{-}17}$ (Conforming Specimens)

From the data presented in Table 5.20 and Figure 5.12, the results presented below are obtained.

The $V_{j,pre.}$ overestimates shear strength for 65 specimens with a mean absolute error (MAE) of 19.2%, while underestimates for 128 specimens with a MAE of 15.9%,

which is validates the conservativeness of the equation The predictions displayed a standard deviation of 21.4%, indicating an adequate accuracy. When all code conforming specimens are considered, the mean absolute error becomes 17.0%. In contrast, $V_{j,ASCE\ 41.17}$ overpredicts shear strength for 110 joints with a significantly higher MAE of 33.0%, and underpredicts 83 joints with a MAE of 15.5%. The standard deviation for $V_{j,ASCE\ 41.17}$ was notably higher at 32.6%, which is consistent with higher dispersion of data. The mean absolute error for conforming specimens is 25.5%, indicating lower accuracy compared to the $V_{j,pre.}$ equation.

Table 5.21 Comparison of $V_{j,pre.}$ vs $V_{j,ACI\ 41\text{-}17}$ (Nonconforming Specimens)

	$V_{j,pre.}$	$V_{j,ASCE\ 41.17}$
Total Number of Specimens	58	58
No. of Over Predicted Specimens	35	11
MAE_{over}	23.7%	22.0%
No. of Under Pred. Specimens	23	47
MAE_{under}	16.7%	26.3%
Standard Deviation	21.6%	23.8%
Overall Mean Absolute Error	21.0%	25.4%

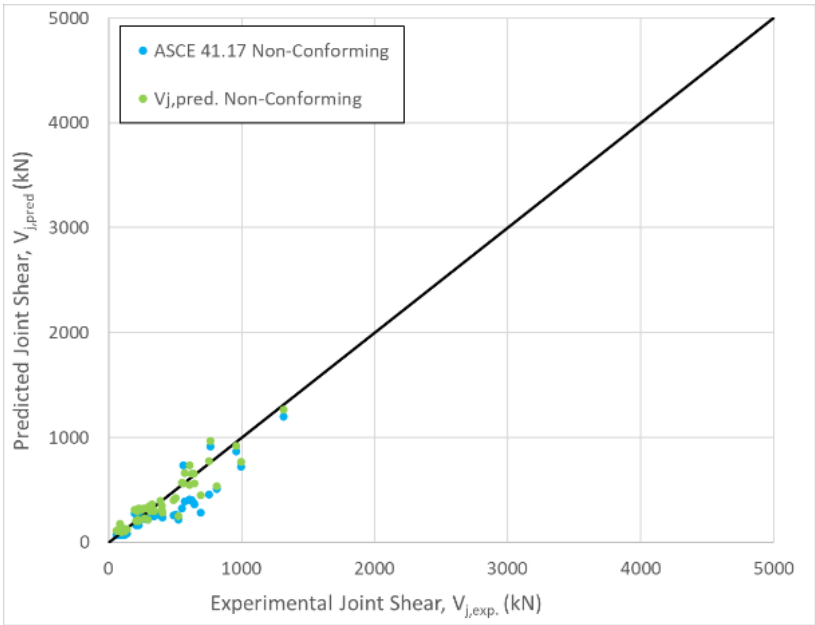


Figure 5.13. Comparison of $V_{j,pre.}$ vs $V_{j,ASCE\ 41\text{-}17}$ (Nonconforming Specimens)

The $V_{j,pre}$ results in overprediction of the shear strength for 35 specimens with a mean absolute error (MAE) of 23.7%, whereas $V_{j,ASCE\ 41\text{-}17}$ overpredicts only 11 specimens with a slightly lower MAE of 22.0%. On the other hand, $V_{j,pre}$ under predicts the strength for 23 specimens with a MAE of 16.7%, compared to $V_{j,ASCE\ 41\text{-}17}$ under-predictions for 47 specimens, which constitutes the majority of the joints, with a higher MAE of 26.3%. This indicates the tendency of ASCE 41-17 to underpredict the joint shear strength for deficient specimens. The MAE for all deficient joints is 21.0% for $V_{j,pre}$, whereas it is 25.4% for $V_{j,ASCE\ 41\text{-}17}$.

This underestimation of joint shear strength by $V_{j,ASCE\ 41\text{-}17}$ indicates the deficient joints are over penalized by the code requirements. However, the proposed equation has low mean absolute error and standard deviation, which confirms its accuracy and makes it a viable option for the shear strength prediction of deficient joints.

5.4.6 Comparison with CSA A23.03-19

In this section, the comparison of joint shear strength prediction equations of CSA.A23.03-19 with the proposed one is carried out.

The conforming specimens are evaluated first and then, the comparison for nonconforming specimens is presented.

Table 5.22 Comparison of $V_{j,pre.}$ vs $V_{j,CSA.A23.03\text{-}19}$ (Conforming Specimens)

	$V_{j,pre.}$	$V_{j,CSA.A23.03\text{-}19}$
Total Number of Specimens	93	93
No. of Over Predicted Specimens	32	28
MAE_{over}	16.3%	20.8%
No. of Under Pred. Specimens	61	65
MAE_{under}	13.3%	19.3%
Standard Deviation	18.0%	22.9%
Overall Mean Absolute Error	14.3%	19.7%

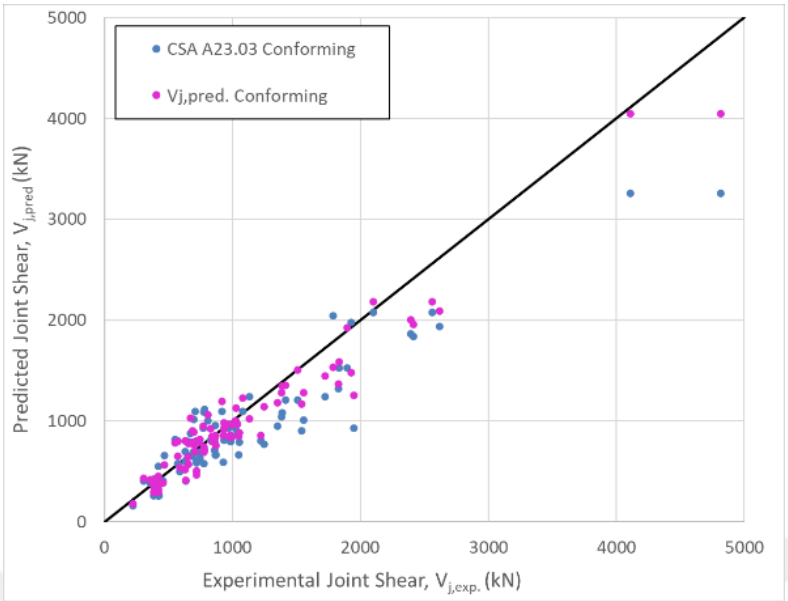


Figure 5.14. Comparison of $V_{j,pre.}$ vs $V_{j,CSA\ A23.03\text{-}19}$ (Conforming Specimens)

A total of 93 conforming specimens based on CSA.A23.03-19 requirements are evaluated.

The $V_{j,pre}$ model overpredicts shear strength for 32 specimens with a mean absolute error (MAE) of 16.3%, which is lower than the $V_{j,CSA.A23.03\text{-}19}$ overprediction MAE of 20.8% for 28 specimens. $V_{j,pre}$ underpredicts 61 specimens with a MAE of 13.3%, compared to $V_{j,CSA.A23.03\text{-}19}$ which underpredicts 65 specimens with a higher MAE of 19.3%.

The standard deviation for $V_{j,pre}$ was 18.0%, indicating less data scatter than $V_{j,CSA.A23.03\text{-}19}$, which has a standard deviation of 22.9%.

The overall mean absolute error for $V_{j,pre}$ was 14.3%, lower than the MAE of 19.7% for $V_{j,CSA.A23.03\text{-}19}$.

Essentially, the proposed equation has a better performance in terms of mean absolute errors and exhibited less data scatter in its predictions when compared to $V_{j,CSA.A23.03\text{-}19}$.

Table 5.23 Comparison of $V_{j,pre.}$ vs $V_{j,CSA.A23.03-19}$ (Nonconforming Specimens)

	$V_{j,pre.}$	$V_{j,CSA.A23.03-19}$
Total Number of Specimens	158	158
No. of Over Predicted Specimens	68	89
MAE_{over}	22.9%	34.8%
No. of Under Pred. Specimens	90	69
MAE_{under}	17.8%	24.4%
Standard Deviation	26.5%	38.9%
Overall Mean Absolute Error	20.0%	30.2%

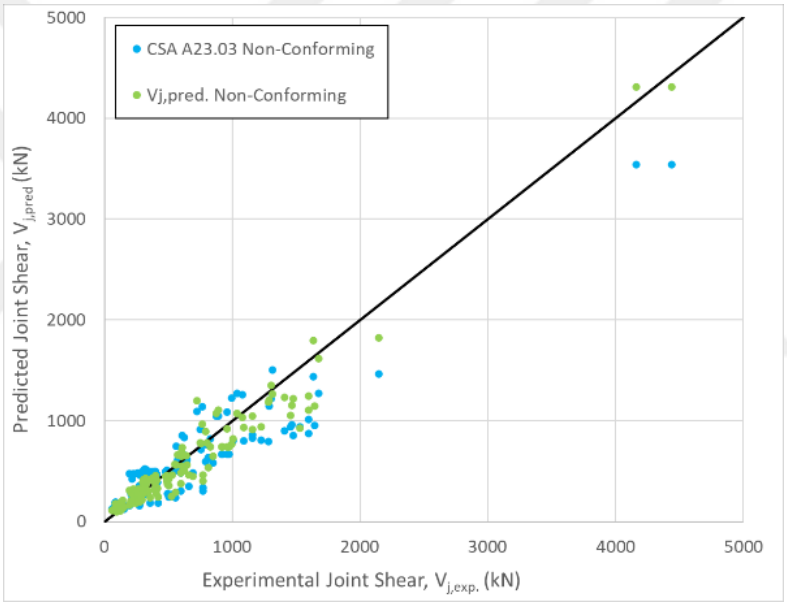


Figure 5.15. Comparison of $V_{j,pre.}$ vs $V_{j,CSA\ A23.03-19}$ (Nonconforming Specimens)

The proposed equation predicts the shear strength of nonconforming joints based on CSA A23.03-19 requirements with a MAE of 20.0 %. The standard deviation of the predictions is also reasonably low, with a value of 26.5%.

5.4.7 Comparison with TEC2007

TEC2007 is the only evaluated structural code, predicting the joint shear strength based on the design compressive strength of concrete, f_{cd}, considering the failure is related to the capacity of compression struts instead of $\sqrt{f_{cd}}$ representing tension failure. Therefore, the comparison of the proposed prediction equation with TEC2007 requirements is important to evaluate the effect of the concrete compressive strength implication in the equation, in addition to the validation of the accuracy of the proposed equation in comparison with TEC2007.

First, conforming specimens are compared and evaluated. The subsection will be finalized with the evaluation of nonconforming specimens.

Table 5.24 Comparison of $V_{j,pre.}$ vs $V_{j,TEC2007}$ (Conforming Specimens)

	$V_{j,pre.}$	$V_{j,TEC2007}$
Total Number of Specimens	90	90
No. of Over Predicted Specimens	30	78
MAE_{over}	16.6%	65.4%
No. of Under Pred. Specimens	60	12
MAE_{under}	15.1%	15.1%
Standard Deviation	19.5%	56.1%
Overall Mean Absolute Error	15.6%	58.7%

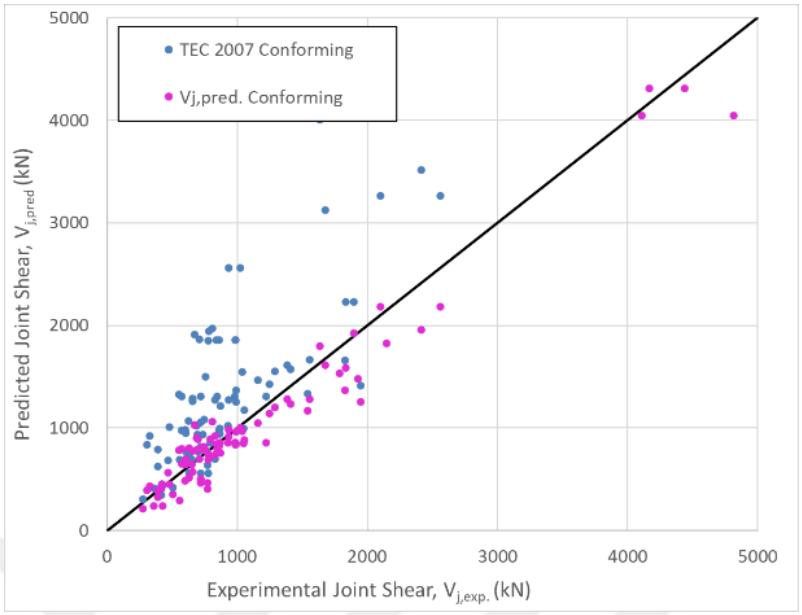


Figure 5.16. Comparison of $V_{j,pre.}$ vs $V_{j,TEC2007}$ (Conforming Specimens)

The $V_{j,pre.}$ equation overpredicts shear strength in 30 specimens with a mean absolute error (MAE) of 16.6%, while the $V_{j,TEC2007}$ overpredicts in a significantly higher number of cases, totaling 78 specimens, with a much larger MAE of 65.4%. On the underprediction side, the $V_{j,pre.}$ equation underpredicts for 60 specimens with an MAE of 15.1%, identical to the MAE_{under} for $V_{j,TEC2007}$, which underpredicts for only 12 specimens.

The standard deviation for the equation $V_{j,pre.}$ is at 19.5%, indicating a moderate dispersion of data. In contrast, the $V_{j,TEC2007}$ exhibits a very high standard deviation of 56.1%, suggesting a much greater variability in its predictions.

Overall, the mean absolute error for the $V_{j,pre.}$ equation is substantially lower at 15.6% compared to the $V_{j,TEC2007}$ overall MAE of 58.7%. This indicates that the $V_{j,pre.}$ equation generally provides much more accurate and consistent predictions for the joint shear strength than the predictions based on the TEC2007 standard, which also indicates the necessity of using tensile strength representation for joint capacity estimations.

Table 5.25 Comparison of $V_{j,pre.}$ vs $V_{j,TEC2007}$ (Nonconforming Specimens)

	$V_{j,pre.}$	$V_{j,TEC2007}$
Total Number of Specimens	161	161
No. of Over Predicted Specimens	70	150
MAE_{over}	22.6%	112.4%
No. of Under Pred. Specimens	91	11
MAE_{under}	16.6%	9.3%
Standard Deviation	25.7%	89.1%
Overall Mean Absolute Error	19.2%	105.3%

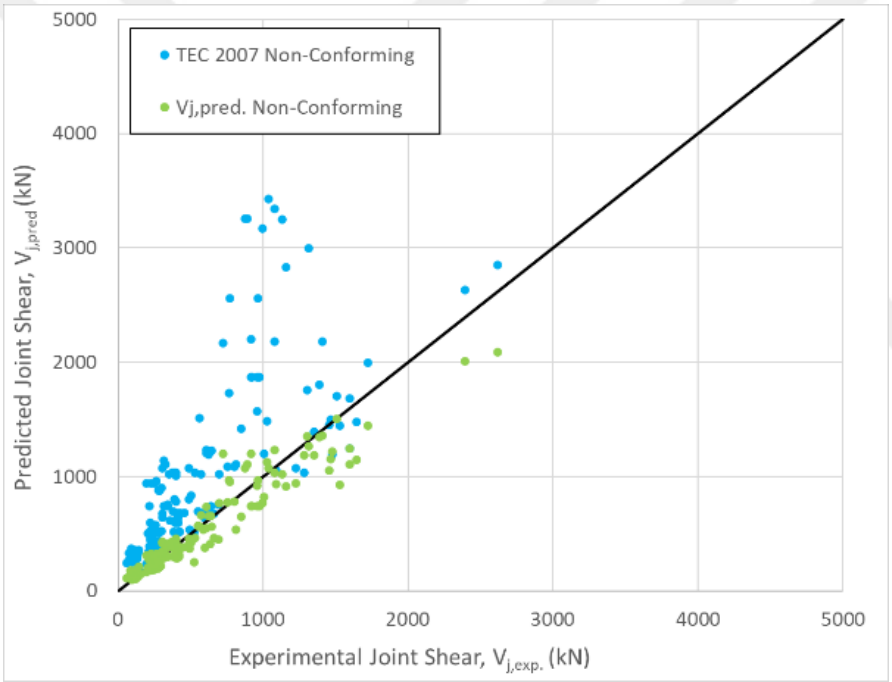


Figure 5.17. Comparison of $V_{j,pre.}$ vs $V_{j,TEC2007}$ (Nonconforming Specimens)

The proposed formula predicts the shear strength of nonconforming joints based on TEC2007 recommendations with a mean absolute error (MAE) of 19.2%. Additionally, the standard deviation of the predictions is reasonably low, standing at 25.7%.

5.4.8 Comparison with TEC2018

Finally, the comparison of results is extended to the evaluation of TEC2018 predictions with the proposed joint shear strength values. Moreover, the improvement achieved by the revision of the shear capacity prediction equation of TEC2018 when compared to TEC2007 is investigated.

Table 5.26 Comparison of $V_{j,pre.}$ vs $V_{j,TEC2018}$ (Conforming Specimens)

	$V_{j,pre.}$	$V_{j,TEC2018}$
Total Number of Specimens	90	90
No. of Over Predicted Specimens	30	27
MAE_{over}	16.6%	31.0%
No. of Under Pred. Specimens	60	63
MAE_{under}	15.1%	24.0%
Standard Deviation	19.5%	31.5%
Overall Mean Absolute Error	15.6%	26.1%

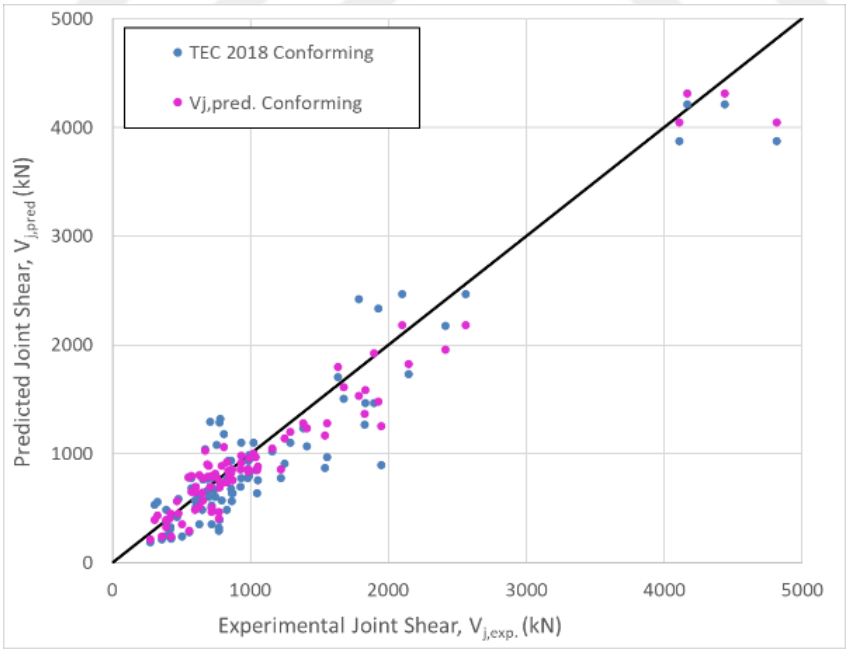


Figure 5.18. Comparison of $V_{j,pre.}$ vs $V_{j,TEC2018}$ (Conforming Specimens)

The $V_{j,pre}$ equation and $V_{j,TEC2018}$ are each assessed on a dataset of 90 conforming specimens to predict the shear strength.

The $V_{j,pre}$ equation overpredicts the shear strength for 30 specimens with a mean absolute error (MAE) of 16.6%, whereas $V_{j,TEC2018}$ overpredicts for a slightly lower number of specimens, 27, but with a higher MAE of 31.0%. When it comes to underprediction, the $V_{j,pre}$ equation underpredicts for 60 specimens with an MAE of 15.1%, while the $V_{j,TEC2018}$ standard underpredicts for 63 specimens with a significantly higher MAE of 24.0%.

The standard deviation associated with the $V_{j,pre}$ equation is 19.5%, which indicates a moderate data scatter. On the other hand, TEC2018 has a higher standard deviation of 31.5%, suggesting greater variability in its predictions.

Overall, the mean absolute error for the $V_{j,pre}$ equation is 15.6%, which is notably lower than the overall MAE of 26.1% for the $V_{j,TEC2018}$. This comparison indicates that the $V_{j,pre}$ equation provides more accurate and consistent predictions for the joint shear strength than $V_{j,TEC2018}$.

Moreover, the revision of the shear strength prediction equation with the implication of square root of characteristic compressive strength, $\sqrt{f_{ck}}$ instead of the design compressive strength, f_{cd}, improved the accuracy of the TEC2018 predictions from an MAE value of %58.7 for TEC2007 to %26.1. From these results, it is clear that $Vj_{,TEC2018}$ provides more accurate and consistent predictions than $V_{j,TEC2007}$. The standard deviation and overall MAE are both significantly lower for $V_{j,TEC2018}$, indicating that its predictions are closer to the actual shear strengths when compared to TEC2007 .

However, it should be noted that the mean absolute error is still high for shear strength prediction of joints when compared to the proposed equation and other contemporary structural codes.

The comparison for nonconforming specimens is provided in Table 5.27 and Figure 5.19.

Table 5.27 Comparison of $V_{j,pre.}$ vs $V_{j,TEC2018}$ (Nonconforming Specimens)

	$V_{j,pre.}$	$V_{j,TEC2018}$
Total Number of Specimens	161	161
No. of Over Predicted Specimens	70	103
MAE_{over}	22.6%	47.0%
No. of Under Pred. Specimens	91	58
MAE_{under}	16.6%	21.8%
Standard Deviation	25.7%	46.6%
Overall Mean Absolute Error	19.2%	38.0%

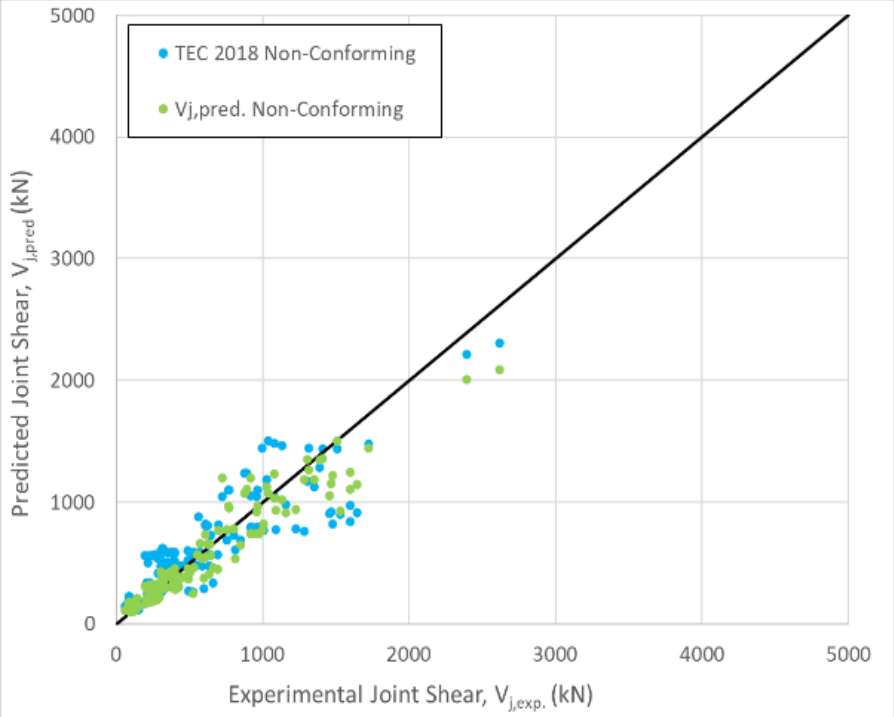


Figure 5.19. Comparison of $V_{j,pre.}$ vs $V_{j,TEC2018}$ (Nonconforming Specimens)

The proposed equation predicts the shear capacity of nonconforming joints based on TEC2018 requirements with a MAE of 19.2% and a standard deviation of 25.7%. As a final comparison of the joint shear strength prediction equations from the Turkish

Earthquake Codes TEC2007 and TEC2018, the importance of the improvement of the accuracy for both conforming and nonconforming specimens must be underlined.

From the unfortunate experience of Kahramanmaraş Earthquakes encountered in February 2023, it is observed that many existing reinforced concrete buildings experienced inadequate member capacities, not surprisingly, including beam-column joints, an unfortunate example of which is presented in Figure 5.20.



Figure 5.20. Beam-Column Joint Failure Mechanism

The accurate prediction of joint shear strength in deficient buildings, which are frequently encountered in the building stock of Turkey, is of paramount importance for evaluating the structural performance of such buildings. Given the unique

challenges posed by nonconforming structures, the development of an accurate equation capable of predicting the shear capacities of deficient joints is imperative for the Turkish Earthquake Code. This necessity is underscored by the seismic events that unfolded during the Kahramanmaraş Earthquakes in February 2023, serving as an important reminder of the critical need for reliable predictive tools in seismic-prone regions like Turkey. By accurately predicting the seismic behavior of these structures, engineers can make informed decisions to enhance the safety and resilience of buildings, ultimately contributing to better disaster preparedness and mitigation strategies for potential seismic hazards.

CHAPTER 6

VERIFICATION OF ANALYTICAL MODEL

6.1 Overview

An analytical model is developed to predict the behavior of beam-column connections, focusing specifically on the shear strength and deformation characteristics of joints under cyclic loading. The model is integrated within a computational framework to facilitate a rigorous validation process. The validation process employs experimental data extracted from prior research studies. For this purpose, analytical models representing beam-column connection subassemblies under cyclic loading are developed. Subsequently, a detailed comparison between the analytical and experimental results is conducted to verify that the developed model accurately reflects the connection response.

In the verification of the proposed beam-column joint non-linear behavior model, structural analysis and design software SAP2000 is utilized due to the popularity and widespread use of this software in structural engineering design and analysis, internationally.

6.2 Description of Modeling and Elements

Two distinct models have been created to represent the interior and exterior beam-column connections for the analytical verification process. Beams and columns are modeled as line elements defined in the software and joint element which is defined as “Panel Zone” serves to connect the line elements. The cyclic loading histories of tested subassemblies are applied from the column end, in line with the experimental loading scheme. Detailed descriptions of the elements constituting the connection model are provided in the subsequent sections.

A sample beam-column connection subassembly is presented in Figure 6.1.

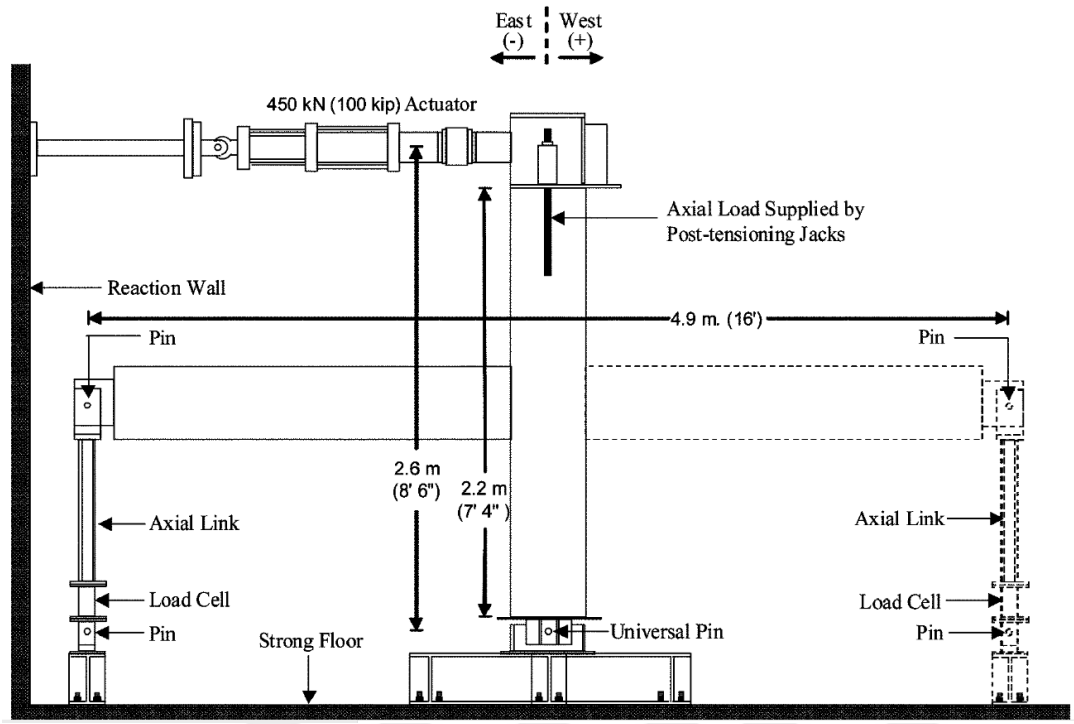


Figure 6.1. Beam-Column Connection Subassembly (Burak & Wight, 2008)

6.2.1 Modeling of Beam-Column Connection Subassemblies

As briefly presented in Figure 6.2, the beam-column connection subassembly is idealized using line elements representing beams and columns, whereas the joint region is represented using the panel zone element provided in the software. Nonlinear properties of beams and columns are concentrated at the end of members, using zero length rotational elements called “nonlinear hinges”. The remaining part of the line elements are defined as linear elastic elements with reduced stiffness properties to account for the cracked section characteristics under excessive deformations resulting from earthquake loading.

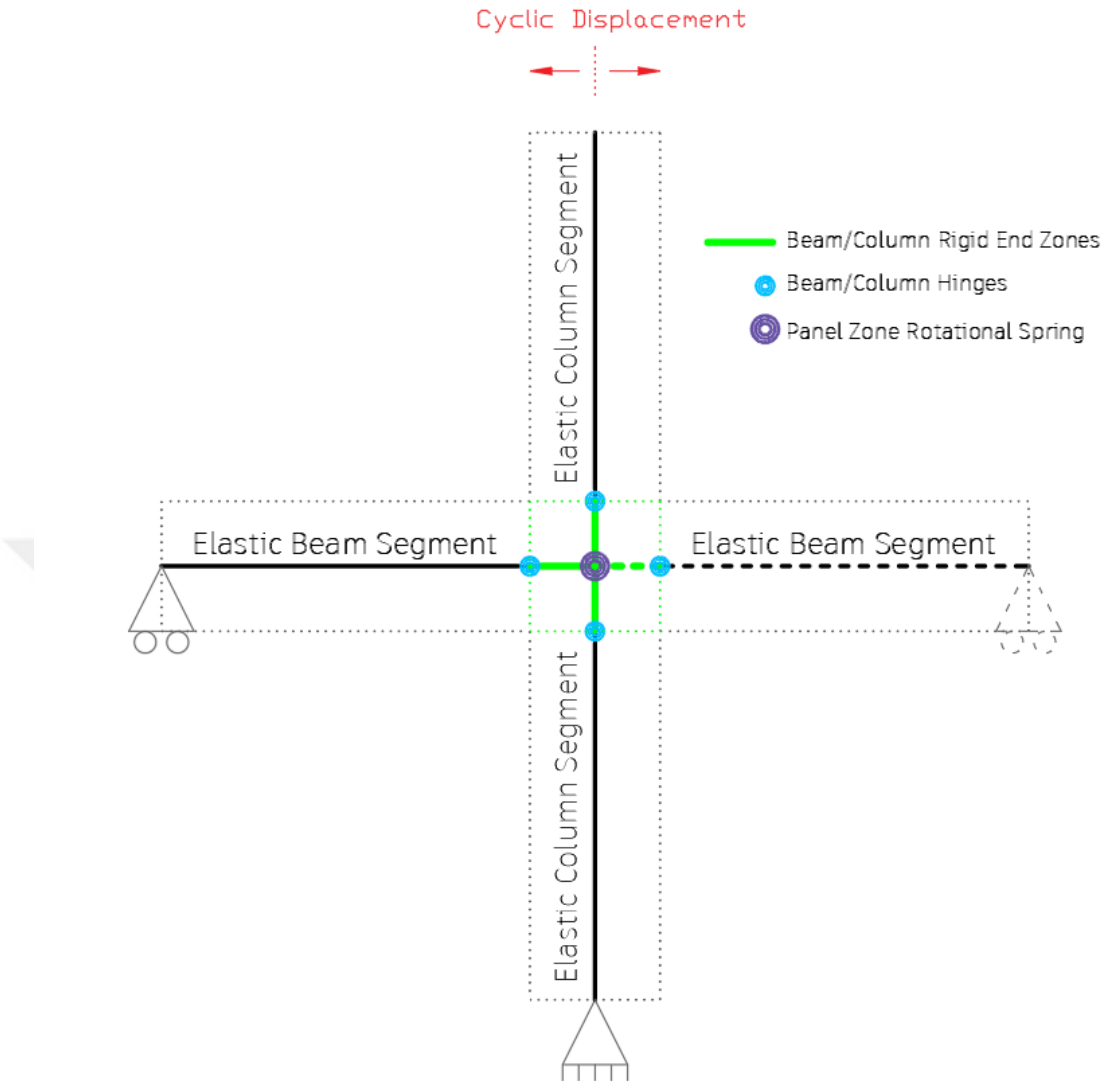


Figure 6.2. Beam-Column Subassembly Model

Definition of Elastic Beam and Column Segments

In order to model the beam and column elements in SAP 2000, the required inputs are the sectional dimensions and material properties. The modulus of elasticity is defined in accordance with the definition presented in ACI 318-19, in relation to the compressive capacity of concrete, utilizing Eqn. 6.1.

$$E_c = 4700\sqrt{f_c'}\ (\text{MPa}) \tag{6.1}$$

Moment - Rotation Relationship of Beams and Columns

Utilizing *'Response2000, Reinforced Concrete Sectional Analysis*' software, the relationship between moment and curvature for beams and columns is established. Then, obtained curvature values are multiplied by the plastic hinge lengths to derive moment vs. rotation relationship of the structural members. Beam and column elements are connected with the joint panel through rotational springs of zero length, which have their moment-rotation behavior characterized by a hysteretic model.

In order to account for the cracked stiffness of members, cracked moment of inertia (I_{cr}) of beams and columns are determined in accordance with the provisions of ACI 318-19 utilizing Eqn. 6.2.

$$\begin{aligned} I_{cr,beams} &= 0.35\, I_{beam,gross} \\ I_{cr,columns} &= 0.70\, I_{beam,gross} \end{aligned} \qquad (6.2)$$

According to ACI 318-19, Section 6.6.3.1.1, the gross moment of inertia can be determined as twice the moment of inertia of the web, for flanged sections.

$$I_{g,flanged} = 2\left(\frac{b_w\, h^3}{12}\right) \qquad (6.3)$$

In 6.6.3.1.2 clause of the same reference, the cracked stiffness under lateral loading is assumed as, moment of inertia of the web for flanged sections.

$$I_{cr,flanged} = \left(\frac{b_w\, h^3}{12}\right) \qquad (6.4)$$

Plastic Hinge Lengths

Accurate estimation of plastic hinge length is required in order to adequately define the moment-rotation characteristics of beams and columns. Based on ACI 318-19 requirements, plastic hinges are designated as the segment within a frame element where flexural yielding is expected due to seismic deformations. This segment must extend at least a distance equal to the member depth (h) from the point where flexural yielding starts. Whereas Turkish Earthquake Code (TEC 2018) recommends a plastic hinge length of half the member depth (h/2). After evaluation of both alternatives, it is determined that ACI 318-19 plastic hinge length yields better results in terms of connection response. Consequently, both for columns and beams, the plastic hinge length is specified as the member depth (h).

Rigid End Zones

As presented in Figure 6.2, the end zones of members within the joint are represented as "rigid end zones". In the subassembly models in which the joint response is addressed via nonlinear panel zones, the segments of members adjoining within the joint are considered as rigid end zones with a rigidity factor of 1.0. This way, the nonlinear joint response is concentrated in the joint panel zone. To evaluate the possibility of defining the joint nonlinear response by reducing the rigidity of the members within the joint without utilizing a joint model, 2 individual subassembly models with rigid end zones having rigidity factor of 1.0 and 0.5 are generated without assigning any panel zones at the joint. The first model represents the rigid joint assumption, while the second one corresponds to semi-rigid joints without the use of any joint model.

To summarize, 3 models are generated for each subassembly.

Model 1: Panel zone assigned to the joint, with rigid end zones having rigidity factors of 1.0.

Model 2: Panel zones are NOT assigned to the joint, with rigid end zones having rigidity factors of 1.0.

Model 3: Panel zones are NOT assigned to the joint, with rigid end zones having rigidity factors of 0.5.

Joint Panel Zones

For joints where beams and columns are framing into, a nonlinear element referred to as “Panel Zone” is provided in SAP 2000 software. The segments of the members within the joint are defined as rigid (or semi-rigid) end zones in the analytical models as discussed before and the joint behavior is defined using a nonlinear rotational spring called panel zone. The spring is employed to link two nodes automatically generated at the joint, each of which is utilized to connect the longitudinal members oriented in one principal direction, either columns or beams. The generated panel zone definition is presented in Figure 6.3.

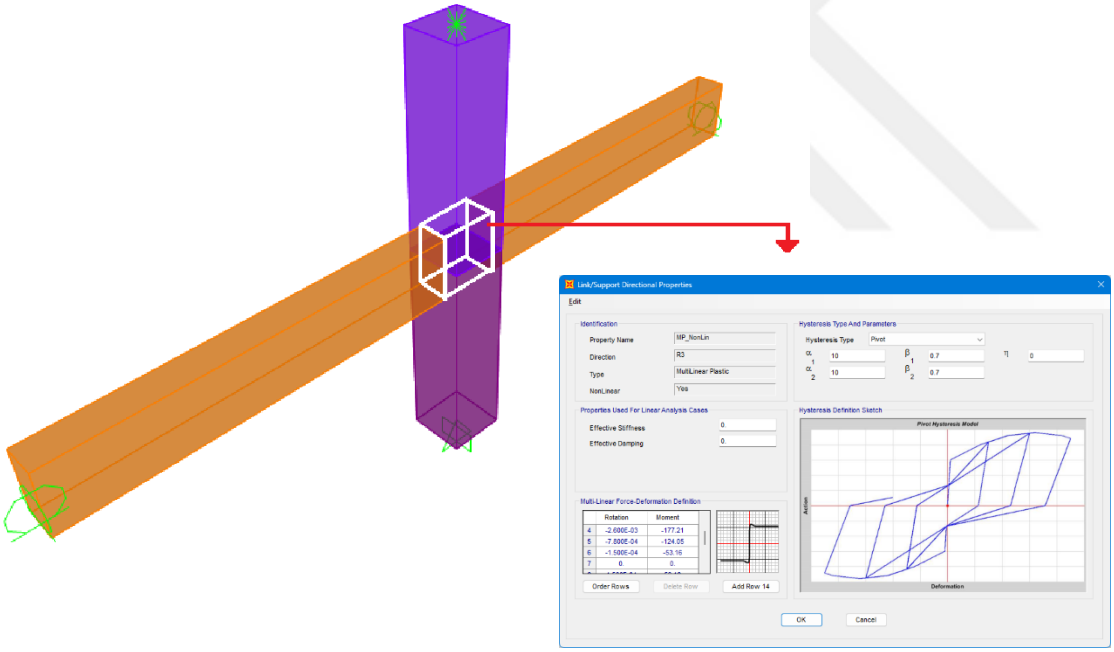


Figure 6.3. Panel Zone Model

In SAP2000, the behavior of both plastic hinges and panel zones can be defined considering a number of hysteresis model alternatives. In this research, the hysteretic response model, which provides a more accurate overall response of the subassemblies, “Pivot Hysteresis Model” is selected after comparison with the other

evaluated response model, “Takeda Model”. Both models are presented in Figure 6.4 and Figure 6.5.



Figure 6.4. Takeda Hysteresis Model

Takeda Hysteresis Model (Takeda et al.,1970), uses a deteriorating hysteretic loop and is considered to be more suitable for reinforced concrete modeling than for steel. This model does not require any parameters to define the behavior and exhibits unloading along elastic segments. During reloading, the curve follows a secant line to the backbone curve for loading in the opposite direction, with the target point for this secant at the maximum deformation that occurred in that direction under previous load cycles. This leads to a decrease in the amount of energy dissipation with increasing deformations.

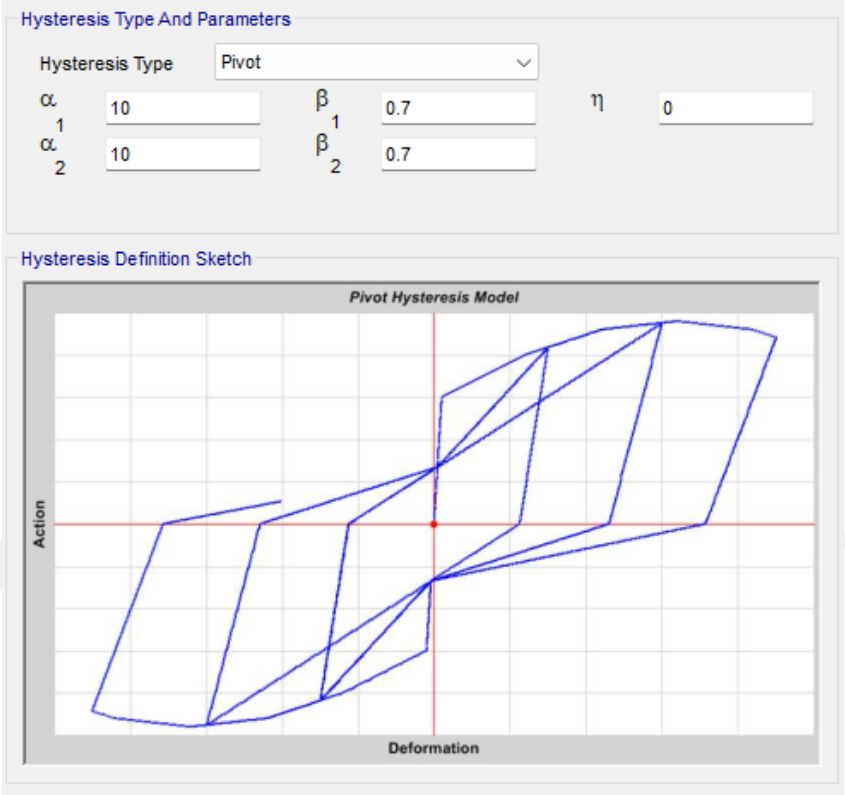


Figure 6.5. Pivot Hysteresis Model

In Pivot Hysteresis Model, the unloading and reverse loading actions gravitate towards specific pivotal points, dictating the impact of strength degradation via the 'α' parameter and the pinching of hysteresis loops through the 'β' parameter. The 'α' parameter serves as a primary pivotal point governing the unloading stiffness of the member, while the 'β' parameter acts as a pivotal point controlling the pinching behavior of the element. Detailed information regarding these parameters is presented below.

- α_1: Determines the pivotal point for unloading from a positive force to origin. Unloading progresses towards a point on the extension of the positive elastic line, but at a negative force value equivalent to α_1 multiplied by the positive yield force.

- α_2: Specifies the pivotal point for unloading from a negative force to origin. Unloading targets a point on the extension of the negative elastic line, but at a positive force value of α_2 times the negative yield force.
- β_1: Identifies the pivotal point for reverse loading from origin towards positive force. Reloading advances towards a point on the positive elastic line at a force value of β_1 times the positive yield force, where $0.0 < \beta_1 < 1.0$. Beyond this point, loading follows the secant to the previous maximum positive deformation on the backbone curve.
- β_2: Designates the pivotal point for reverse loading from origin towards negative force. Reloading proceeds towards a point on the positive elastic line at a force value of β_2 times the positive yield force, where $0.0 < \beta_2 < 1.0$. Beyond this point, loading follows the secant to the previous maximum negative deformation on the backbone curve.
- η: Governs the degree of degradation of the elastic slopes post plastic deformation, where $0.0 < \eta < 1.0$.

In the analyses, parameter α is defined as 10, whereas β is defined as 0.7, keeping the default values in the software after comparison of analytical results with the experimental data. The lateral load vs story shear results for Specimen 1 of Raffaelle & Wight (1995) is presented in the Figure 6.6 to illustrate the difference in structural response for the cases where Takeda and Pivot Hysteresis Models are utilized.

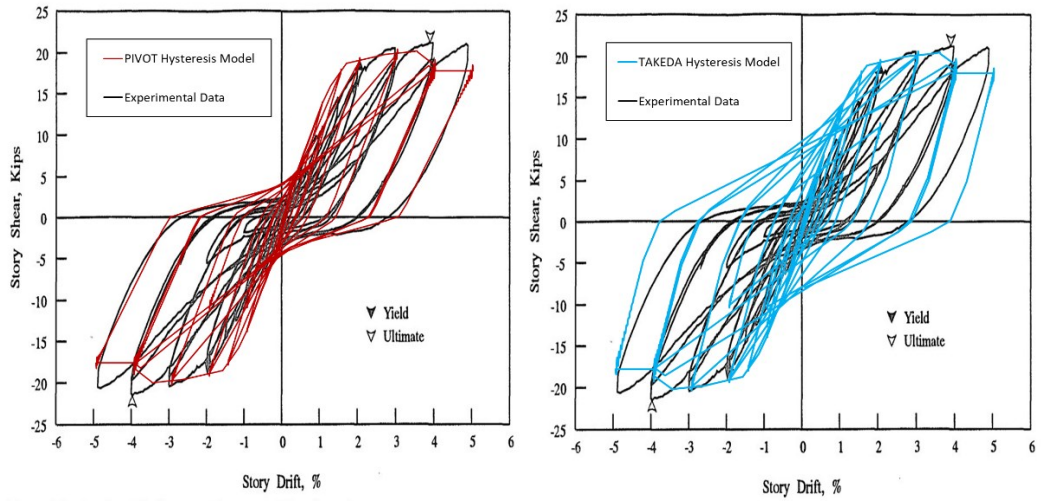


Figure 6.6. Comparison of Takeda and Pivot Hysteresis Models (Raffaelle & Wight, 1995)

Determination of Moment Arm for Joint Shear Conversion

The next step in the definition of nonlinear moment-rotation characteristics of the panel zone, the proposed joint shear force needs to be converted to moment. For this purpose, a moment arm should be defined. Since SAP 2000 does not provide any recommendation for the moment arm a parametric study is conducted to determine the moment arm which gives accurate estimations of the experimental structural response. The alternatives evaluated for the moment arm include beam depth (h_b), effective beam depth (d_b), defined as the distance between outermost compression fiber to the centroid of tension reinforcement, and the distance between the centroid of outermost tension and compression reinforcement layers (d'') as illustrated in Figure 6.7.

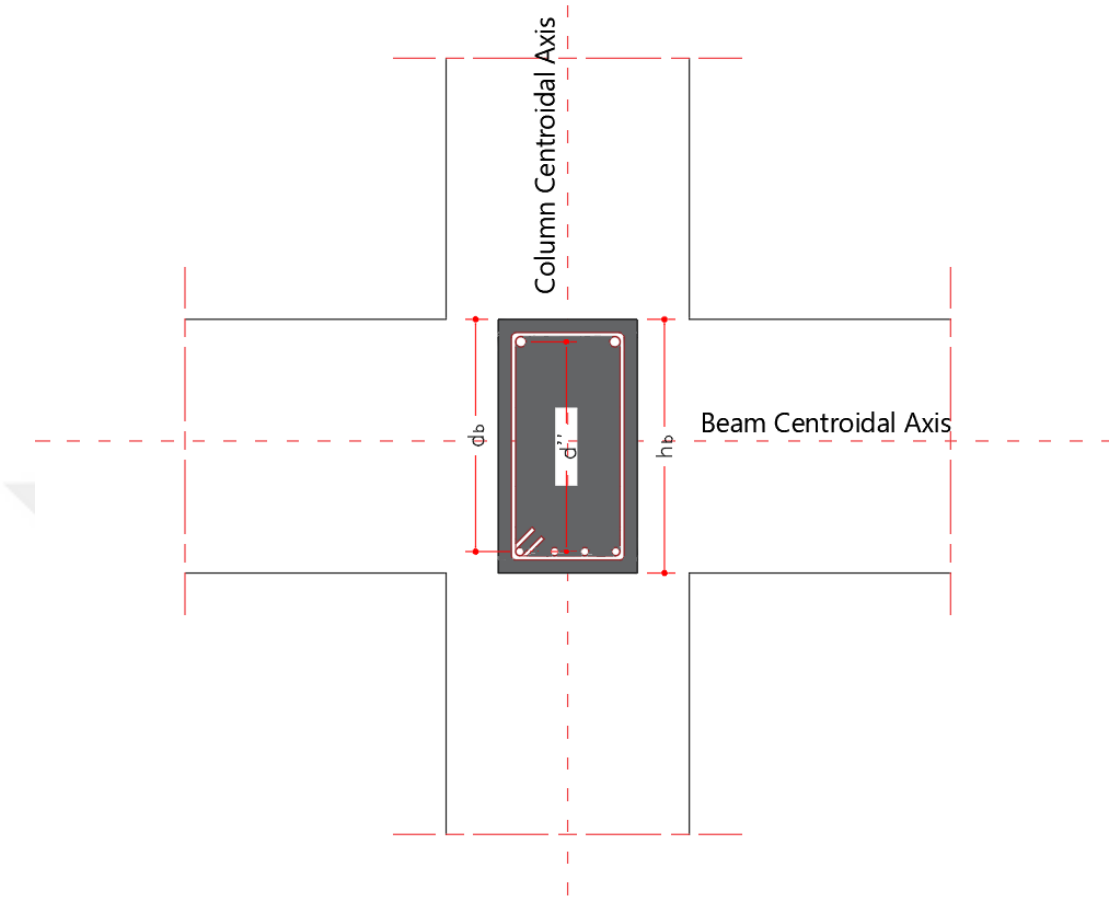


Figure 6.7. Alternatives Evaluated for Moment Arm

The comparison of results obtained by each moment arm alternative is performed on the specimen, 2-S, tested by (Burak & Wight,2008), due to the high accuracy of the proposed joint model compared with the experimental results, which is presented in Section 6.5.1

6.3 Loading Procedures

For the verification of the proposed nonlinear joint shear response model, 14 specimens from 3 different experimental studies are selected, (Burak & Wight, 2008; Raffaelle & Wight, 1995; Shin & LaFave, 2004) in which cyclic displacements are

applied laterally from the top of the column as illustrated in Figure 6.1 and Figure 6.2.

In the generated analytical models of the subassemblies, the lateral deformations defined in each experimental study are applied as nonlinear time histories to the top of the columns.

The displacement history applied in the experimental setup of Raffaelle & Wight, (1995) and its analytical counterpart are presented in Figure 6.8 as an example.

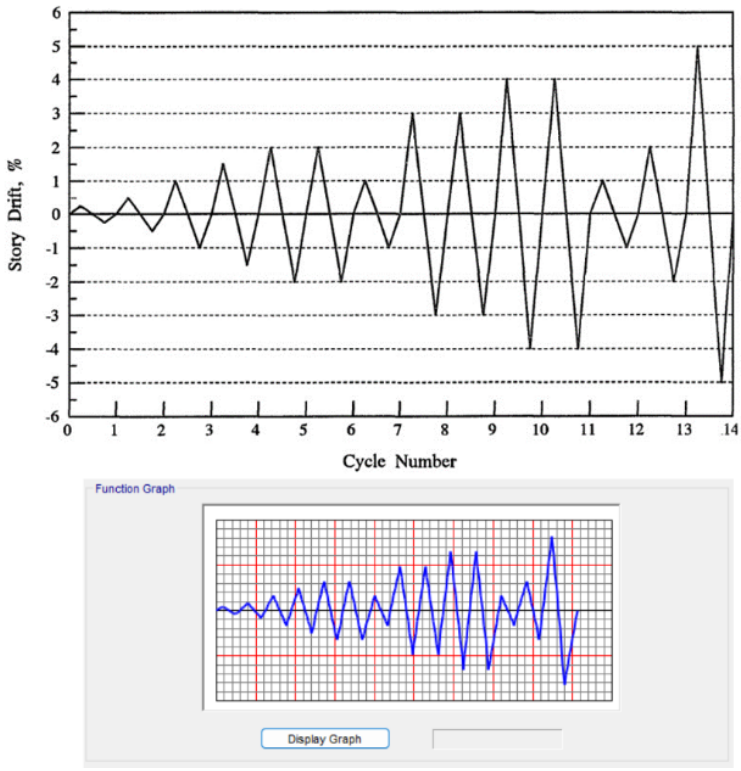


Figure 6.8. Cyclic Deformation Time History Definition

6.4 Loading Case Definition

For each beam-column subassembly, a unit deformation is assigned to the top of the column, with a magnitude of 1.0 mm in the analytical models. This unit displacement is then multiplied with the deformation time history function as the one provided in Figure 6.8.

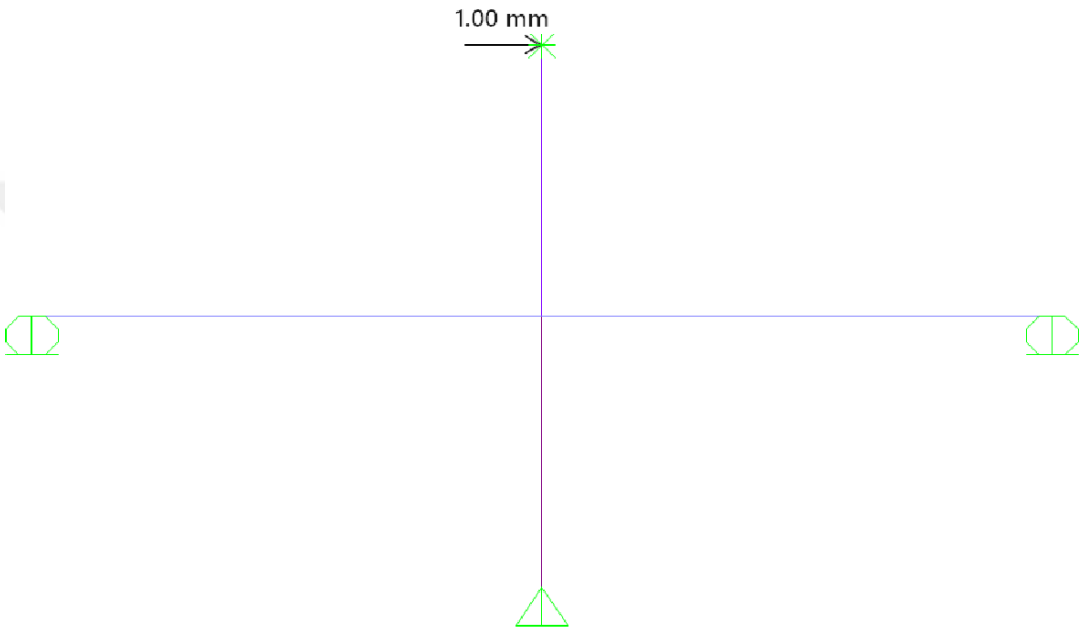


Figure 6.9. Unit Displacement Defined at the Top of the Column

A nonlinear time history load case is then generated to start the analysis, which records each output in a stepwise manner. To simulate the experimental investigation accurately, first a nonlinear static load case in which dead loads are applied to the structure is completed and then, the cyclic displacement history is imposed on the subassembly, for all 14 specimens. The load case definition for subassemblies is presented in Figure 6.10

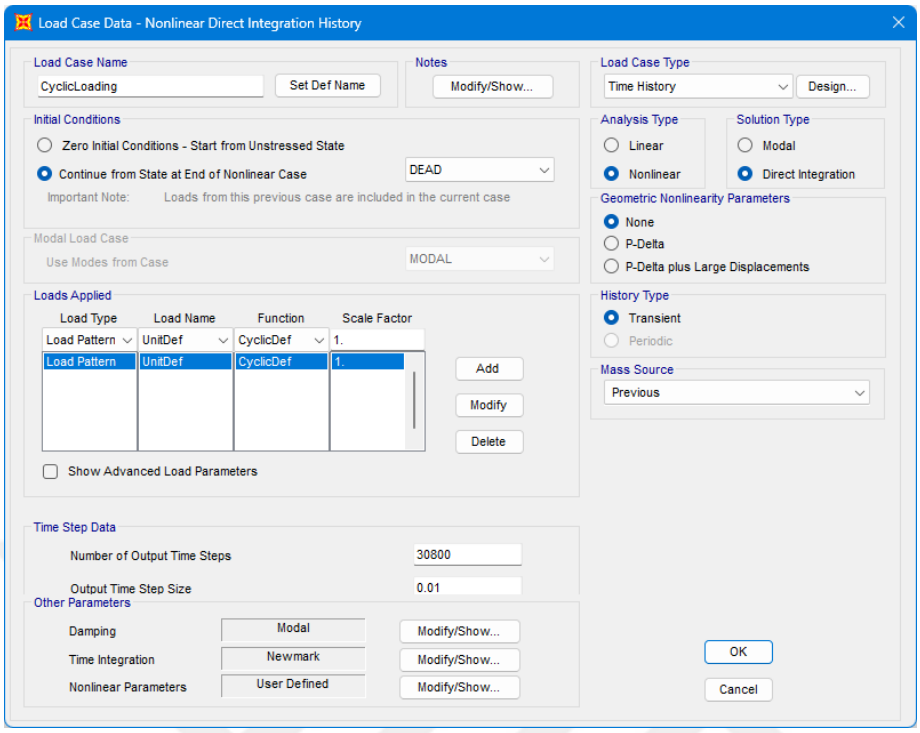


Figure 6.10. “Cyclic Loading” Load Case Definition

6.5 Comparison of Analytical and Experimental Results

This section of the document presents a comparison between experimental data and the results of the analyses conducted with SAP2000. The purpose of this comparison is to validate the accuracy of the developed nonlinear behavior model. To validate the analytical model, the joint shear force versus shear strain responses of the connections is utilized primarily as this curve provides a direct representation of the seismic behavior of the joints. Furthermore, to examine the overall behavior of the subassemblies, the relationships between lateral forces and displacement are illustrated for each specimen. Additionally, since experimental results are presented in the research study, comparison of beam moment rotation response of the specimens are presented for the specimens of Burak and Wight (2008).

Due to the availability of comprehensive data, specimens of Burak and Wight serve as the principal source of verification (Burak & Wight, 2008). Moreover, in order to

evaluate the joint shear stress versus strain response and lateral load versus lateral drift, specimens by Raffaelle and Wight, Shin and LaFave are presented (Raffaelle & Wight, 1995; Shin & LaFave, 2004).

6.5.1 Specimens of Burak and Wight

To verify the accuracy of the model, specimens of Burak and Wight constitute an important source since the constructed specimens possess varying geometrical properties reflecting the parameters studied in the preparation of the behavior model. All the specimens are constructed with floor slabs, and also eccentricities in between the beam and column axes are present for the spandrel beam direction.

Specimen 1 (1-S), Loading in the Spandrel Beam Direction

The first specimen tested by Burak and Wight is loaded in the spandrel beam direction, with an eccentricity between the column and beam axes. The subassembly includes a transverse beam and floor slab.

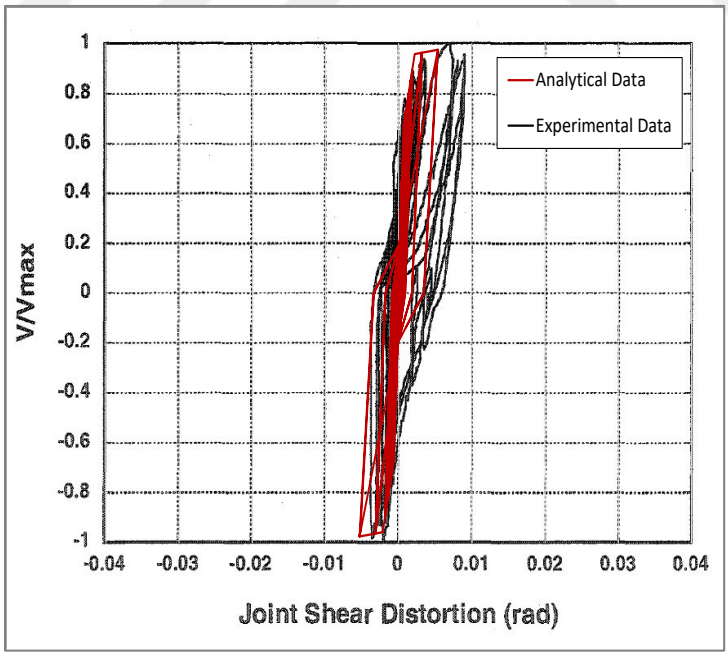


Figure 6.11. Specimen 1-S Joint Shear Force vs. Shear Strain Comparison

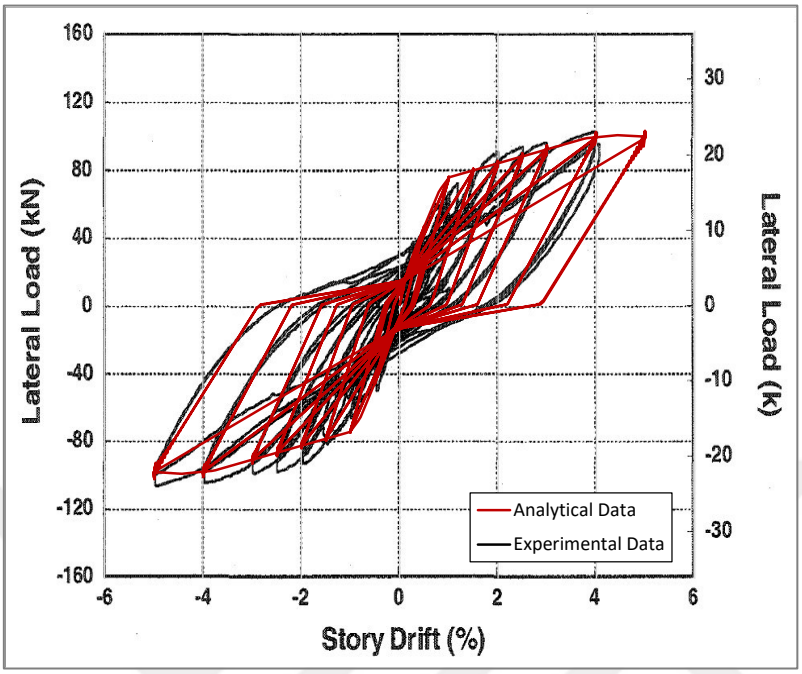


Figure 6.12. Specimen 1-S Lateral Load vs. Story Drift Comparison

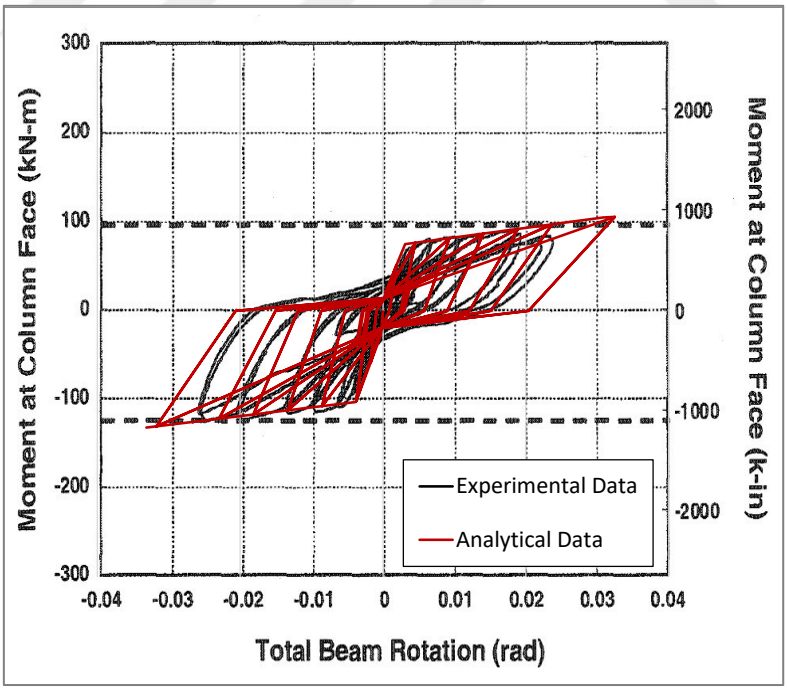


Figure 6.13. Specimen 1-S Beam Moment - Rotation Comparison

The comparison of the joint shear force vs. shear strain data clearly indicates that the analytical model represents the actual behavior successfully. The predicted shear strength of the joint, at 744.00 kN, closely matches with the experimentally observed value of 774.84 kN. As the joint shear strength is predicted slightly below the experimental value, story drift lateral load response is slightly below the experimental results. The developed nonlinear model accurately predicts the joint shear force vs. strain response. The maximum analytical strain is obtained as 0.005 radians for both positive and negative loading directions, which align with the experimental strains of 0.009 radians and 0.003 radians, respectively.

Finally, it can be seen that although the beam moment rotation response is satisfactorily presented, a higher pinching and consequently, a larger rotational deformation is monitored than experimental value. The experiment measured the beam rotation as 0.024 radians, compared to a predicted rotation of 0.032 radians.

Specimen 2 (2-S), Loading in the Spandrel Beam Direction

The second specimen differs from the first specimen in that it features a rectangular column. Moreover, the reinforcement detailing of the joint and geometrical properties of the beams are altered.

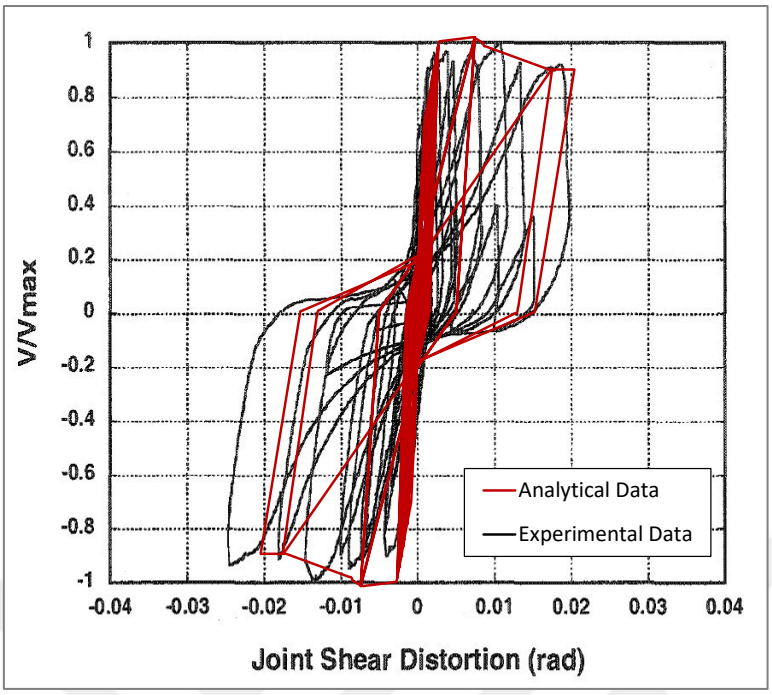


Figure 6.14. Specimen 2-S Joint Shear Force vs. Joint Shear Strain Comparison

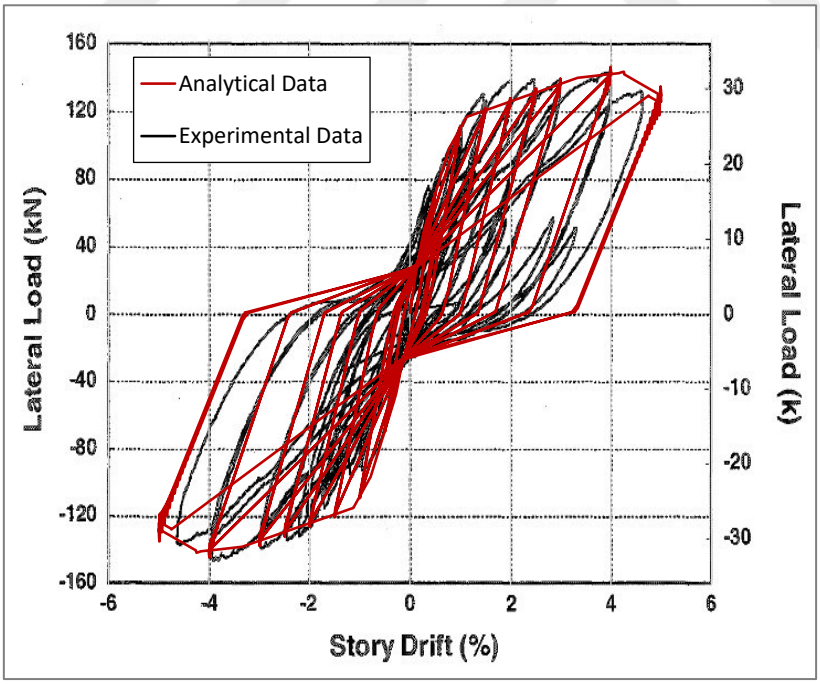


Figure 6.15. Specimen 2-S Lateral Load vs. Story Drift Comparison

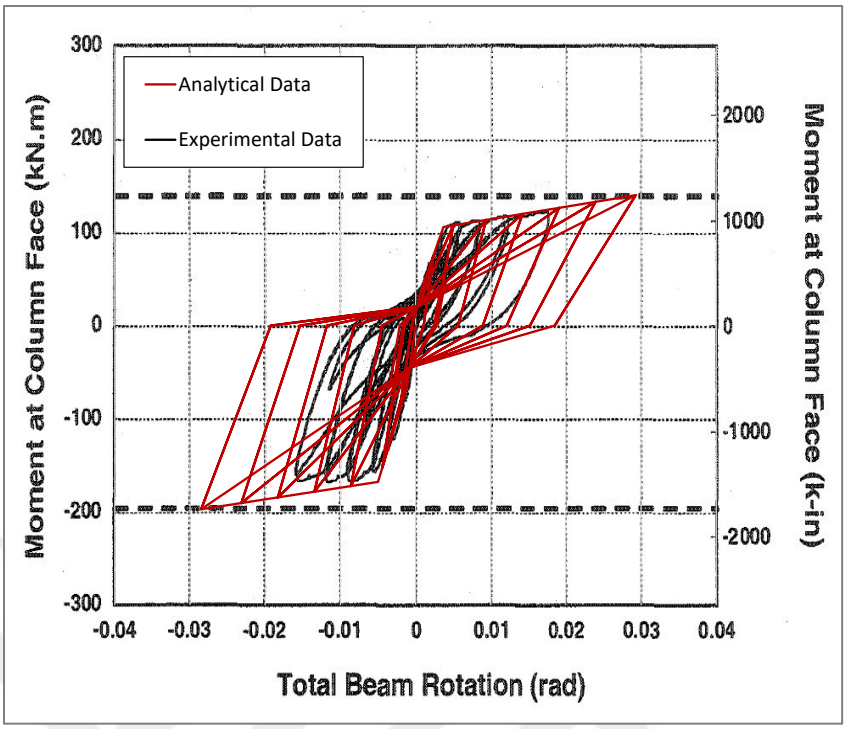


Figure 6.16. Specimen 2-S Beam Moment – Rotation Response Comparison

The second specimen in the test setup is one of the specimens for which the joint shear strength and joint shear behavior is predicted with high accuracy. The predicted shear strength of the joint, which is 859.52 kN, aligns closely with the shear strength measured through testing, which is 862.95 kN.

As can be seen from the joint shear response, the analytical results accurately represent the experimental observations. The maximum shear strain observed in the joint during experiments was 0.02 radians for positive loading and 0.025 radians for negative loading directions, which matches the analytical predictions of 0.02 radians for both positive and negative loading directions. Additionally, the analytical lateral load story drift response of the model also satisfactorily represents the overall behavior of the structure.

Although the beam moment rotation response is parallel to the experimental results, the observed hinge rotation is slightly over the experimental measurements with the predicted maximum rotation of the beam is 0.03 radians, while the rotation measured

experimentally is 0.18 radians. This variation in the result stems from the over-predicted initial rigidity of the joint model, whereas the overall behavior of all members is presented successfully.

Specimen 2 (2-S), Loading in the Spandrel Beam Direction, Comparison of Moment Arms

As previously stated, specimen 2-S is used to demonstrate the use of different moment arm alternatives in the definition of moment-rotation characteristics of the beam-column joints. In Figure 6.17 the lateral load – story drift (P-Δ) responses obtained using d_b, d'' and h_b are presented.

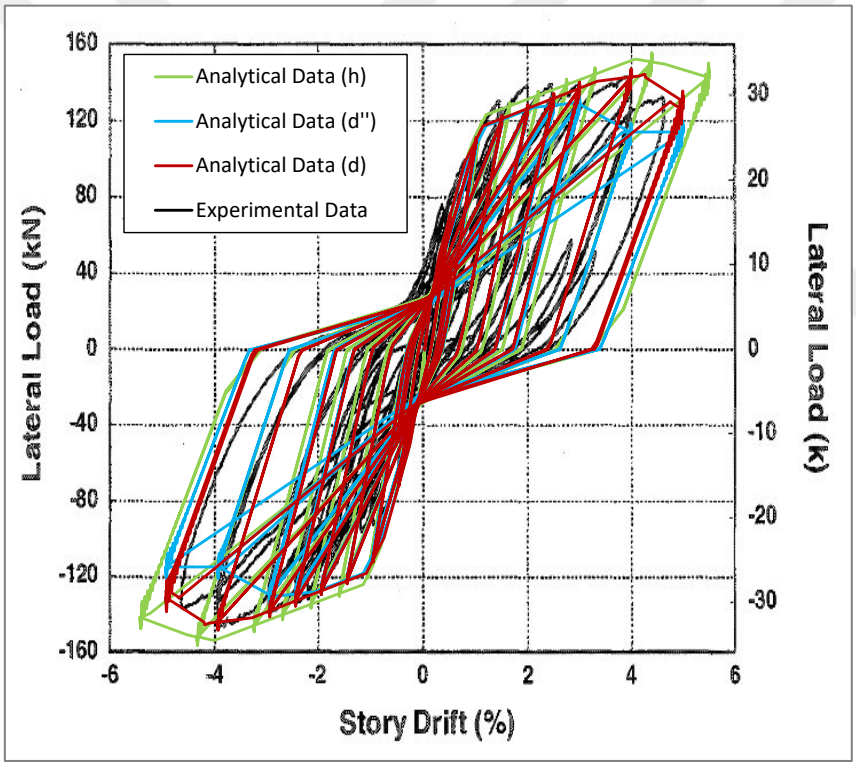


Figure 6.17. Specimen 2-S Lateral Load vs. Story Drift Comparison for Various Moment Arm Assumptions

In the investigation of subassembly response under cyclic loading, a general tendency of lower lateral loads than experimental forces are observed, in the cases where d'' are considered as moment arms. Additionally, as the other extremity of the

moment arm alternatives, a rotational spring behavior using beam depth (h_b) is also studied. As presented in the Figure 6.17, the use of beam depth leads to a higher predicted strength for the moment rotation response of the joint and resulted in observation of larger forces in lateral load deformation responses.

Consequently, the use of effective depth of the beam as joint moment arm is deemed necessary for adequate representation of the joint behavior.

Specimen 3 (3-S), Loading in the Spandrel Beam Direction

The third specimen of the experimental investigation is similar to specimen 2-S, except in the loading direction, a wide beam frames to the joint instead of a conventional beam that has a width lower than the column width.

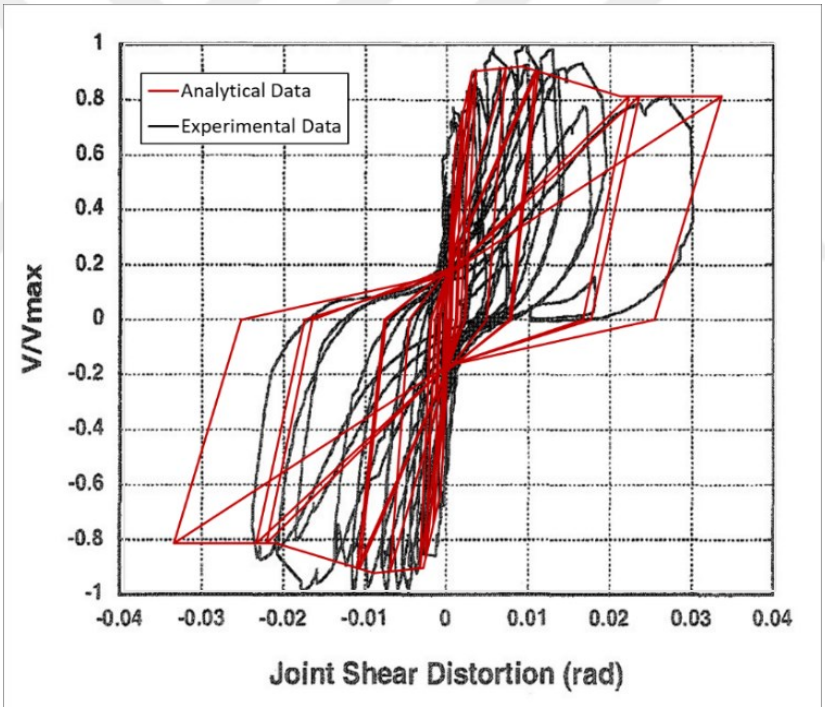


Figure 6.18. Specimen 3-S Joint Shear Force vs. Shear Strain Comparison

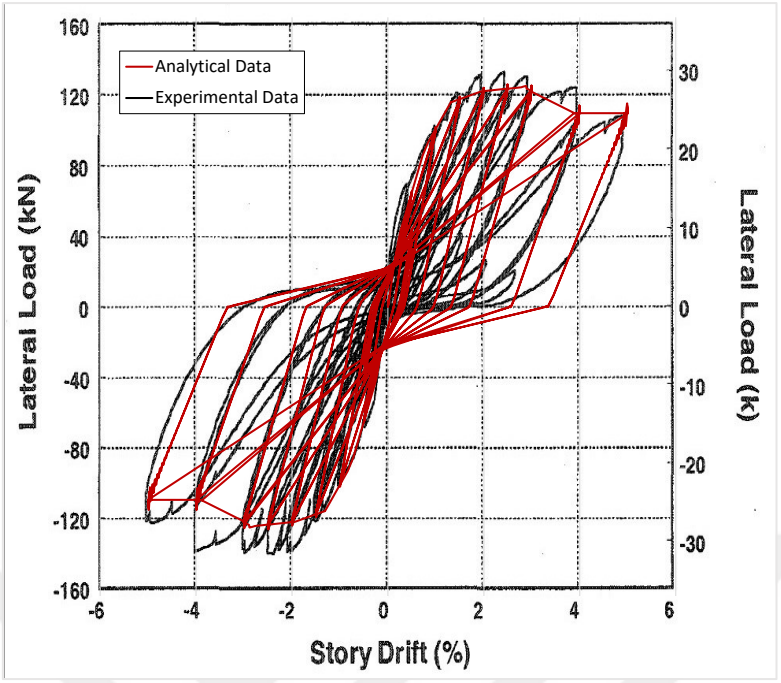


Figure 6.19. Specimen 3-S Lateral Load vs. Story Drift Comparison

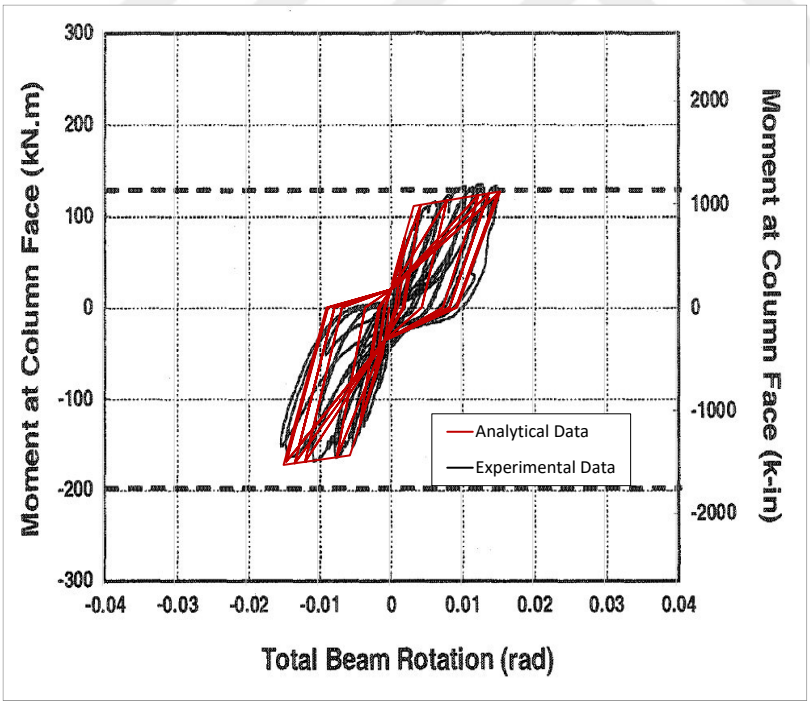


Figure 6.20. Specimen 3-S Beam Moment – Rotation Response Comparison

In the third specimen, the predicted joint shear strength is lower than the experimental investigation, as can be seen in Figure 6.18, with an experimental result of 827.37 kN compared to an analytical result of 739.06 kN. As expected, the lower prediction of joint shear strength leads to a lower lateral load observation than expected in the story drift response.

It can be revealed from the comparison of the results that the initial stiffness and general structural response is still predicted satisfactorily for both the pre-yield and post-yield phases of the structural behavior whereas the maximum joint strain is predicted as 0.033 radians, as compared to the experimental value of 0.024 radians.

Specimen 1 (1-N), Loading in the Normal Beam Direction

In the direction of the normal beam, the test setup depicts an exterior beam-column connection with concentric alignment, as there are no beams framing into the joint in the opposite direction. It is important to note that for the analyses conducted in the normal beam direction, the specimens were initially tested in the spandrel beam direction, resulting in a reduction in the stiffness of the connections.

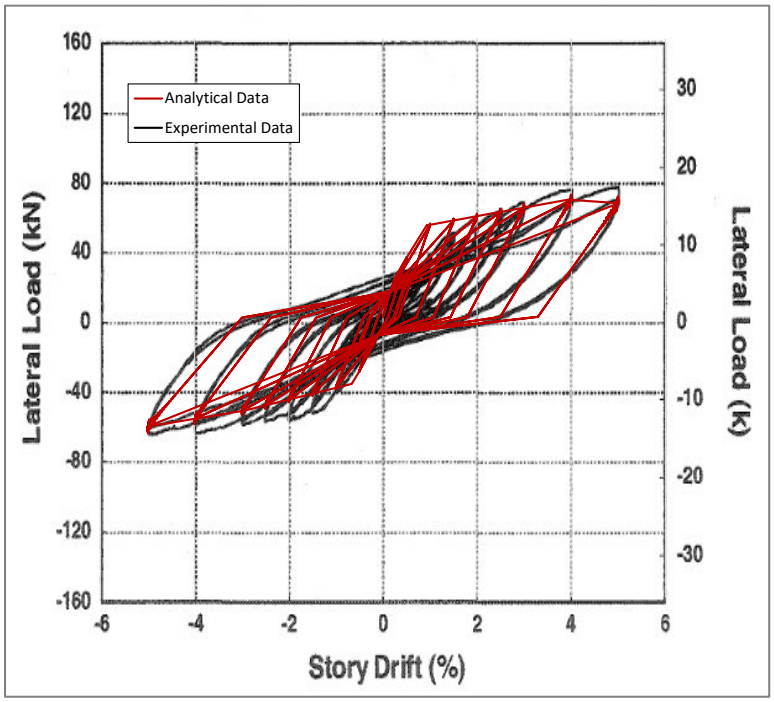


Figure 6.21. Specimen 1-N Lateral Load vs. Story Drift Comparison

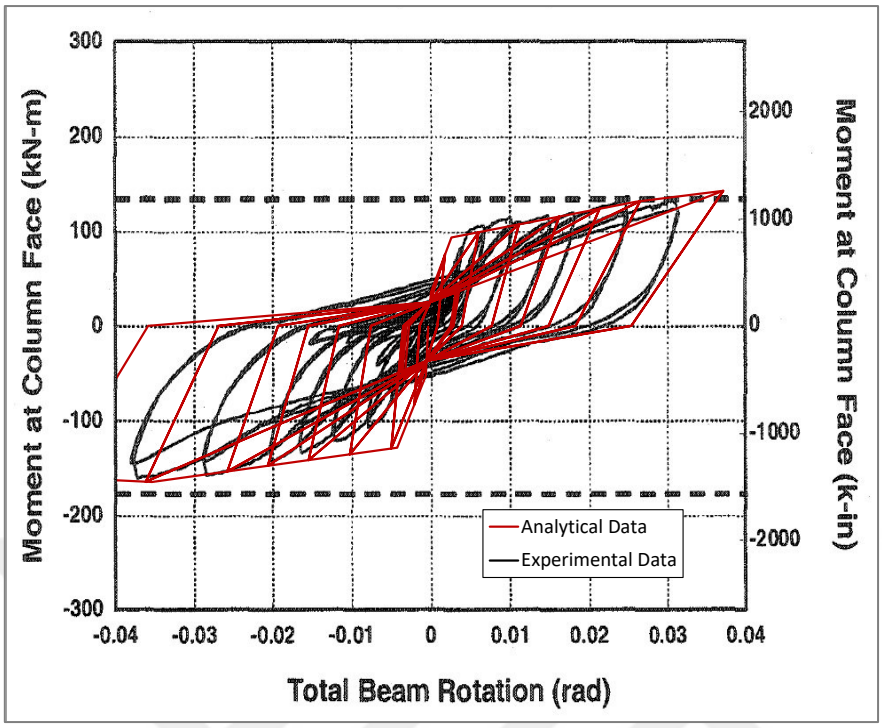


Figure 6.22. Specimen 1-N Beam Moment – Rotation Response Comparison

From both the lateral load and story drift response and the beam-moment rotation curves, it can be observed that the response of the beam-column connection subassembly is predicted satisfactorily. Although, the over pinching encountered in the beam moment rotation analytical response leads to larger beam end rotations. Since the proposed model includes a reduction factor for the joint shear strength, the capacity of the connection is predicted satisfactorily with a predicted value of 648.94 kN compared to the experimentally observed 569.37 kN. It should be noted that, the stiffness of this specimen is reduced considerably due to prior loading in the perpendicular direction, therefore the rigidity of the analytical model is higher than the experimental one, and the beam response governs the connection behavior. Beam rotation response is also represented satisfactorily as the maximum beam rotation is predicted as 0.038 and 0.048 radians in positive and negative loading directions, respectively, whereas the experimentally observed values are 0.032 and 0.038 radians.

Specimen 2 (2-N), Loading in the Normal Beam Direction

This connection, like the one for the first specimen, is also loaded from the normal beam direction and constitutes an exterior joint. Asymmetrical beam reinforcement is utilized in the beam and the connection is constructed with a floor slab, with prior loading in the spandrel beam direction. It should be also noted that the beam in the normal direction of Specimen 2 frames into the strong direction of the rectangular column.

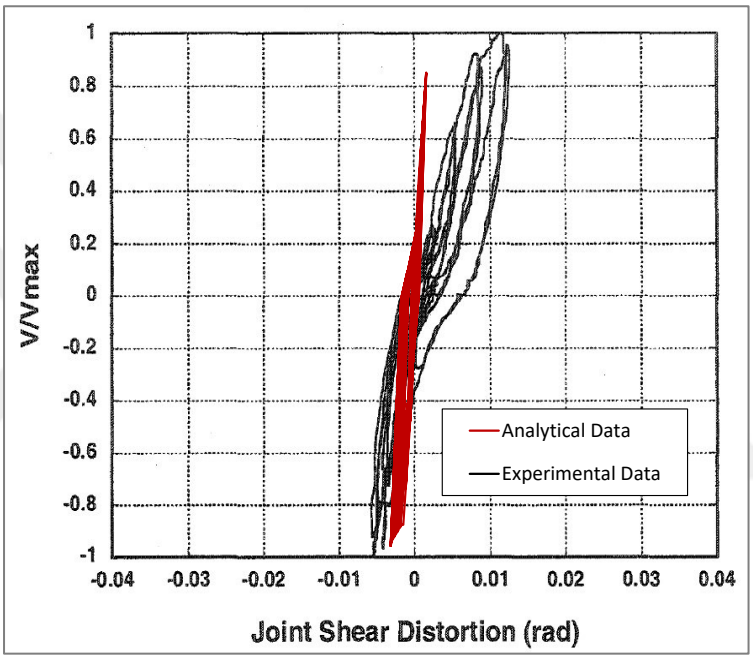


Figure 6.23. Specimen 2-N Joint Shear Force vs. Joint Shear Strain Comparison

In the evaluation of the 2-N, it can be clearly observed that the reduction in stiffness stemming from the prior loading could not be presented in the model. The shear strain is predicted as 0.003 radians in both positive and negative loading directions with a joint force of 1063.18 kN. Whereas the experimentally observed value of 809.58 kN at a strain of 0.011 and 0.005 radians in positive and negative loading directions indicates the proposed model predicts a stiffer response. Consequently, since the experimental response of the joint is steep and the connection does not exhibit considerable plastic deformations, higher prediction of the initial stiffness also leads to an overprediction of the beam moment rotation response (Figure 6.25).

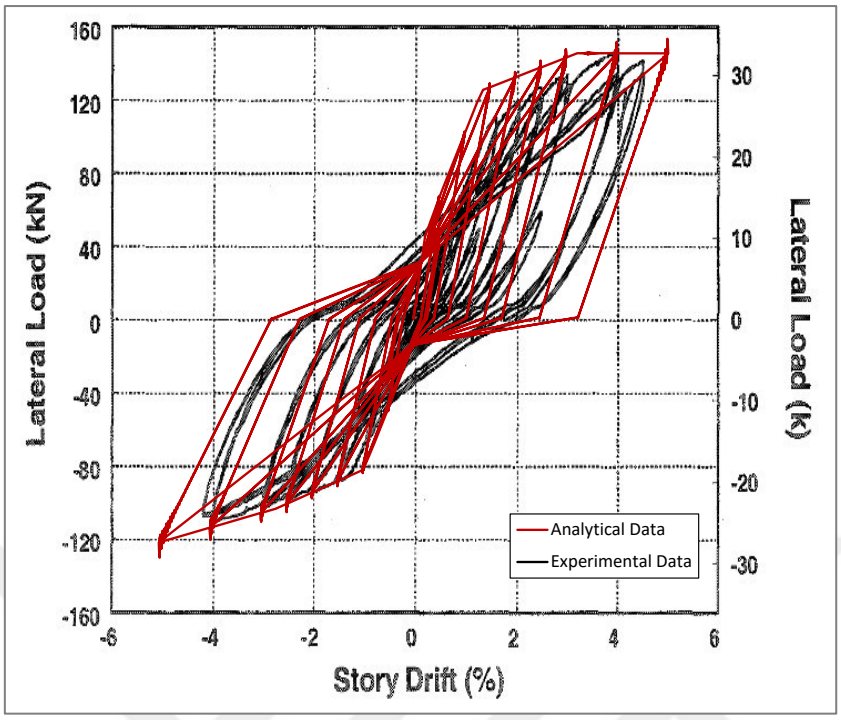


Figure 6.24. Specimen 2-N Lateral Load vs. Story Drift Comparison

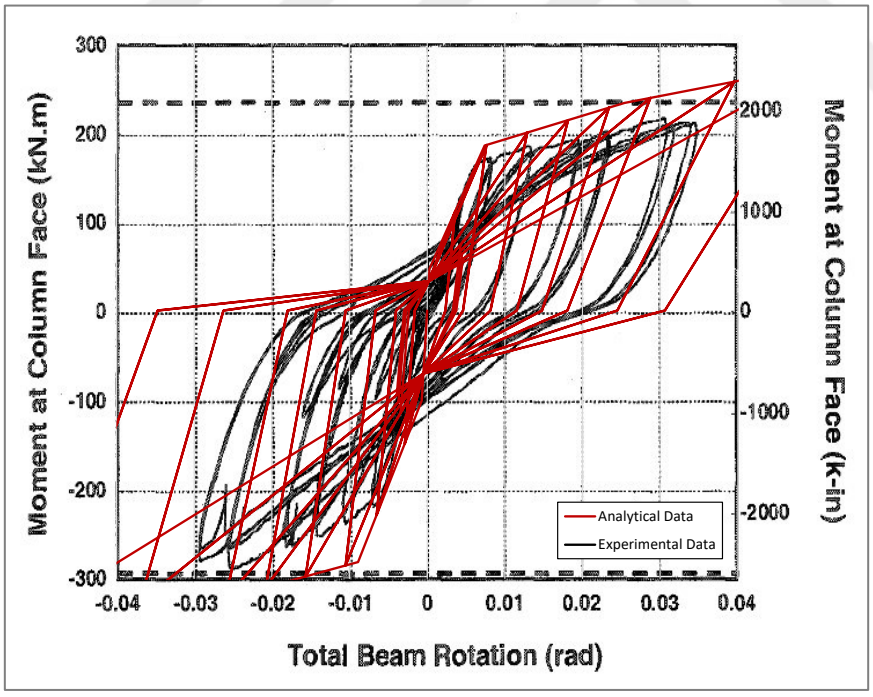


Figure 6.25. Specimen 2-N Beam Moment – Rotation Response Comparison

On the contrary, the lateral load – story drift response of the subassembly still reflects the experimental behavior quite satisfactorily.

Specimen 3 (3-N), Loading in the Normal Beam Direction

When subjected to loading in the normal beam direction, the response of Specimen 3 is similar to that of Specimen 2. Asymmetric deformation occurs in the joint due to unequal top and bottom beam reinforcement areas, and the behavior of the subassembly in terms of lateral load vs. story drift is controlled by the properties of the beam.

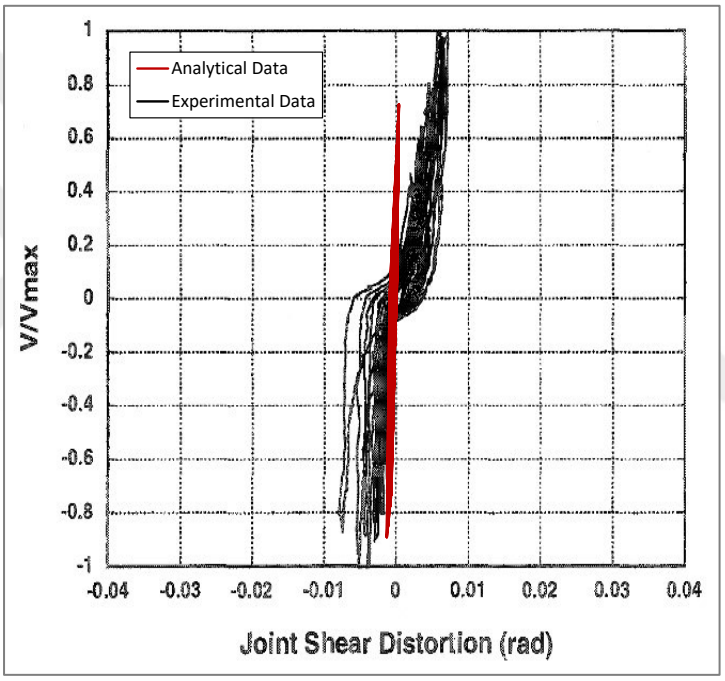


Figure 6.26. Specimen 3-N Joint Shear Force vs. Shear Strain Comparison

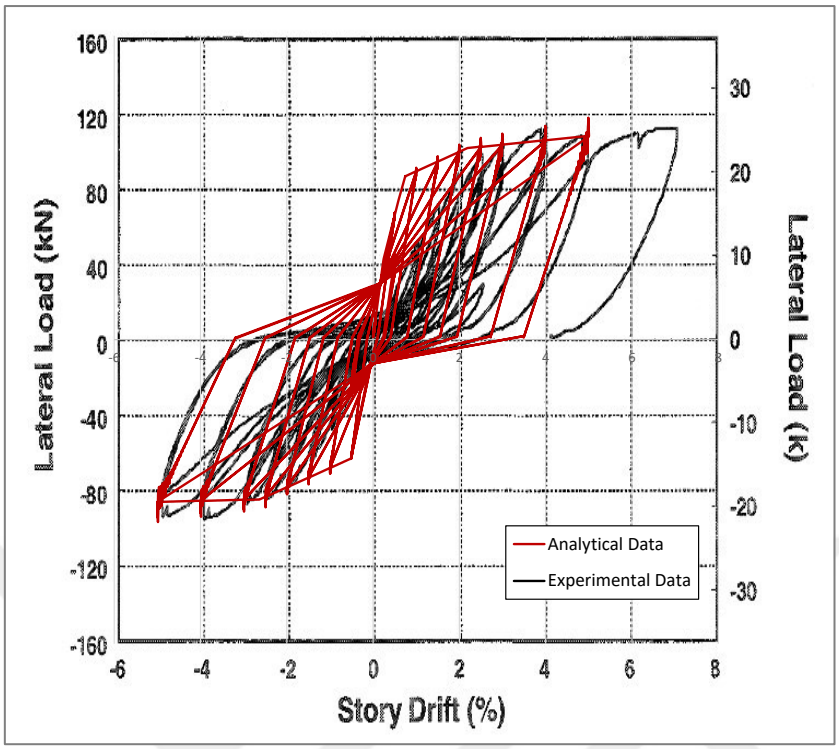


Figure 6.27. Specimen 3-N Lateral Load vs. Story Drift Comparison

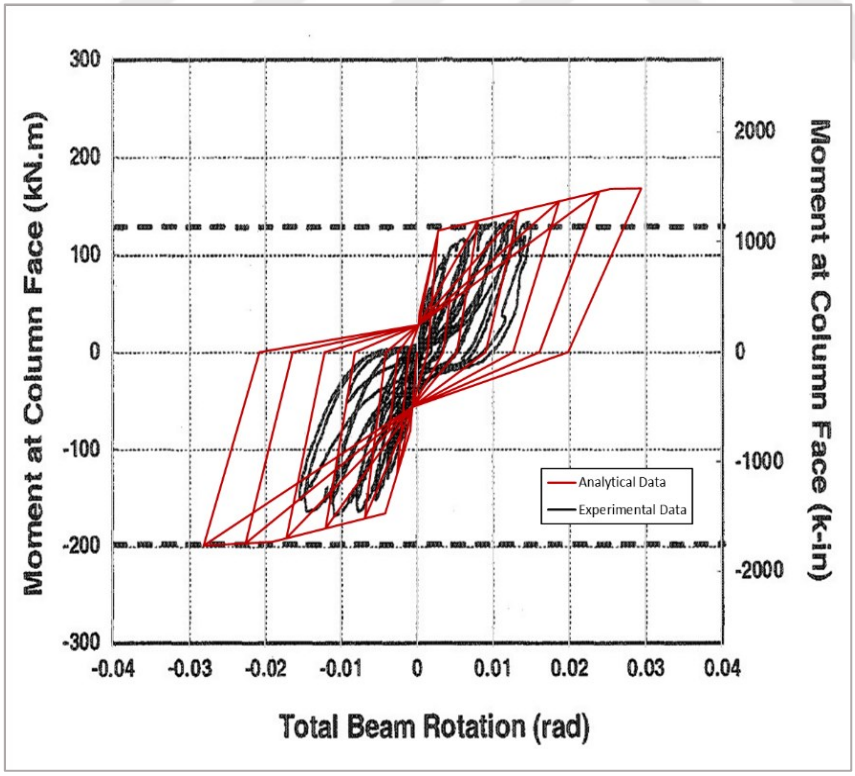


Figure 6.28. Specimen 3-N Beam Moment – Rotation Response Comparison

The shear strength of the joint in specimen 3-N is adequately captured by an analytical value of 1045.58 kN, in comparison to the experimental value of 1156.54 kN. In relation to this observation, it can be concluded from the analytical results that the overall behavior of the structure is estimated accurately, as presented in Figure 6.28. Since the reduction in the stiffness of the beams due to prior loading cannot be resembled in the model, the joint strains are lower than the experimental ones and the response of the subassembly is governed by the beam behavior. The beam rotation is over predicted as 0.029 radians, when compared to the experimental beam rotation, 0.015 radians.

6.5.2 Specimens of Raffaelle and Wight

Raffaelle and Wight experimentally investigated the cyclic response of 4 subassemblies that have eccentric spandrel beams with varying cross sectional dimensions and reinforcement detailing (Raffaelle & Wight, 1995). All specimens had column axial loads of 20.0 kN and no slabs or transverse beams representing the floor system.

Specimen 1

The first specimen in the experimental investigation had an eccentricity of 50.8 mm (2 inches) in the direction of the load. The beam dimensions were 254 mm x 381 mm (10" x 15") with 3 ϕ19 (#6) bars and 3 ϕ16 (#5) bars serving as the top and bottom longitudinal reinforcement, respectively. The joint shear force vs. strain response of the subassembly is presented in Figure 6.29.

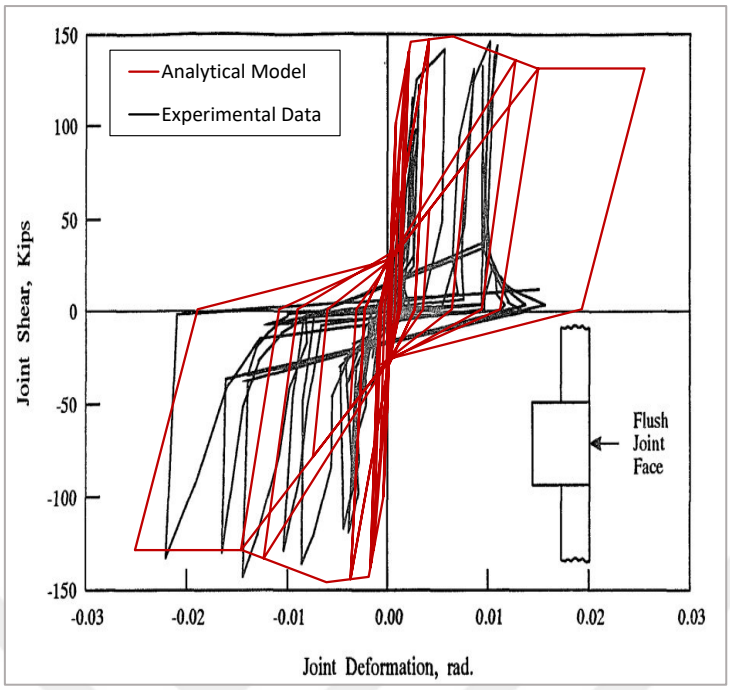


Figure 6.29. Specimen 1 Joint Shear Force vs. Shear Strain Comparison

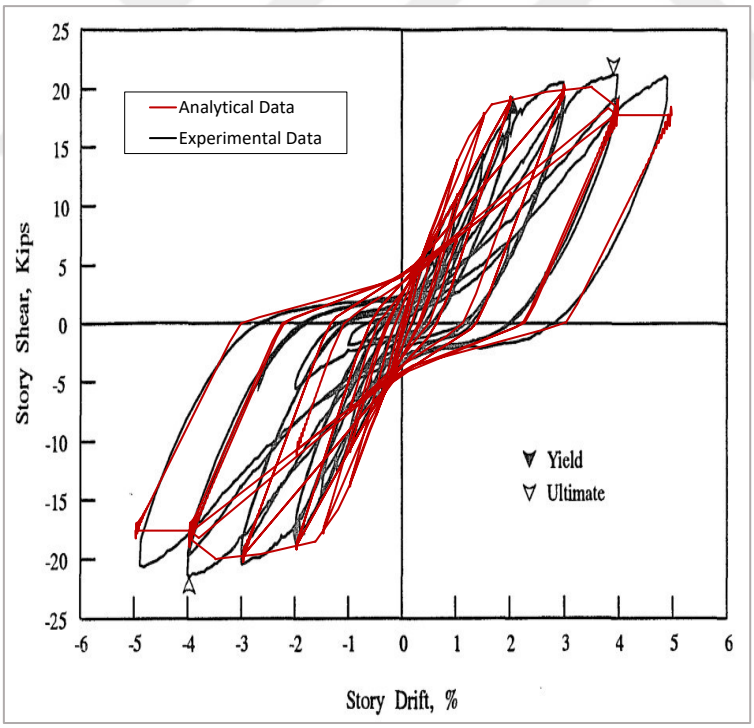


Figure 6.30. Specimen 1 Lateral Load vs. Story Drift Comparison

Based on the lateral load versus story drift graph shown in Figure 6.30, it can be deduced that the model predicts a more rigid response from the beam-column

connection subassembly. Furthermore, the lateral load capacity of the subassembly is slightly underestimated, with an analytical value of 89.7 kN compared to the experimental value of 95.2 kN. However, the analytical response of the joint shear force versus shear strain behavior indicates a close resemblance to the experimental behavior of the joint, indicating that the overestimation of stiffness and lateral load capacity is not attributed to the joint but to other structural members. The discrepancy in the beam moment versus rotation relationship from the experimental data may lead to an overestimation of the lateral load response of Specimen 1. Unfortunately, since there is no available experimental data on beam moment versus rotation response for this test series, a comparison cannot be performed.

Specimen 2

Specimen 2, differing from Specimen 1, featured a narrow beam with dimensions of 177.8 mm x 381 mm (7" x 15") with 2 ϕ19 (#6) top bars and 2 ϕ16 (#5) bottom bars. Specimen 2 had an eccentricity of 88.9 mm (3.5") due to the beam face being flush with the column face.

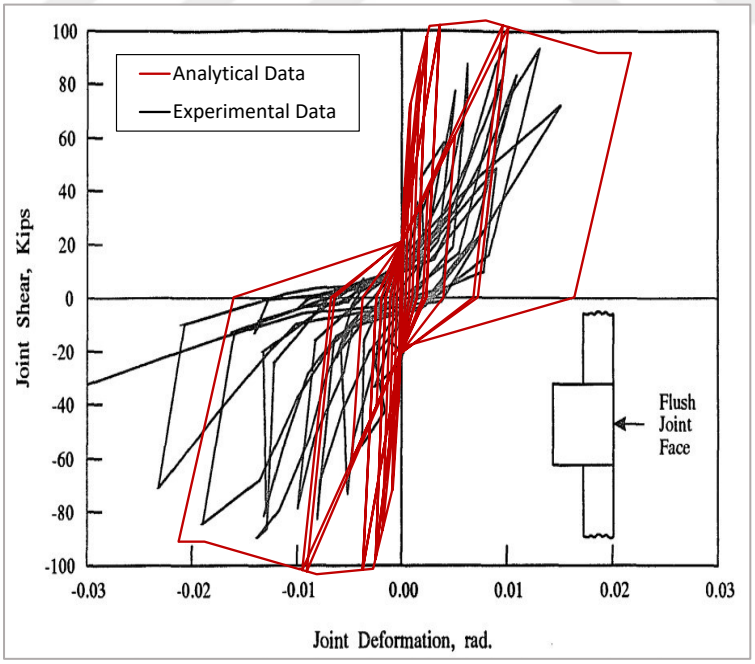


Figure 6.31. Specimen 2 Joint Shear Force vs. Shear Strain Comparison

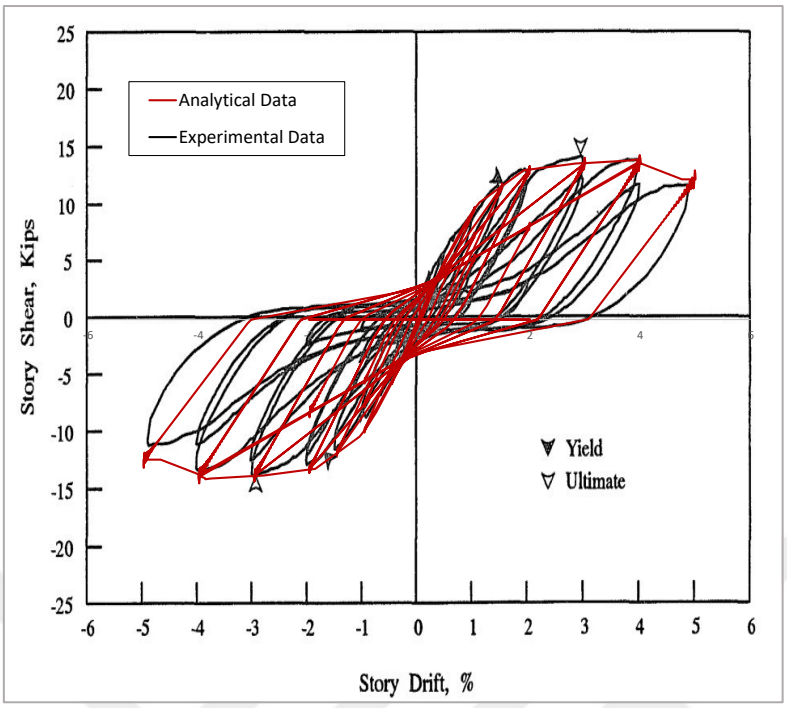


Figure 6.32. Specimen 2 Lateral Load vs. Story Drift Comparison

The experimental lateral load versus story drift response of the subassembly is successfully represented by the analytical results, as shown in Figure 6.32. The analytically predicted maximum lateral load of 63.3 kN shows strong resemblance with the experimental value 62.3 kN, although the joint shear response of the structure is overestimated both in terms of the joint shear strength and the initial rigidity of the beam-column joint. As the behavior of beam-column connection subassemblies under large deformations depend on both the beam and column characteristics as well as the joint characteristics, the effect of overestimated joint capacity and rigidity must be evaluated also considering the beam moment rotation results. Unfortunately, this data is not provided in the research study and cannot be compared.

Specimen 3

The beam dimensions were adjusted slightly in the third specimen by widening it to 190.5 mm (7.5"). In this specimen, 3 ϕ16 (#5) bars were used as the top reinforcement and 2 ϕ16 (#5) bars as the bottom reinforcement. The joint eccentricity decreased to 82.55 mm (3.25"). A comparison between the experimental and analytical outcomes is provided in Figures 6.33 and 6.34.

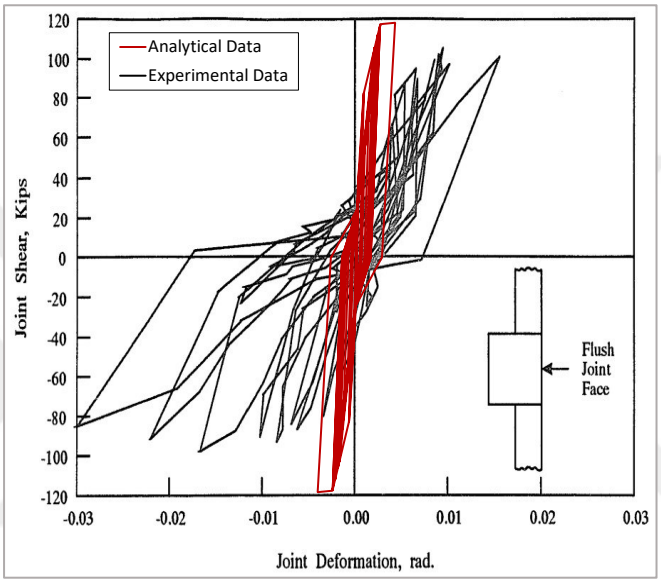


Figure 6.33. Specimen 3 Joint Shear Force vs. Shear Strain Comparison

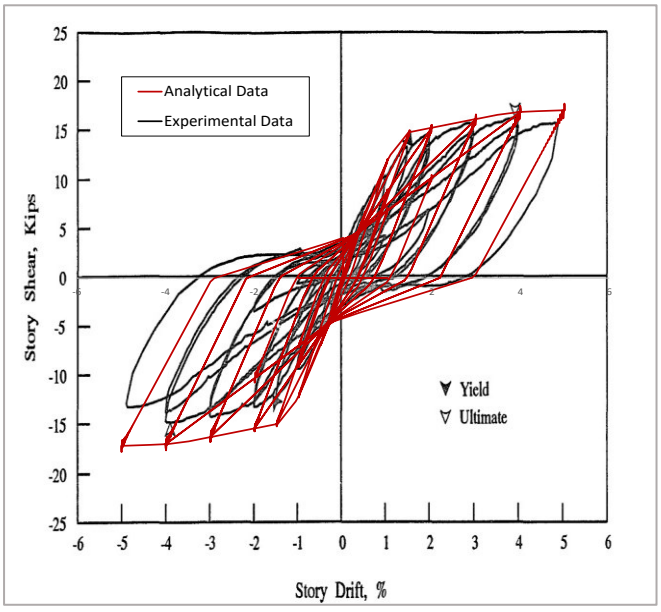


Figure 6.34. Specimen 3 Lateral Load vs. Story Drift Comparison

The third specimen of the group investigated by Raffaelle and Wight is one of the specimens the joint shear strength of which is considerably over predicted as 566.17 kN when compared to the experimental joint shear strength of 469.73 kN. The specimen has a lower experimental rigidity than the one predicted by the analytical model. Although the joint response could not be represented satisfactorily, the overall behavior is still represented adequately since the predicted lateral load capacity, 78.86 kN, is very close to the experimental value, 72.06 kN. The subassembly rigidity is perfectly matched in the positive loading direction whereas both the rigidity and the joint strength is over predicted in the negative loading direction.

Specimen 4

Specimen 4 closely resembles Specimen 3, with the only variation being an increase in the beam depth to 558.8 mm (22"). The longitudinal reinforcement and eccentricity ratios remained the same. An essential distinction of Specimen 4 is the inclusion of 6 layers of shear reinforcement in the joint area, in contrast to the 3 layers used in the other specimens in this test series.

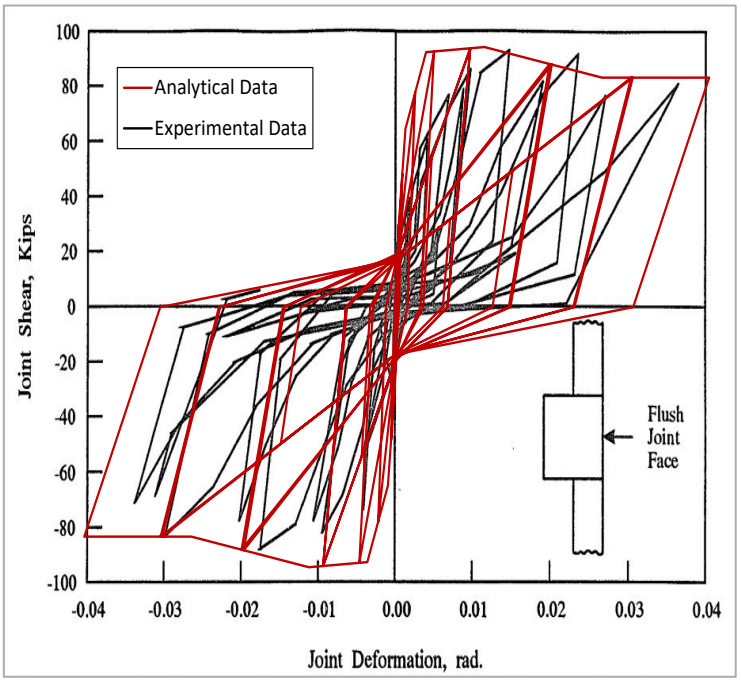


Figure 6.35. Specimen 4 Joint Shear Force vs. Shear Strain Comparison

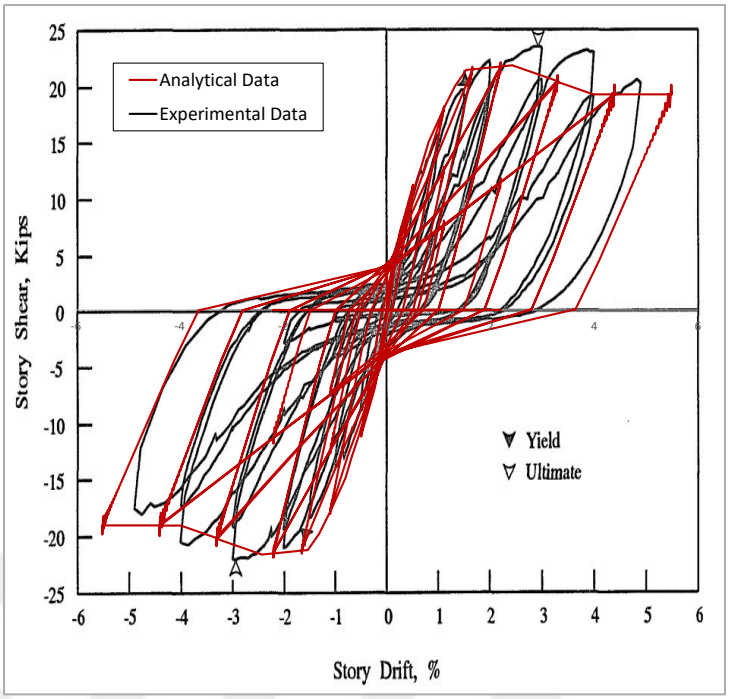


Figure 6.36. Specimen 4 Lateral Load vs. Story Drift Comparison

The last specimen of the group has one of the joints the strength and nonlinear behavior of which are successfully predicted. As the joint shear strength is predicted with high accuracy, $V_{j,pre.}$ = 408.64 kN vs. $V_{j,exp}$ = 412.35 kN, both the rigidity and inelastic behavior of the joint is effectively represented by the model. The predicted lateral load for the subassembly, 102.68 kN, also matches with the experimental lateral load of 113.42 kN. It should also be noted that the pinching characteristics of the joint and the subassembly are also simulated by the model satisfactorily.

6.5.3 Specimens of Shin and LaFave

Shin and LaFave conducted a series of experiments on four exterior beam-column-slab connection specimens (Shin & LaFave, 2004). Two of these specimens had eccentric joints. During testing, lateral loading was applied from the top of the column in the spandrel beam direction, with no applied axial load. Lateral load versus story drift and joint shear force versus joint strain data were presented as experimental results, whereas, beam moment-rotation response was not provided.

Specimen SL1

The first specimen in the experimental investigation had an eccentricity of 88.9 mm (3.5") in the direction of loading. The beam dimensions were 279.4 mm x 406.4 mm (11" x 16") with 4 ϕ16 (#5) bars and 2 ϕ16 (#5) as the top and bottom longitudinal reinforcement, respectively, for the beam in the loading direction. The subassembly also has a 101.6 mm (4") thick slab and a transverse beam with 330.2 mm x 406.4 mm (13" x 16") cross sectional dimensions. The beam-column joint had 3 layers of hoop reinforcement and 1 ϕ10 (#3) tie in each direction.

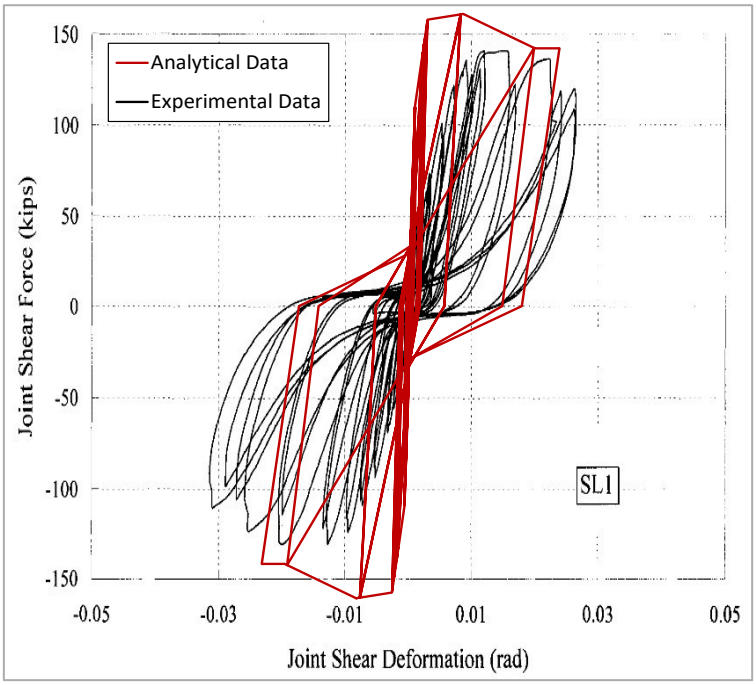


Figure 6.37. SL1 Joint Shear Force vs. Shear Strain Comparison

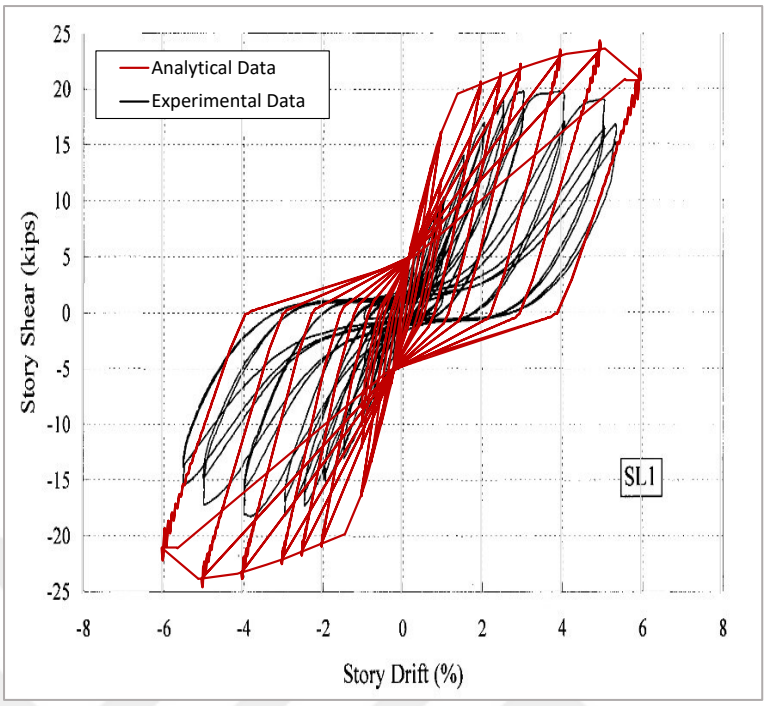


Figure 6.38. SL1 Lateral Load vs. Story Drift Comparison

The first specimen in the group stands out for its considerably overestimated joint shear strength. The specimen demonstrates a noticeably lower stiffness than what is predicted by the analytical model. The overestimation in the joint shear strength is reflected in the structural response, evident in the lateral load versus story drift behavior. This suggests that the structural deformation aligns harmoniously with the joint deformation.

Specimen SL2

The second specimen is constructed with the same detailing as SL1 but has a narrower beam with a width of 177.8 mm (7"). The beam-column joint was constructed with 3 layers of hoop reinforcement and 1 tie in each direction, with a diameter of 10 mm (#3). The eccentricity was further increased to 139.7 mm (5.5").

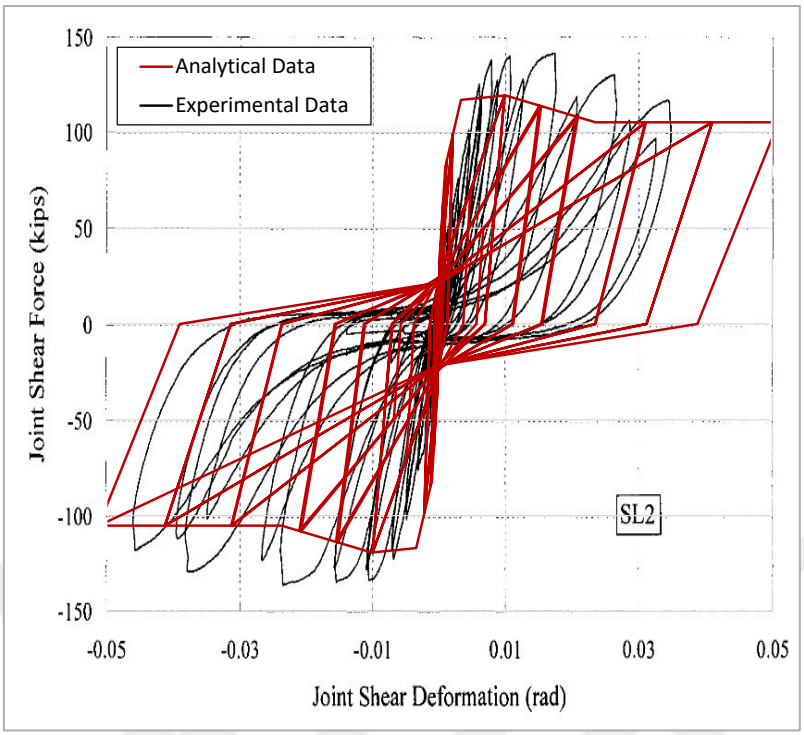


Figure 6.39. SL2 Joint Shear Force vs. Shear Strain Comparison

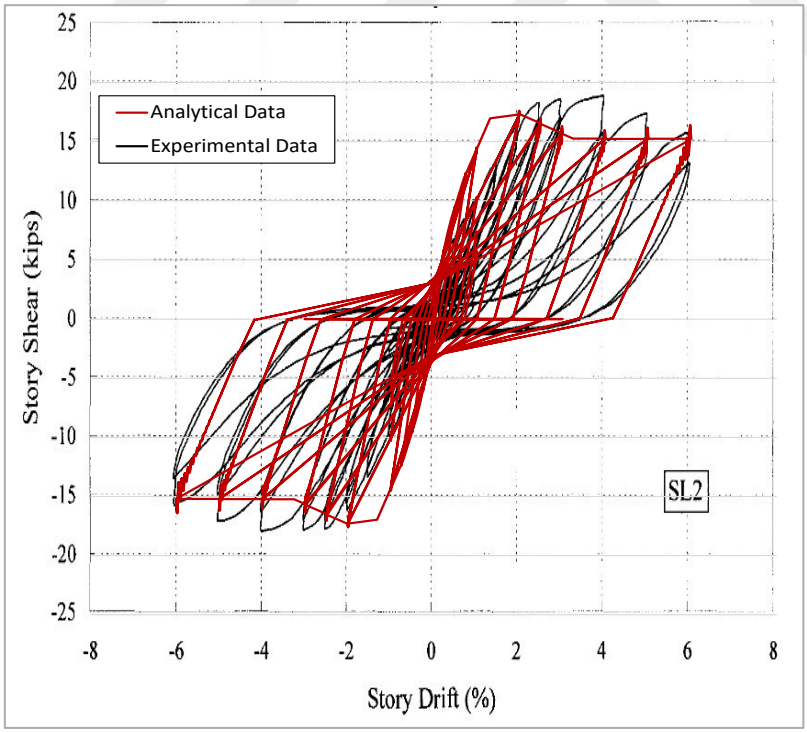


Figure 6.40. SL2 Lateral Load vs. Story Drift Comparison

The response of the overall structure resembles the experimental response of the joint, with a lower predicted joint shear strength and a stiffer initial response. The comparison of lateral load versus story shear and joint force vs. joint strain data verifies that the general response of the structure is successfully predicted. This clearly demonstrates that the joint strength or lateral load capacity should not be reduced significantly due to the presence of eccentric joints, which is the common recommendation of contemporary structural codes.

The comparison cannot be extended to the evaluation of beams due to lack of data.

Specimen SL3

The third specimen has exactly the same reinforcement detailing as SL1, but the joint eccentricity is omitted. The loading is applied concentrically in the direction of the spandrel beam.

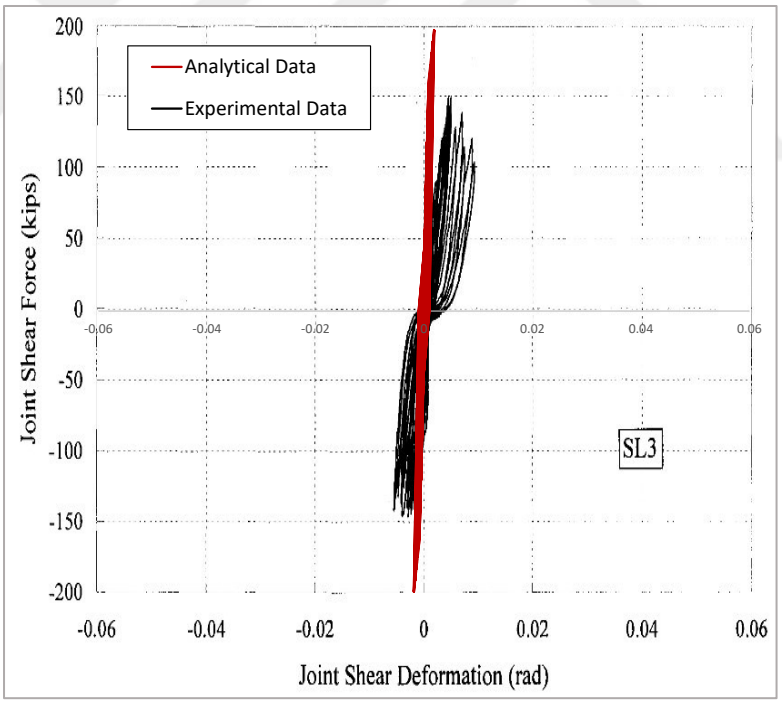


Figure 6.41. SL3 Joint Shear Force vs. Shear Strain Comparison

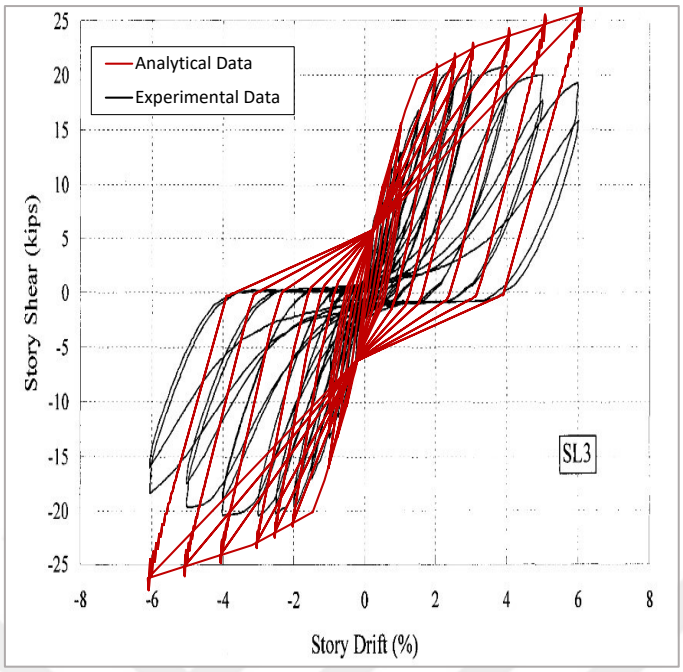


Figure 6.42. SL3 Lateral Load vs. Story Drift Comparison

It is noteworthy to underline that, although most of the properties of SL3 are the same as SL1, the response of the joint differs considerably. While the joint of SL1 shows a high strain (0.03 rad.), the joint of SL3 deforms much less than SL1 (0.01 rad.). This difference is significant in terms of evaluation of the effect of eccentricity in beam-column joints. The proposed model is effective in the addressing the joint behaviour for both specimens, presenting a limited strain in SL3, although predicts a higher joint shear strength. The effect of high joint shear strength prediction leads to a higher lateral load capacity.

Specimen SL4

The last specimen in the experimental investigation has beam dimension of 279.4 mm x 406.4 mm (11" x 16") with 4 ϕ16 (#5) bars and 4 ϕ16 (2 #5) bars serving as the top and bottom longitudinal reinforcement, same as SL1 and SL3. The loading is applied to the subassembly concentrically, only altering the column orientation where the stronger axis of the rectangular column lies parallel to the loading direction.

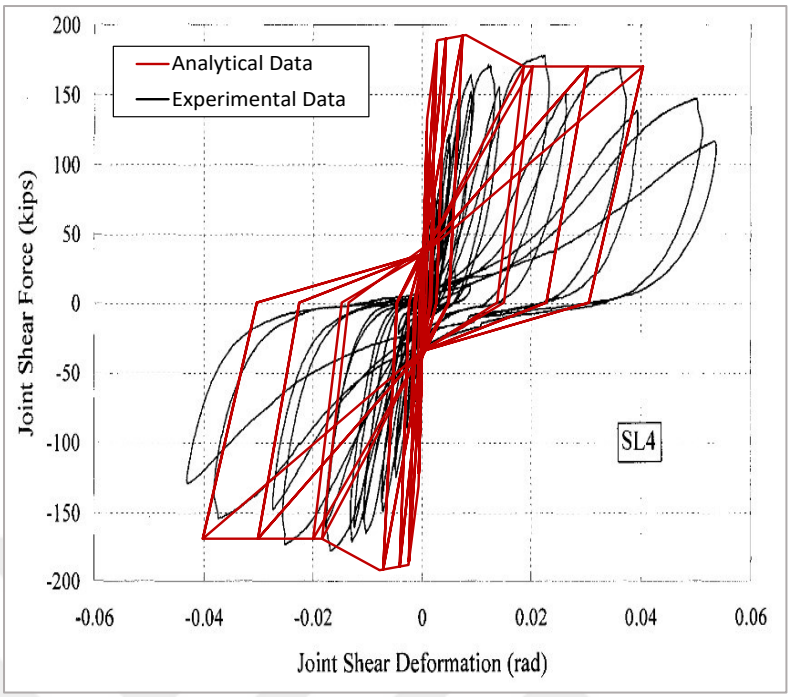


Figure 6.43. SL4 Joint Shear Force vs. Shear Strain Comparison

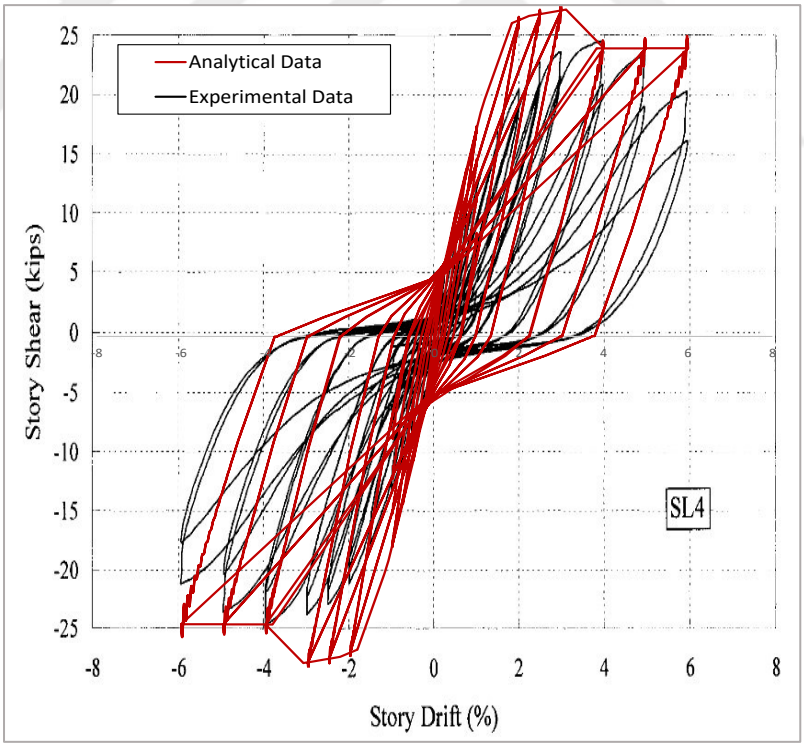


Figure 6.44. SL4 Lateral Load vs. Story Drift Comparison

The response SL4 analytical model resembles the response of the experimental investigation, despite a higher joint shear strength prediction. The pinching characteristics of the experimental investigation are similar to the model, whereas higher initial stiffness of the joint model affects the lateral load versus story drift response.

6.5.4 Comparison of Joint Model with Rigid and Semi Rigid Joint Assumptions

In this part of the thesis, 3 different alternatives applied in beam-column joint modeling of reinforced concrete structures is evaluated, in the light of the results of 2 specimens of Burak and Wight, 1-S and 3-S, due to the diverse response characteristics of the specimens. Also, due to the availability of beam moment-rotation data, the effect of different modeling techniques on the response of beam moment-rotation response is also evaluated. Both specimens are modeled first utilizing the proposed joint model that has nonlinear behavior characteristics in combination with the rigid end zones. Then, models without the panel zone that defines the joint model but with only rigid end zones that have rigidity factors of R = 1.0 and R = 0.5, representing the rigid and semi rigid joint assumptions, respectively are analyzed to evaluate the overall structural behavior.

Specimen 1-S

The evaluation of specimen 1-S is significant in the comparison of the effect of modeling techniques since the joint does not experience excessive strains and the response of the subassembly is shaped accordingly. The expected and analytical joint shear force versus joint strain data is presented in Figure 6.45.

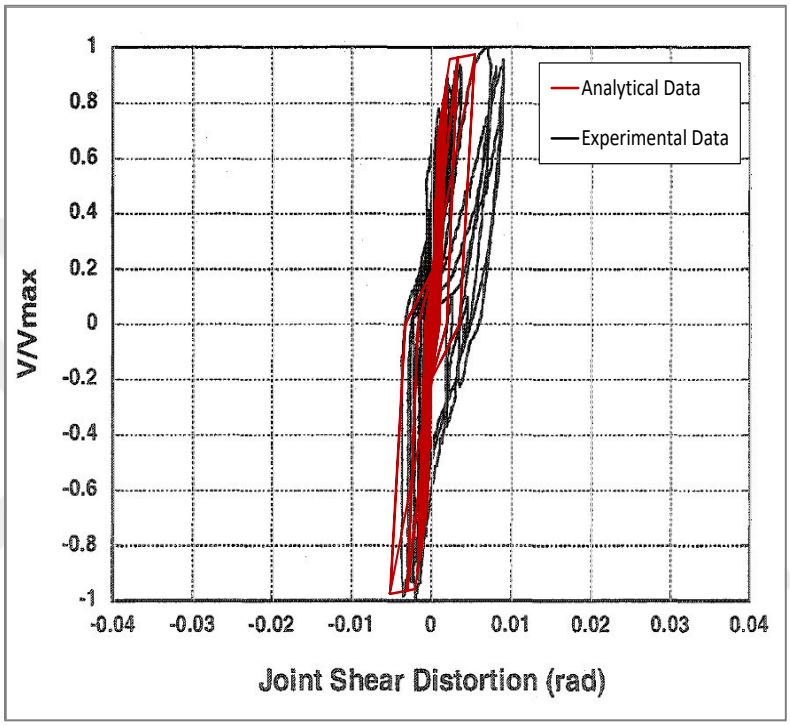


Figure 6.45. Analytical and Experimental Joint Reponse of Specimen 1-S

The subassembly is analized with the joint model using rigid end zones combined with nonlinear panel zone, solely the rigid end zones and semi rigid end zones. Figure 6.46 and Figure 6.47 represent the respective responses.

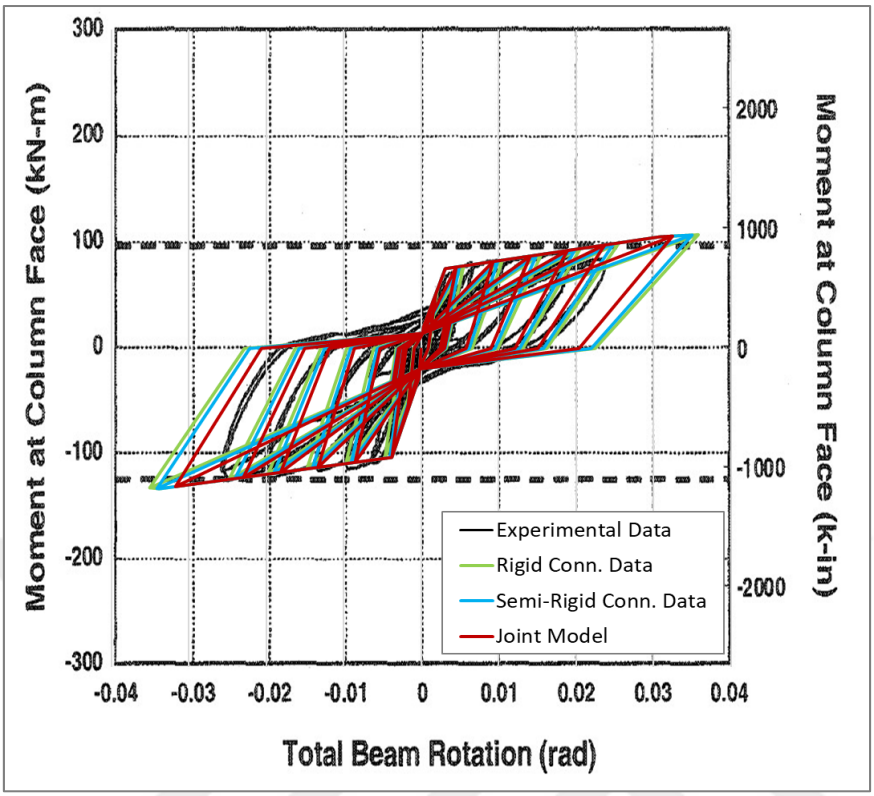


Figure 6.46. Comparison of Beam Moment-Rotation Response for Sp.1-S

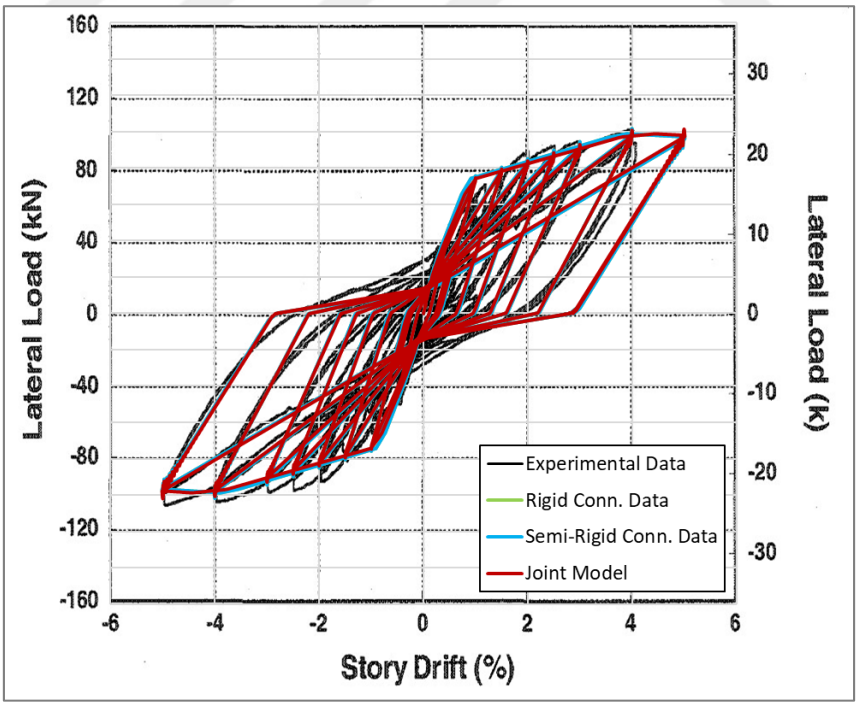


Figure 6.47. Comparison of Lateral Load vs Story Drift for Sp.1-S

From the evaluation of results presented in Figure 6.46 and Figure 6.47, it can be observed that the overall response of the subassembly is not significantly affected by the rigid joint assumption, in comparison with the joint panel zone model. Moreover, the utilization of semi-rigid end zones does not considerably affect the reponse of the structure. However, it should be noted that, the response of the beam alters with the utilization of rigid and semi rigid end zones. The rigid and semi rigid end zone definition present a higher beam end rotations compared to the proposed joint model. The is only a minor difference between the use of rigid and semi-rigid end zonesfor this specimen.

Specimen 3-S

The analysis of specimen 3-S also holds importance in comparing the impact of different modeling methods, especially due to the substantial joint strains experienced and the influence of these strains in the structural response. The graphs depicting the experimental and analytical joint shear force versus shear strain responses utilizing the joint model are provided in Figure 6.48.

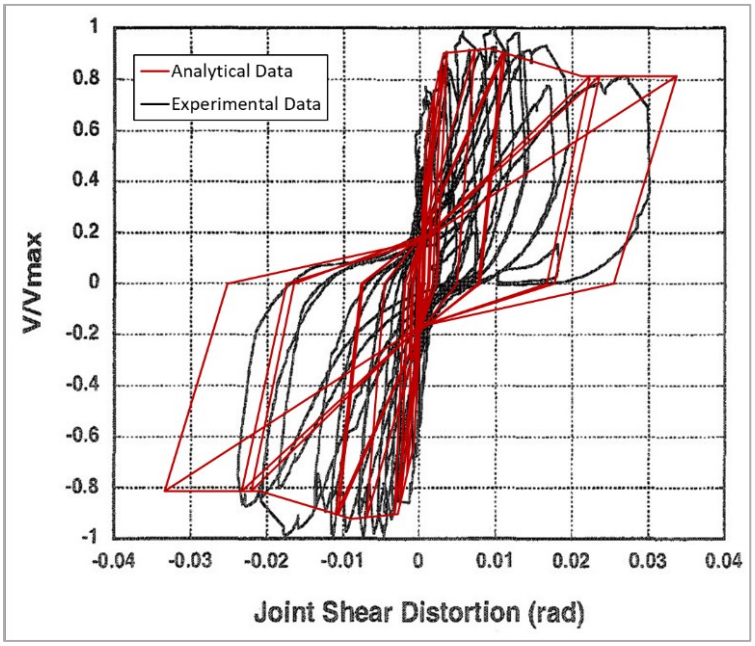


Figure 6.48. Analytical and Experimental Joint Reponse of Specimen 3-S

The subassembly is analyzed using the joint model which incorporates rigid end zones in combination with the nonlinear panel zone, rigid end zones by themselves, and semi-rigid end zones. Figure 6.49 and Figure 6.50 illustrate the corresponding responses for each case.

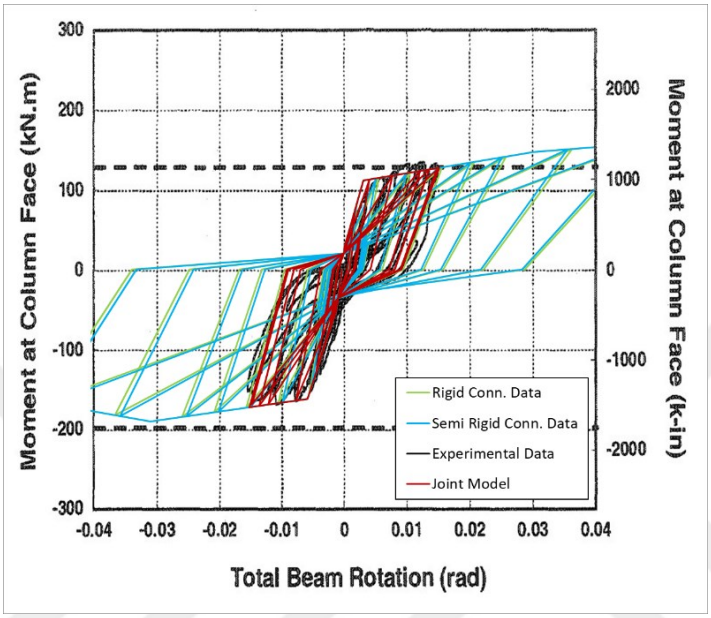


Figure 6.49. Comparison of Beam Moment Rotation Response for Sp. 3-S

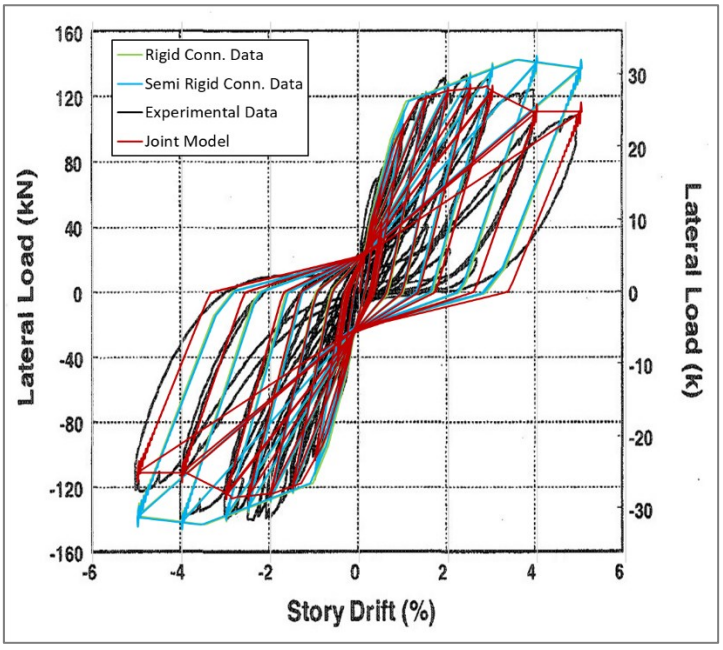


Figure 6.50. Comparison of Lateral Load vs Story Drift for Sp. 3-S

The beam moment rotation and overall structural response comparison figures presented in Figure 6.49 and Figure 6.50 clearly indicate that, the effect of rigid end zone definition without the implication of nonlinear response behavior of joints by utilizing a joint model leads to erroneous outcomes, especially for joints where excess strains are experienced. The moment rotation response obtained by utilizing the joint panel zone with the proposed nonlinear behavior model successfully resembles the experimental beam maximum rotation values 0.015 radians and 0.016 radians with predictions of 0.015 radians in both the positive and negative loading directions. Whereas both the rigid and semi-rigid joint definitions lead to excessive beam rotations of 0.048 radians and 0.046 radians in both positive and negative loading directions, clearly indicating the misinterpretation of the member behavior for the subassembly.

Although the general response of the structure seems to follow the experimental behavior for rigid and semi-rigid end zone assumptions, the beam rotations for these models significantly deviate from the experimental response. Moreover, the use of semi-rigid end zones does not improve the analytical response of the structure and only have minor difference when compared to rigid joint assumption.

Based on the analytical results, the implication of the nonlinear behavior of beam-column joints by the use of a joint model is crucial for determining structural performance accurately, especially under seismic loading where excessive structural deformations are expected.

CHAPTER 7

APPLICATION OF JOINT MODEL TO FRAME ANALYSIS

In this section of the thesis, the verification of the proposed nonlinear joint model, which is discussed in detail in the prior sections and validated in the light of subassembly tests will also be verified using the frame test data gathered from a half scale three story, three bay reinforced concrete frame, tested in the Middle East Technical University Structural Mechanics Laboratory in 2011 (Unal & Burak, 2013b).

Further explanation of the conducted test and analytical model is presented in the subsequent sections.

7.1 Overview

While evaluating the seismic performance of reinforced concrete moment resisting frame buildings, it is not sufficient to solely consider the overall performance, as the base shear versus roof drift response is quite resilient. Although the base shear versus roof drift response may not be significantly affected by particular changes in cross sectional or member properties, structural member response might experience substantial modifications. Columns, beams, and beam-column joints are crucial parts of a reinforced concrete structure that need detailed assessment, in addition to evaluating overall load-story drift response of the frame. A thorough assesment should be conducted by evaluating the performance of each structural member at different loading steps as earthquake ground motion intensity rises. This objective can be accomplished by conducting a multi-level performance evaluation of each individual member as earthquake ground motion intensity increases.

In the experimental study conducted at the Middle East Technical University in 2011, a well-detailed half scale reinforced concrete frame structure that has 3 stories

and 3 bays was tested. The frame structure is loaded with 4 different earthquake scenarios with return periods of 72, 475 and 2475 years, also altering the soil conditions from soft to firm soil, the details of which are presented in Section 7.2.3.

In this study, an analytical frame model using SAP2000 Version 20.1 Ultimate Edition is generated, and a displacement based time history analysis is performed to represent the Pseudo Static loading applied in the experimental investigation.

The overall structural response of the model is then compared with the experimental one in terms of load versus interstory drift response for each story as well as the moment versus rotation response of the beams. Moreover, the beam-column joint response is compared with experimental results considering both rigid joint assumption and utilizing the joint model with the “Panel Zone” definition in combination with the rigid end zones in the analytical model.

7.2 Description of the Test Frame

7.2.1 Frame Properties

In the experimental study, the seismic response of a 3-story 3-bay reinforced concrete frame depicted in Figure 7.1 is investigated. The frame was designed based on Turkish Earthquake Code (TEC) 2007 requirements and failed by the formation of a joint mechanism.

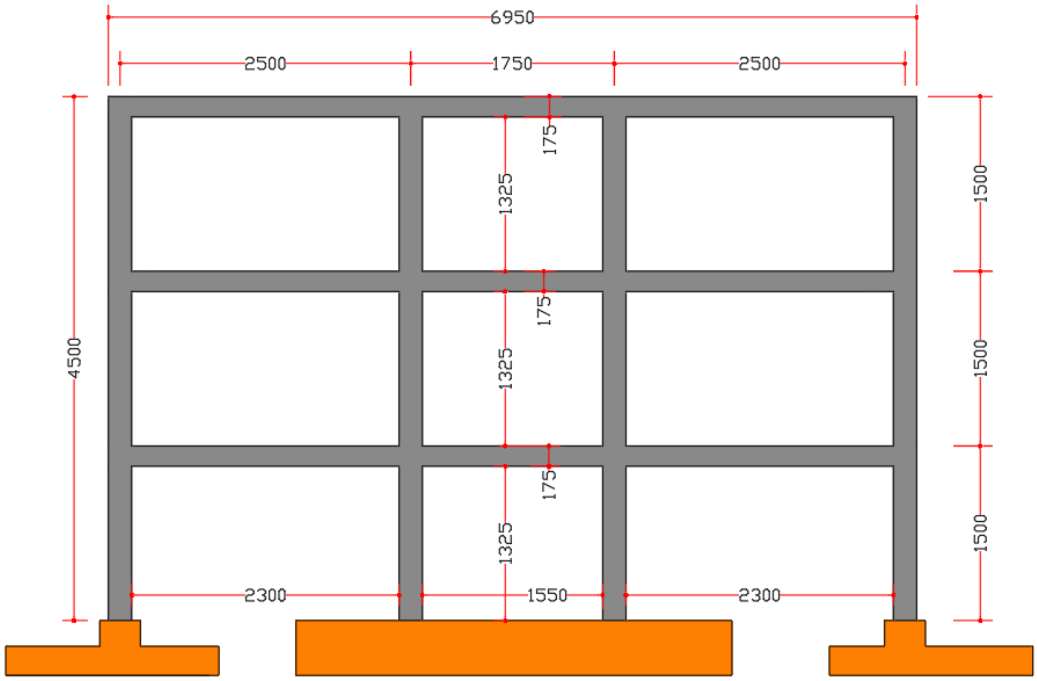


Figure 7.1. Test Frame (all dimensions are in mm.)

The cross sectional properties and reinforcement detailing of the frame members are presented in Figure 7.2. The specimen has slabs at every floor level with an effective flange width (b_e) roughly eight times the slab thickness. This design accounts for the contribution of the slab to the beam behavior and confinement of the joint and provides means for application of gravity loading by the use of steel plates. Shear reinforcement detailing for the interior and exterior joints is presented in Figure 7.3.

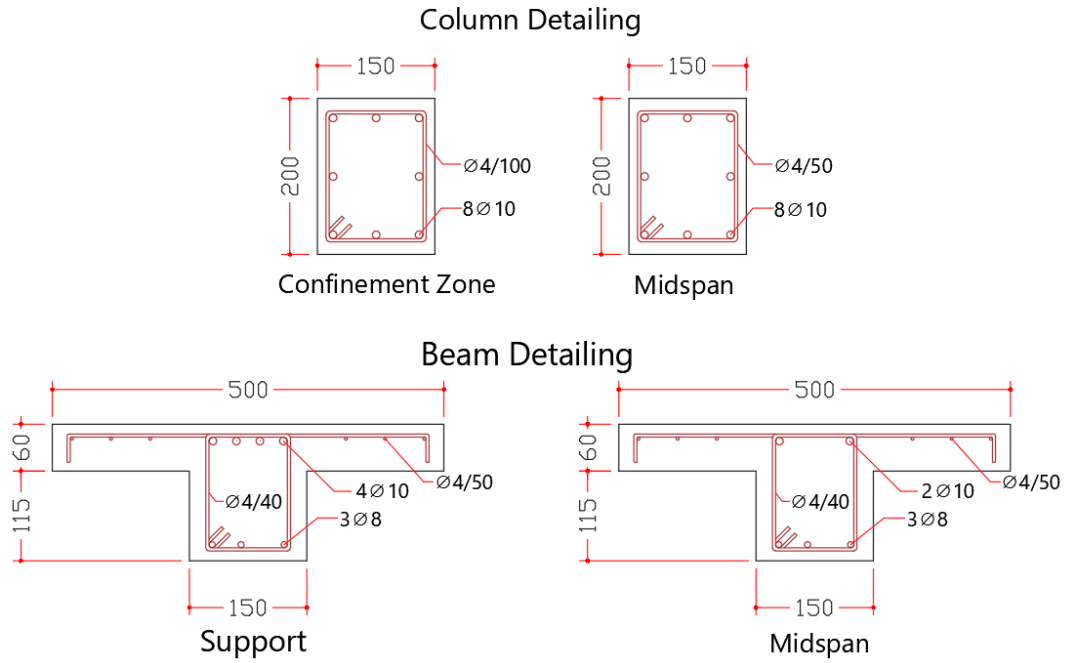


Figure 7.2. Beam and Column Detailing (all dimensions are in mm.)

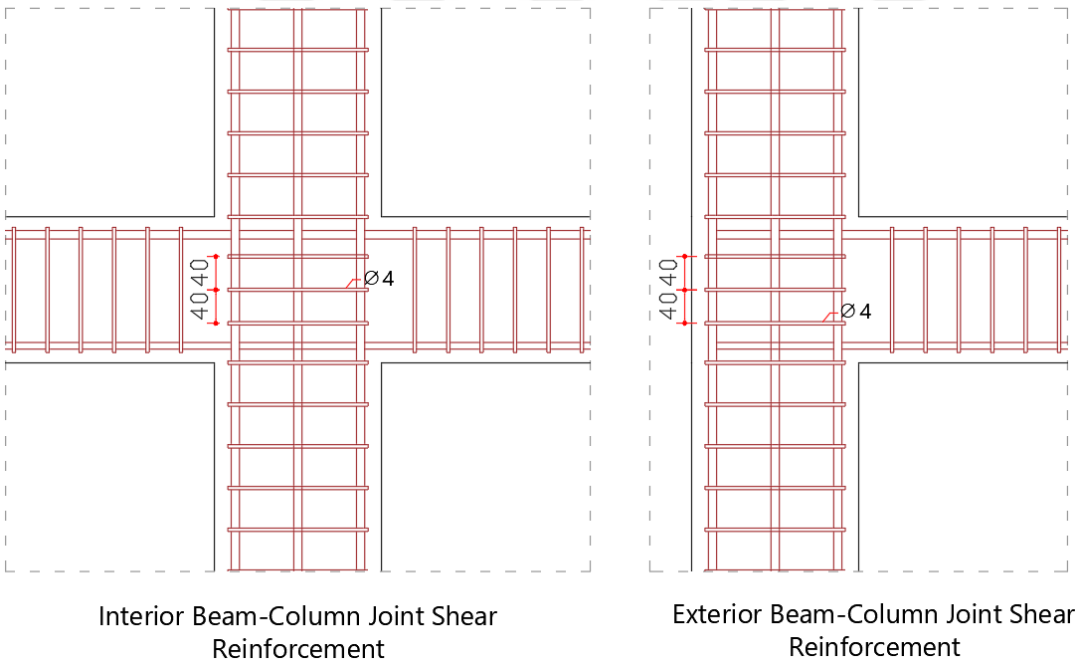


Figure 7.3. Interior and Exterior Beam-Column Joint Shear Reinforcement Detailing (all dimensions are in mm.)

7.2.2 Material Properties

In this subsection, the material properties utilized in the construction of test frame are presented. Concrete compressive strengths obtained from the experimental data are presented for each floor separately. The modulus of elasticity of concrete is determined using the formula recommended by ACI 318-19 and provided as Eqn. 7.1. Test frame concrete and rebar properties are presented in Tables 7.1 and 7.2.

$$E_c = 4700\sqrt{f_c'}\ (\text{MPa}) \tag{7.1}$$

Table 7.1 Test Frame Concrete Properties

Floor	f_c' (MPa)	E_c (MPa)
Floor 1	26.4	24136.7
Floor 2	35.6	28038.8
Floor 3	39.5	29523.3

Table 7.2 Test Frame Rebar Properties

Type	f_y (MPa)	f_u (MPa)
8 mm (Deformed Bar)	430.0	560.0
10 mm (Deformed Bar)	430.0	680.0
8 mm (Plain Bar)	320.0	460.0
10 mm (Plain Bar)	355.0	555.0
4 mm (Plain Bar)	240.0	340.0

7.2.3 Frame Loading

The dead load is applied to the frame structure by the use of steel blocks placed on the slab representing the self-weight of the structure and the ground acceleration time histories are applied at each floor level representing seismic loading. The stepwise application of the seismic loads to the structure based on probability of exceedance, soil type and return period (RP) is summarized below.

D1 : Probability of exceedance of 50% in 50 years, Z1 (RP:72 years)

D2 : Probability of exceedance of 10% in 50 years, Z1 (RP: 475 years)

D3 : Probability of exceedance of 10% in 50 years, Z3 (RP: 475 years)

D4 : Probability of exceedance of 2% in 50 years, Z1 (RP: 2475 years)

The ground acceleration time histories are presented schematically in Figure 7.4.

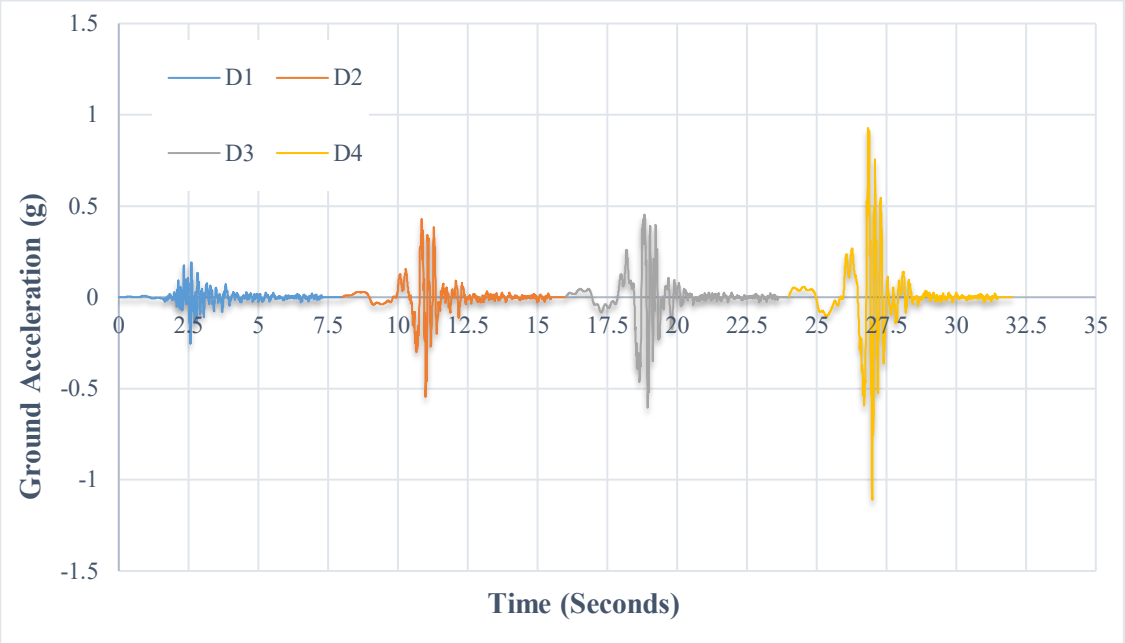


Figure 7.4. Ground Acceleration Time Histories for Frame Test

At each floor level, hydraulic actuators are utilized to impose the displacement demands computed by solving the dynamic equilibrium of the three degree-of-freedom system.

The imposed dead load magnitudes and the application points of displacement time histories are schematically represented in Figure 7.5.

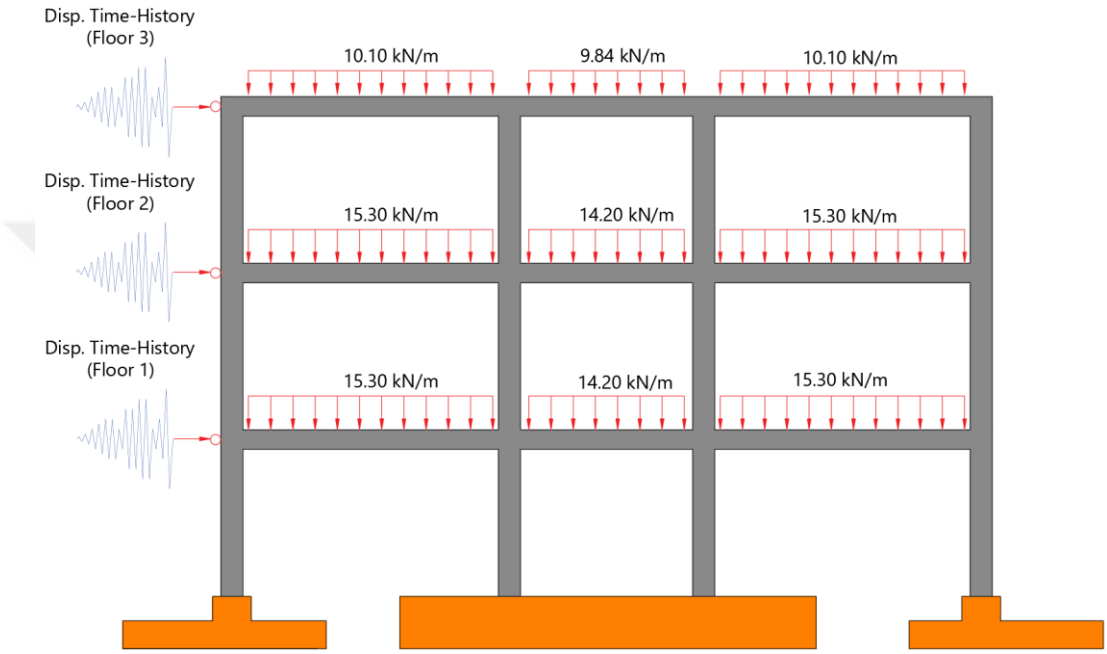


Figure 7.5. Imposed Dead Load Magnitudes and Point of Application of Seismic Displacement Time Histories

Finally, the displacement time history data applied at each floor level are presented graphically in Figure 7.6 to Figure 7.9, which led to the formation of a joint failure mechanism during the application of D4 displacement time history.

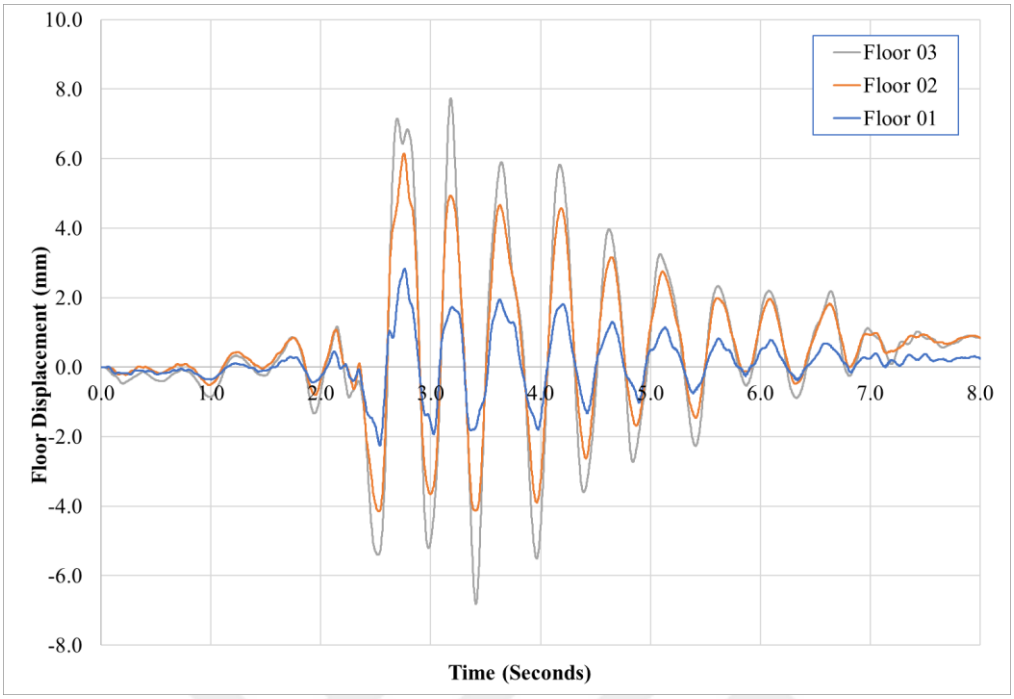


Figure 7.6. D1 Displacement Time Histories Applied to the Frame

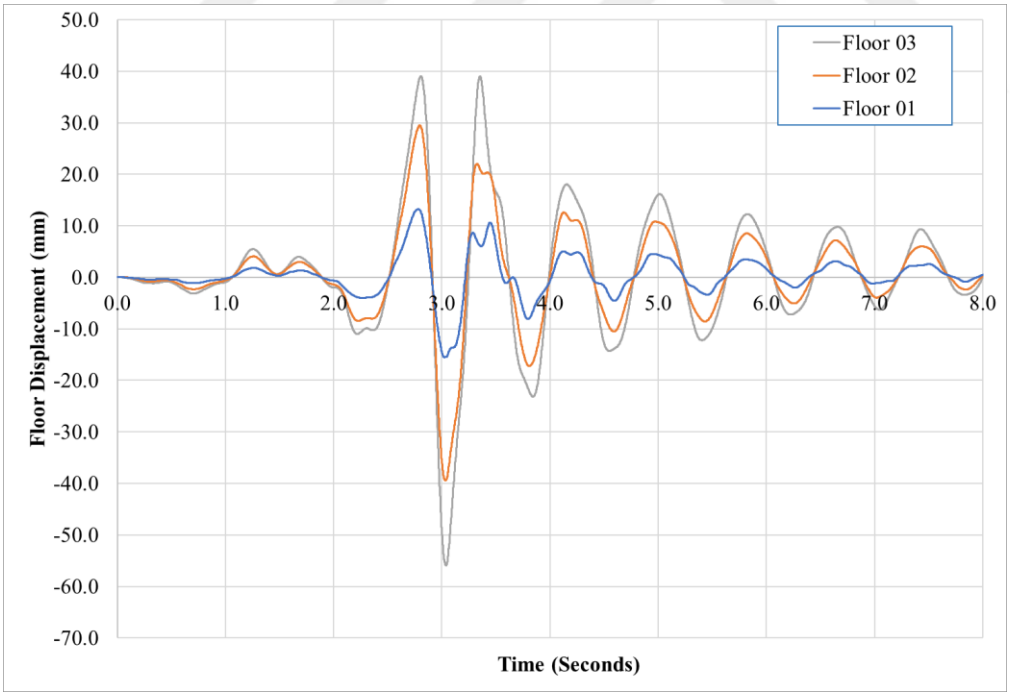


Figure 7.7. D2 Displacement Time Histories Applied to the Frame

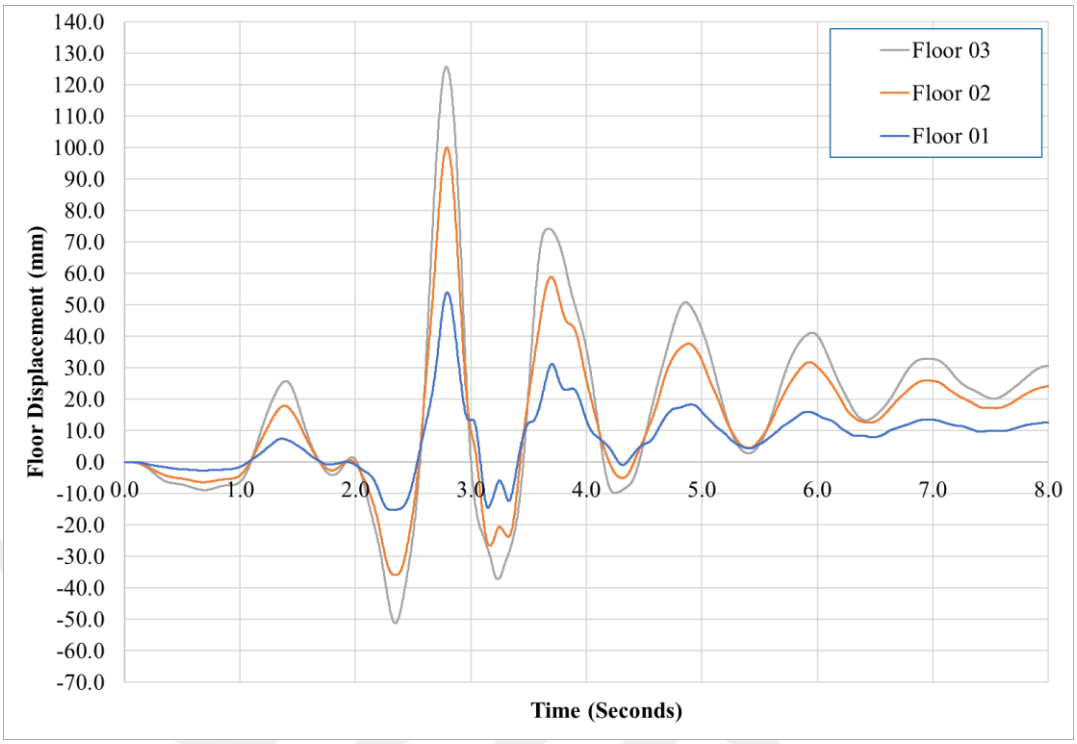


Figure 7.8. D3 Displacement Time Histories Applied to the Frame

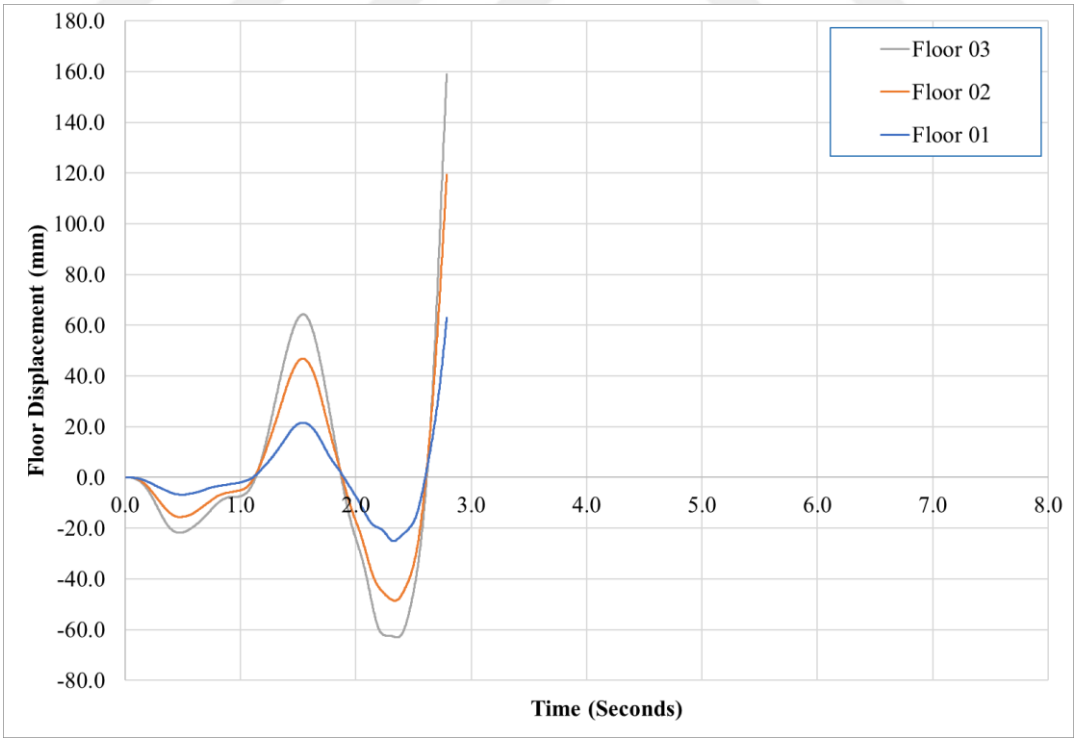


Figure 7.9. D4 Displacement Time Histories Applied to the Frame

7.3 Modeling of the Test Frame

As explained in the previous sections, the test frame is modeled in SAP 2000 software and related geometrical, material and loading properties are defined. In this section the analytical model is explained in detail.

7.3.1 Geometrical and Material Properties

The generated 3D model of the test frame is presented in Figure 7.10. Beams and columns are defined as line elements whereas the joints in between line elements are defined as “Panel Zones”.

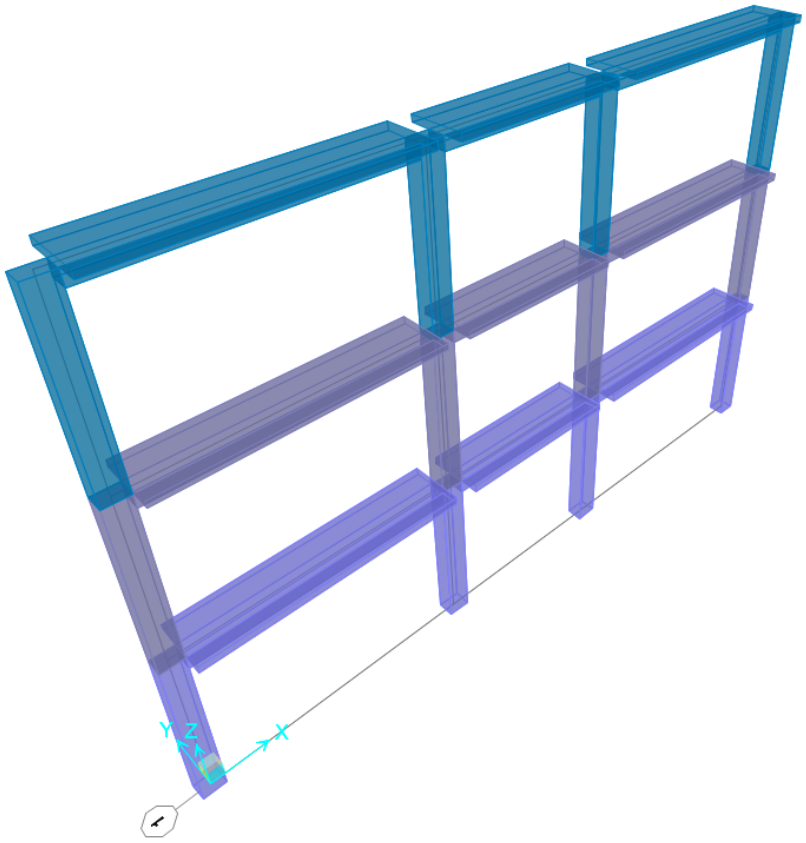


Figure 7.10. 3D Model of the Test Frame

Definition of Material Properties

Based on the data extracted from the experimental study, the material properties are defined separately for each floor.

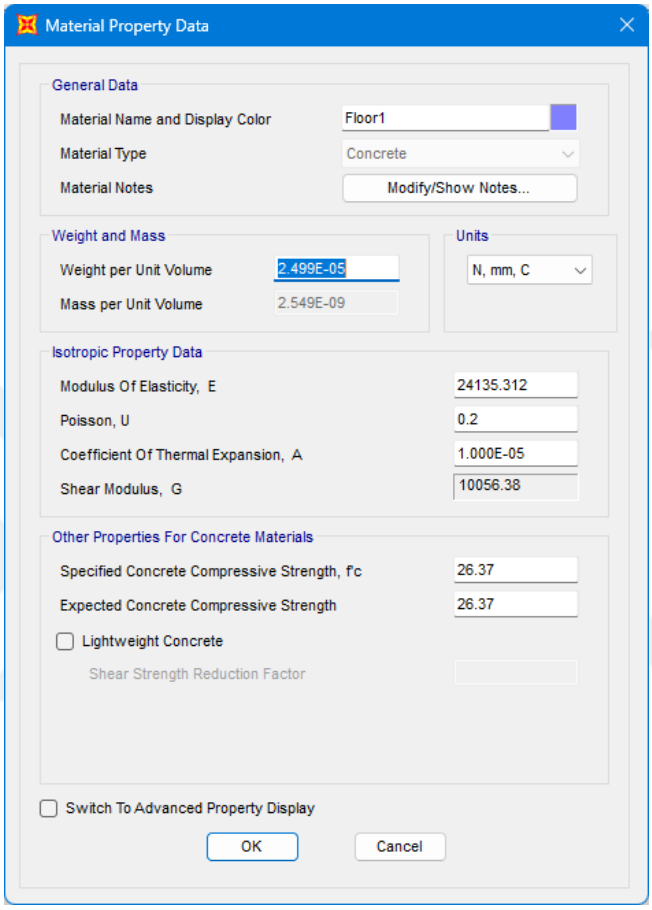


Figure 7.11. Sample Concrete Properties Definition (Floor 1)

Beam and Column Cross Sections

The cross sectional properties of frame members are also defined considering the geometrical and material properties assigned to the members.

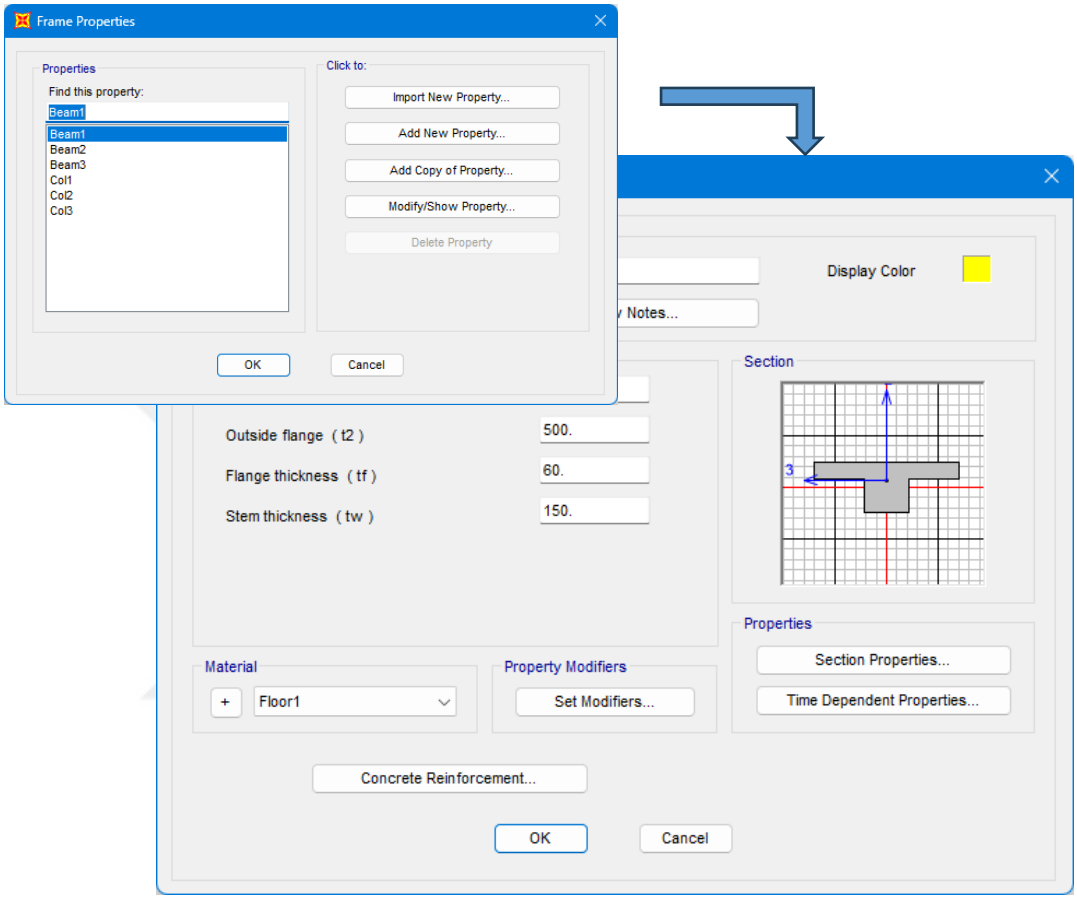


Figure 7.12. Sample Cross Sectional Properties Definition (Floor 1)

The cracked section characteristics of the beam and column members are defined based on the ACI 318-19 regulations. For the T-sections cracked stiffness is considered as the moment of inertia of the rectangular section whereas for rectangular beams and columns the cracked stiffness is taken as 0.35 ($I_{beam,cr} = 0.35\ I_{beam,gross}$) and 0.7 ($I_{col,cr} = 0.70\ I_{col,gross}$) of the moment of inertia, respectively as previously presented in Section 6.2.

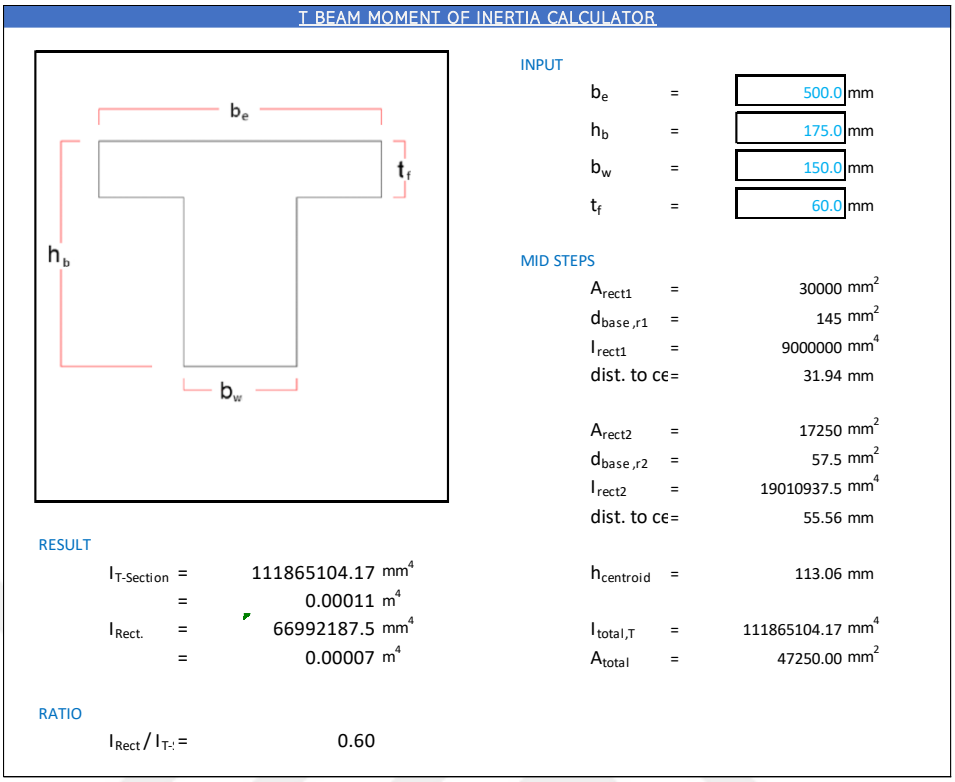


Figure 7.13. Test Frame Beam Cracked Section Stiffness Determination

The moment-rotation relationship of beams and columns are obtained utilizing "Response 2000" software and applied as concentrated rotational springs to the frame model using "nonlinear hinges". A sample moment-rotation calculation and corresponding definition of nonlinear frame hinge are presented in Figure 7.14.

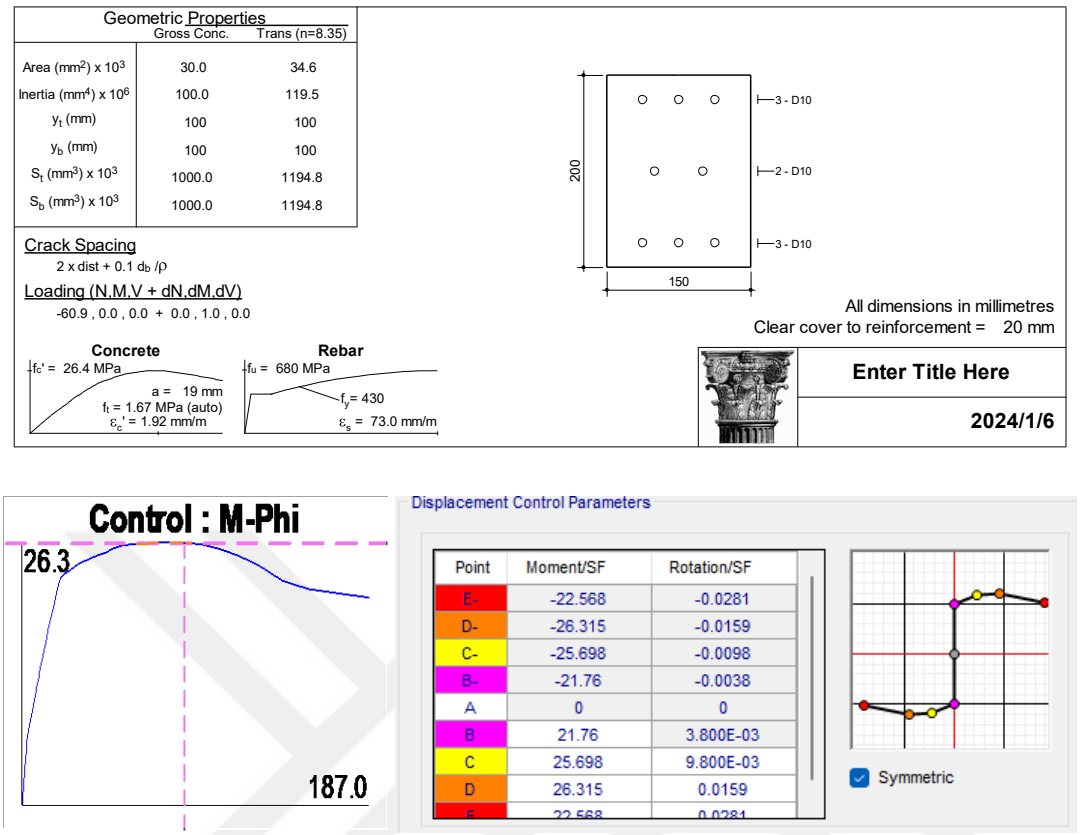


Figure 7.14. Moment-Rotation Relationship for Beams and Columns

Hinge Lengths

In ACI 318-19, plastic hinge regions are defined as "the length of frame element over which flexural yielding is intended to occur due to earthquake design displacements, extending not less than a distance h from the critical section where flexural yielding initiates". Accordingly, the plastic hinge length is defined as the depth of the member (h) for both columns and beams.

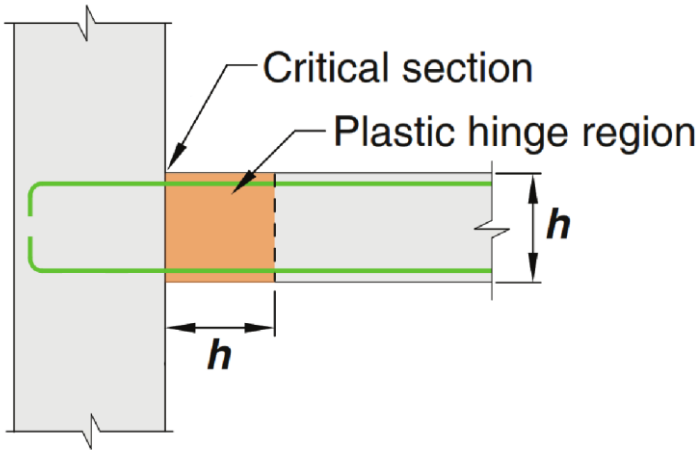


Figure 7.15. Hinge Length Definition for Beams and Columns

Rigid End Zones

In nonlinear analysis, rigid segments of beams and columns within the joint are simulated using rigid end zones. These end zones are defined as segments of the member assumed to be infinitely rigid and are measured from the face of the joint. The schematical representation of the rigid end zones is presented in Figure 7.16.

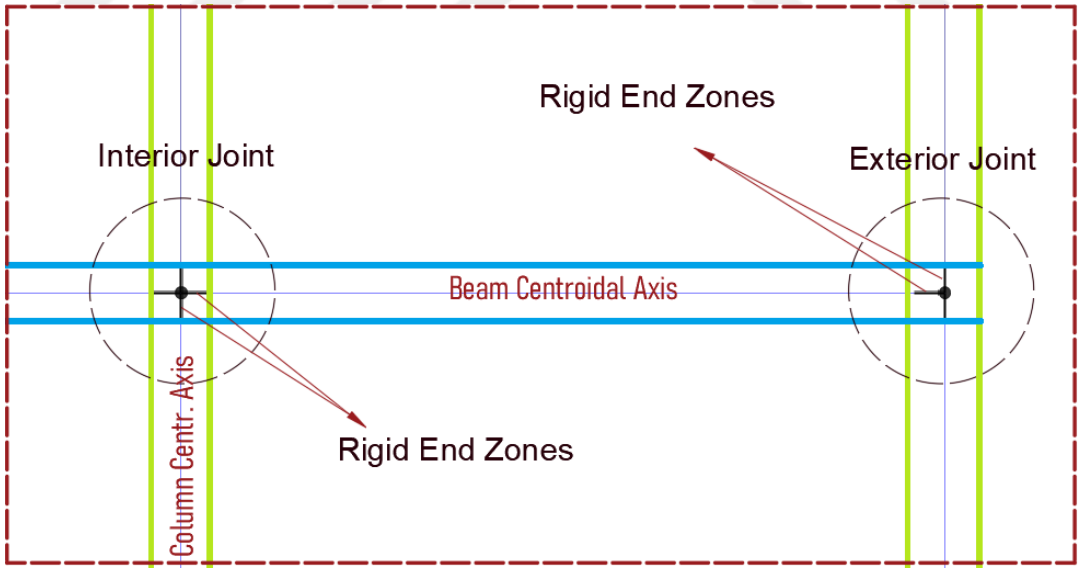


Figure 7.16. Rigid End Zones

In the analysis, to monitor the effect of utilizing a joint model by panel zone application, 2 additional models with rigid end zone factors of 1.0 and 0.5 are created, without panel zone assignment at the beam-column joints. This way the analytical results obtained by using the joint model are compared with the rigid and semi-rigid joint assumptions, which is presented in Section 7.4.

7.3.2 Determination of Panel Zone Characteristics

As previously discussed, SAP 2000 enables the use of nonlinear panel zones as beam-column joints by defining nonlinear moment-shear distortion relationship for the joints.

For the tested frame, since the joints on each floor are exposed to different axial load levels, a total of 6 different panel zones are defined. For this purpose, first a dead load analysis considering all vertical loads applied to the frame is performed, then, the proposed nonlinear joint models are generated based on the obtained axial load levels and integrated into analytical model of the frame analytical model.

The level of axial loads obtained from the dead load analysis are presented in Section 7.3.4. The panel zone assignment in the model is illustrated in Figure 7.17.

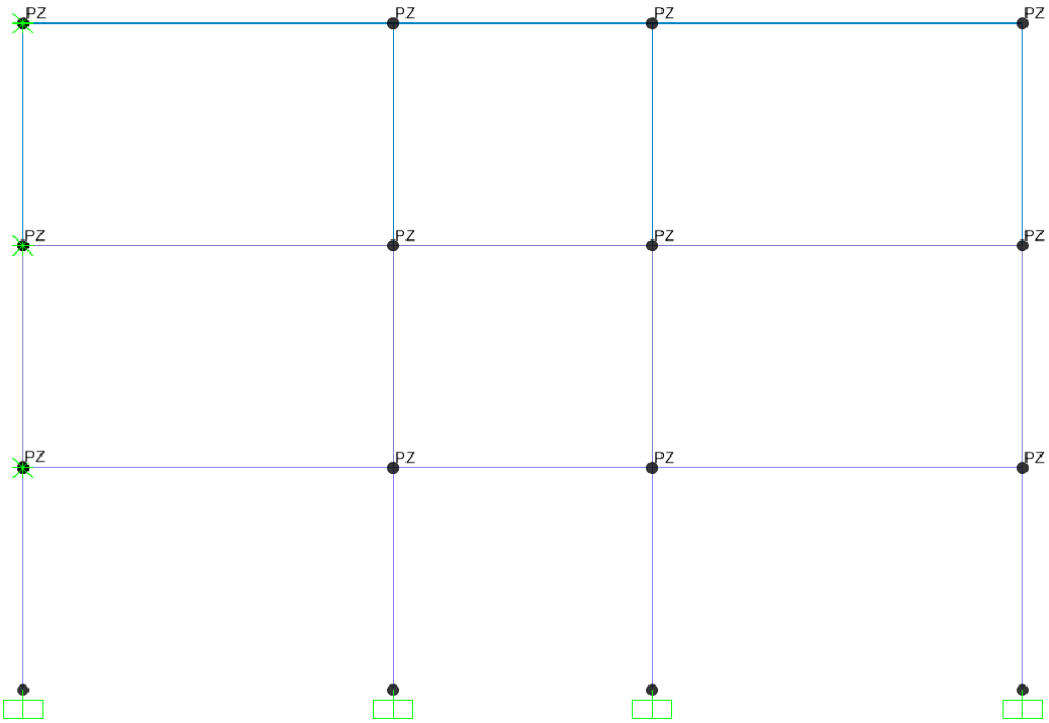


Figure 7.17. Panel Zone Assignment in the Model

6 individual panel zone characteristics assigned to the model are presented in Figure 7.18. On each floor, due to the different axial load level on the column, the panel zone properties are defined for the exterior and interior connections, separately. In the definition of the joint panel zone, the floor and location of the panel zones are identified.

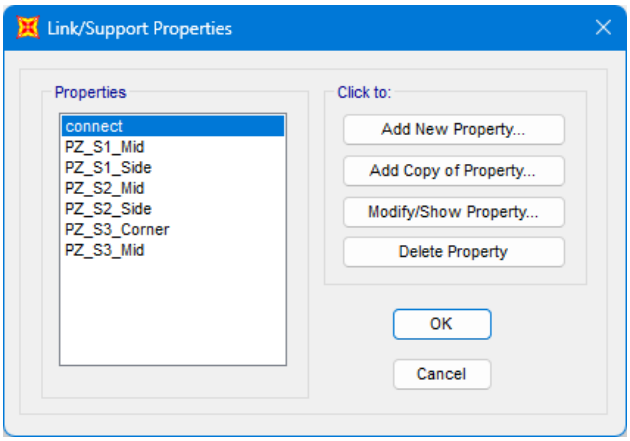


Figure 7.18. Panel Zone Location in the Model

The panel zone characteristics defined in the model are presented in Figure 7.19. For the hysteretic behavior of the nonlinear panel zone, "Pivot" hysteresis behavior model, the details of which are presented in 6.2.1, is implemented.

Sample moment-rotation relationship utilized in the models is presented in Figure 7.19.

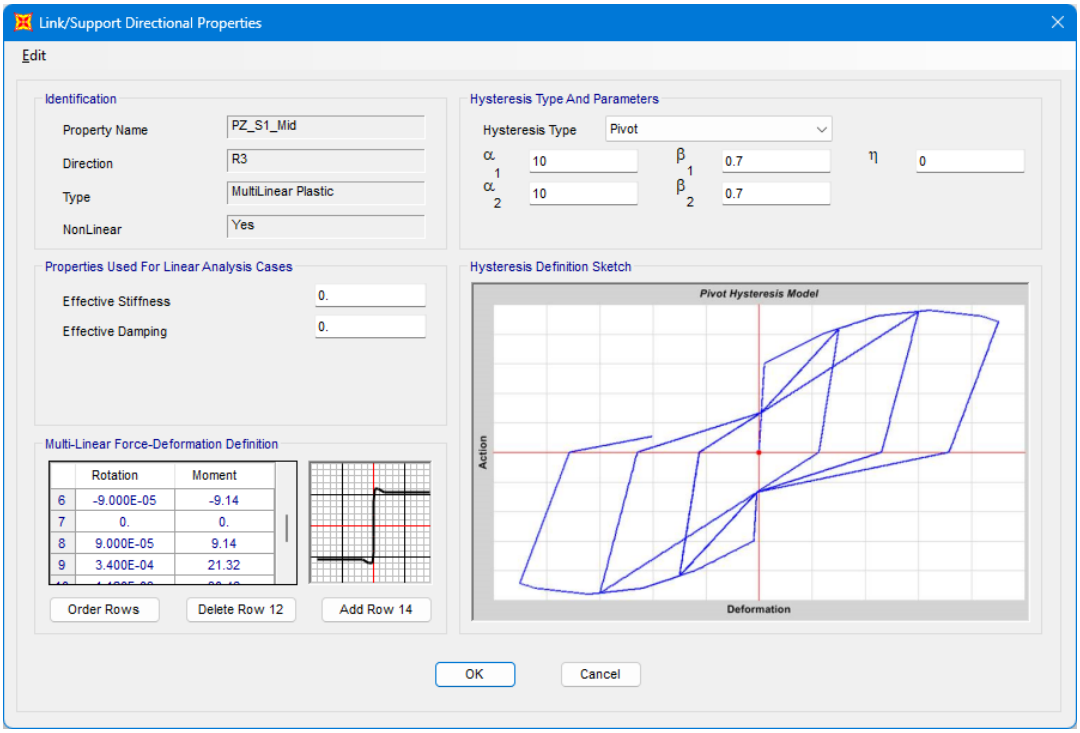


Figure 7.19. Sample Panel Zone Definition for Frame Model

7.3.2.1 Determination of Joint Shear Strength

Computation of the Confinement Score and Shear Strength Factor for the Test Frame

To determine the nonlinear behavior characteristics of the beam-column joints of the test frame, first, the "Joint Shear Strength Factor" is computed considering the confinement provided by the surrounding members, as presented in 4.2.1.

Beam Width (b_b) = 150.0 mm (for all members)

Column Width (b_c) = 150.0 mm (for all members)

Beam Width (b_c) / Column Width (b_c) = 1.00 (for all members)

Consequently, the confinement scores and related Joint Shear Strength Factors for all joints are summarized in Table 7.3 Confinement Score and Joint Shear Strength Factors for the Test Frame.

Table 7.3 Confinement Score and Joint Shear Strength Factors for the Test Frame

Beam-Column Joint	Number of Beams	Conf. Score (CS)	Joint Shear Strength Factor (γ)
Floor 1 Interior	2.00	2.00	14.00
Floor 1 Exterior	1.00	1.00	10.00
Floor 2 Interior	2.00	2.00	14.00
Floor 2 Exterior	1.00	1.00	10.00
Floor 3 Interior	2.00	2.00	14.00
Floor 3 Exterior	1.00	1.00	10.00

Computation of the Modification Factors

To determine the Modification factors, first, the axial load level on the beam-column connections must be determined. For this reason, as the first step of analytical investigation, a simple, static analysis is carried out to determine the axial forces on the beam-column joints. The axial forces imposed on the beam-column joints are significant in the determination of nonlinear force-strain characteristics of the connection regions, as explained in Section 4.2.2.2. The axial forces imposed on the beam-column joints and related axial load factors are presented in Table 7.4.

Table 7.4 Axial Loads and Factors

Beam-Column Joint	Axial Force N (kN)	Concrete Str. f_c' (MPa)	Column Depth h_c (mm)	Column Width b_c (mm)	Axial Load Index AxI $N / (b_c h_c f_c')$	Axial Load Factor AxF $1 + (AxI/2)$
Floor 1 Int.	60.82	26.37	150.00	200.00	0.077	1.038
Floor 1 Ext.	36.07	26.37	150.00	200.00	0.046	1.023
Floor 2 Int.	25.28	35.59	150.00	200.00	0.024	1.012
Floor 2 Ext.	14.68	35.59	150.00	200.00	0.014	1.007
Floor 3 Int.	0.00	39.46	150.00	200.00	0.000	1.000
Floor 3 Ext.	0.00	39.46	150.00	200.00	0.000	1.000

Then, the volumetric shear reinforcement ratios ($\rho_{singlelayer,core}$) are calculated and presented in Table 7.5.

Table 7.5 Shear Reinforcement Ratios for the Test Frame

Beam-Column Joint	Shear Reinf. Area (A_0) (mm^2)	Eff. Shear Reinf. Length (l_c) (mm)	Spacing (s) (mm)	Col. Core Depth ($h_{c,core}$) (mm)	Col. Core Width ($b_{c,core}$) (mm)	Shear Reinf. Ratio ($\rho_{singlelayer,core}$)
Floor 1 Int.	12.57	504.00	40.00	168.00	118.00	0.0080
Floor 1 Ext.	12.57	504.00	40.00	168.00	118.00	0.0080
Floor 2 Int.	12.57	504.00	40.00	168.00	118.00	0.0080
Floor 2 Ext.	12.57	504.00	40.00	168.00	118.00	0.0080
Floor 3 Int.	12.57	504.00	40.00	168.00	118.00	0.0080
Floor 3 Ext.	12.57	504.00	40.00	168.00	118.00	0.0080

Shear reinforcement factors (SR) are calculated next, as presented below.

Shear Reinforcement Index (SI) = 0.008 - 0.01 = -0.002

Since $\rho_{singlelayer,core} < 1.0$ %,

$$SR = 1 - \sqrt{SI} = 1 - \sqrt{0.002} = 0.955$$

Finally, since there are slabs in the test frame, the slab index (SI) and the slab factor (SF) are calculated as,

$$\text{Slab Index (SI)} = \frac{t_f}{h_b} = 60 / 175 = 0.34$$

$$\text{Slab Factor (SF)} = 1+SI^2 = 1 + 0.34^2 = 1.116$$

Calculation of the Effective Joint Width, b_j

For all the listed joints, the effective joint width (b_j) is determined as 150.0 mm, as the column width governs (Eqn. 4.24). No eccentricity Modification is required since all the connections are concentric.

Joint Shear Strength Determination of Beam-Column Joints of the Test Frame ($V_{j,pre.}$)

In the light of the determined Joint Shear Strength Factor, Modification Factors, and effective joint width; the joint shear capacities of the beam-column connections are determined as presented in Table 7.6.

Table 7.6 Joint Shear Strength Values of the Beam-Column Connections of Test Frame

Beam-Column Joint	Joint Shear Strength Factor	Concrete Comp. Str.		Eff. Joint Width	Column Depth	Basic Jnt Shear Str. Pred.	Axial Load Factor	Shear Reinf. Factor	Slab Factor	Final Joint Shear Str. Pred.
	γ	f_c' (MPa)	$\sqrt{f_c'}$	b_j (mm)	h_c (mm)	$V_{j,pre.,basic}$ (kN)	AxF	SR	SF	$V_{j,pre.}$ (kN)
Floor 1 Interior	14.00	26.37	5.14	150.00	200.00	179.01	1.04	0.96	1.12	198.42
Floor 1 Exterior	10.00	26.37	5.14	150.00	200.00	127.87	1.02	0.96	1.12	139.60
Floor 2 Interior	14.00	35.59	5.97	150.00	200.00	207.97	1.01	0.96	1.12	224.61
Floor 2 Exterior	10.00	35.59	5.97	150.00	200.00	148.55	1.01	0.96	1.12	159.65
Floor 3 Interior	14.00	39.46	6.28	150.00	200.00	218.98	1.00	0.96	1.12	233.74
Floor 3 Exterior	10.00	39.46	6.28	150.00	200.00	156.41	1.00	0.96	1.12	166.96

7.3.2.2 Determination of Joint Performance Points

The joint shear performance points of the test frame are determined considering the procedure presented in Section 7.3.2.2. The basic strain at the inelasticity point ($\gamma_{inel,basic}$) values and mid-steps utilized in the determination of the basic inelastic strain are summarized in Table 7.7.

Table 7.7 Basic Inelastic Strain Value Determination, Test Frame

Beam-Col. Joint	$V_{j,pre.}$ (kN)	$V_{j,inel}$ = 0.70 $V_{j,pre.}$ (mm^2)	Eff. Joint Shear Area A_j (mm^2)	Joint Shear Stress, Inel. Pt. $v_{j,inel}$ (MPa)	Conc. Comp. Str. f_c' (MPa)	Modulus of Elasticity E_c ($4700\sqrt{f_c'}$) (MPa)	Shear Mod. of Elas. (elastic) G_{elas} ($0.4 E_c$) (mm)	Shear Mod. of Elas. (inel.) G_{inl} ($0.3 G_{elas}$) (mm)	Strain at $V_{j,inel}$, basic $\gamma_{inel,basic}$ (kN)
FL1-I	198.4	138.9	30000.0	4.6299	26.37	24135.31	9654.12	2896.24	0.0016
FL1-E	139.6	97.7	30000.0	3.2573	26.37	24135.31	9654.12	2896.24	0.0011
FL2-I	224.6	157.2	30000.0	5.2410	35.59	28038.96	11215.58	3364.67	0.0016
FL2-E	159.6	111.7	30000.0	3.7252	35.59	28038.96	11215.58	3364.67	0.0011
FL3-I	233.7	163.6	30000.0	5.4540	39.46	29524.08	11809.63	3542.89	0.0015
FL3-E	166.9	116.8	30000.0	3.8957	39.46	29524.08	11809.63	3542.89	0.0011

After the basic strain at the inelastic curve is defined, to determine the final inelastic curve, strain Modification factors due to the adjoining beam confinement and shear reinforcement within the joint volume are calculated, as explained in detail in Section 4.4. The computed values are presented in Table 7.8.

Table 7.8 Strain Modification Factors, Test Frame

Beam-Column Joint	Strain Adj. Factor, Beam Conf. (F_{BC})	Strain Adj. Factor, Shear Reinf (F_{SR})	Total Adj. Factor
FL1-Int	1.00	1.201	1.201
FL1-Ext	2.00	1.201	2.403
FL2-Int	1.00	1.201	1.201
FL2-Ext	2.00	1.201	2.403
FL3-Int	1.00	1.201	1.201
FL3-Ext	2.00	1.201	2.403

The final nonlinear joint strain curves for the beam-column joints of the test frame are determined using the modified strain and force data constructed using the proposed procedure. The force-strain curves are as presented in Figure 7.21 to Figure 7.23.

The proposed joint strain data presented in the related figures are then multiplied by the effective joint depth (d), defined as the distance between the centroid of the tension reinforcement and outermost compression fiber of the beam. Moment arm determination is previously explained in section 6.2.1.

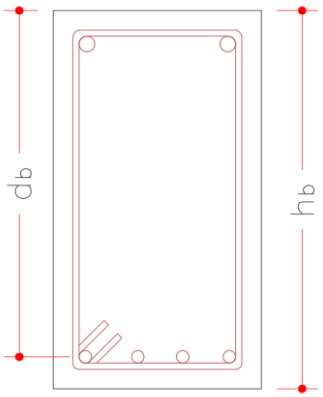
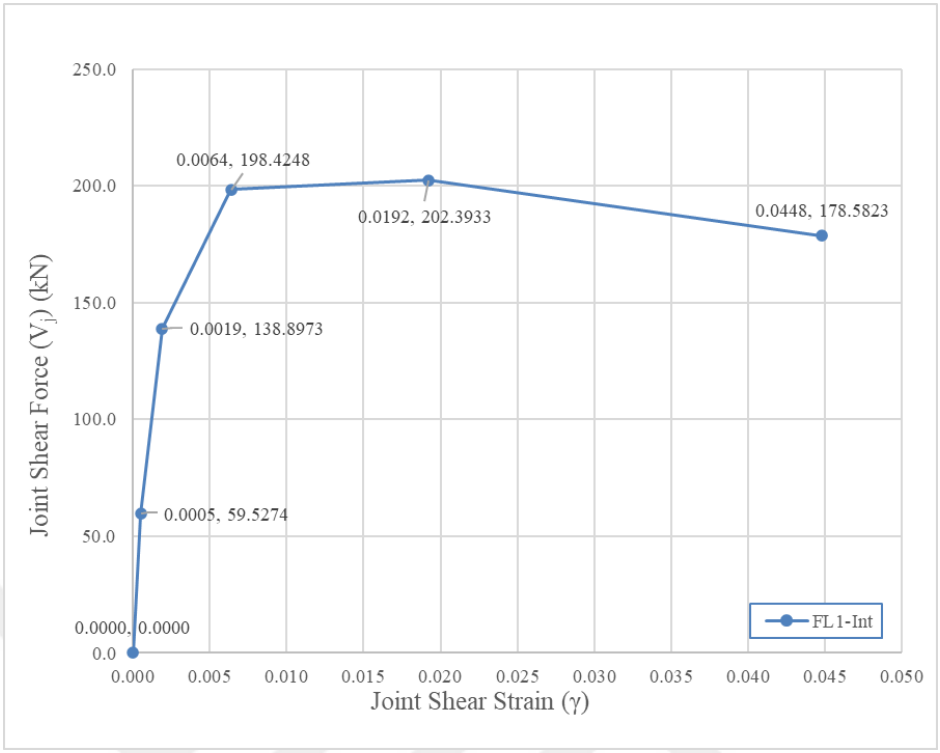


Figure 7.20. Considered Moment Arm in Moment-Rotation Calculations



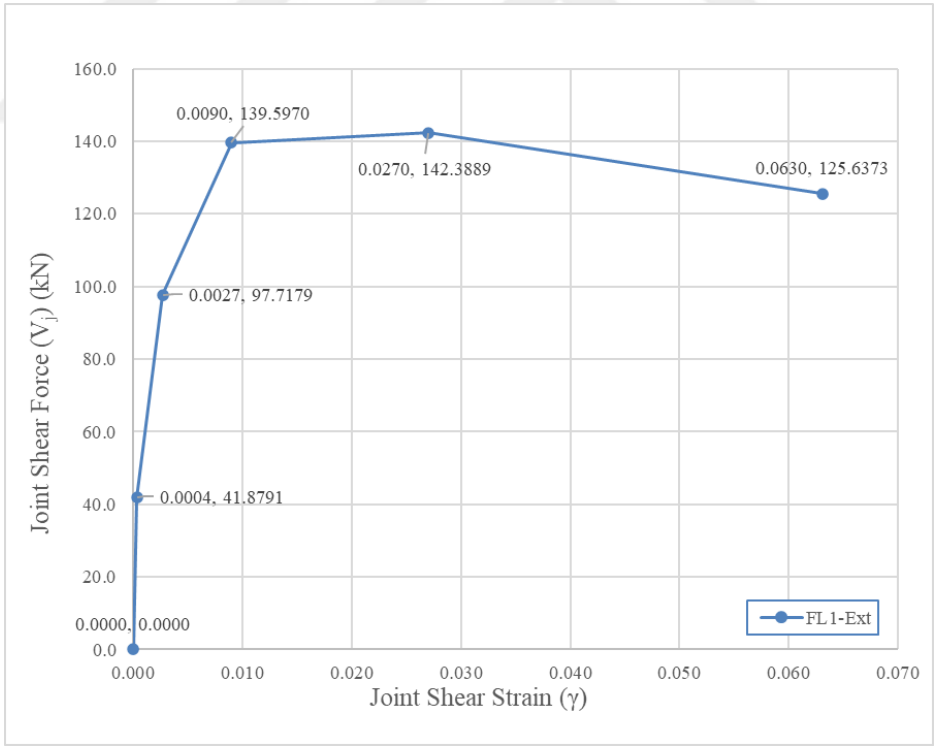
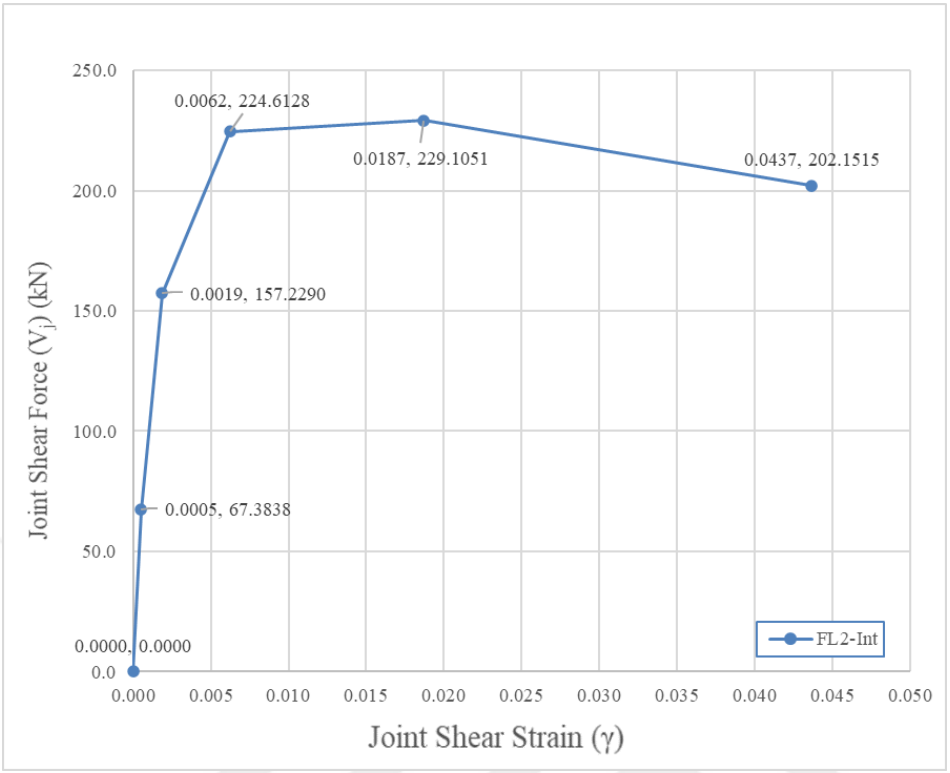


Figure 7.21. Joint Shear Force – Shear Strain Curves, Floor 1 Joints



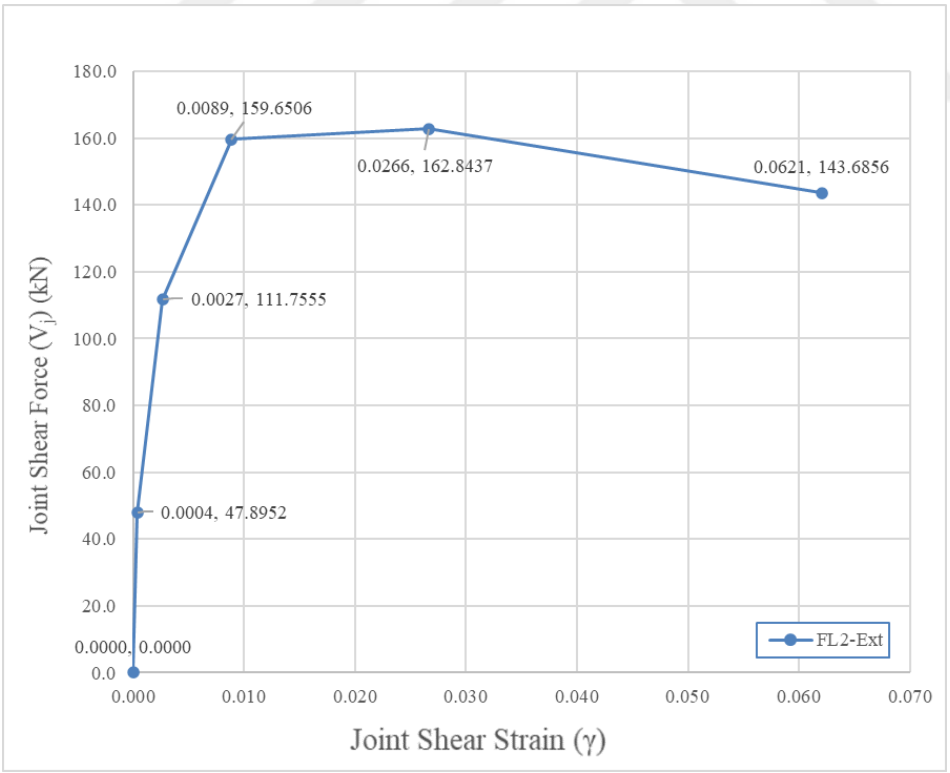
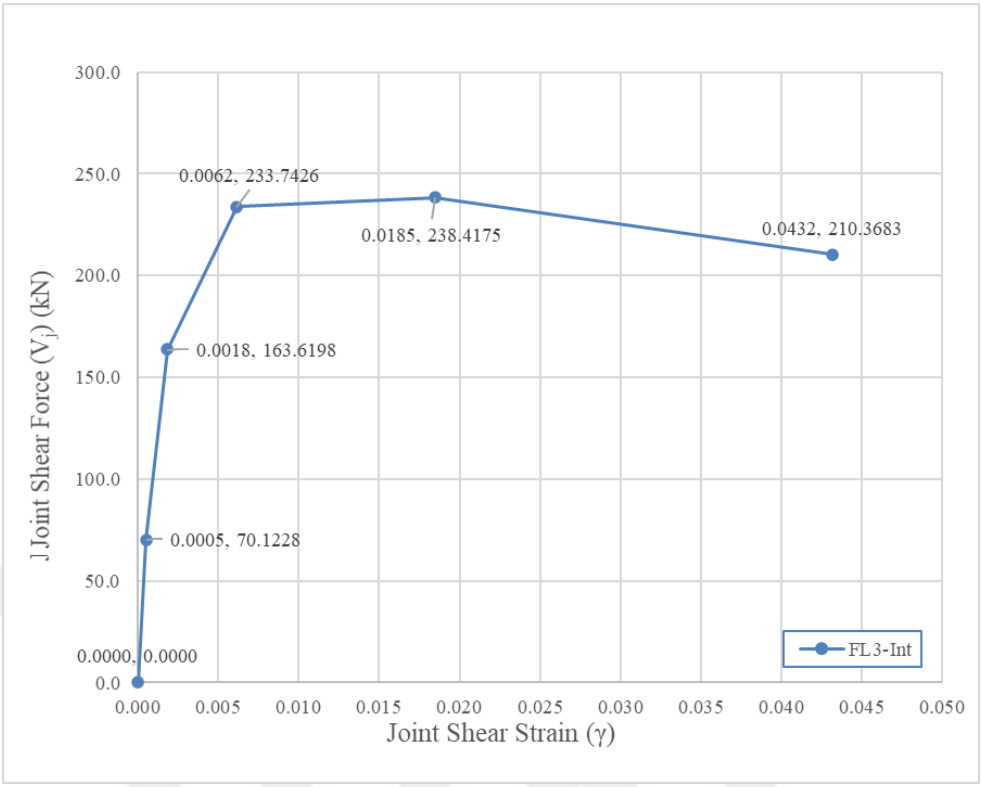


Figure 7.22. Joint Shear Force – Shear Strain Curves, Floor 2 Joints



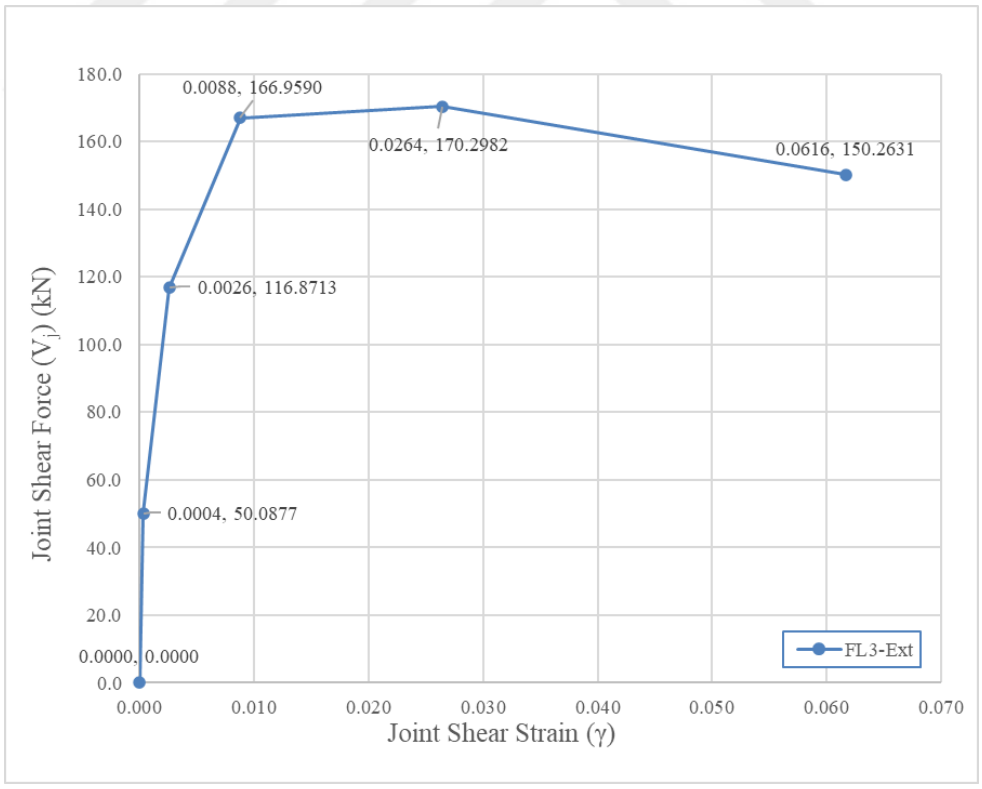


Figure 7.23. Joint Shear Force – Shear Strain Curves, Floor 3 Joints

7.3.3 Loads Applied to the Structure

Loads applied to the structure are classified into 5 load patterns, 2 of which are used to define the vertical loads on the structure and the rest are used to identify the displacements implied at each floor level. The load patterns are identified as DEAD, SDEAD (representing superimposed dead load), UD_F1 to UD_F3 (representing unit displacements applied at each floor level).

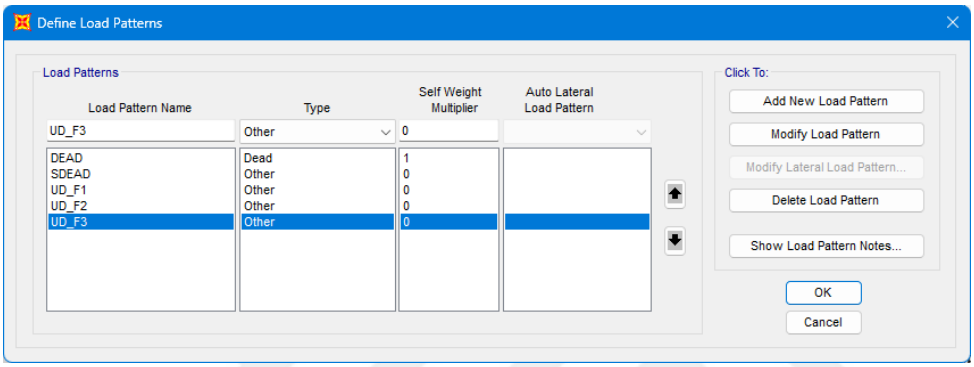


Figure 7.24. Load Pattern Definitions for the Model

DEAD : Load pattern including the self-weight of the structure, defined as material unit weight.

SDEAD : Superimposed dead load pattern to account for the weight of steel blocks on the frame, the magnitudes of which are provided in Figure 7.25.

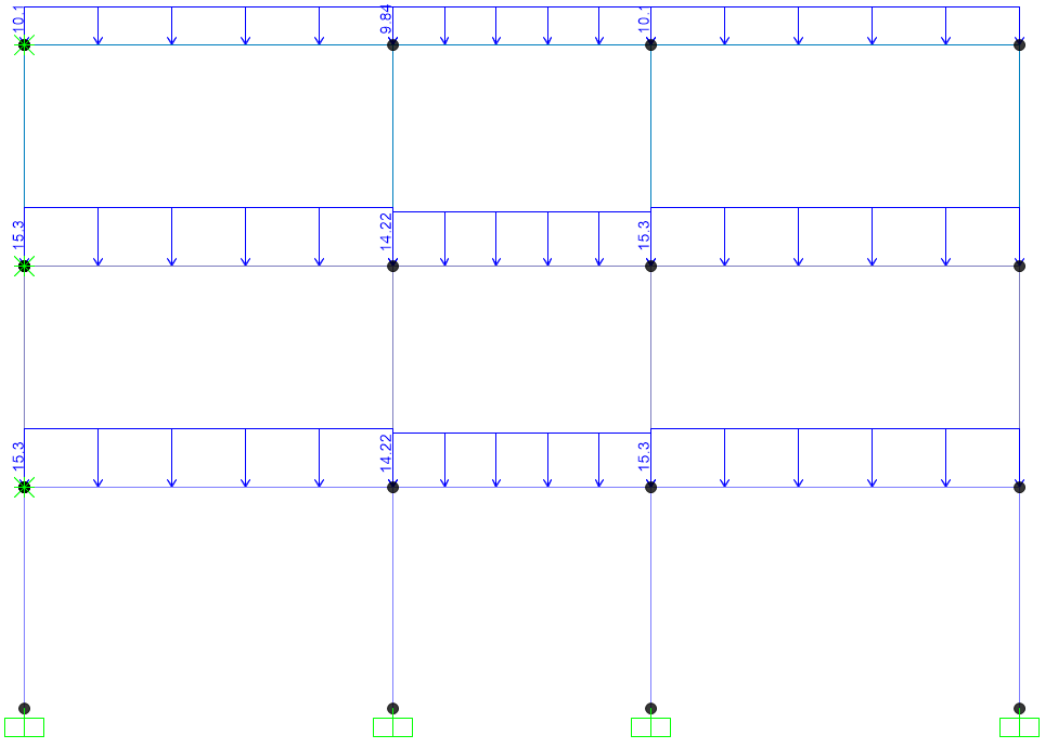


Figure 7.25. Superimposed Dead Loads on the Structure

UD_F1 : Unit displacement defined as 1.0 mm at floor 1.

UD_F2 : Unit displacement defined as 1.0 mm at floor 2.

UD_F3 : Unit displacement defined as 1.0 mm at floor 3.

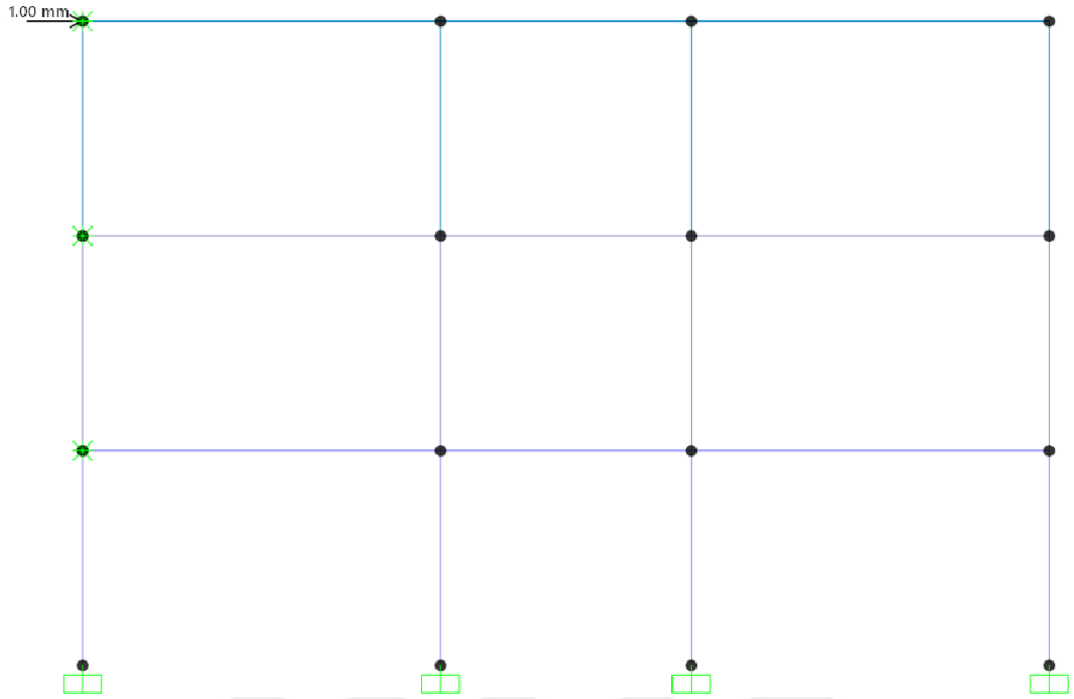


Figure 7.26. Unit Displacement Assigned at Floor 3

The assigned unit displacements at each floor are then multiplied by the displacement time history functions for each floor, in order to impose the seismic displacements created on the structure, as a result of D1, D2, D3 and D4.

Displacement Time History Functions

The displacements exerted to the test setup is determined as a result of solving the dynamic equilibrium of the three degree-of-freedom system, as mentioned in Section 7.2.3.

Each unit displacement defined on the structure is multiplied by 4 displacement time-history functions, to impose the seismic displacements, constituting a total of 12 displacement time histories. A sample function definition is presented in Figure 7.27.

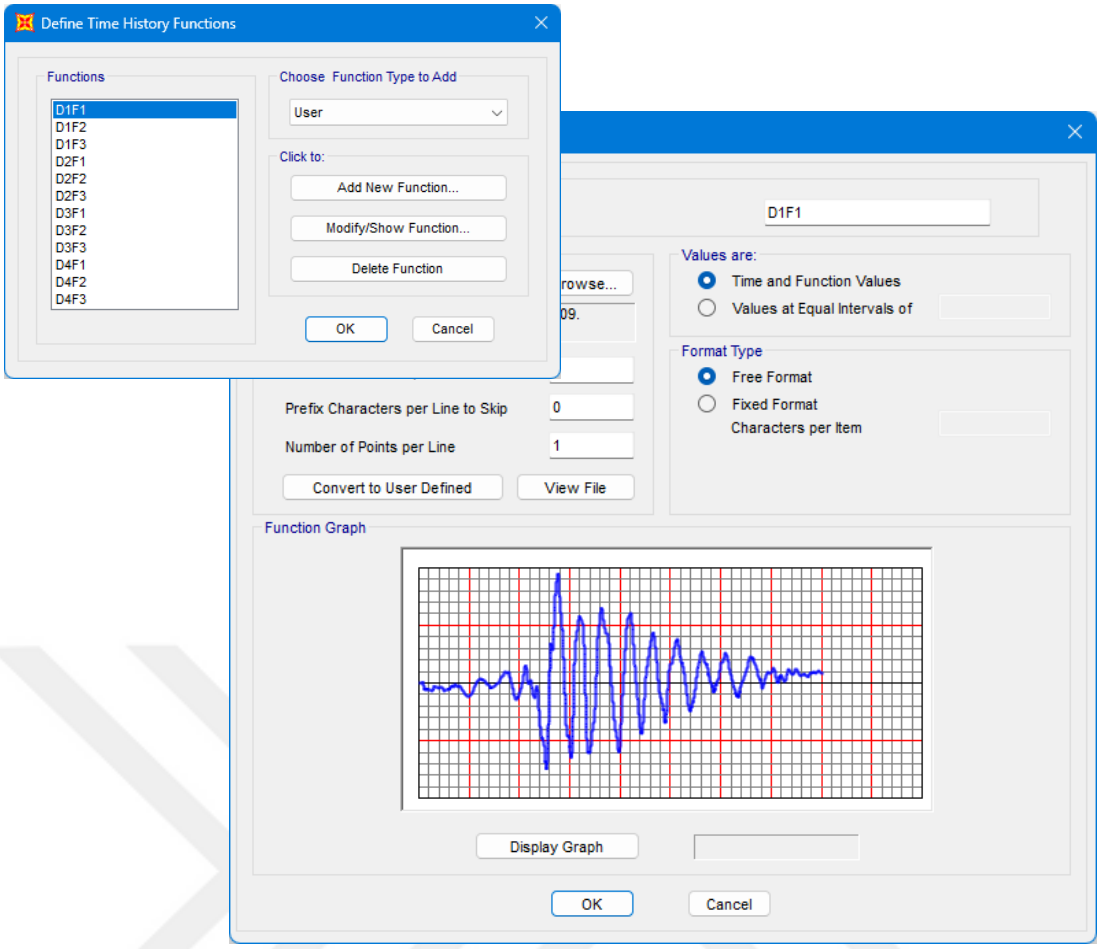


Figure 7.27. Time History Function Application

7.3.4 Description of Nonlinear Time History Load Case

In order to represent the experimental load application, a sequence of nonlinear time history load cases is defined in the model. To define the static conditions where only the gravity loads are effective on the structure, a basic load case in which only the self-weight and superimposed dead loads are active is generated. This load case, which is presented in Figure 7.28, is labeled as “D+SDEAD”.

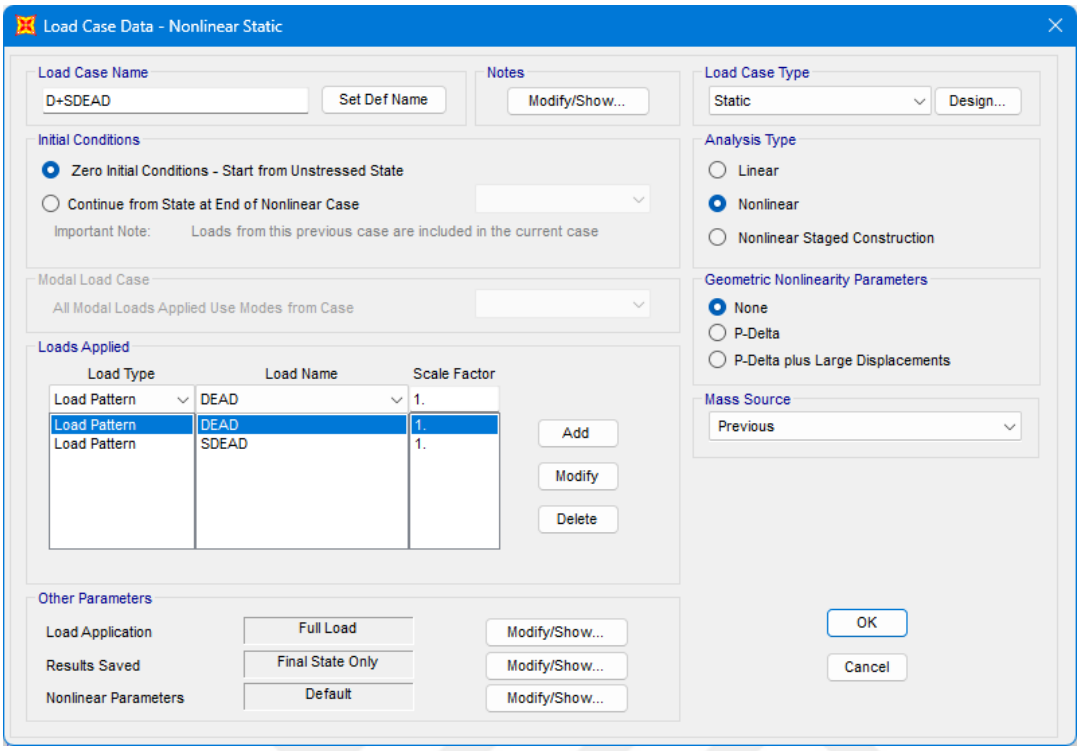


Figure 7.28. Dead Load Case Definition

After the dead load application, a sequence of earthquakes is applied to the structure, namely, D1, D2, D3 and D4, in a stepwise manner following the final conditions of the structure after the prior case. Consequently, the geometrical, material and loading conditions under which the test frame is constructed and experimentally investigated are modeled analytically and the results of the nonlinear time history analysis cases are recorded.

A sample definition of the seismic load case is presented in Figure 7.29.

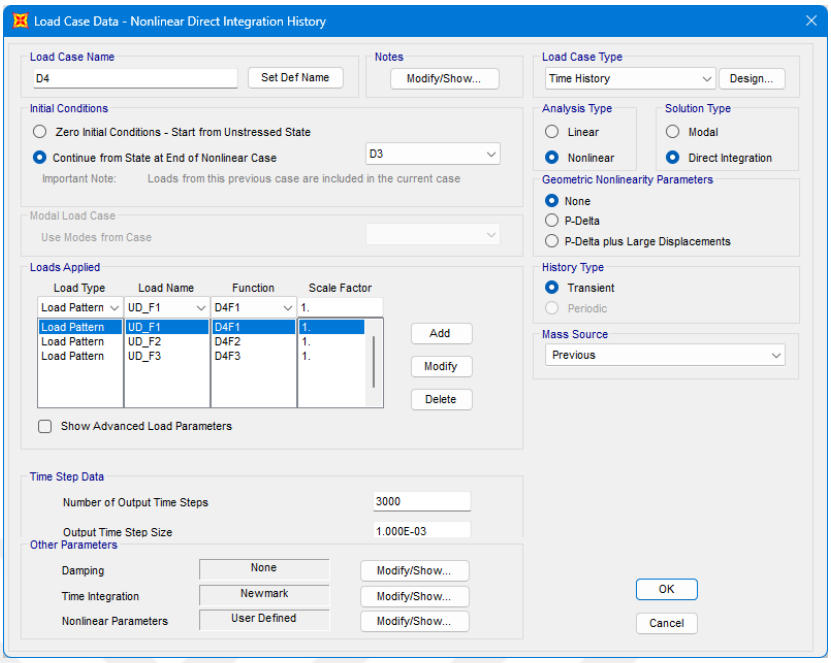


Figure 7.29. Sample Seismic Load Case Definition

Finally, the generated analytical model is evaluated under seismic displacement time histories and the results are compared with the experimental results of the test frame.

In Section 7.4, the comparison of experimental and analytical data is carried out to verify the generated analytical model and the accuracy of the proposed nonlinear joint shear behavior model.

7.4 Verification of Analytical Results with Experimental Data

In this section of the thesis, the analytical results obtained from the nonlinear model representing the test frame will be compared to the experimental results. For this comparison, first the proposed nonlinear behavior models for the interior and exterior beam-column joints are compared to the experimental joint responses. Moreover, the responses of beam plastic hinge regions are compared to the experimental moment-rotation response. Finally, the overall behavior of the structure is compared with the experimental results in terms of lateral load vs. story drift responses of the structure.

7.4.1 Comparison of the Cyclic Joint Response

The analytical responses of the beam-column joints shown in Figure 7.30 are compared with the experimental results considering each earthquake level applied to the structure. In the figures below, the comparisons are presented separately for each earthquake level. First, the responses of interior beam-column joint are presented in Figure 7.32 to Figure 7.34, then the exterior in Figure 7.35 to Figure 7.38.

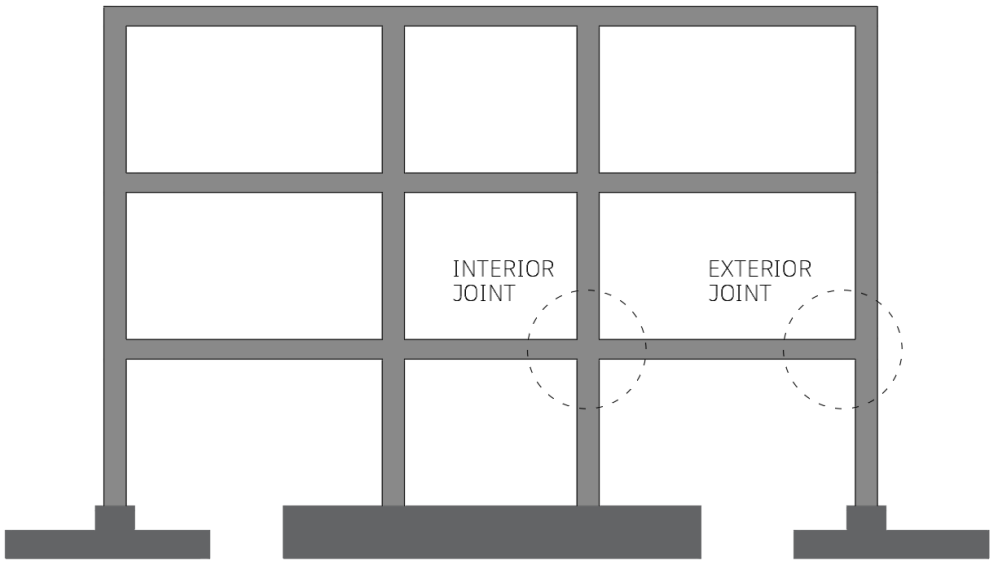


Figure 7.30. Selected Interior and Exterior Joints for Verification

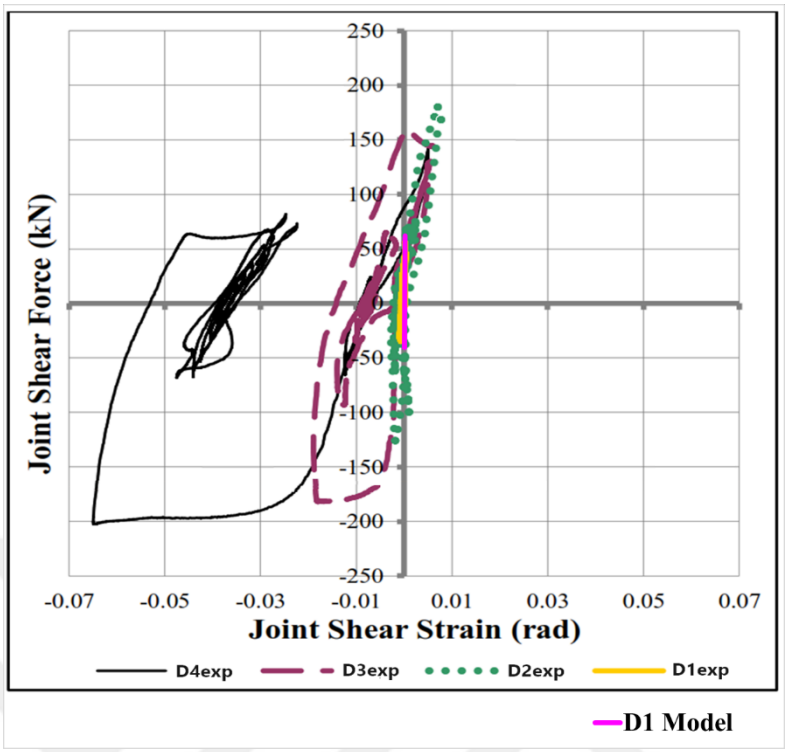


Figure 7.31. Interior Joint, D1 Response Comparison

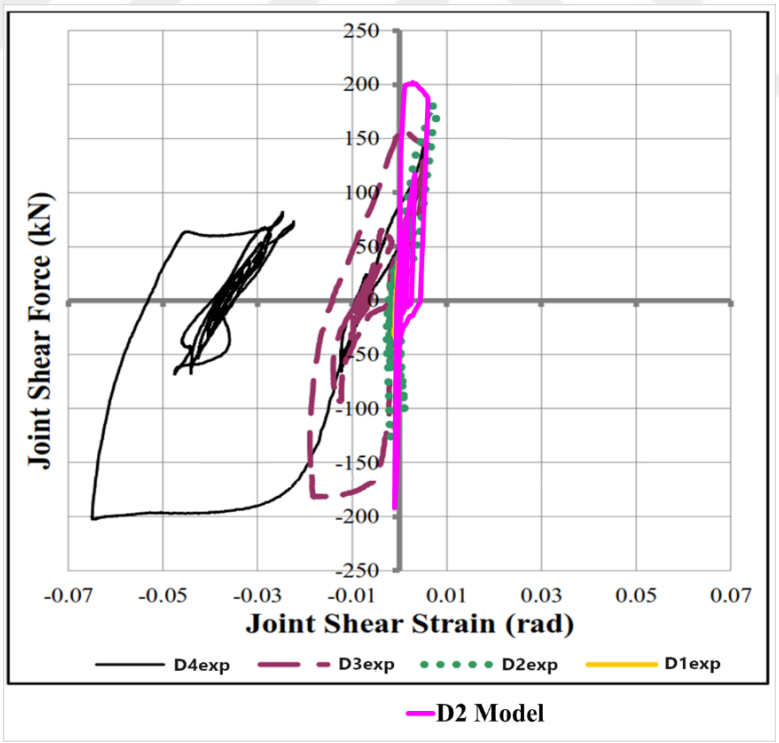


Figure 7.32. Interior Joint, D2 Response Comparison

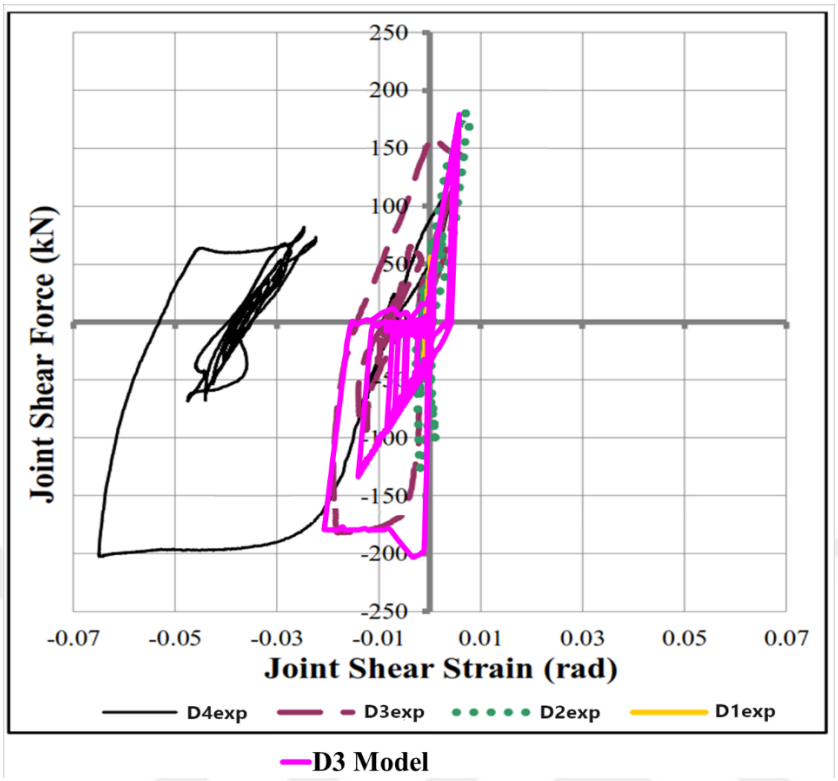


Figure 7.33. Interior Joint, D3 Response Comparison

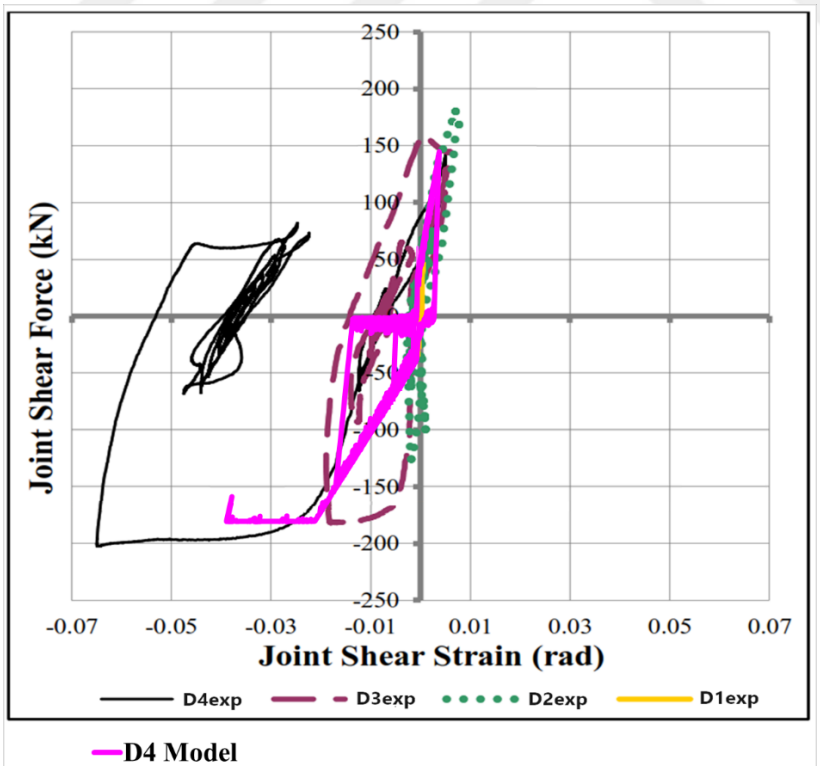


Figure 7.34. Interior Joint, D4 Response Comparison

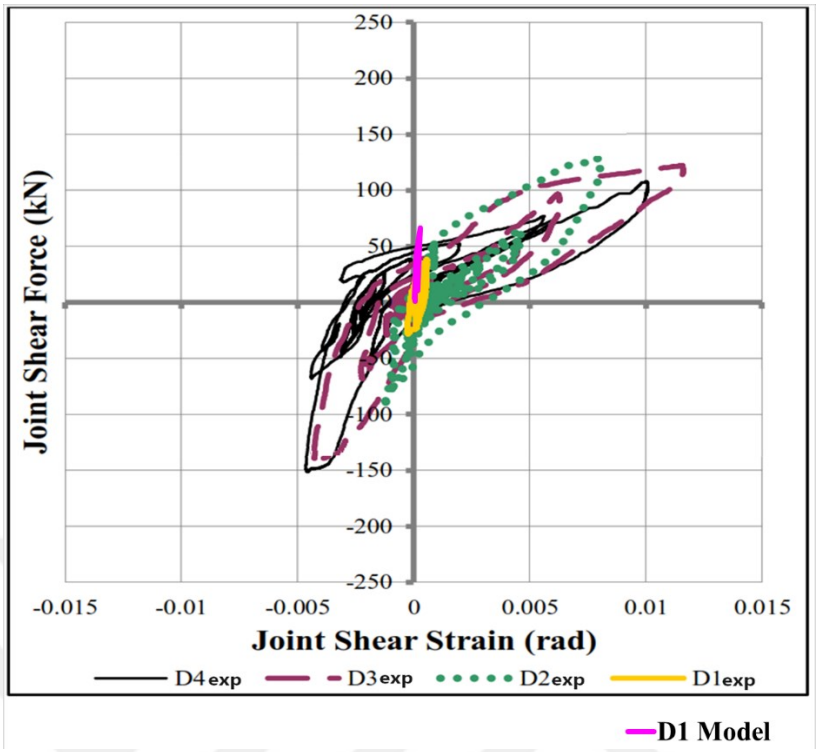


Figure 7.35. Exterior Joint, D1 Response Comparison

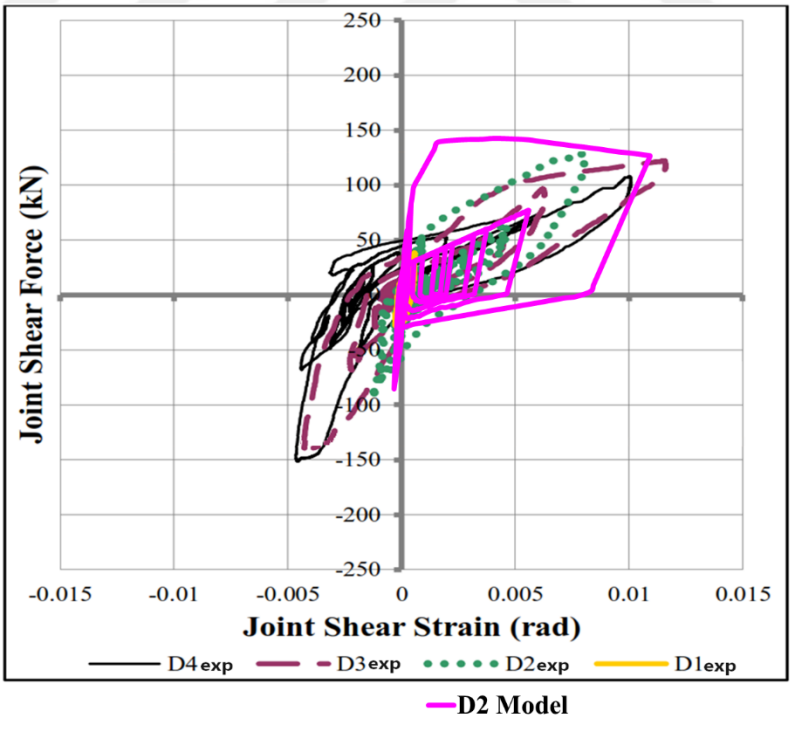


Figure 7.36. Exterior Joint, D2 Response Comparison

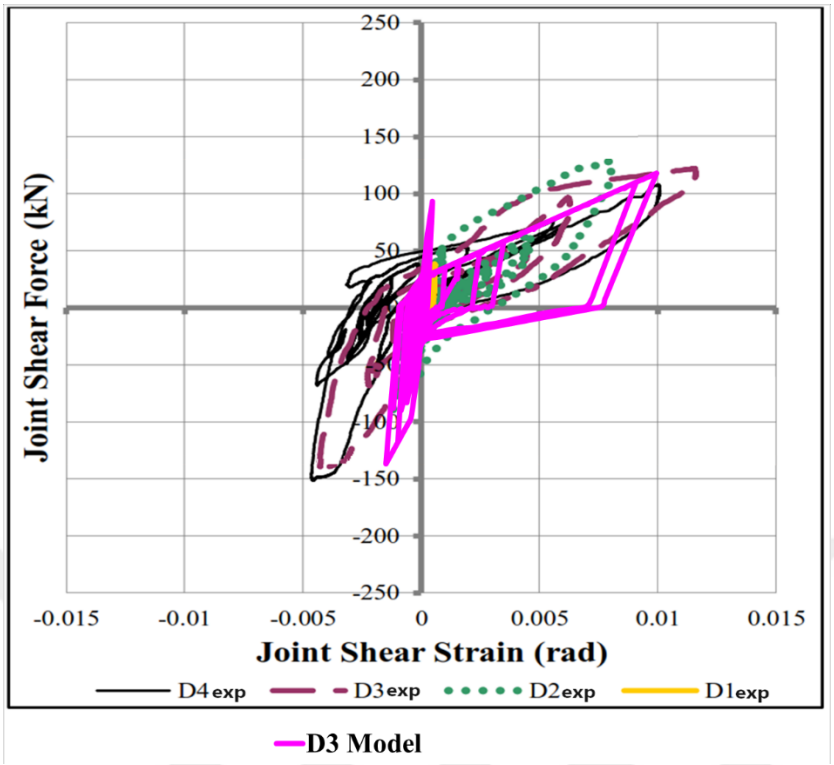


Figure 7.37. Exterior Joint, D3 Response Comparison

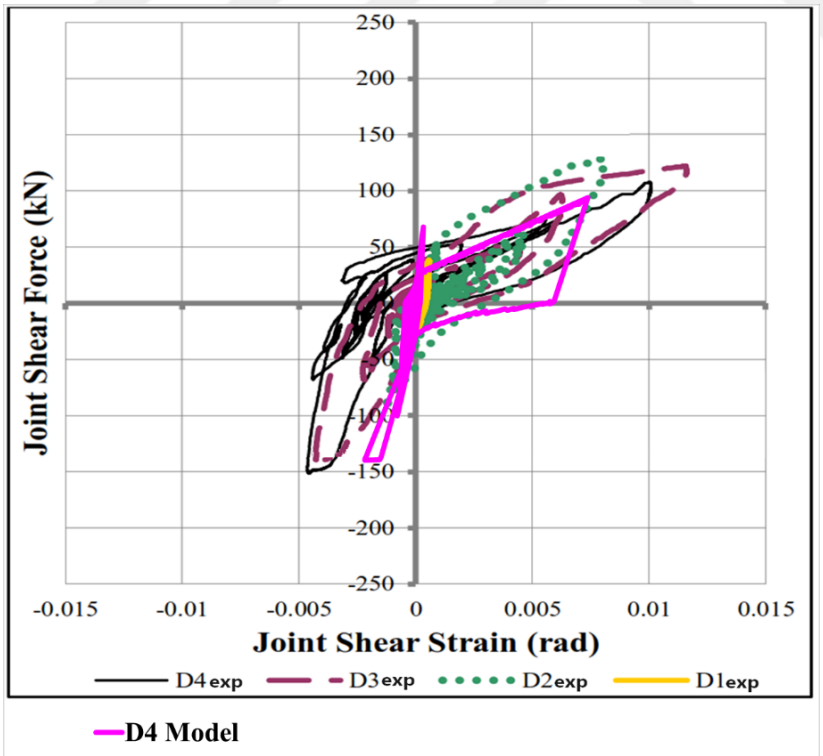


Figure 7.38. Exterior Joint, D4 Response Comparison

In the assessment of the analytical joint shear response, it can be observed that a joint shear failure mechanism akin to that of the experimental frame is successfully attained. The joint shear force responses of the model adequately capture the experimental hysteresis curves. Furthermore, the behavior of both the interior and exterior beam-column joints aligns parallel to that of the experimental frame across all four earthquake levels, as individually assessed in the figures.

7.4.2 Comparison of the Beam Moment – Rotation Response

In addition to the beam-column joint response, the beam response is one of the key analytical results that is monitored. The evaluation of the moment response of the plastic hinge defined at the beam end is significant in the adequate determination of the damage level of the structure. Most structural design codes define limit for beam end rotations and relate them to the level of damage. Additionally, the range of the beam rotations is significantly affected by the behavior of the beam-column joint, therefore a reliable joint model is required to accurately evaluate the structural behavior.

In this section, beam moment-rotation response of the structure is evaluated in the light of experimental results.

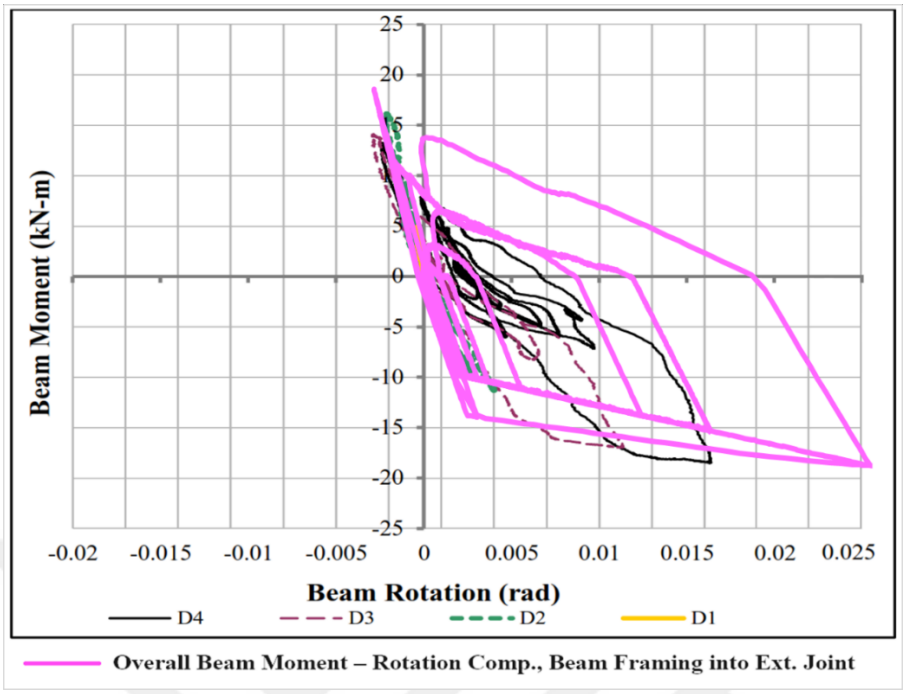


Figure 7.39. Beam Moment – Rotation Comparison, Exterior Beam Framing into Exterior Joint

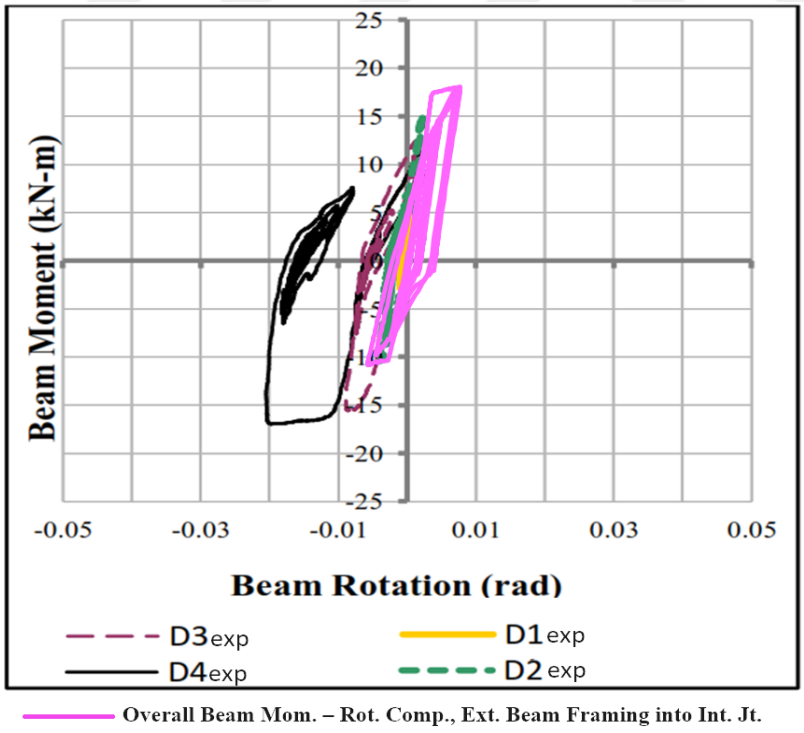


Figure 7.40. Beam Moment – Rotation Comparison, Exterior Beam Framing into Interior Joint

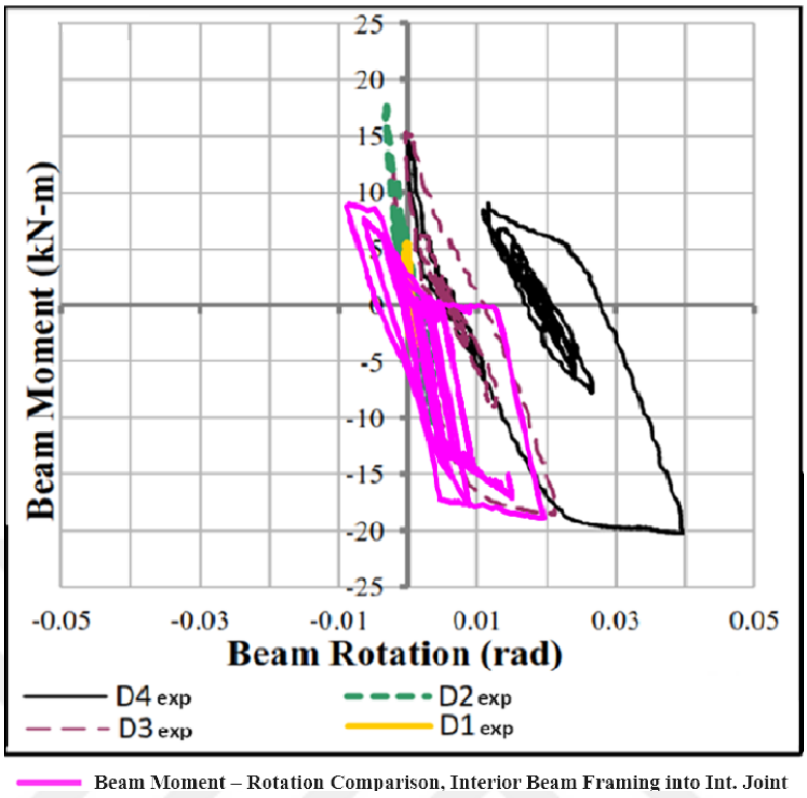


Figure 7.41. Beam Moment – Rotation Comparison, Interior Beam Framing into Interior Joint

The evaluation of the beam moment-rotation responses yield similar results to joint shear force - shear strain comparisons. The response of the beams is in compatibility with the experimental results.

In the next subsection, the overall response of the structure is evaluated with the comparison of experimental and analytical lateral load vs story drift response.

7.4.3 Comparison of the Lateral Load – Story Drift Response

In this part of the thesis, the response of overall structure is evaluated considering the lateral load-story drift response of the structure. In Figure 7.42 to Figure 7.57, the lateral load vs story drift response of the analytical model is compared with the experimental results considering interstory drifts and the roof drift. These figures reveal that for all earthquake magnitudes, the behavior of the structure is predicted by the analytical model with significant accuracy.

Comparison for Story 1

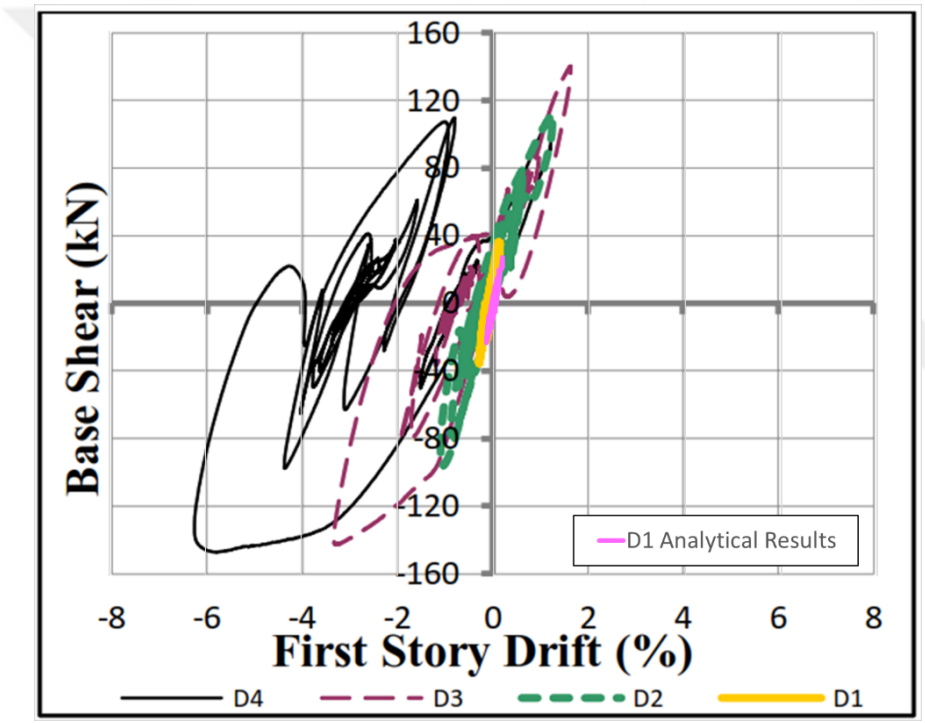


Figure 7.42. Story 1, D1 Lateral Load – Interstory Drift Response

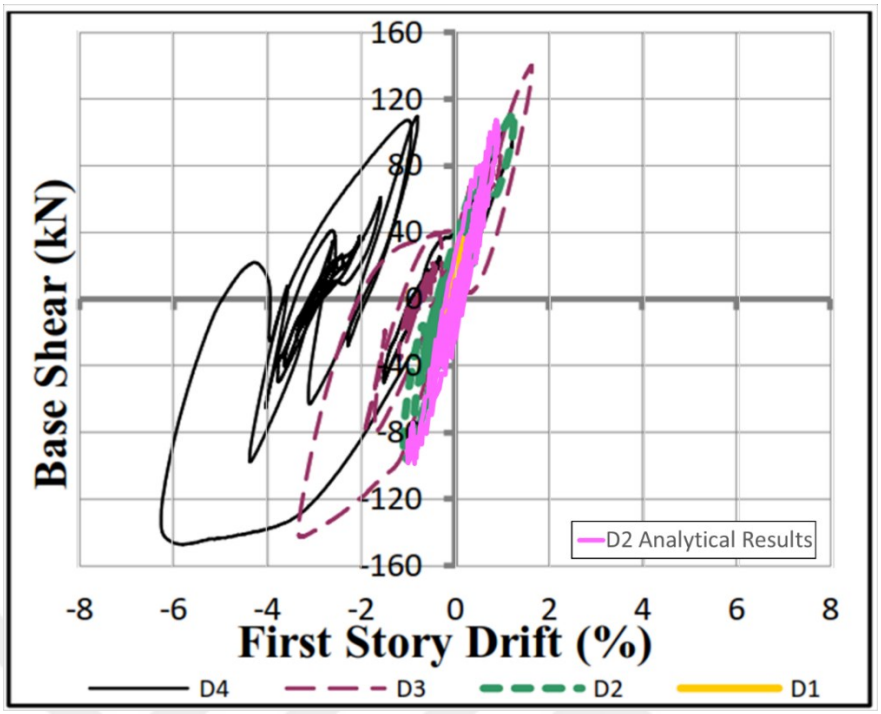


Figure 7.43. Story 1, D2 Lateral Load – Interstory Drift Response

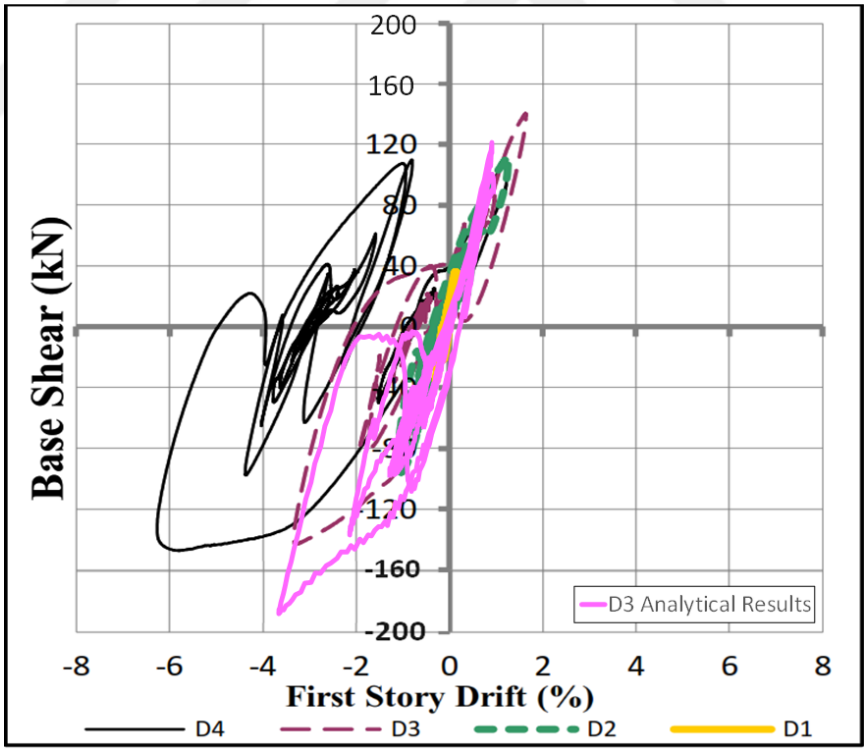


Figure 7.44. Story 1, D3 Lateral Load – Interstory Drift Response

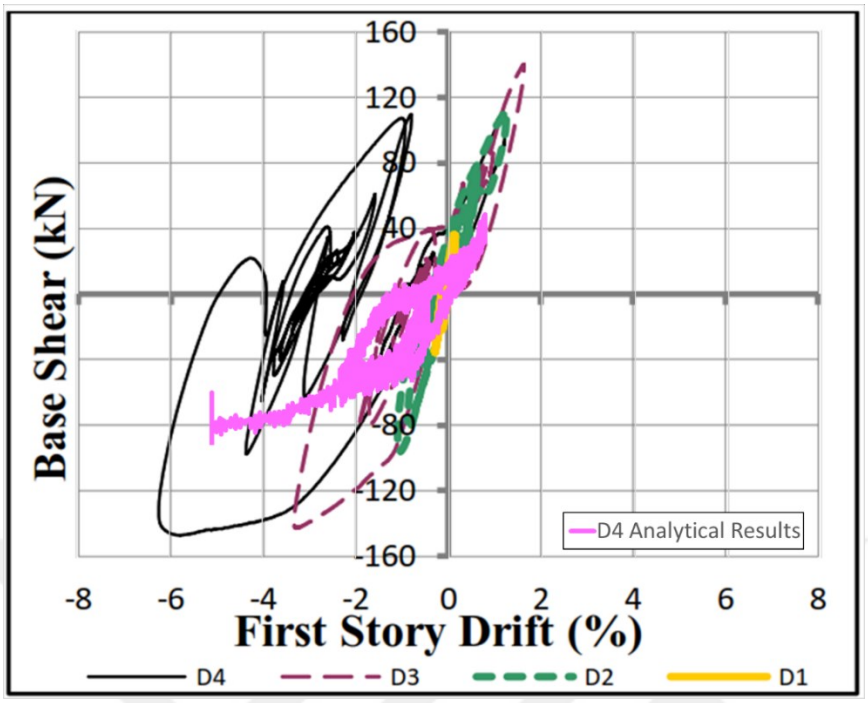


Figure 7.45. Story 1, D4 Lateral Load – Interstory Drift Response

Comparison for Story 2

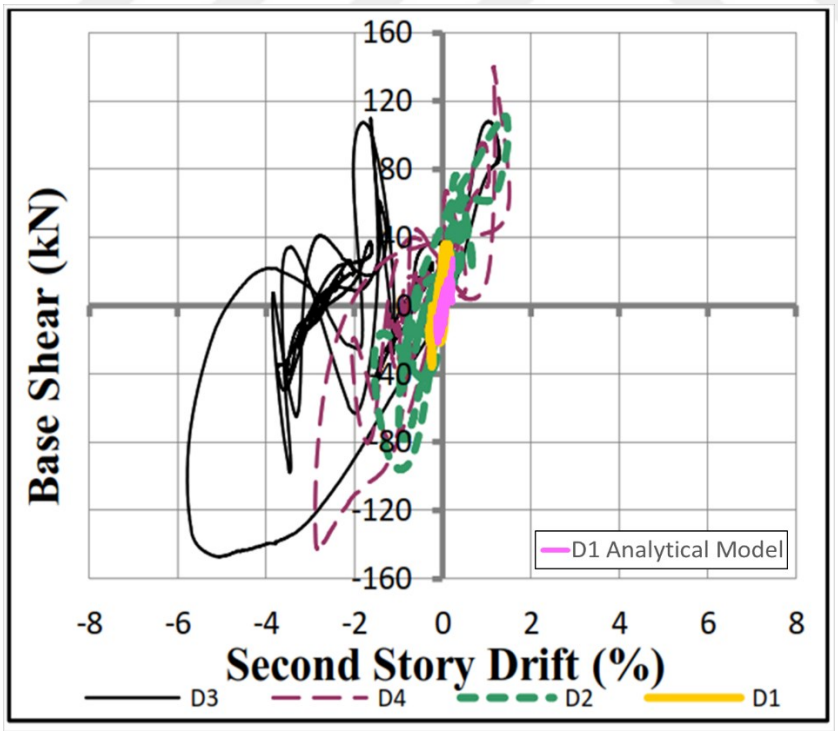


Figure 7.46. Story 2, D1 Lateral Load – Interstory Drift Response

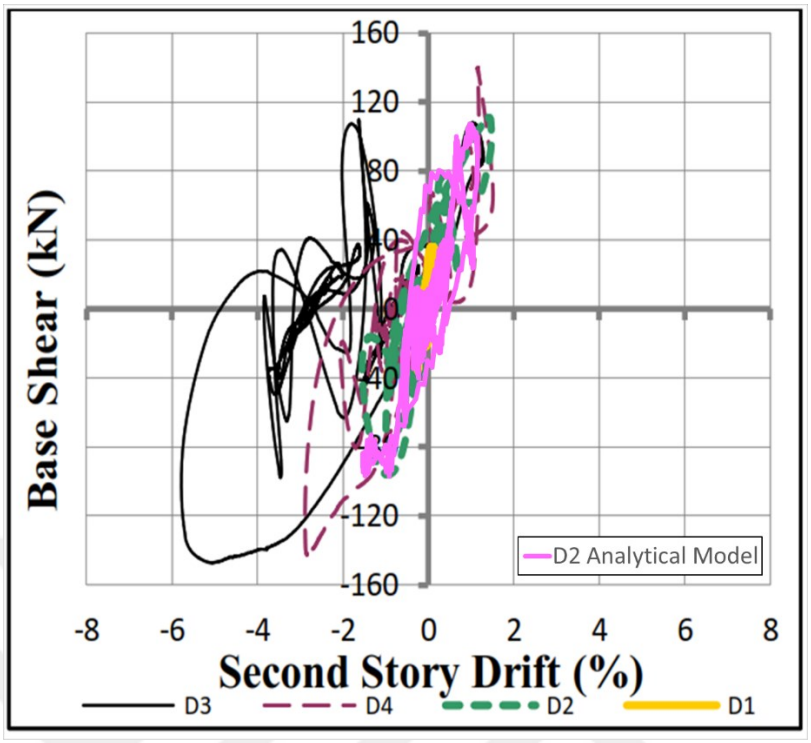


Figure 7.47. Story 2, D2 Lateral Load – Interstory Drift Response

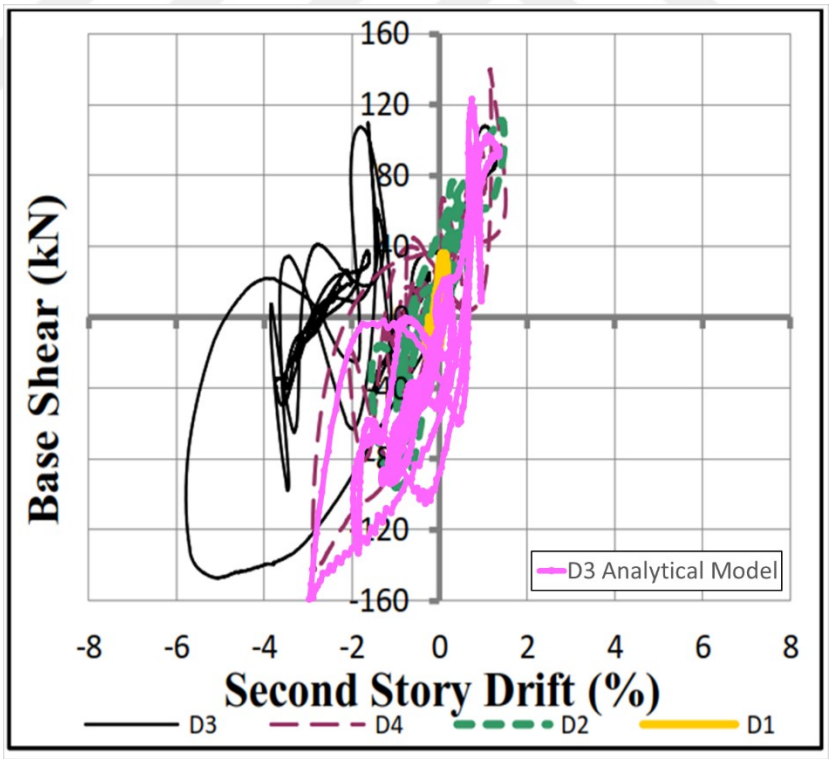


Figure 7.48. Story 2, D3 Lateral Load – Interstory Drift Response

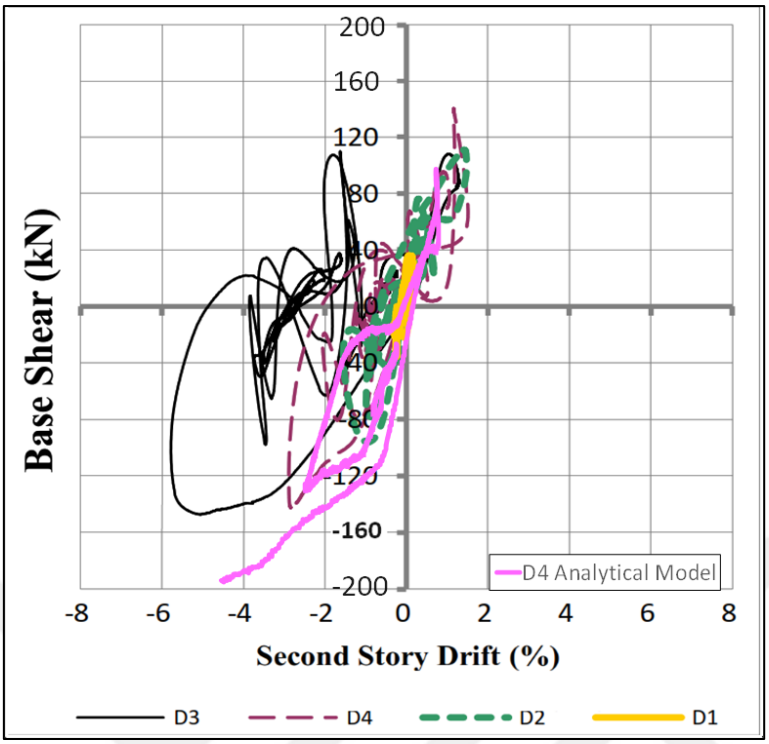


Figure 7.49. Story 2, D4 Lateral Load – Interstory Drift Response

Comparison for Story 3

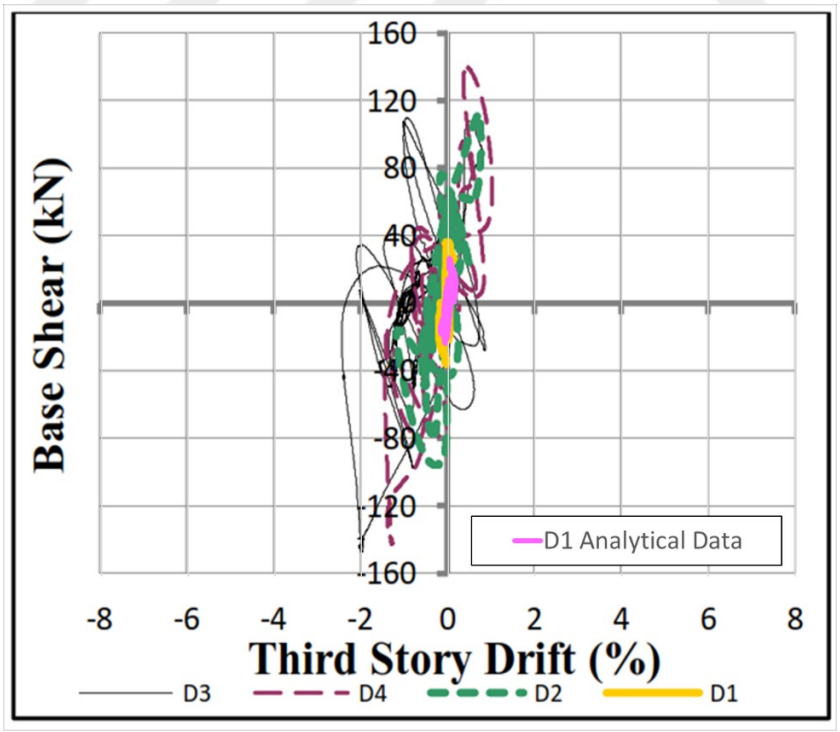


Figure 7.50. Story 3, D1 Lateral Load – Interstory Drift Response

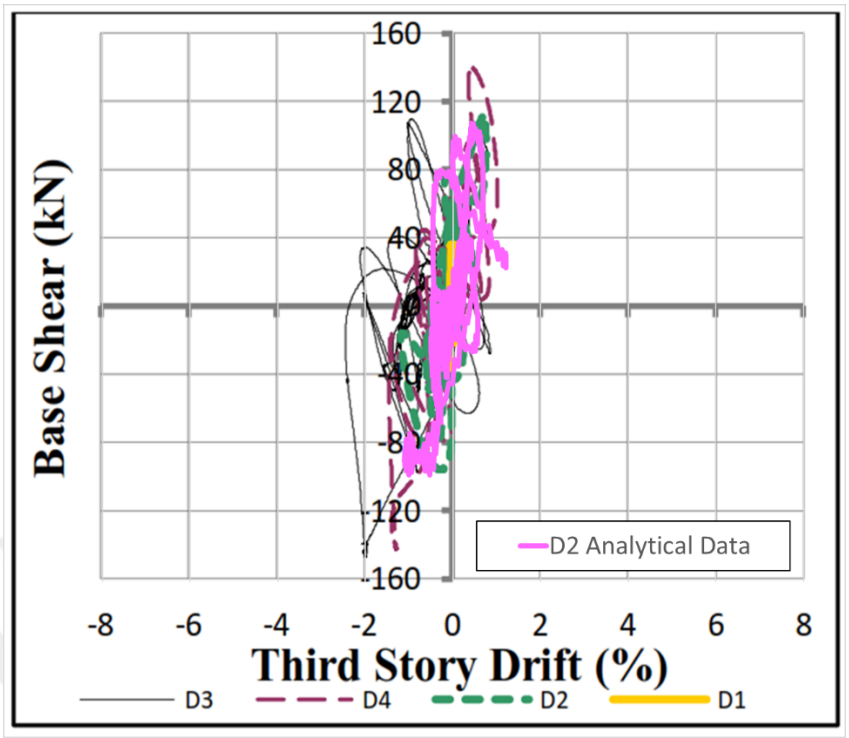


Figure 7.51. Story 3, D2 Lateral Load – Interstory Drift Response

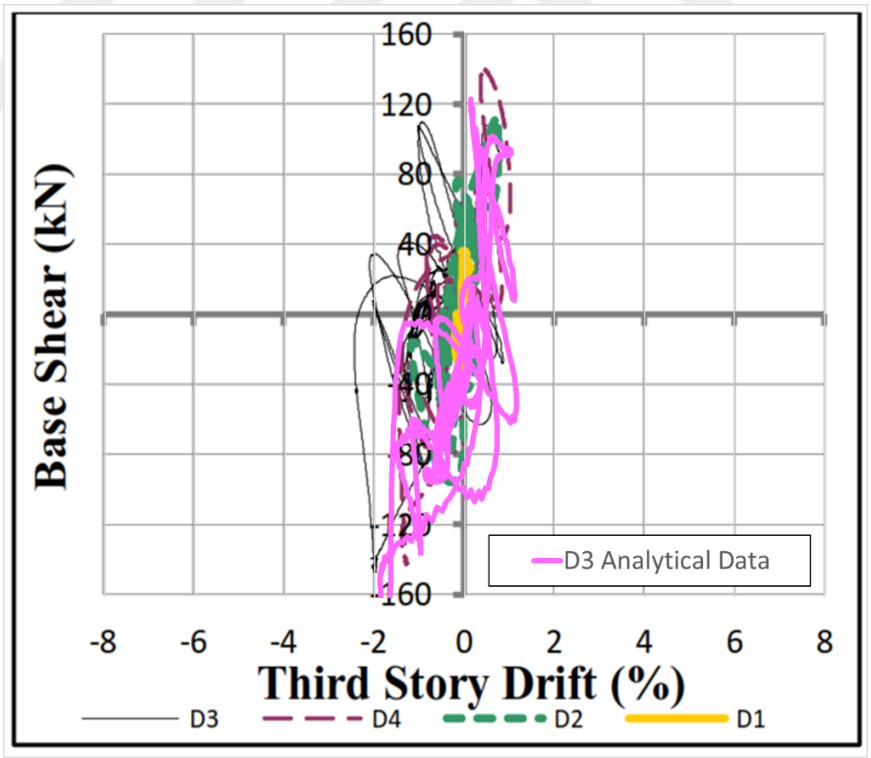


Figure 7.52. Story 3, D3 Lateral Load – Interstory Drift Response

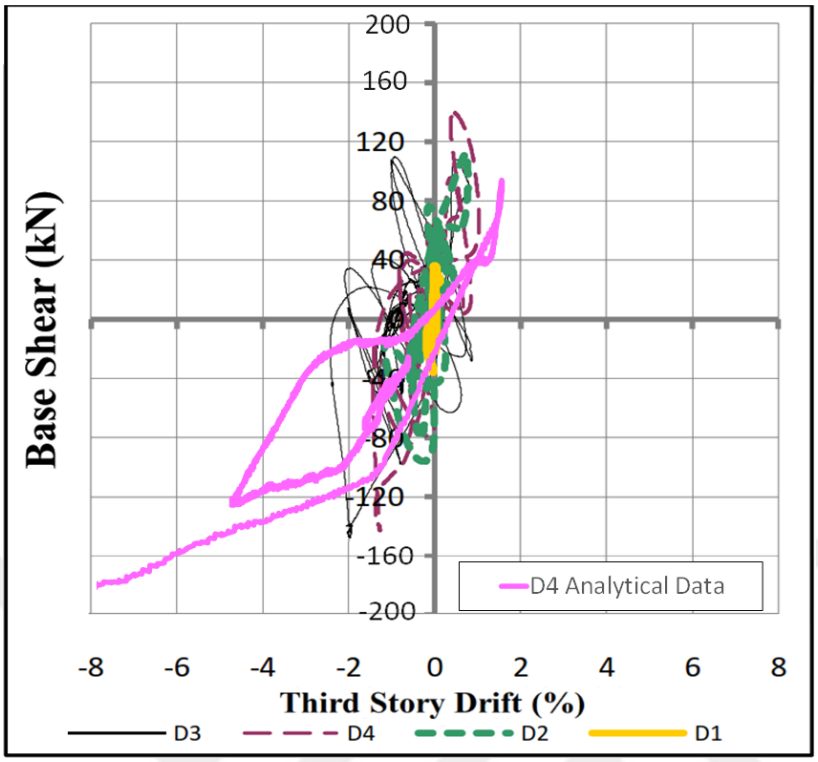


Figure 7.53. Story 3, D4 Lateral Load – Interstory Drift Response

Comparison for Roof Drift

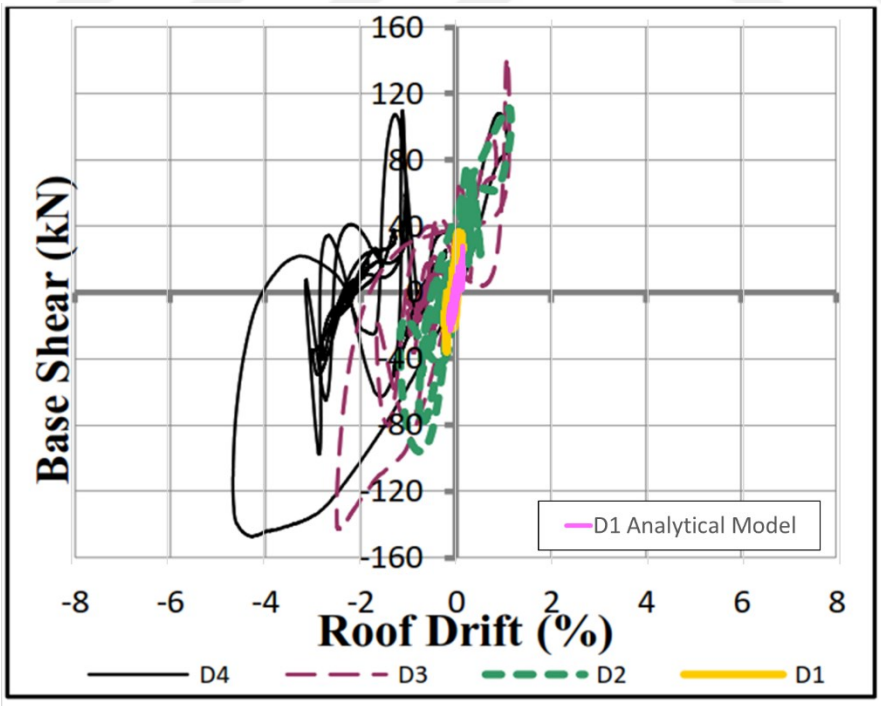


Figure 7.54. Roof Level, D1 Lateral Load – Interstory Drift Response

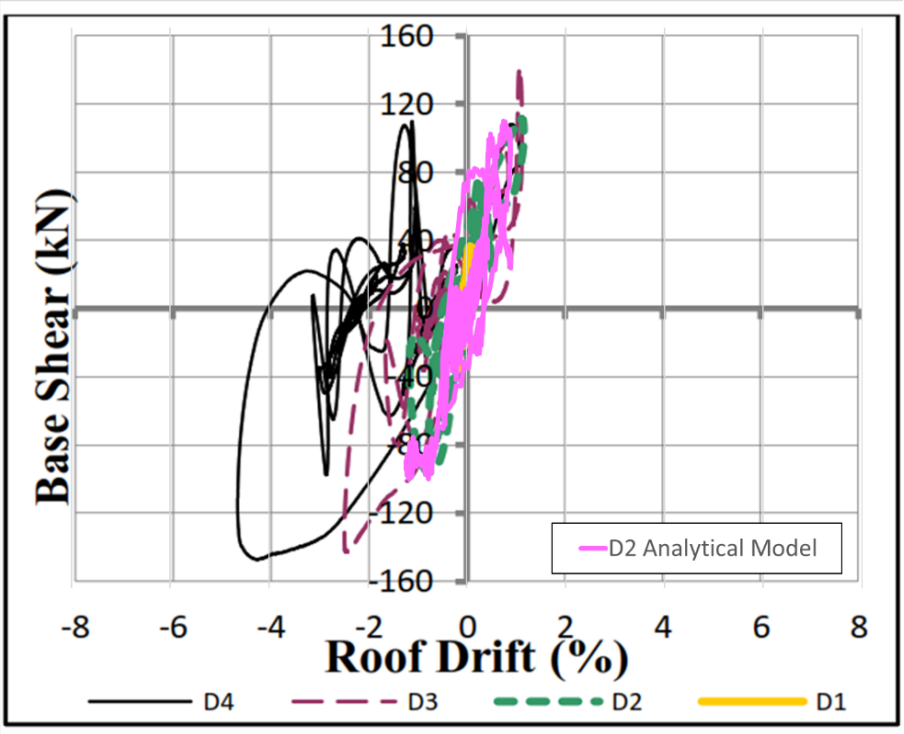


Figure 7.55. Roof Level, D2 Lateral Load – Roof Drift Response

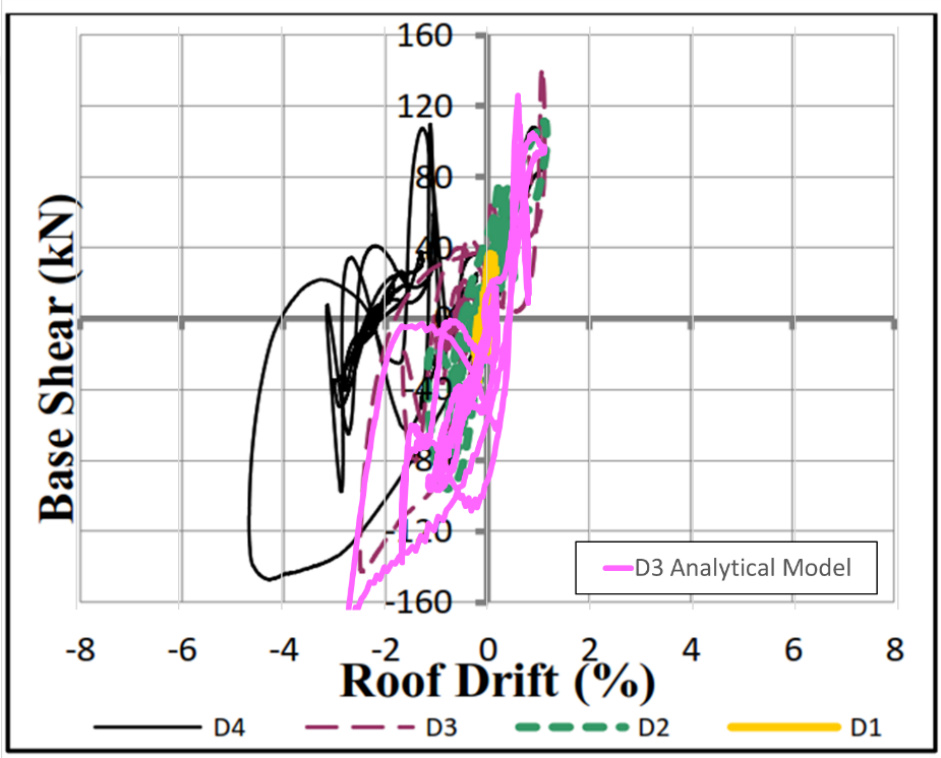


Figure 7.56. Roof Level, D3 Lateral Load – Roof Drift Response

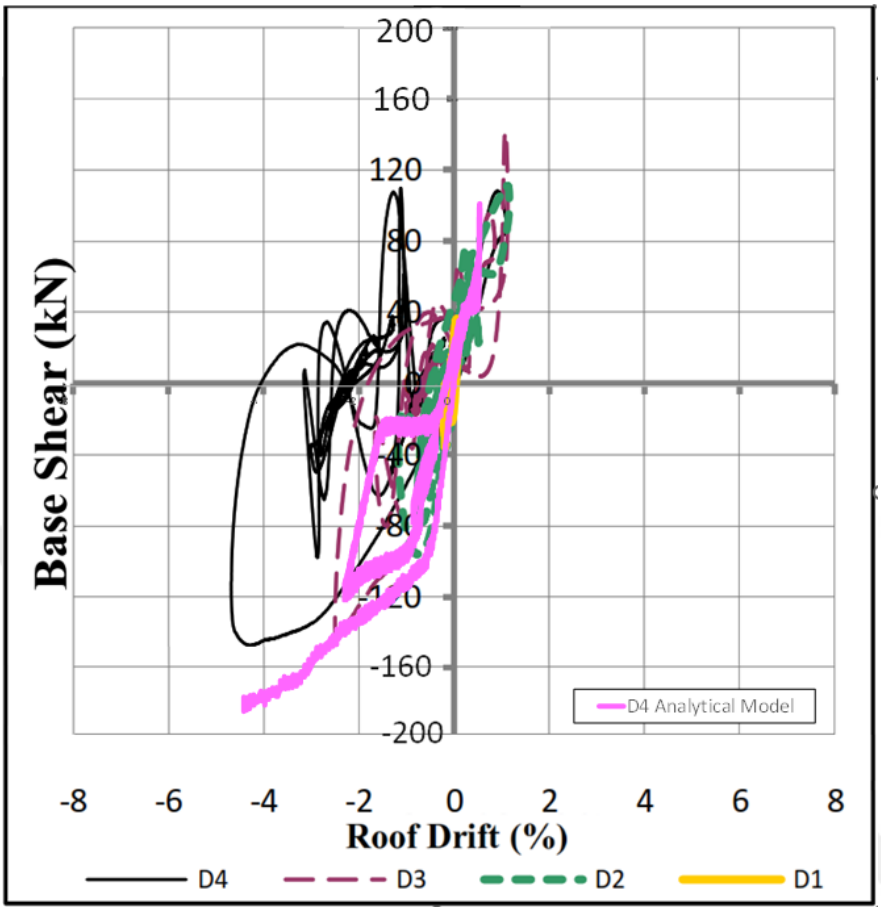


Figure 7.57. Roof Level, D4 Lateral Load – Roof Drift Response

7.4.4 Evaluation of Analytical Model

From the results presented in the previous sections comparing the joint response, beam moment-rotation relationship and the overall structural behavior by means of lateral load vs story drift response obtained from the analytical model with the experimental results, it is observed that the proposed model yields significantly accurate estimations. Utilization of the model leads not only to the adequate prediction of the joint shear response, but also the overall structural response.

In the following section, the analytical behavior is compared to a model generated with rigid joint assumption, without the use of the nonlinear panel zone for the beam-column joints.

7.4.5 Comparison of Rigid Joint Assumption with the Joint Model

In this section, the overall structural behavior obtained from the use of nonlinear panel zone, is compared to rigid joint assumption generated as a nonlinear model with only rigid end zones (REZ), without the implementation of the joint model, which is the common practice in structural design industry.

In Figure 7.58 to Figure 7.61, the lateral load vs roof displacement response of both models is presented.

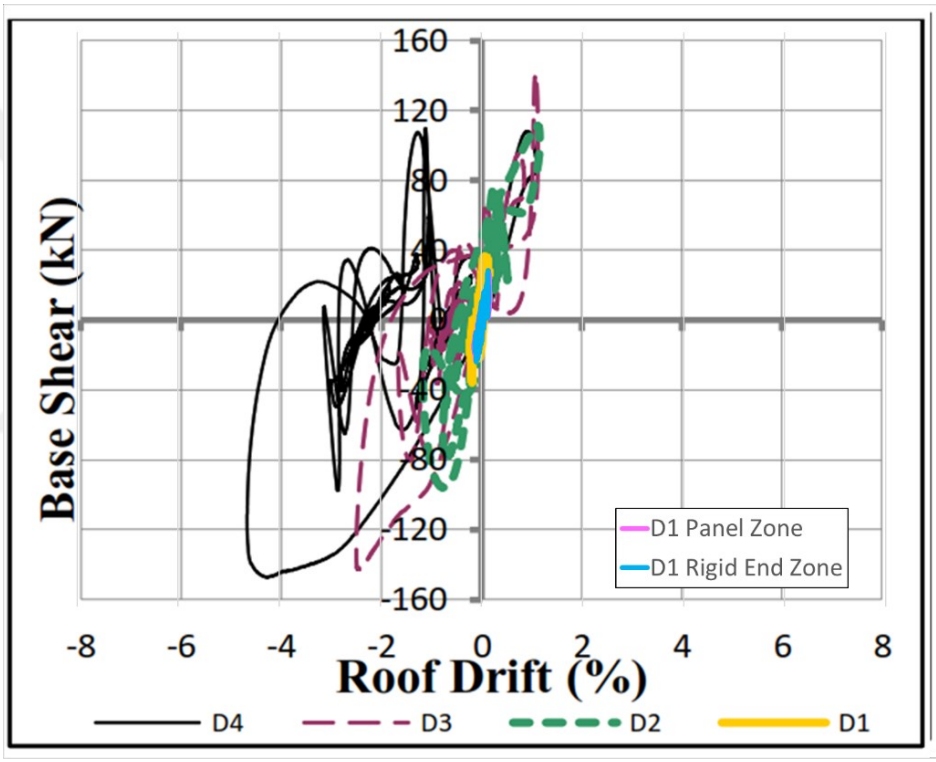


Figure 7.58. Joint Model vs Rigid Joint Assumption, D1

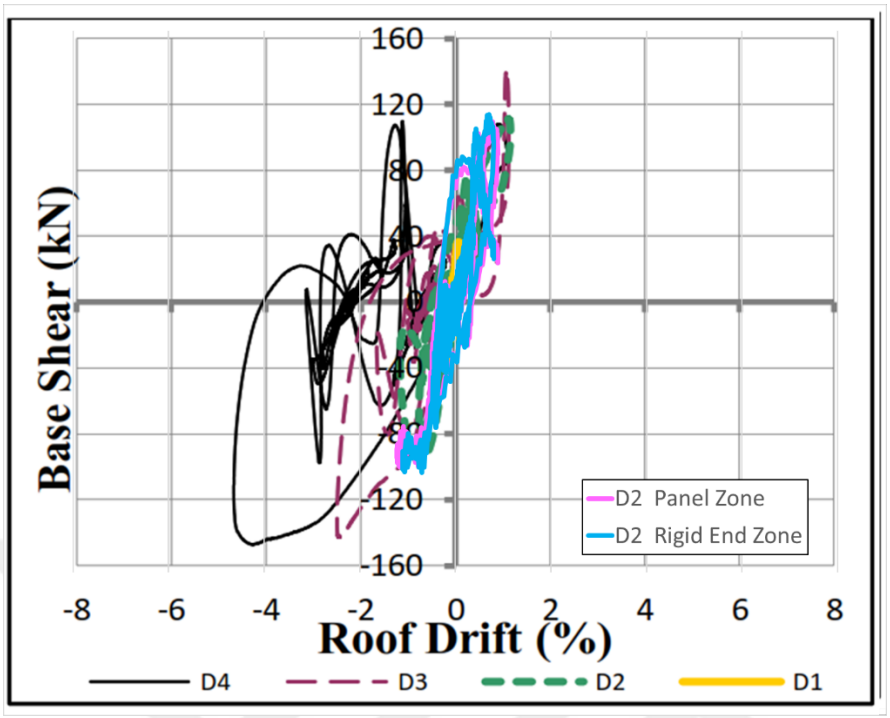


Figure 7.59. Joint Model vs Rigid Joint Assumption, D2

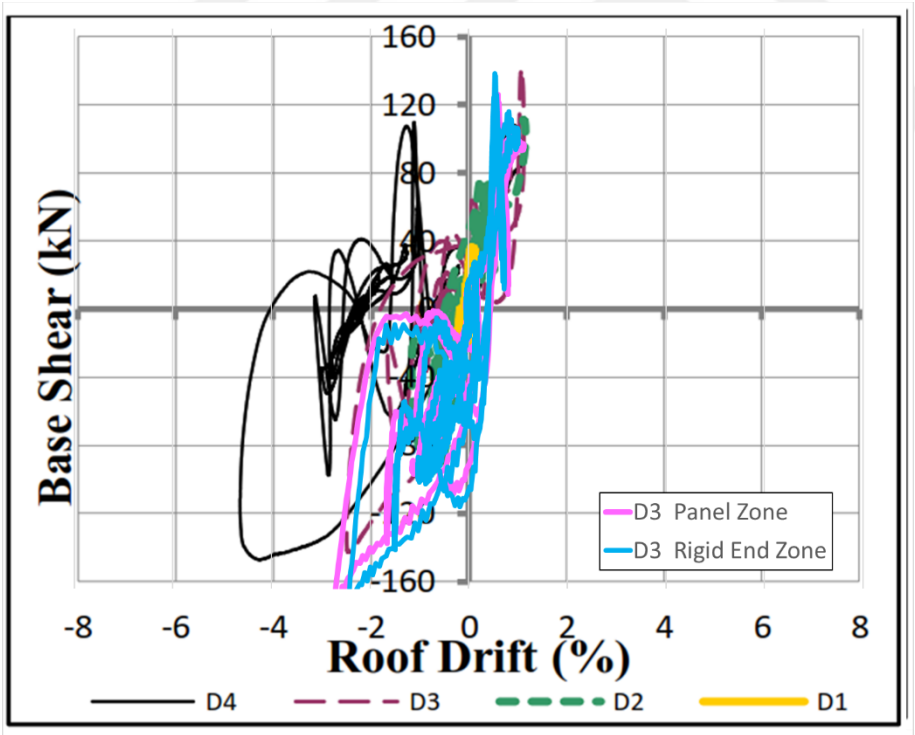


Figure 7.60. Joint Model vs Rigid Joint Assumption, D3

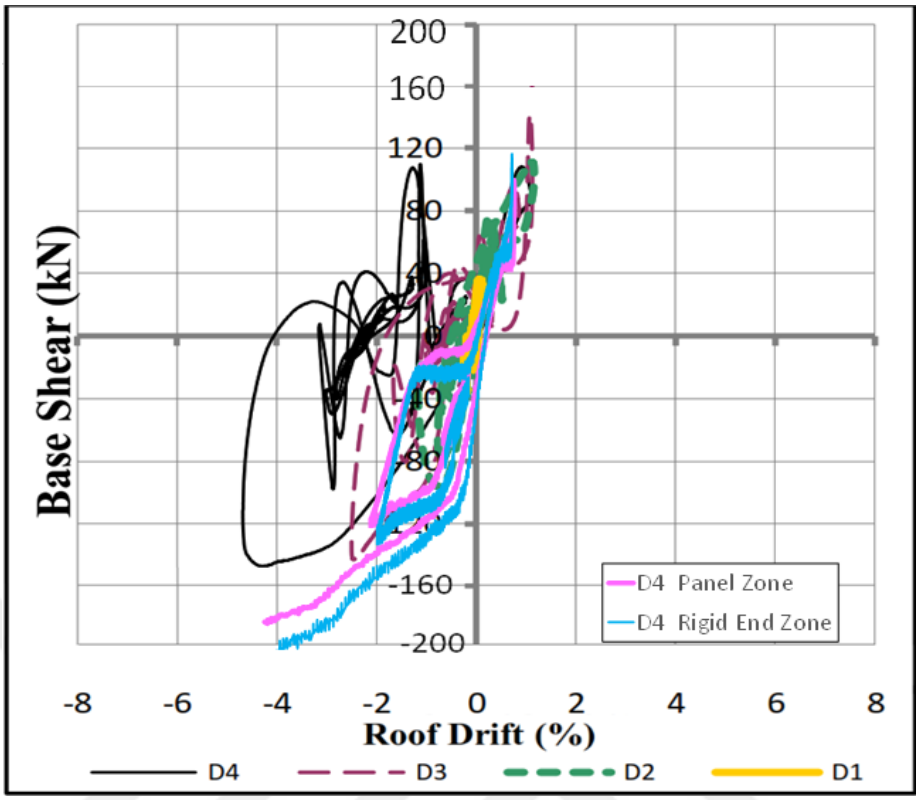


Figure 7.61. Joint Model vs Rigid Joint Assumption, D4

After the evaluation of the lateral load vs roof drift results, it can be concluded that a slight rigidity difference is observed, especially for D3 and D4 earthquake levels, though the difference is not significant. However, when member behavior is considered, there is a significant difference in between the two models as can be observed from the beam moment-rotation responses discussed next.

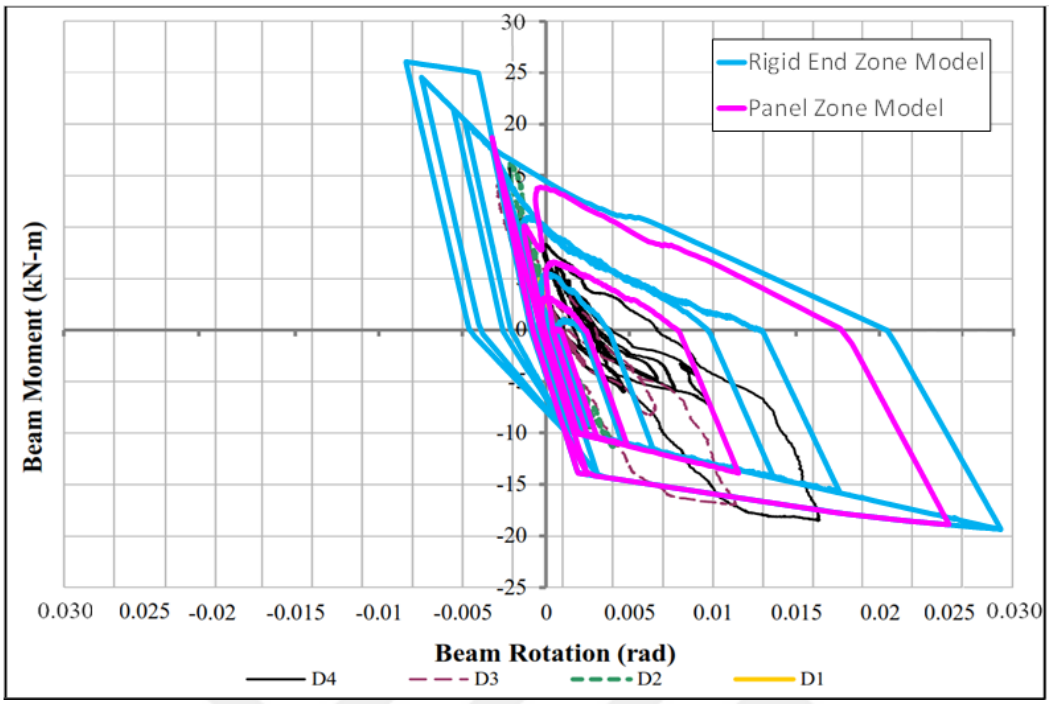


Figure 7.62. Overall Beam Moment - Rot., Joint Model vs REZ Model, Beam Framing into Ext. Joint

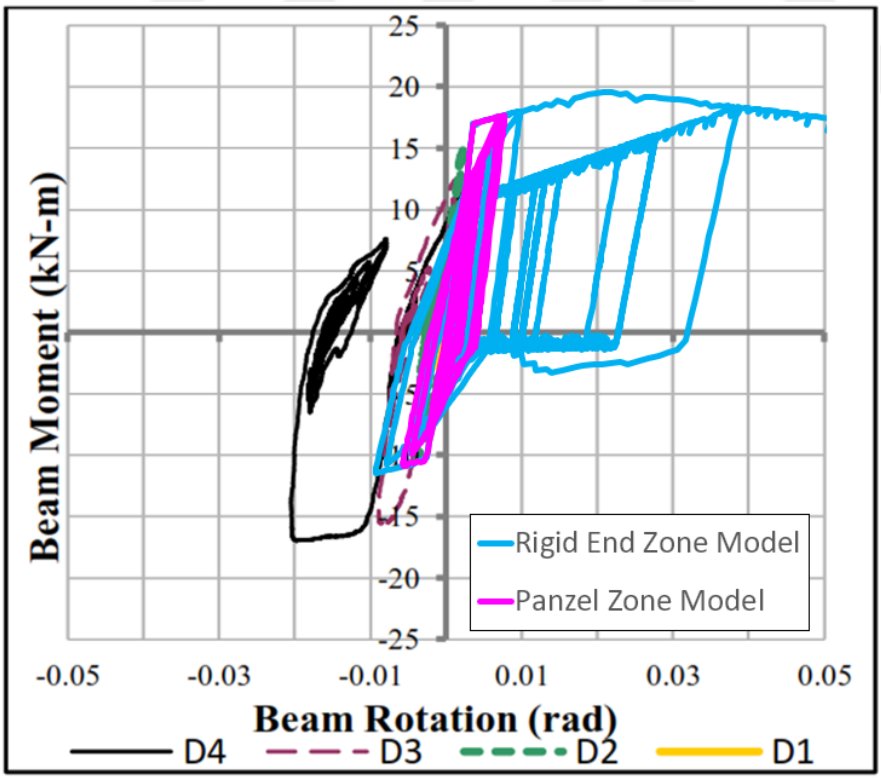


Figure 7.63. Beam Moment - Rot., Joint Model vs REZ Model, Beam Ext Beam Framing into Int. Joint

The beam moment - rotation relationship of the rigid joint assumption (REZ Model) and joint model utilization differ significantly, as can be inferred from

Figure 7.62 and Figure 7.63. Although both analytical models estimate the overall structural behavior without major difference, the effect of the utilization of the proposed nonlinear joint model is significantly observed in the response of the beams.

It is important to underline that the beam hinge rotations are crucial in the assessment of the damage levels of reinforced concrete structures. Hence, an inaccurate prediction of the beam moment-rotation response can lead to inappropriate evaluation of the structural performance under seismic loading. The necessity of the utilization of an effective joint model, hence, reveals itself in the proper determination of the structural behavior under seismic deformations, which may avoid unfounded demolition of existing structures and financial loss.

CHAPTER 8

SUMMARY AND CONCLUSIONS

8.1 Summary

The primary goal of this study is to develop an analytical model to accurately define the nonlinear shear behavior of beam-column joints when subjected to cyclic loading. During model development the main purpose is to achieve a delicate balance, while ensuring that the model is sufficiently comprehensive so that a wide range of parameters affecting the joint shear response can be considered, a level of simplicity that facilitates its practical application should be maintained.

The initial stage of this research involves the elaborate assembly of a database, which is composed of various experimental studies focusing on beam-column joint subassemblies. This database is notable for its diversity, covering various joint types and spanning a broad spectrum of geometric configurations and material characteristics. The compilation of such a comprehensive database serves as a foundational step, enabling a thorough evaluation of the properties associated with the selected specimens. This evaluation is critical in developing a methodology for predicting the shear strength of beam-column joints, with a particular emphasis on incorporating the pivotal characteristics that define these connections.

The first step in the construction of the nonlinear model is determination of a basic joint shear strength ($V_{j,pre.,basic}$) based on the geometrical properties of the connection, mainly focusing on the extent of the column face covered by the beam width that frames into the column. While following the general methodologies addressed by the contemporary structural codes, the joint shear prediction differs from the codes in terms of defining a continuous approach for computing the joint shear strength factor (γ) instead of a discrete definition. The initial computation of the basic joint shear strength is subsequently enhanced through the application of Modification factors.

These factors are carefully determined based on the geometrical, material, reinforcement and loading characteristics. Following a thorough assessment of the extent of the effect of crucial parameters on the joint shear strength, drawing on insights from previous experimental and analytical studies, a comprehensive shear strength prediction model is formulated. This model is designed to be versatile, making it suitable for a broad range of connection types.

The next step in developing a response model for beam-column joints under reversed cyclic loading involves identifying fundamental shear strain and shear strength benchmarks points. To achieve this objective, the key performance points for the joint shear response, namely P_{cr}, P_{inel}, P_{max1}, P_{max2} and P_{final}, are determined using data from experimental studies that provide joint shear force versus shear strain relationship. Among these key points, P_{inel} is recognized as the most accurately determinable point. Therefore, a predictive method rooted in the basic joint shear strength is recommended to accurately establish P_{inel}. The shear force and shear strain values for the remaining performance points are calculated in relation to P_{inel}, leading to the creation of backbone curves. These curves articulate the relationship between shear force and shear strain for both external and internal beam-column joints, providing a comprehensive view of their behavior under cyclic loading.

The validation of the developed backbone curves utilized as the joint model is conducted using the SAP2000 software. For the analytical validation process, the beam-column joint “Panel Zone” element in the software is utilized along with the “Pivot” hysteretic material model, to accurately depict the provided experimental shear force versus shear strain relationships of the joints. The outcomes from the analyses of beam-column connection subassemblies under reversed cyclic loading are compared with experimental data for not only the joint shear behavior but beam flexural behavior and overall structural response to confirm the accuracy of the analytical model. The efficiency of the model is further verified by comparing the analytical results of the utilization of the joint model by defining nonlinear panel zone elements with the response of rigid and semi-rigid joint assumptions.

Finally, the proposed joint shear behavior model is verified by the comparison of experimental and analytical responses of a well detailed, code conforming 3-story 3-bay structure, previously tested in the Middle East Technical University Structural Mechanics Laboratory.

8.2 Conclusions

1. The study provides an accurate shear strength prediction equation developed for beam-column connections under reversed cyclic loading. The use of Modification factors based on geometric and material properties of the connections enhances the accuracy of the model and applicability to a wide range of connection properties.
2. The application of a continuous approach in the determination of the joint shear strength factor proves to be effective in comparison to the contemporary structural codes, accurately predicting both the code conforming and nonconforming specimens defined based on the limitations of each design code.
3. While contemporary structural codes provide detailed requirements on obtaining the shear strength of beam-column joints, the prescribed methodologies for calculating joint shear strength could potentially lead to incorrect estimations of the joint shear capacity. The proposed joint shear strength prediction equation, which has lower mean absolute error and data dispersion when compared to all evaluated structural design codes, proves to be a viable option for integration into structural codes, which will aid in more accurate estimation of the reinforced concrete beam-column joint shear strength.
4. The method proposed for determining the key performance points, especially P_{inel}, proves to be effective. By accurately establishing P_{inel} through the joint shear strength, the study facilitates a more precise calculation of shear force and shear strain relationship for reinforced concrete joints.

5. The generation of backbone curves that define the shear force versus shear strain relationship for both exterior and interior beam-column joints provide valuable insight into their behavior under reversed cyclic loading. These curves are instrumental in understanding the complex dynamics of beam-column joints and offer a solid foundation for further research and practical applications.
6. The employment of SAP2000 software utilizing the beam-column joint panel zone element and the Pivot hysteretic material model, demonstrates a robust approach to obtain the joint shear force versus shear strain relationships. The verification process underscores the reliability of the analytical joint model when compared with the experimental data.
7. In order to accurately evaluate the performance of a frame structure under cyclic loading, a nonlinear joint model should be utilized. The inaccurate estimation of the joint shear response may lead to erroneous evaluation of the response of the adjoining members and the overall structure.
8. There is no joint shear strength estimations for deficient connections provided by structural design codes except for ASCE 41-17. Although ASCE 41-17 can be utilized to predict the joint shear strength for nonconforming structures, the high mean absolute error and standard deviation values indicate the ineffectiveness of the joint shear strength estimation methodology. The utilization of the proposed joint shear strength prediction equation as the design requirement in a structural code is a feasible option due to its suitability for practical applications.
9. The rigid or semi rigid joint assumptions do not provide satisfactory representations of the overall structural response and member responses. These assumptions result in excess beam rotations, which will lead to inaccurate performance assessment of frame structures.
10. When compared to the “Takeda” hysteresis model, “Pivot” hysteresis model predicts the shear behavior of reinforced concrete joints more accurately

under cyclic loading, also the pinching of the hysteresis curves can be successfully represented by the utilization of this model.

8.3 Recommendations for Future Research

While the proposed joint shear behavior model yields favorable outcomes for a broad spectrum of beam-column connections and offers a straightforward method for obtaining the joint behavior, it is imperative to highlight several critical areas that warrant additional investigation.

1. There is only limited data for the shear strain levels observed after the peak shear load is reached. For a more accurate estimation of the joint shear response under cyclic loading, new experimental studies should be performed in which the specimens are loaded till joint failure to obtain the post-peak response of the beam-column joint.
2. The hysteretic behavior coefficients for models such as “Pivot” hysteresis model and other hysteretic models that can be utilized for defining the behavior of various reinforced concrete structural members must be evaluated for a better understanding and representation of the overall structural response.
3. From experimental data, it can be observed that some exterior joints demonstrate a varying response in the positive and negative loading directions. The shear behavior of exterior beam column joints should be studied in detail to develop an unsymmetrical joint model for cyclic loading.
4. There is only limited experimental data for the cyclic behavior of deficient beam-column joints. The accuracy of the developed joint model can be improved for nonconforming joints as new experimental data becomes available.
5. It is observed that the significant revision in the joint shear strength estimation of the Turkish Earthquake Code improved the accuracy of the joint shear strength predictions, yet this improvement is not adequate for a

sufficient evaluation of the joint behavior. The equation should be evaluated and modified accounting for the experimental data and the requirements provided by other structural codes.

REFERENCES

ACI Committee 318. (2011). *318-11 Building Code Requirements for Structural Concrete and Commentary*. American Concrete Institute.

ACI Committee 318. (2014). *318-14 Building Code Requirements for Structural Concrete and Commentary*. American Concrete Institute.

ACI Committee 318. (2019). *318-19 Building Code Requirements for Structural Concrete and Commentary*. American Concrete Institute. https://doi.org/10.14359/51716937

Alameddine, F., & Ehsani, M. R. (1991). High-Strength RC Connections Subjected to Inelastic Cyclic Loading. *Journal of Structural Engineering*, *117*(3), 829–850. https://doi.org/10.1061/(ASCE)0733-9445(1991)117:3(829)

Alath, S., & Kunnath, S. K. (1995). Modeling Inelastic Shear Deformation in RC Beam-Column Joints. *Engineering Mechanics*, 822–825. https://api.semanticscholar.org/CorpusID:138509183

Anderson, J. C., & Townsend, W. H. (1977). Models for RC Frames with Degrading Stiffness. *Journal of the Structural Division*, *103*, 2361–2376. https://api.semanticscholar.org/CorpusID:106997356

ASCE/SEI 41. (2017). *Seismic Evaluation and Retrofit of Existing Buildings*. American Society of Civil Engineers. https://doi.org/10.1061/9780784414859

Attaalla, S. A. A. (1997). *Seismic Shear Capacity of Beam-Column Joints in Multistory Reinforced Concrete-Frame Buildings* [M.Sc]. Faculty of the Graduate School University of Southern California.

Behnam, H., Kuang, J. S., & Huang, R. Y. C. (2017). Exterior RC wide beam-column connections: Effect of beam width ratio on seismic behaviour. *Engineering Structures*, *147*, 27–44. https://doi.org/10.1016/j.engstruct.2017.05.044

Bolong, Z., & Yuzhou, C. (1991). Behavior of Exterior Reinforced Concrete Beam Column Joints Subjected to Bi-Directional Cyclic Loading. *SP-123: Design of Beam-Column Joints for Seismic Resistance*. https://doi.org/10.14359/2815

Bonacci, J., & Pantazoupoulou, S. (1993). Parametric Investigation of Joint Mechanics. *ACI Structural Journal*, *90*(1). https://doi.org/10.14359/4211

Briss, G. R., Paulay, T., & Park, R. (1978). *The Elastic Behaviour of Earthquake Resistant Reinforced Concrete Interior Beam-Column Joints*.

Burak, B. (2010, July 25). ANALYTICAL VERIFICATION OF A SIMPLIFIED REINFORCED CONCRETE JOINT MODEL . *Proceedings of the 9th U.S. National and 10th Canadian Conference on Earthquake Engineering*.

Burak, B., & Wight, J. K. (2008). Experimental Investigation on Seismic Behavior of Eccentric Reinforced Concrete Beam-Column-Slab Connections. *ACI Structural Journal*, *105*(2). https://doi.org/10.14359/19730

Canadian Standards Association. (2019). *Design of concrete structures*.

Cheung, P., Paulay, T., & Park, R. (1991). New Zealand Tests on Full-Scale Reinforced Concrete Beam-Column-Slab Subassemblages Designed for Earthquake Resistance. *SP-123: Design of Beam-Column Joints for Seismic Resistance*, 1–37. https://doi.org/10.14359/10258

Durrani, A. J., & Wight, J. K. (1985). Behavior of Interior Beam-to-Column Connections Under Earthquake-Type Loading. *ACI Journal Proceedings*, *82*(3). https://doi.org/10.14359/10341

Durrani, A. J., & Zerbe, H. E. (1987). Seismic Resistance of R/C Exterior Connections with Floor Slab. *Journal of Structural Engineering*, *113*(8), 1850–1864. https://doi.org/10.1061/(ASCE)0733-9445(1987)113:8(1850)

Ehsani, M. R., & Wight, J. K. (1985). Effect of Transverse Beams and Slab on Behavior of Reinforced Concrete Beam-to-Column Connections. *ACI Journal Proceedings*, *82*(2). https://doi.org/10.14359/10327

El-Metwally, S. E., Ashour, F., & Chen, W. F. (1990). Instability Analysis of Eccentrically Loaded Concrete Walls. *Journal of Structural Engineering*, *116*(10), 2862–2880. https://doi.org/10.1061/(ASCE)0733-9445(1990)116:10(2862)

Elmorsi, M., Kianoush, M. R., & Tso, W. K. (2000). Modeling bond-slip deformations in reinforced concrete beam-column joints. *Canadian Journal of Civil Engineering*, *27*(3), 490–505. https://doi.org/10.1139/l99-085

French, C. W., & Boroojerdi, A. (1989). Contribution of R/C Floor Slabs in Resisting Lateral Loads. *Journal of Structural Engineering*, *115*(1), 1–18. https://doi.org/10.1061/(ASCE)0733-9445(1989)115:1(1)

Fu, J., Chen, T., Wang, Z., & Bai, S. (2000). Effect of axial load ratio on seismic behavior of interior beam–column joints. *Proc. 12th World Conf. Earthquake Eng*.

Fujii, S., & Morita, S. (1991). Comparison Between Interior and Exterior R/C Beam-Column Joint Behavior. *SP-123: Design of Beam-Column Joints for Seismic Resistance*. https://doi.org/10.14359/2836

Gentry, T. R., & Wight, J. K. (1994). Wide Beam-Column Connections under Earthquake-Type Loading. *Earthquake Spectra*, *10*(4), 675–703. https://doi.org/10.1193/1.1585793

Guimaraes, G. N., Kreger, M. E., & Jirsa, J. O. (1993). Evaluation of Joint-Shear Provisions for Interior Beam-Column-Slab Connections Using High-Strength Materials. *ACI Structural Journal*, *89*(1). https://doi.org/10.14359/1299

Hanson, N. W., & Conner, H. W. (1967). Seismic Resistance of Reinforced Concrete Beam-Column Joints. *Journal of the Structural Division*, *93*, 533–560. https://api.semanticscholar.org/CorpusID:135932736

Hegger, J., Sherif, A., & Roeser, W. (2003). Nonseismic Design of Beam-Column Joints. *ACI Structural Journal*, *100*(5). https://doi.org/10.14359/12807

Higazy, E. M. M., Elnashai, A. S., & Agbabian, M. S. (1996). Behavior of Beam-Column Connections under Axial Column Tension. *Journal of Structural Engineering*, *122*(5), 501–511. https://doi.org/10.1061/(ASCE)0733-9445(1996)122:5(501)

Hwang, S.-J., Lee, H.-J., Liao, T.-F., Wang, K.-C., & Tsai, H.-H. (2005). Role of Hoops on Shear Strength of Reinforced Concrete Beam-Column Joints. *ACI Structural Journal*, *102*(3). https://doi.org/10.14359/14416

Joh, O., Goto, Y., & Shibata, T. (1991a). Behavior of Reinforced Concrete Beam-Column Joints With Eccentricity. *SP-123: Design of Beam-Column Joints for Seismic Resistance*. https://doi.org/10.14359/2863

Joh, O., Goto, Y., & Shibata, T. (1991b). Influence of Transverse Joint and Beam Reinforcement and Relocation of Plastic Hinge Region on Beam Column Joint Stiffness Deterioration. *SP-123: Design of Beam-Column Joints for Seismic Resistance*. https://doi.org/10.14359/2849

Joint ACI-ASCE Committee 352. (2010). *ACI PRC-352-02: Recommendations for Design of Beam-Column Connections in Monolithic Reinforced Concrete Structures(Reapp 2010)*.

Kaku, T., & Asakusa, H. (1991). Ductility Estimation of Exterior Beam-Column Subassemblages in Reinforced Concrete frames. *SP-123: Design of Beam-Column Joints for Seismic Resistance*. https://doi.org/10.14359/2842

Karayannis, C. G., Chalioris, C. E., & Sirkelis, G. M. (2008). Local Retrofit Of Exterior RC Beam–Column Joints Using Thin RC Jackets—An Experimental Study. *Earthquake Engineering & Structural Dynamics*, *37*(5), 727–746. https://doi.org/10.1002/eqe.783

Kim, C. G., & Park, H. G. (2015). *Effect of Shear Reinforcement on Seismic Performance of RC Beam-Column Joints*. https://api.semanticscholar.org/CorpusID:204746314

Kim, J., LaFave, J. M., & Song, J. (2007). A new statistical approach for joint shear strength determination of RC beam-column connections subjected to lateral earthquake loading. *Structural Engineering and Mechanics*, *27*(4), 439–456. https://doi.org/10.12989/sem.2007.27.4.439

Kun, H. (2003). *Design And Detailing Of Diagonally Reinforced Interior Beam-Column Joints For Moderate Seismicity Regions* [Ph.D.]. The University of Hong Kong.

Kurose, Y., Guimaraes, G. N., Zuhua, L., Kreger, M. E., & Jirsa, J. O. (1991). Evaluation of Slab-Beam-Column Connections Subjected to Bidirectional lLoading. *SP-123: Design of Beam-Column Joints for Seismic Resistance*. https://doi.org/10.14359/2807

Kusuhara, F., Azukawa, K., Shiohara, H., & Otani, S. (2004, August 1). Tests Of Reinforced Concrete Interior Beam-Column Joint Subassemblages with Eccentric Beams. *13th World Conference on Earthquake Engineering*.

LaFave, J. M., & Wight, J. K. (1999). Reinforced Concrete Exterior Wide Beam-Column-Slab Connections Subjected to Lateral Earthquake Loading. *ACI Structural Journal*, *96*(4). https://doi.org/10.14359/694

Lee, H.-J., & Ko, J.-W. (2008). Eccentric reinforced concrete beam-column connections subjected to cyclic loading in principal directions. *Aci Structural Journal*, *105*, 380–382.

Lee, J.-Y., Kim, J.-Y., & Oh, G.-J. (2009). Strength Deterioration Of Reinforced Concrete Beam–Column Joints Subjected To Cyclic Loading. *Engineering Structures*, *31*(9), 2070–2085. https://doi.org/10.1016/j.engstruct.2009.03.009

Lehman, D., Stanton, J., Anderson, M., Alire, D., & Walker, S. (2004, August 1). Seismic Performance Of Older Beam-Column Joints. *13th World Conference on Earthquake Engineering*.

Leon, R. T. (1990). Shear Strength and Hysteretic Behavior of Interior Beam-Column Joints. *ACI Structural Journal*, *87*(1). https://doi.org/10.14359/3198

Li, B., & Leong, C. L. (2015). Experimental and Numerical Investigations of the Seismic Behavior of High-Strength Concrete Beam-Column Joints with Column Axial Load. *Journal of Structural Engineering*, *141*(9). https://doi.org/10.1061/(ASCE)ST.1943-541X.0001191

Meinheit, D. F., & Jirsa, J. O. (1977). *Shear Strength of Reinforced Concrete Beam-Column Joints*.

Murty, C. V. R., Rai, D. C., Bajpaj, K. K., & Jain, S. K. (2003). Effectiveness of Reinforcement Details in Exterior Reinforced Concrete Beam-Column Joints for Earthquake Resistance. *ACI Structural Journal*, *100*(2). https://doi.org/10.14359/12478

Noguchi, H., & Kashiwazaki, T. (1992). Experimental Studies On Shear Performances Of RC Interior Column-Beam Joints With High-Strength Materials. *Earthquake Engineering, Tenth World Conference*, 3193–3168.

Ohmori, N., Takahashi, T., Tsubota, H., Inoue, N., Kurihara, K., & Watanabe, S. (1989). Experimental Studies on Nonlinear Behaviour of Reinforced Concrete Panels Subjected to Cyclic In-plane Shear. *Journal of Structural and Construction Engineering (Transactions of AIJ)*, *403*(0), 105–118. https://doi.org/10.3130/aijsx.403.0_105

Park, R. (2002). Summary Of Results of Simulated Seismic Load Tests On Reinforced Concrete Beam-Column Joints, Beams And Columns With Substandard Reinforcing Details. *Journal of Earthquake Engineering*, *6*(2), 147–174. https://doi.org/10.1080/13632460209350413

Park, R., & Milburn, J. R. (1983). Comparison of recent New Zealand and United States seismic design provisions for reinforced concrete beam-column joints and test results from four units designed according to the New Zealand code.

Bulletin of the New Zealand Society for Earthquake Engineering, *16*(1), 3–24. https://doi.org/10.5459/bnzsee.16.1.3-24

Park, R., & Ruitong, D. (1988). A Comparison of The Behaviour Of Reinforced Concrete Beam-Column Joints Designed For Ductility And Limited Ductility. *Bulletin Of the New Zealand National Society For Earthquake Engineering*, *21*(4), 255–278.

Parker, D. E., & Bullman, P. J. M. (1997). Shear Strength Within Reinforced Concrete Beam-Column Joints. *The Structural Engineer*, *75*(4).

Paulay, T., Park, R., & Priestley, M. J. N. (1978). Reinforced Concrete Beam-Column Joints Under Seismic Actions. *ACI Journal Proceedings*, *75*(11). https://doi.org/10.14359/10971

Quintero-Febres, C. G., & Wight, J. K. (2001). Experimental Study of Reinforced Concrete Interior Wide Beam-Column Connections Subjected to Lateral Loading. *ACI Structural Journal*, *98*(4). https://doi.org/10.14359/10300

Raffaelle, G. S., & Wight, J. K. (1995). Reinforced Concrete Eccentric Beam-Column Connections Subjected to Earthquake-Type Loading. *ACI Structural Journal*, *92*(1). https://doi.org/10.14359/1474

Scott, R. H. (1992). The Effects of Detailing on RC Beam/Column Connection Behaviour. *The Structural Engineer*, *70*(18), 318–324.

Shin, M., & LaFave, J. M. (2004). Seismic Performance of Reinforced Concrete Eccentric Beam-Column Connections with Floor Slabs. *ACI Structural Journal*, *101*(3). https://doi.org/10.14359/13100

Shiohara, H., & Kusuhara, F. (2006). *Proposed Benchmark Problem for Blind Analysis: Tests for Validation of Mathematical Models on R/C Beam-column Joints*.

Sugano, S., Nagashima, T., Kimura, H., & Ichikawa, A. (1991). Behavior of Beam Column Joints Using High-Strength Materials. *SP-123: Design of Beam-Column Joints for Seismic Resistance*. https://doi.org/10.14359/2866

Teng, S., & Zhou, H. (2003). Eccentric Reinforced Concrete Beam-Column Joints Subjected to Cyclic Loading. *ACI Structural Journal*, *100*(2). https://doi.org/10.14359/12477

Tsonos, A. G. (2007). Cyclic Load Behavior of Reinforced Concrete Beam-Column Subassemblages of Modern Structures. *ACI Structural Journal*, *104*(4). https://doi.org/10.14359/18777

Turkish Disaster and Emergency Management Presidency. (2018). *Turkish Earthquake Code 2018*.

Turkish Ministry of Public Works and Settlement. (2007). *Turkish Earthquake Code 2007*.

Unal, M., & Burak, B. (2012). Joint shear strength prediction for reinforced concrete beam-to-column connections. *Structural Engineering and Mechanics*, *41*(3). https://doi.org/10.12989/sem.2012.41.3.421

Unal, M., & Burak, B. (2013a). Development and analytical verification of an inelastic reinforced concrete joint model. *Engineering Structures*, *52*, 284–294. https://doi.org/10.1016/j.engstruct.2013.02.032

Unal, M., & Burak, B. (2013b). Performance of Beam-to-Column Connection of a Well-Detailed RC Moment Frame Building under Pseudo dynamic Loading. *Journal of Structural Engineering*, *139*(6), 886–896. https://doi.org/10.1061/(ASCE)ST.1943-541X.0000700

Uzumeri, S. M. (1977). Strength and Ductility of Cast-In-Place Beam-Column Joints. *SP 53-12: Reinforced Concrete Structures in Seismic Zones*, 293–350.

Wong, H. F., & Kuang, J. S. (2008). Effects of beam—column depth ratio on joint seismic behaviour. *Proceedings of the Institution of Civil Engineers - Structures and Buildings*, *161*(2), 91–101. https://doi.org/10.1680/stbu.2008.161.2.91

Zaid, S., Shiohara, H., & Otani, S. (1999, October 30). Test of a Joint Reinforcing Detail Improving Joint Capacity Of R/C Interior Beam-Column Joint. *The 1st Japan-Korea Joint Seminar on Earthquake Engineering for Building Structures*.

CURRICULUM VITAE

Surname, Name: Akın, Umut

EDUCATION

Ph.D.	Middle East Technical University Civil Engineering Department, Structural Mechanics The Effect of Inelastic Behavior of Beam-to-Column Connection Regions on The Seismic Performance of RC Frame Structures Supervisor: Assoc. Prof. Dr. Burcu Burak Bakır	2014-2024
M.Sc.	Middle East Technical University Civil Engineering Department, Structural Mechanics Seismic Assessment of Reinforced Concrete Beam-to-Column Connections Under Reversed Cyclic Loading Supervisor: Assoc. Prof. Dr. Burcu Burak Bakır	2008-2011
B.S.	Middle East Technical University Civil Engineering Department	2003-2008
High School	Mehmet Emin Resulzade Anatolian High School, Ankara	1996-2003

EMPLOYMENT

2018 -	Su Yapı Engineering and Consulting Inc., Ankara
	Design Director, Structural and Geotechnical Projects (2023 -) Head of Structural and Architectural Dept. (2021-2023) Design Engineer (2018-2021)
2015 - 2018	SWS Engineering, Ankara
	Design Engineer
2014 - 2015	Hidrokon Engineering, Ankara
	Design Engineer
2011 - 2014	Stucky Teknik Engineering and Consulting Ltd., Ankara
	Design Engineer
2008 - 2010	Erges Engineering and Consulting Ltd., Ankara
	Design Engineer

TEACHING EXPERIENCE

2021 Spring	Bilkent University Department of Architecture
	ARCH332 – Structural Design II

RESEARCH INTERESTS

Seismic design of frame structures.

Nonlinear behaviour of reinforced concrete members.

Beam-column joint response mechanisms against cyclic loading.

Post tensioned bridge design.

ORGANIZATIONS / INTERESTS

ACI Concrete Convention and Exposition, 2019 - Cincinnati, Ohio, USA

“Post Tensioned Highway Bridge Design” Poster Presentation

4th Symposium on Bridges and Viaducts, 2019 - Ankara, Turkey

“Post Tensioned Highway Bridge Design” Technical Presentation

Chamber of Architects “Dreams on the City” Competition #2, 2007 - Ankara

“Hasanoğlan Köy Enstitüsü” Re-evaluation Project 2nd Prize